LOCAL SOURCE INFLUENCES UPON THE STRUCTURE OF DUST PLUMES IN THE CHANNEL COUNTRY OF WESTERN QUEENSLAND, AUSTRALIA.

A thesis

submitted in the fulfilment

of the requirements of the degree

doctor of philosophy

By

Harry Butler B.Sc.(Hons.), Dip.Ed.

15th December, 2003

This work has not previously been submitted for a degree or diploma in any university. To the best of my knowledge and belief, the thesis contains no material previously published or written by another person except where due reference is made in the thesis itself.

_____

(Harry James Butler)

Contents

List of Figures

List of Tables

Abstract

Most of the early wind erosion research undertaken in Australia, concentrated on how wind erosion affects cultivated farm land. However, in the 1990's the focus of wind erosion research in Australia started to shift to include rangeland environments. Initially these rangeland experiments used experimental configurations that were developed for cultivated fields. This meant that in most cases a sampler was set up in the middle of a field and it was assumed that the data collected was representative of the field as a whole. It was also assumed that temporal changes in dust fluxes/concentration reflect overall changes in the land type erodibility and wind erosivity. However, recent experiments and field observations within the rangelands of the Channel Country suggest that this assumption is not valid. These experiments and observations suggest that there are substantial spatial and temporal variations in erodibility within individual land types. Such variations complicate the interpretation of temporal and spatial erosion trends. In particular, this variability implies that it is difficult to compare sampler data between different wind erosion events.

To begin quantifying and comparing sampler data between events within the rangeland environments, the Dust Source Interaction Simulation Model (DSism) was developed to simulate the effect that physical processes and spatial variations in erodibility have upon observed dust concentration profiles. The modelling/simulation approach used is closely linked to experimental data via the extensive use of sensitivity testing. Another key feature of the DSism approach, is its flexibility in allowing different dust source areas

to have particle emission characteristics. This combined sensitivity testing and simulation approach has provided new insights into the wind erosion processes.

By using DSism, it has been possible to identify several key features of the wind erosion process within rangeland environments. The first observation is that spatial and temporal changes in erodibility produce distinct changes in both the vertical and crosswind dust concentration profiles. Further investigations, indicate that the dispersion processes in operation vary from event to event. In particular, the results presented here indicate that surface heating plays an important role in some wind erosion events. These results also suggest that even small variations in the vertical dust concentration profile can reflect temporal and spatial changes in processes and erodibility. Finally the simulation results show that the particle size distribution of a vertical dust concentration profile depends on (a) the processes in operation during a given event and (b) the spatial variation in the particle size emission characteristics of the various source areas. These findings have several important implications. In particular, they indicate that both the crosswind and vertical dust concentration profiles can be viewed as amalgamation of several distinct plumes from different dust source areas and that dust concentration profiles contain significant information about both the spatial distribution of sources and the processes in operation during any given event.

Most field studies have used regression models to describe the variation in dust concentration with height. A problem with this approach is that it assumes that the variation in dust concentration with height, always has a given functional form (or shape) and that dust concentration always decreases with height. Field observations, indicate that this assumption is only valid for some events within rangeland environments and that dust concentration does not always decrease with height in these environments. In most cases, such variations from the regression fit have been assumed to be the result of experimental "noise" (error) or spatial variations in erodibility. This thesis

presents, modelling and field evidence, which suggests that such variations, are the result of a combination of spatial variations in erodibility and changes in thermal conditions.

Acknowledgements

I would like to thank all the people that have helped me throughout the last few years in preparing this thesis. A special thanks goes to the following people who's help has been invaluable to me.

- Prof. W.L. Hogarth and Assoc. Prof. G.H. McTainsh for their patience, understanding and time they given me in the last few years.
- Deslie Smith for helping to organise the meeting times and other administration hassles that occurred from time to time.
- All my friends who have put up with my mood changes.
- Craig Strong, Kenn Tews, John Leys and the rest of the experimental team for there help in organising and collecting the field data.
- All those who helped with the proof reading.
- All the staff at the University of Southern Queensland and Griffith University. Especially Christine McDonald, Tim Passmore, Alison Mander and Patricia Cretchley who helped with much of the proof reading.
- Miss Anita Frederiks for her continued support and understanding over the last few years. Especially in understanding why I had to work, rather than being with her. I owe you so much for that.

Dedication

I would like to dedicate this dissertation to my Mother and Father, for their continued support and encouragement in helping me reach this level in my Academic studies. Without their support and understanding this thesis would not have been possible.

Part I

Introduction and background

Chapter 1

Introduction

Wind erosion is a major geomorphic process in much of arid central Australia. Soil particles entrained during wind erosion events, in this area of Australia, are often transported in dust plumes over large distances and off the Australian mainland. Wind eroded sediment from these regions has been identified as far away as New Zealand (Knight et al., 1995). Wind erosion therefore not only impacts on the local environment at its source, but also impacts on the global environment.

At the continental and regional scale the dust from wind erosion events is also a contributer to air pollution in cities (McTainsh, 1998). This was dramatically illustrated by the dust storms that hit Melbourne in 1983, Adelaide in May 1994 (Raupach et al., 1994) and Griffith in November 2002 (Fig. 1.1). While such events are a spectacular illustration of the erosive power of wind, the visible effects of smaller or more distant events are often much more subtle. Evidence of such events is often only a slight haze (Fig. 1.2), red dust on a car after a shower of rain, or a bright red sunset. In addition, many dust events are missed or mistaken for other natural phenomena, such as smoke haze or for urban derived air pollution.

At source, wind erosion removes significant amounts of topsoil, and nutrients from the soil (Leys et al., 1993). This removal of nutrients etc is estimated to cost South Australia alone 23 million Australian dollars per annum (William

Figure 1.1: Large dust plume approaching Griffith, New South Wales, Australia on the 12th November, 2002. This plume covered much of eastern Australia and was the result of one of Australia's worst droughts.

and Young, 1999), while the Melbourne dust storm of 1984, was estimated to cost Australia four million Australian dollars (Raupach et al., 1994).

With the increasing emphasis, in Australia, on sustainable and environmental friendly agriculture, the impact that certain pesticides have on the environment is also becoming an important issue. The movement of soil by wind has been identified as one of the major means by which pesticide contaminated soil may be redistributed within the natural environment (Hawthorne et al., 1996). Such redistribution of contaminated soil has been linked to the degradation of water quality in several major catchments in Australia (Raupach and Leys, 1999). Therefore, to protect our fragile natural environment, and provide a sustainable economic return to farmers, it is important to understand the role of wind erosion in the natural environment.

It is surprising that detailed research on the impact of wind erosion, in Australia, only began in the mid 1980's (Offer and Goossens, 2001). However

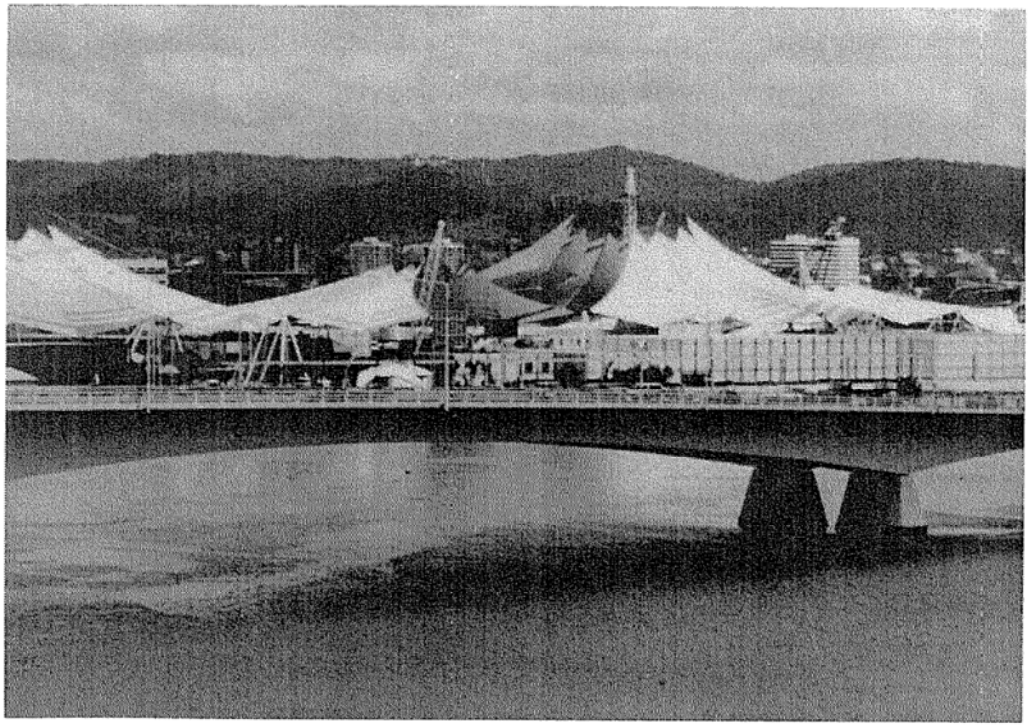

(a) Brisbane on a clear day

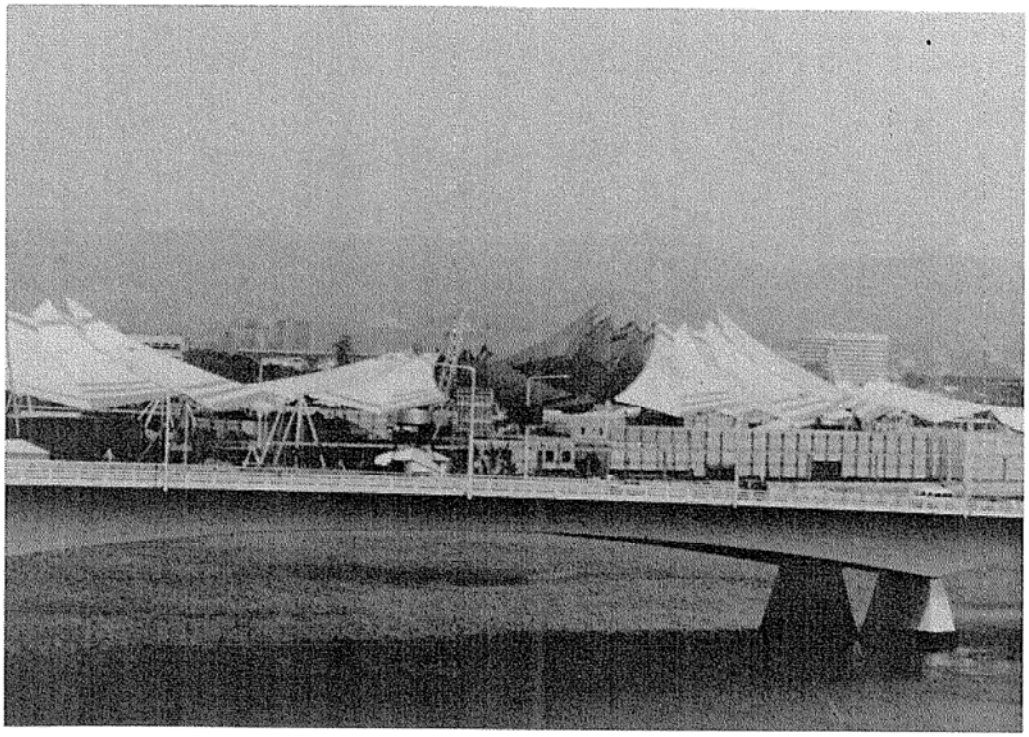

(b) Brisbane during a dust haze

Figure 1.2: Photographic comparison of the visibility in Brisbane on a clear day (a) and as a result of dust haze (b). Photos courtesy of G.H. McTainsh.

since then most of the research effort has focused on experiments, carried out on cultivated agricultural land, often with the aid of portable wind tunnels (Leys, 1998). These experiments have increased our knowledge of the environmental factors governing wind erosion of cultivated agricultural land in Australia. In addition the analysis of meteorological data on dust storm occurrence within Australia has also increased our understanding of the wind erosion process on a regional and continental scale (McTainsh et al., 1998). However, little is known about the influence spatial changes in surface conditions have on wind erosion at the local scale, especially in the Australian rangelands. The major aim of this research was to improve our understanding of how spatial and temporal variations in dust source areas and physical processes in rangeland environments influence how dust is vertically and laterally distributed during wind erosion events.

To address this problem, several field sites were established in the Channel Country of western Queensland in 1994, to monitor wind erosion and dust emission rates on a medium to long term basis (Fig. 1.3). The Channel Country is located some 1500km from Brisbane and contains some of Australia's largest cattle stations. It also forms the major drainage system of the Lake Eyre Basin and is one of the more environmentally sensitive and remote areas of Australia. Over the past century much has been written in Australian folklore about the dusty nature of large parts of the Channel Country. This long history of wind erosion and environmental sensitivity of the region makes it the ideal location to study wind erosion.

The data collected to date at these long term sites, has consisted of vertical and stream-wise dust flux, deposition rates, vertical dust concentration profiles, surface cover information and meteorological conditions (Nickling et al., 1999; McTainsh et al., 1998). In addition, the particle size characteristics of many of the collected sediments have been analysed. This data set, represents one of the best spatial and temporal records of wind erosion available in Australia.

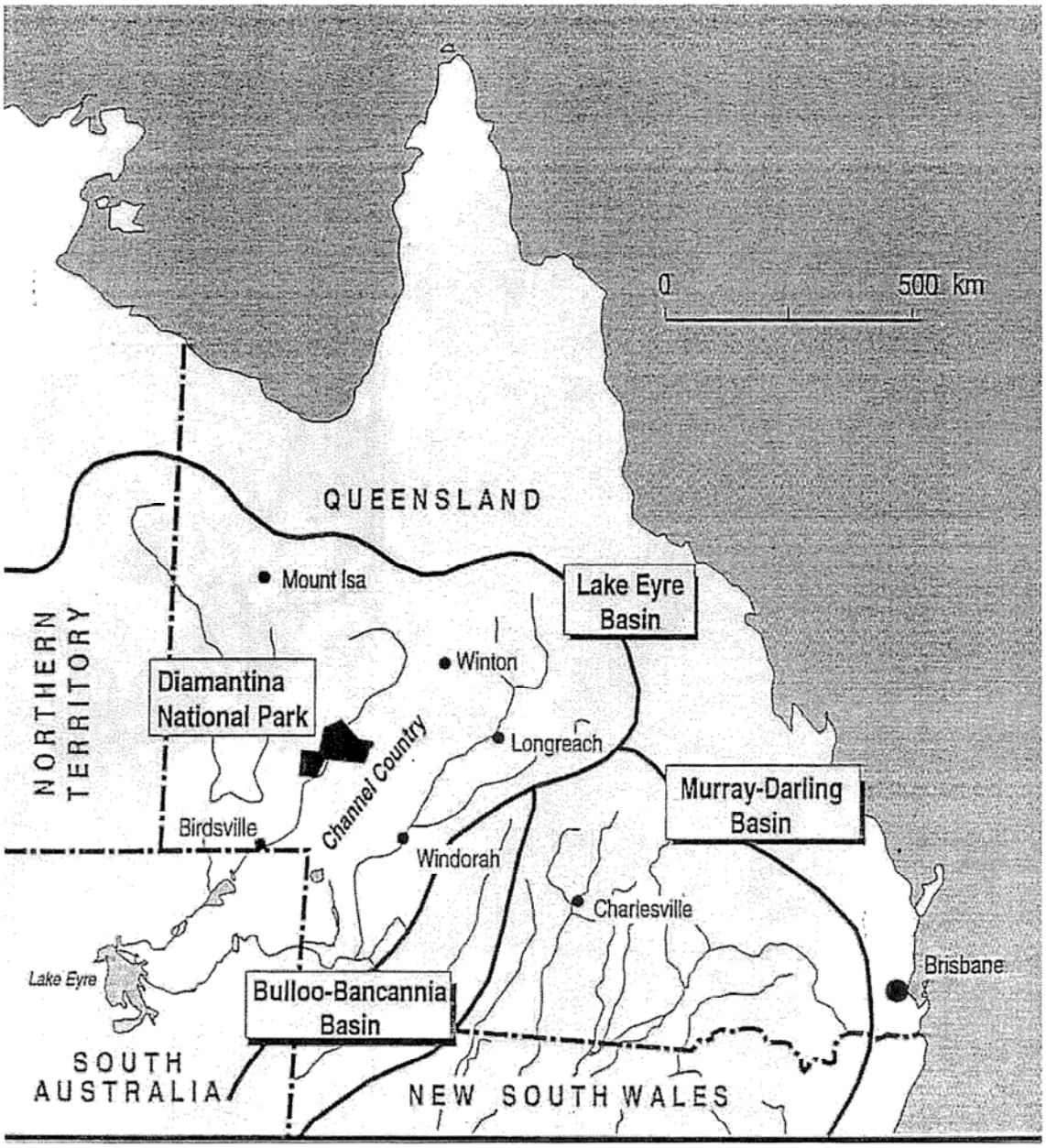

Figure 1.3: Location of the Channel Country in relation to Brisbane, and other major regional centres in Queensland, Australia.

Initial analysis of data collected at the Channel Country field sites by Nickling et al. (1999), indicates that in the field, both dust flux and dust concentration, are affected by spatial changes in erodibility of the surface. While these conclusions are supported by field studies undertaken in both America and Africa, by Gillette (1977) and Nickling and Gillies (1993) respectively, little is known about how localised spatial changes in the erodibility of natural soil surfaces affects dust concentration profiles, since it is difficult to quantify

these changes on an event basis.

Over the last decade in Australia there have been several experimental studies using portable wind tunnels that show how soil erodibility and vegetation cover affect wind erosion rates. Few studies (Nickling et al., 1999; Chappell et al., 2003), however, have considered the question of how changing spatial patterns of erodibility and vegetation cover affect dust concentration profiles. This is due largely to the difficulty of being able to precisely locate the dust sources that are active during any given dust event. One of the reasons it is difficult to locate these sources, is that wind erosion unlike water erosion, is not confined to channels (or well defined catchment boundaries). Thus wind transported sediments could have come from any direction and been re-entrained many times, whereas water transported sediments originate within the boundaries of the local catchment. Another reason it is difficult to isolate actual dust sources during wind erosion events, is the variability of wind in speed and direction during any given event. Thus it is quite feasible for several different dust sources to be active at different stages of a single wind erosion event.

Most models that have been used to fit dust concentration profiles such as, Vories and Fryrear (1991), Fryrear and Saleh (1993), and Leys (1998), have assumed that deviations from the predicted fit are mainly due to experimental noise in the data. Thus many process induced effects which may be due to spatial variations in erodibility and which may appear as noise in the data, have tended to be ignored to date. One reason for ignoring such processes is that most of these modelling studies have been carried on cultivated agricultural fields, where the surface conditions are fairly uniform. The lack of surface variability in this case would imply that any spatial effects should be small. However, Shao et al. (1996), have suggested that temporal and spatial variations in erodibility within these fields is also likely to be an important consideration.

The Channel Country of western Queensland is a large and diverse region, therefore, in contrast to cultivated land where the surface conditions are fairly

uniform, there is significant variation in soil surface conditions and vegetation cover. Variations in wind erosion rates in the Channel Country are therefore a direct result of changes in surface conditions and vegetation cover. The main aim of this project in terms of the Channel Country, was to determine to what extent spatial/temporal variations in erodibility and processes affect recorded dust concentration profiles.

To further understand how important the above aim is to understanding wind erosion in rangeland environments, such as the Channel Country, consider the following two scenarios. In Scenario A (Fig. 1.4), a dust sampler is set up in the middle of a land type, as in a typical field measurement scenario. Two Events (A and B) now occur while this site is active. For Event A (Fig. 1.4(a)) a given set of dust sources are active and wind is coming from a given direction. In Event B (Fig. 1.4(b)), the same sources are active but the wind is now coming from a different direction. Provided the wind speed remains constant in these events, the amount of sediment collected by the sampler will be different. This difference will be the result of the change in source strength and distribution of the dust sources upwind of the sampler.

However, the wind speed is unlikely to be constant between events. There are two consequences of such a change in wind speed. The first of these consequences relates to the deposition rate of particles within the plume. Provided the deposition velocity remains constant dust particles entrained within the plume will settle out at a constant rate. Consequently, if the wind speed is low more particles will settle out close to the original source area. However, if the wind speed is high these particles will be distributed over a much larger area. Thus, the amount of sediment travelling past the sampler will depend on the distance of the sources upwind and the actual wind speed.

The other effect that changing wind speed can have is to change the source areas that are actually active during a given event. These changes in active source areas, can be further modified by changes in vegetation cover and surface conditions between events. This brings us to Scenario B in Figure 1.5. In this scenario the dust sampler with the land type shown in Figure 1.4

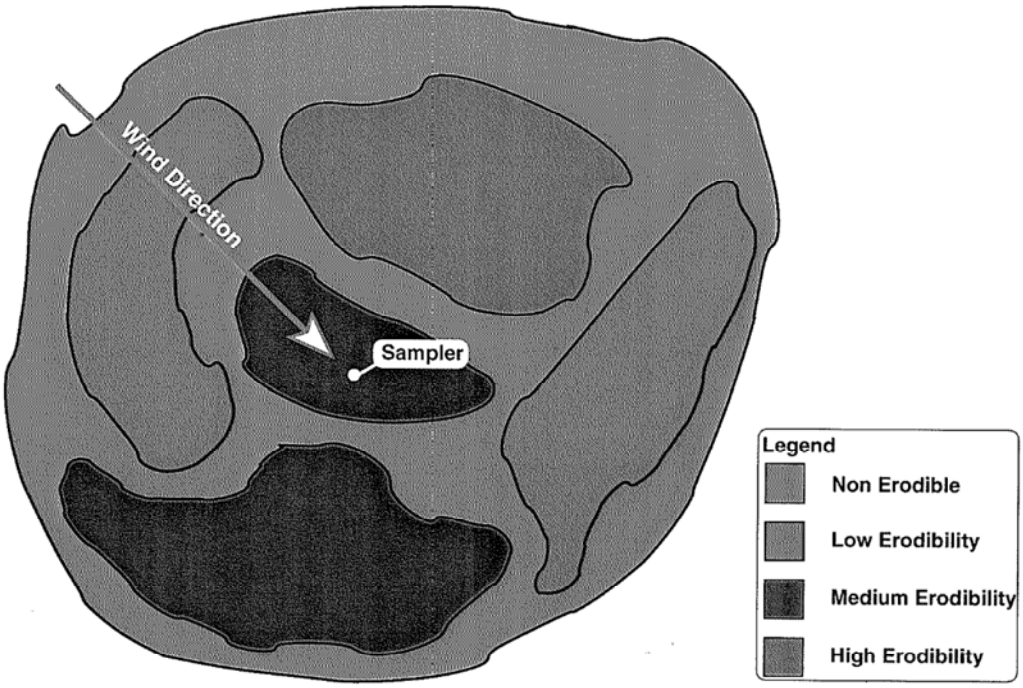

(a) Event A: hypothetical wind erosion event which has several different active dust sources within a single land type.

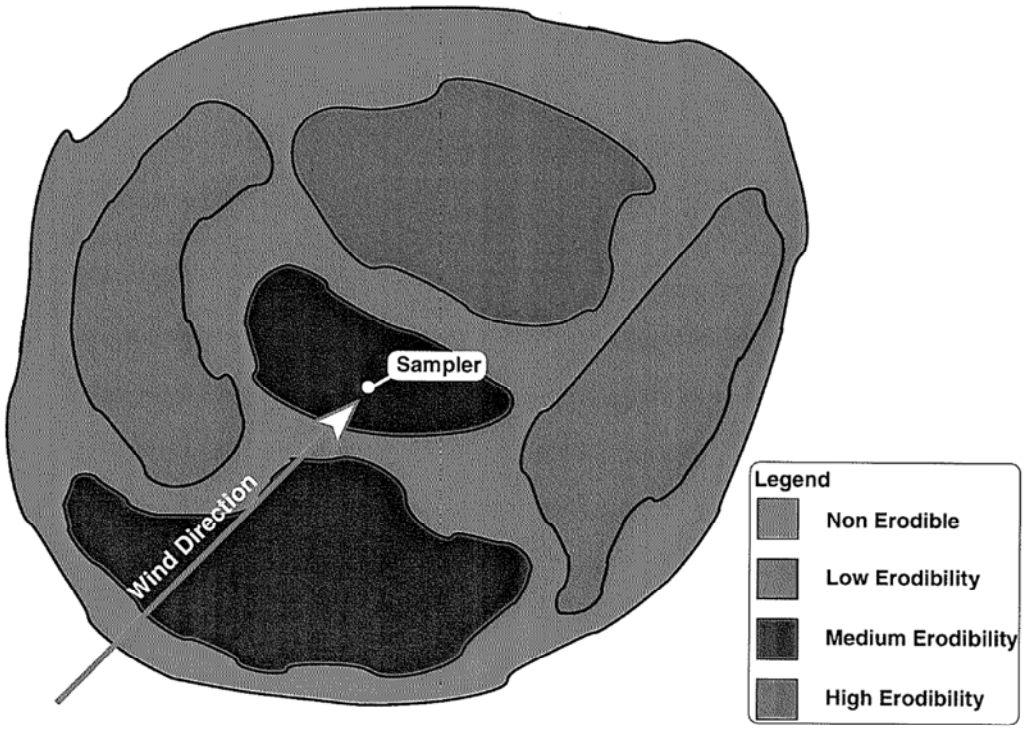

(b) Event B: same active dust source areas as Event A, but with different wind direction.

Figure 1.4: Scenario A: Two wind erosion Events (A and B) with the same potential source areas but different wind directions.

has recorded two further Events (C and D). While the wind direction in each event remains the same, the active source dust source areas are different. Once again the dust collected at the sampler will be different. Under these conditions it is difficult to compare the measurements taken at the sampler for the different Events (A,B,C and D). In particular, it is difficult to isolate whether the changes observed at the sampler are the result of spatial or temporal changes, or are simply the result of changes in wind speed and direction. The aim of this project, when viewed in the context of these scenarios is to begin understanding how spatial and temporal changes in dust sources within rangeland environments affect the measurements taken at the sampler.

A fundamental premise of this thesis is that measured dust concentration profiles can be viewed as a signal that uniquely identifies the characteristics and spatial distribution of dust sources during a dust event. That is, the measured dust concentration profile at any given point, could be thought of as being an amalgam of the distinct dust signals from several dust sources. This is a significantly different approach to that taken by non-spatially oriented models. This assumption means that the resulting model uses a large amount of experimental data and the more data the model has, the better it is likely to perform. The model also does not assume anything about the likely structure/shape of the resulting dust concentration profiles.

Using a signal to noise analogy as a basis, it is possible to view much of the noise, assumed by other models to exist in the experimental data, to actually be the result of other processes occurring during the event, in much the same way that stray electro-magnetic fields affect radio signals. This approach suggests that by understanding the likely nature of the apparent noise in the data, it is possible to gain a much better understanding of the processes occurring during any single event. Taking the signal to noise analogy further it is possible to begin thinking of the dust concentration profile and dust events in a different light. Each dust source can be thought of as being characterised by a distinct signal (or dust concentration profile). This signal can be thought of

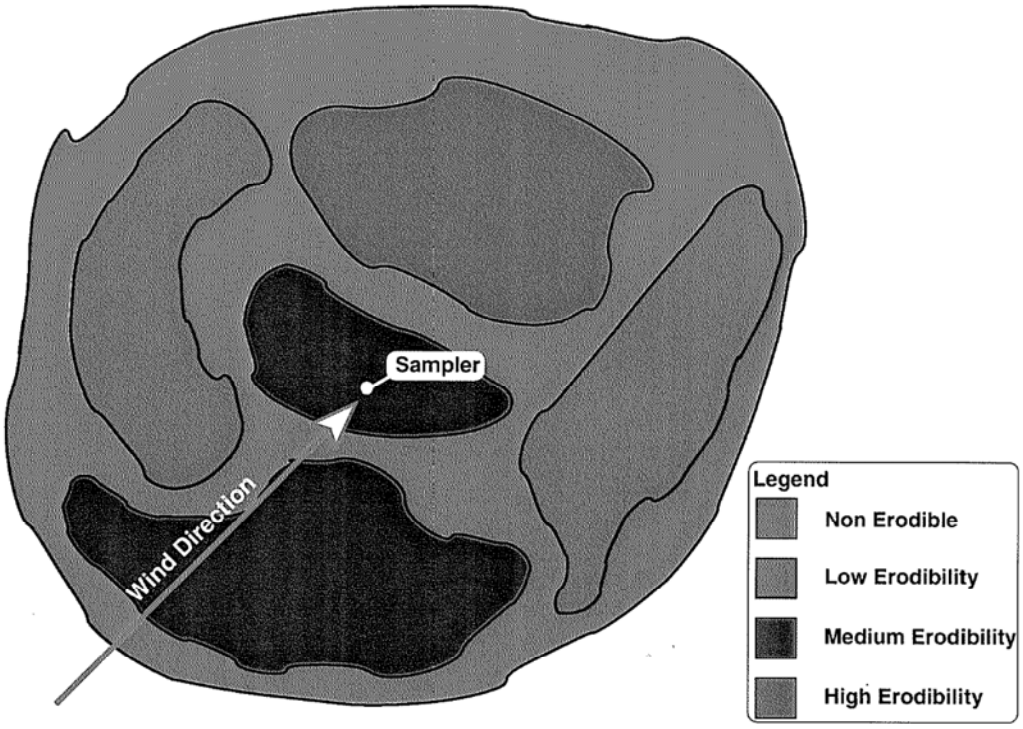

(a) Event C: hypothetical wind erosion event which has several different active dust sources within a single land type.

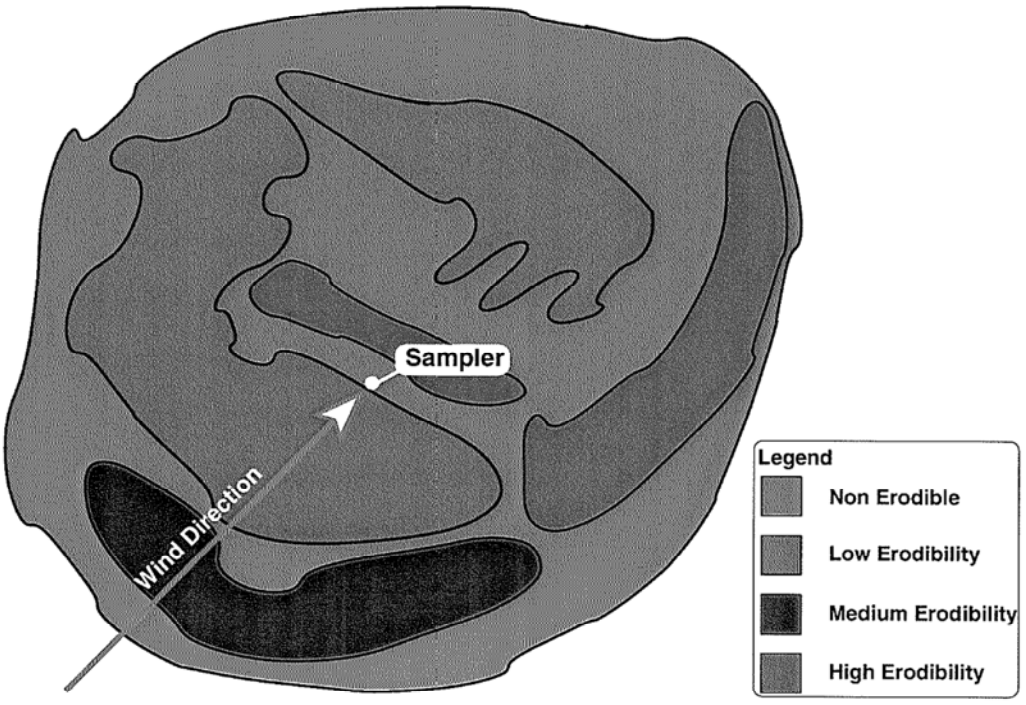

(b) Event D: the wind direction is the same as Event C, only in this event the source areas have changed.

Figure 1.5: Scenario B: Two wind erosion Events (C and D) with the same wind direction but different source areas.

as being a function of the particle size of the soil and other aspects of the erodibility of the soil and the distance the sediment has travelled. The likely dependence of the signal on these characteristics suggests that spatial changes in erodibility will be crucial in determining the structure of any measured dust concentration profile.

To achieve the goals outlined above, the Dust Source Interaction Simulation Model (DSism) was developed which allows the user to simulate the effects that changes in the spatial erodibility patterns would have on dust concentration profiles. The model does not take the traditional wind erosion approach, which is to use dust flux as the dependent variable. Instead, dust (particulate) concentration is used as the dependent variable. As a result DSism is based on the Gaussian Plume model (Hanna et al., 1982; Zannetti, 1990).

While there are several models available that use dust concentration as the dependent variable, DSism, however uses dust concentration data in a rather unique fashion. Instead of just predicting dust concentration values at given points, DSism outputs both vertical and crosswind dust concentration profiles. There are several reasons for doing this.

Dust concentration profiles are a much more sensitive measure of spatial variations than dust flux. In particular, dust flux only measures a given mass flowing through a given area per unit time. It does not provide any information about where in the plume this dust is concentrated. Dust concentration profiles taken at the same point however, gives much more detailed information about where the majority of the dust is being moved within the plume. This extra information is important to successfully link spatial variations in erodibility to changes in wind erosion rates.

Another advantage in using dust concentration profiles, rather than single point estimates of dust concentration, is that more process information can be extracted from a profile. In particular, by comparing observed dust concentration profiles against simulated ones, it is possible to identify process

differences between events. Comparing observed and predicted dust concentration profiles in this fashion, produces a model that is data hungry. That is, if more detailed or accurate observed dust concentration profile data becomes available it is possible to easily incorporate this new information into the modelling process, thus enabling researchers to continuously refine their concepts of how spatial changes in erodibility affect the resulting dust plumes. Therefore, to fully understand the results and the simulation process presented here, it is important that neither the modelling nor the experimental work be viewed in isolation.

The thesis has been divided into four parts. Part I, Introduction and background, contains three chapters and provides detailed background information on both the field site and the current methods used to model wind erosion. Chapter 1 provides the reader with a brief overview and introduction to this thesis. Chapter 2 provides details about the field site within the Channel Country of western Queensland and the likely influences on wind erosion within the site. The final chapter in Part I (Chapter 3) compares different modelling strategies.

Part II, Development of the dust source interaction simulation model (DSism), (Chapters 4 and 5) details the adaption of the Gaussian plume simulation model to rangeland environments. The first chapter of this part (Chapter 4) outlines the basic structure of the simulation model with regard to the measurement techniques employed within the study site, while the following chapter (Chapter 5) details how this basic structure is altered to account for field conditions within rangeland environments, such as the Channel Country of western Queensland.

Part III, Source influences on the structure of dust plumes, chapters 6 to 9, uses the model developed in Part II and experimental data collected within the Channel Country to examine the effect that spatial changes in erodibility has on the wind erosion processes in rangeland environments. Chapter 6, examines the model performance once it has been calibrated using field data. The following chapter (Chapter 7) looks at whether a secondary process may

account for some of the variations observed in the shape of vertical dust concentration profile. Chapter 8 compares model predicted spatial changes in erodibility to observed changes in surface and vegetation conditions within the study site. The final chapter in this part (Chapter 9), examines the likely affect that spatial changes in particle size emission rates have on the resulting vertical dust concentration profile.

Part IV, Concluding comments, consists of two chapters (Chapters 10 and 11). The first chapter (Chapter 10) reviews DSism in the context of the other models discussed in Chapter 3. While, the final chapter (Chapter 11) summaries the results of the research presented in this thesis and discusses the future directions along which this research is likely to proceed.

Chapter 2

Background I: Environmental influences upon wind erosion in the Channel Country

2.1 Introduction

To understand the effect that spatial changes in erodibility have upon wind erosion in the Channel Country it is first necessary to have a mental picture of the region. To make such a mental picture complete it must not only provide details of important geographical features, but should also include a basic understanding of the wind erosion processes in operation within the region. The purpose of this chapter is therefore to describe the field site and the environmental factors in sufficient detail that the reader is able to build their own mental picture of the study site. It is not designed as a detailed review of all the environmental factors that influence wind erosion.

2.2 Field site

The Lake Eyre Basin (Fig. 2.1) covers a large part of inland Australia. This basin contains several of Australia's largest inland rivers, such as the Thompson, Cooper, Diamantina, and Georgina, all of which drain into Lake Eyre. During the summer wet season in northern Australia these rivers inundate their large floodplains. However, during the rest of the year large sections of these river channels are dry and their floodplains dry out and become active wind erosion sites (Fig. 2.2).

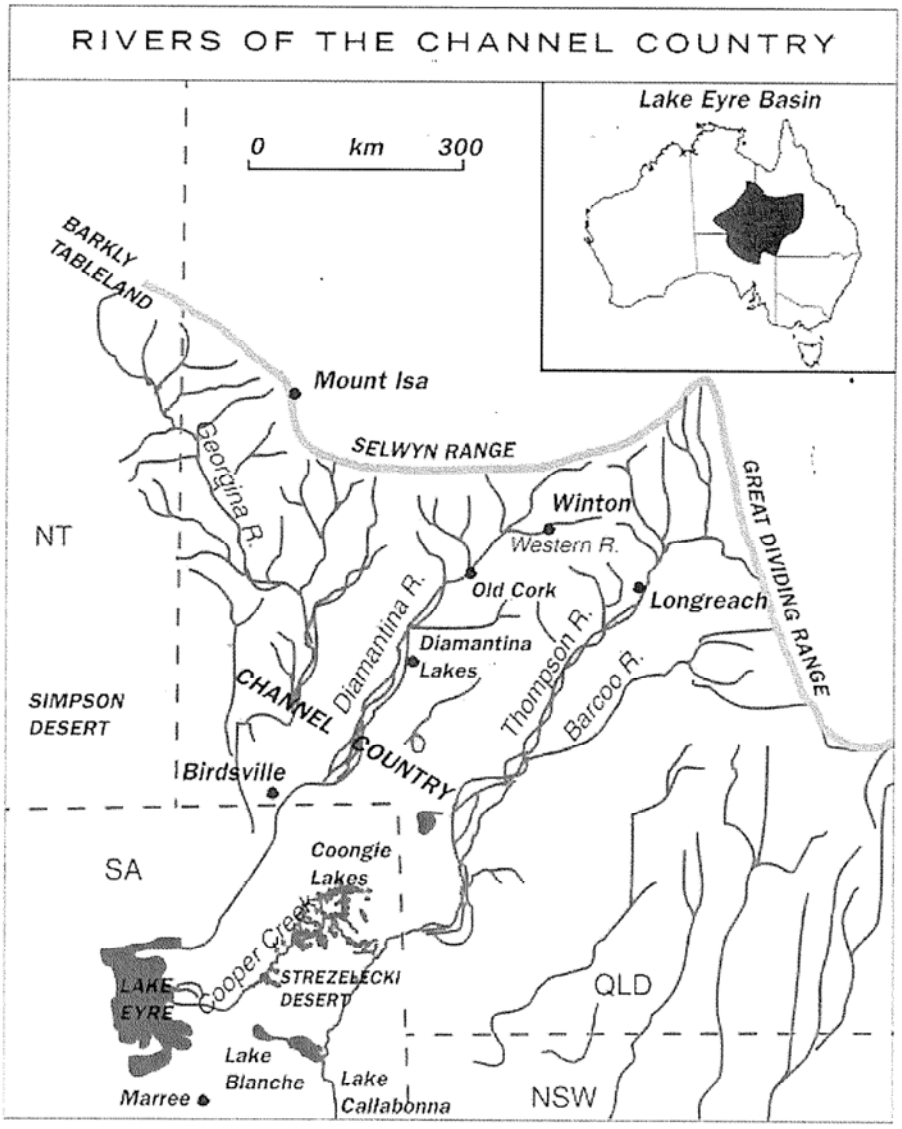

Figure 2.1: Map of the Lake Eyre Basin, indicating the location of Lake Eyre, the Thompson, Cooper, Diamantina, and Georgina rivers.

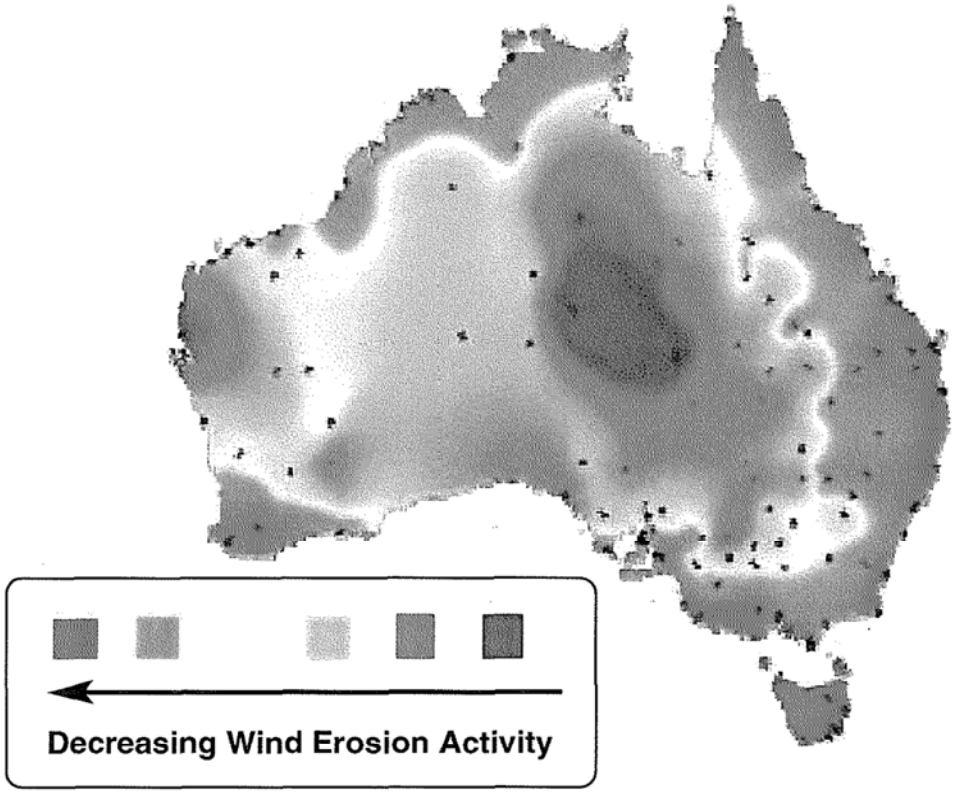

Figure 2.2: Active dust source regions calculated using recorded meteorological data from 1960-1999 (McTainsh, 2002, pers. comm.). The red–brown section in the middle of Australia with high wind erosion activity covers most of the Lake Eyre Basin.

Contained within the Lake Eyre Basin is the Channel Country of western Queensland. This region consists of large floodplains, saline and wind eroded claypans, and source bordering sand dunes. Following flooding or local rainfall, sections of these floodplains may be covered by Mitchell grass and other native grasses, which make them ideal for grazing purposes. As a consequence the area also contains some of Australia's largest cattle stations and makes a significant contribution to Australia's beef exports. During the dry season much of the vegetation on the floodplains dries off or is removed via grazing, leaving claypans which become major areas of wind erosion activity (McTainsh et al., 1998).

Diamantina National Park is located in the centre of the Channel Country.

This National Park contains several land types, within a relatively small area (Fig. 2.3), which are typical of very large areas of the Australian arid zone (McTainsh et al., 1999). These rangelands have sparse grass and shrub cover and any surface cover is strongly affected by rainfall and grazing. The field sites used in this study are located within this National Park and have been a focus of research activity since 1994. The experimental data thus collected forms one of the best records of wind erosion activity available in Australia.

The land types within the Diamantina National Park study site are categorised as Dunes, Downs, Main Channel Floodplain and High Floodplain. These land types are based upon the land systems defined by Wilson et al. (1990) (Table 2.1). The Dunes are relics of former arid conditions (Nanson et al., 1988) and are covered with shrubs and other standing vegetation. In contrast the Downs are normally covered with Mitchell and other native grasses, which grow to a height of 20-30cm. These grasses, also grow on the edge of the channels which characterise the Main Channel Floodplain. In addition, River red gums and other trees, grow along the banks of the larger channels to a height of 10–20m.

Table 2.1: Land type categories used within the field site in terms of the original Wilson et al. (1990) classifications.

Land types used in this Study	Land systems defined by Wilson et al. (1990)
Dunes	Simpson
Downs	Winton/Kallala
Main Channel Floodplain	Cooper
High Floodplain	Woonabootra, Dingara, Cunnawilla

The High Floodplain soils range from grey cracking clays, which are relatively stable and well vegetated, to sandy loams which have been degraded as a result of salinity and wind erosion. Consequently claypans occupy a large proportion of the High Floodplains. On such degraded claypans the topsoil is

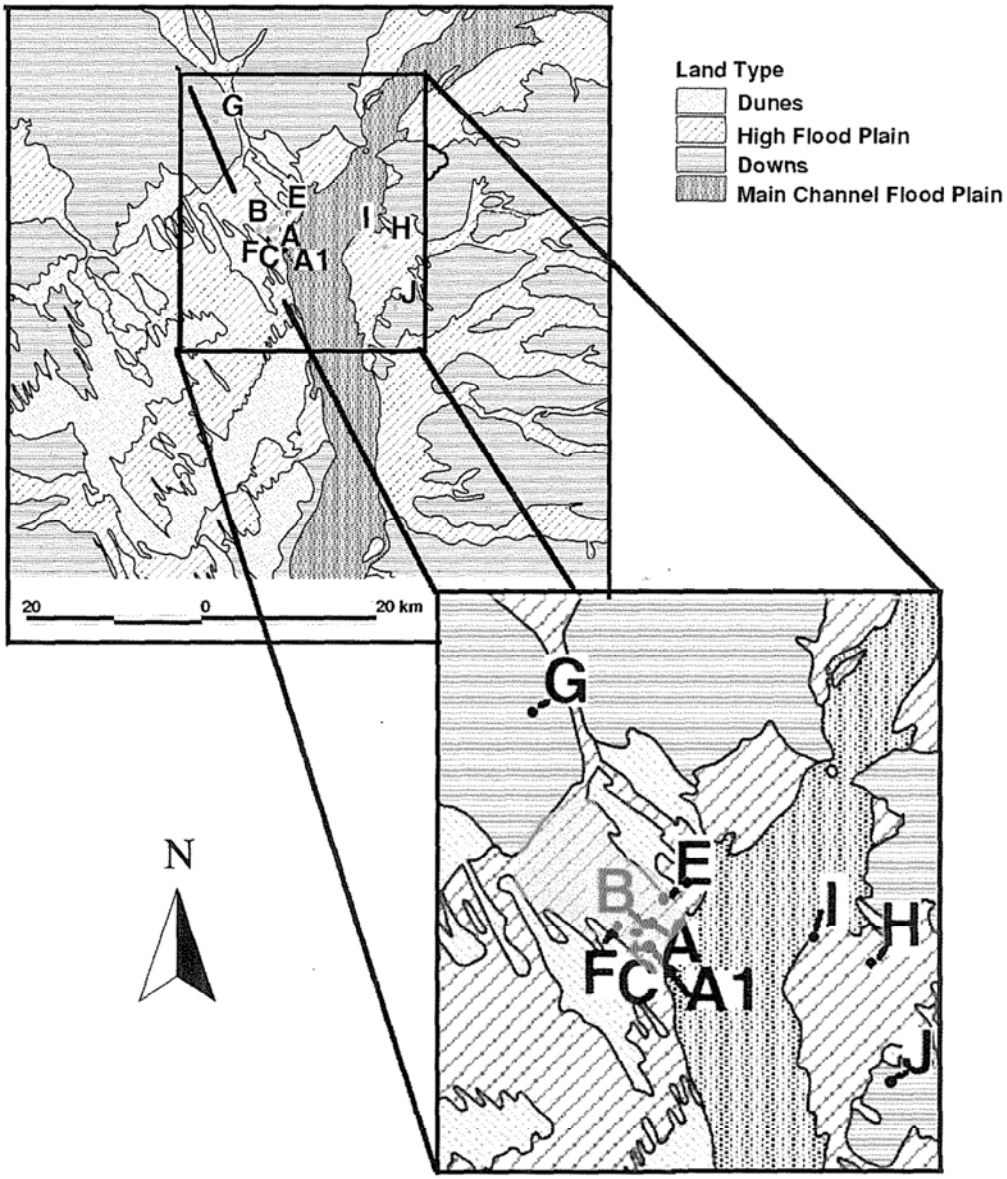

Figure 2.3: Land type map of the Diamantina National Park study site. Labels *A* to *I* indicate sites within the National Park where dust monitoring equipment has been set up. Insert 1 shows the location of the monitoring sites in more detail. The pink shaded area in the insert, shows the location of the Lake Constance claypan.

variably sealed by physical and biological crusts (Strong, 2001, pers. comm.) and in most years little vegetation is present. Any such vegetation is normally isolated to areas where the saline claypans have been flooded or to small drainage channels within these claypans. Other regions of these claypans are covered by gibber (0.5-5cm ironstone gravels) which form a stony surface over the topsoil or have a range of surface conditions as shown in Figure 2.4.

The High Floodplains in the northern part of the Channel Country are adjacent to the main river channels. In the lower reaches of the Cooper, Diamantina and Georgina Rivers, the High Floodplain occupies the whole river channel. Thus, the High Floodplains occupy approximately 8% of the Channel Country. The Dunes are located on the western side of the Main Channel Floodplain and cover about 10% of the Channel Country. The Downs occupy the interfluve areas between the main rivers and cover about 26% of the region. Together the High Floodplains, Dunes and Downs cover approximately 44% of the Channel Country.

The Lake Constance claypan (Fig. 2.3), which forms the basis of this study, is a typical example of the claypans associated with the High Floodplains. As shown in Figure 2.4 it has a wide range of surface conditions within a relatively small area, which makes it ideal for this study. Such changes in surface conditions within the Lake Constance claypan suggest several things about how this study site differs from the cultivated land that has been the primary focus of wind erosion research in Australia, since the early 1980's. The first noticeable difference is that unlike cultivated fields where there are distinct changes in the surface conditions at the boundaries, the changes in surface conditions within the claypan are much more gradual. Thus it is much more difficult on the claypan to isolate regions that are subject to wind erosion. As a result it is much more difficult in the Channel Country to understand how soil and environmental processes influence wind erosion.

The other noticeable difference is that there is much more spatial variability in surface conditions within the claypan, than one would observe in a cultivated field. Such a difference should mean that any dust measurements

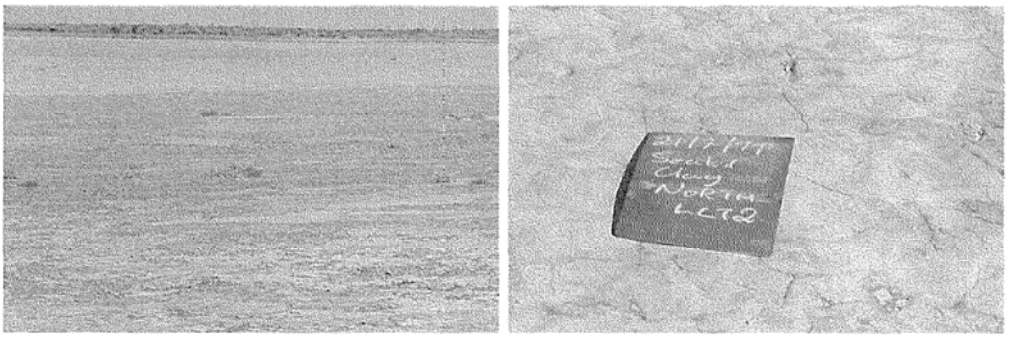

(a) Clay curled surface

(b) Sealed clay surface

(c) Silt and fine sandy deposit on surface

(d) Rippled surface

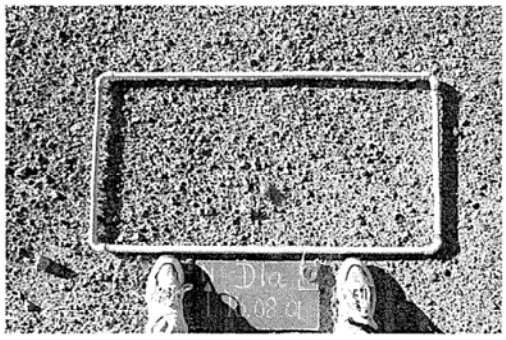

(e) Gibber surface

Figure 2.4: A selection of different surface conditions observed on the Lake Constance claypan.

made on the claypan will have a strong spatial component to them. That is, any measured dust concentration profile, should to some extent reflect the surface conditions that the wind has blown over prior to reaching a sampling location. As a result there should be significant differences in observed dust measurements at sites A to J (Fig. 2.3) for any given dust event. Such measurement differences have been observed by Love (2001) in his study of wind erosion rates at these sites and by McTainsh et al. (1999) in their study of the erodibility of various land types within the Channel Country. These studies however, did not consider the effect that such spatial variations in erodibility would have on the resulting dust plumes. The approach taken in this study is designed to consider this spatial issue in much greater detail, and therefore provide some insights into how this spatial variability affects the distribution of dust within the resulting dust plumes at the local scale.

The surface conditions of these claypans also vary through time. A good example of this is how the surface conditions vary on the Lake Constance claypan as a result of flooding which occurs on a fairly regular basis. Such flooding results in large sections of the claypan being covered in water. As the flood water recedes large amounts of fine sands are deposited on the surface of the claypan. The sun then quickly dries the surface of the claypan. This drying is not uniform with the small depressions and drainage channels drying much slower than the remainder of the claypan. The presence of such processes suggest that the surface conditions within the claypan not only vary spatially but also vary through time.

2.3 Factors affecting wind erosivity and soil erodibility in the Channel Country

Over the past two decades, much has been reported in the literature about how certain environmental processes influence wind erosion. This section is not designed to present a comprehensive review of this literature, but rather

an overview of the factors that are more likely to be relevant to the Channel Country. In particular, this section focuses on what factors are likely to influence wind flow and hence wind erosivity within the study site. It also looks in detail at the various soil and surface characteristics that are likely to influence wind erodibility within the study site.

2.3.1 Wind erosivity

Erosivity is the capacity of the wind to entrain soil particles from the surface. Since Bagnold (1941) first published his classic text on wind erosion, significant progress has been made in understanding which characteristics of the wind influence wind erosivity. This progress has largely been due to the use of portable or indoor wind tunnels in many experiments on erosivity. The following sections examine the implications and assumptions of such experiments in terms of the field site. It also provides information about the characteristics of the wind within the study site that will be important in understanding results presented in later chapters.

2.3.1.1 Wind

As the wind moves across the surface there is a very thin layer of air near the ground where the wind velocity is zero (Fig. 2.5). The wind velocity at the roughness interface is termed the friction velocity of the wind ($u_\star$) and the height of the layer, the roughness height (z_0). The erosivity of the wind is related to the shear at this interface, and hence to the friction velocity $u_\star$.

Bagnold (1941) noted that particle movement does not start until a given threshold value of $u_\star$ is reached and that this velocity is dependent on whether initiating grains were present or not. These threshold velocities, Bagnold (1941) defined as the *impact threshold* ($u_{\star i}$) and the *fluid threshold* ($u_{\star f}$). The impact threshold is the value of $u_\star$ where movement of particles is initiated by saltation bombardment, while the fluid threshold, is the value of $u_\star$ for

which particles begin to move along the surface in a dust cloud without an initial impact being supplied. Under field conditions it is much more difficult to identify the point that grain movement is initiated, therefore identification of these thresholds is much harder. Nickling (1988) suggested that a better definition of threshold velocity would be to define u_{*t} as the value of u_* at which the whole bed starts to move. This definition is used here to denote field threshold values. Figure 2.6 shows that the value of u_{*t} for which entrainment is initiated is also dependent on the particle size of the soil and the type of soil. This implies that the erosivity of the wind is dependent on wind speed and the surface over which the air is flowing.

One major problem with monitoring and modelling wind erosion within the study site is the variability in wind speed during individual events. This variability is illustrated by the wind speeds recorded at site A during a single wind erosion event on 20 August 1995. During this event, which lasted four and half hours, the wind speed at 2m varied between 8.5 and 11.4ms^{-1} with an average speed on 10ms^{-1}. While at 10m the wind speed varied between 9

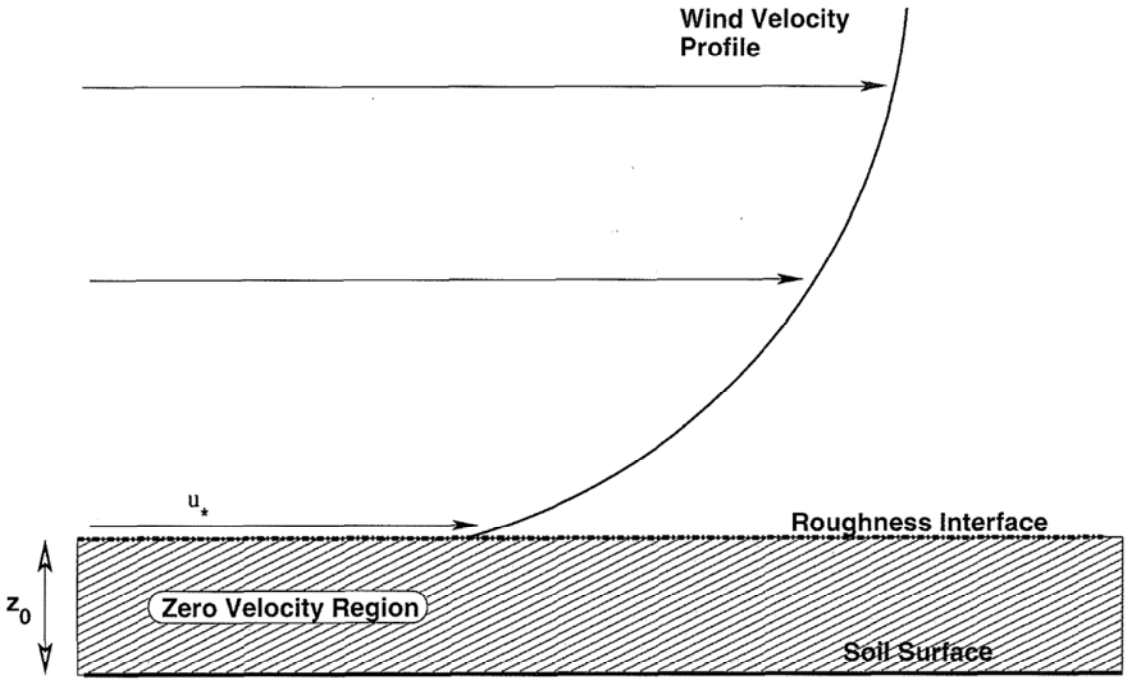

Figure 2.5: A schematic illustration of the concept of wind friction velocity (u_*) and roughness height (z_0). (Diagram not to scale).

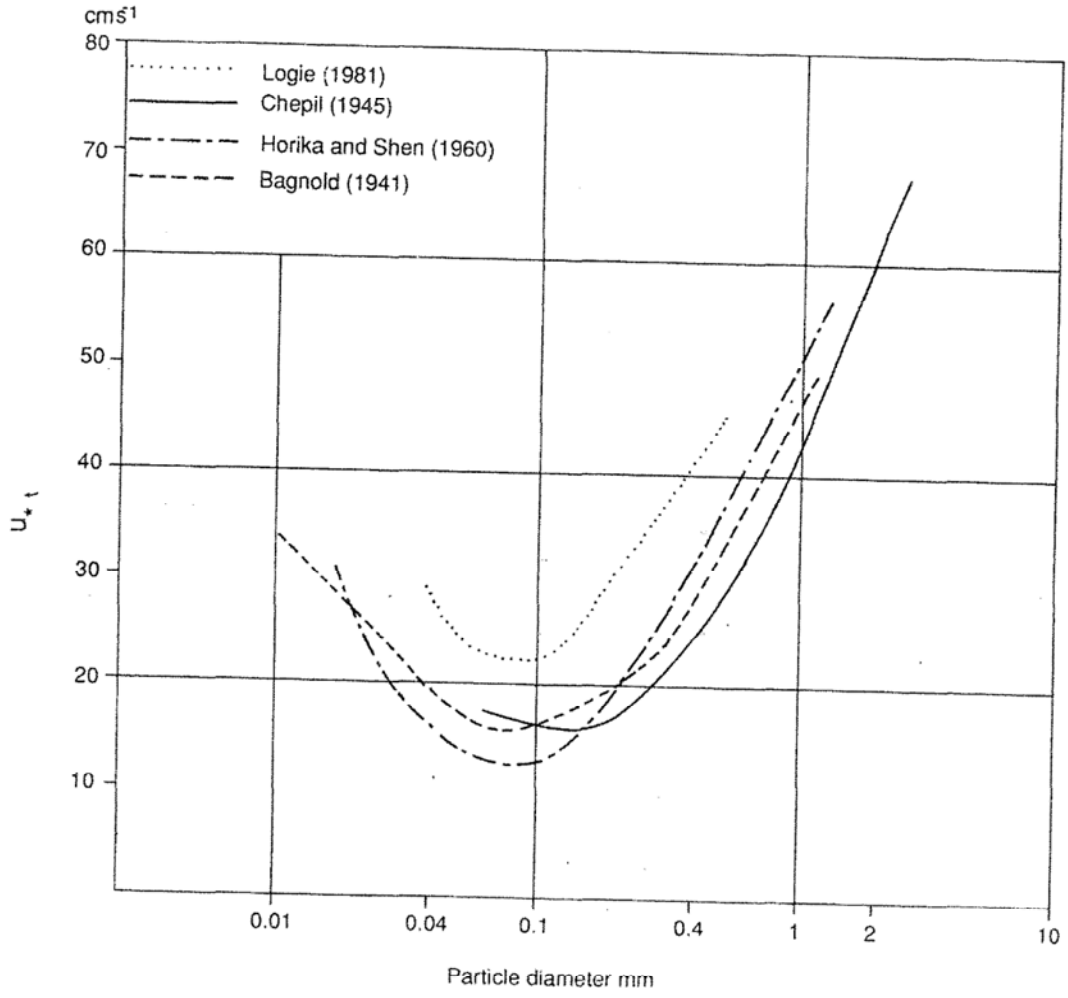

Figure 2.6: Influence of particle diameter on threshold velocity (u_{*t}) as obtained by the studies of Bagnold (1941), Logie (1981), Horikawa and Shen (1960) and Chepil (1945). Source: Cooke et al. (1993).

and 12ms^{-1} with an average speed of 10.7ms^{-1}. Thus, depending on the wind speed threshold (u_{*t}) of the surface, that surface could be active only for brief periods within an event. The wind speed threshold (u_{*t}) also varies spatially within the study site. Thus, different regions of the study site, are active at different times throughout the wind erosion season. These active regions will be referred to in future as dust source areas.

Most wind erosion studies, since Bagnold (1941), have assumed that wind

velocity increases with height, and can be described by the following equation:

$$u = \frac{u_\star}{\mathcal{K}} \ln\left(\frac{z}{z_0}\right) \tag{2.1}$$

where $\mathcal{K}$ is von Kármán's constant, $u_\star$ is the friction velocity at the roughness interface, z_0 is the roughness height and u is the wind speed at height z provided $z > z_0$. This equation assumes that wind velocity increases logarithmically with height (z). However, a number of wind velocity profiles have been measured within the study site that do not fit this logarithmic structure (McTainsh, 2002, pers. comm.). This departure from a logarithmic structure, most likely occurs as a result of either surface heating or topographic effects (Cooke et al., 1993) on the wind flow (these are discussed further in Section 2.3.1.2). Such a change in wind velocity profile should be reflected in how the sediment is dispersed within the resulting dust plume. This possibility is examined in further detail in Chapter 7.

Another problem in measuring and modelling wind erosion is the variability in wind direction, unlike water erosion where the flow is often contained in channels or within clear flow boundaries, the wind within the claypan can come from any direction. Thus, particles can arrive at a sampling location from any point within the site. Therefore, during a single dust event, it is possible for several different source areas to be active, simply depending on the wind direction at the time.

In any open field experiments these changes in wind speed and direction are hard to account for, as little is known about how spatial changes in erodibility affect the resulting dust concentration profiles. Portable wind tunnels, which have been used in several Australian studies (e.g Leys (1998), Raupach et al. (1993)), overcome this problem by providing a controlled wind source, therefore keeping wind speed and dust source area constant. Variability in wind speed, direction, and the susceptibility of the surface to erosion by the wind, can however, play an important role in determining the make up of the resulting dust plume.

2.3.1.2 Topographic and heating affects

The threshold wind velocity (u_{*t}) is the main limiting factor in determining if wind erosion takes place. Therefore, any changes in the wind flow that affect the value of u_{*t} will influence the erodibility of the surface. In this section, two environmental factors which may affect the value of u_{*t}; namely topography and heating are discussed.

A number of studies (e.g Baines (1995) and Dyke (1982)), have shown that obstacles placed in a fluid flow, alter the streamlines of the flow (Fig. 2.7). Studies of wind flow over dunes, have shown that similar changes occur in the wind velocity profile (Walmsley et al., 1982). These studies have also shown that the changes in wind flow depend on the height of the obstacle, the speed of the fluid flow, and the viscosity of the fluid.

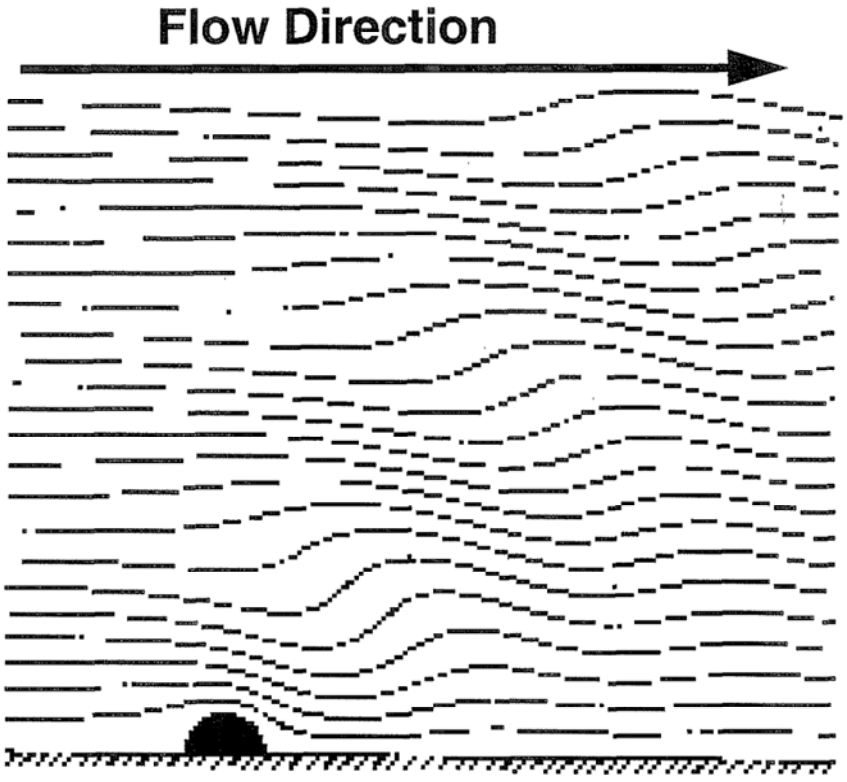

Figure 2.7: The theoretical effect of a 2-Dimensional obstacle on wind flow streamlines. Based on the model results of Baines (1995). Note: The compression and expansion of the streamlines.

Such changes in the streamlines of the flow, appear as alterations in the velocity profile of the wind, similar to those observed within the study site. These changes also suggest that since entrained dust particles tend to move in these streamlines, the dust concentration will increase in regions where the streamlines converge and decrease where the streamlines diverge. Such areas of convergence and divergence might therefore be reflected in the vertical dust concentration profile.

The alterations in the flow streamlines also indicate that the friction velocity (u_*) at the roughness interface, will vary as a result of changes in the topography of the surface. Thus, the amount of dust entrained will either increase or decrease depending on the actual change in u_* at the roughness interface. Such variations in erosion have been observed by Hardisty and Whitehouse (1988), in their experimental study of the effect changes in surface slope has on wind erosion rates and by Goossens (2000) in his study of the effect that topography had on sand movement within the desert landscape.

Other studies, such as the one by Frank and Kocurek (1994), have shown that variations in the thermal stability of the atmosphere have a strong influence upon wind velocity profiles measured in the field. In addition, urban air pollution studies, such as Yoshida (1991) have shown that surface heating, has a major influence on air pollution levels in the urban environment. Since the surface characteristics of the study site vary from vegetated to gibber to bare, the thermal properties of the surface will also vary. These changes will affect the wind velocity profile, and therefore have an influence on the wind erosion rates and the dust concentration profiles within the site.

2.3.2 Vegetation and erodibility

Erodibility is defined as the susceptibility of the soil surface to erosion by wind. Experimental studies carried out over the last 50 years with the aid of wind tunnels and under field conditions, especially by Bagnold (1941), Chepil and Woodruff (1963), Gillette et al. (1980, 1982), and Nickling and Gillies

(1993); Nickling et al. (1999) in the United States, Great Britain, Australia and Africa, have identified many of the factors/processes that affect the erodibility of the surface. In this section, several of these factors/processes, are discussed in terms of their likely applicability to the Channel Country and the Diamantina National Park field site. Such a discussion is designed to provide the reader with a mental picture of the processes which may be in operation within the Channel Country, thus enabling a link to be made between these processes and the modelling results presented in later chapters.

2.3.2.1 Vegetation and roughness

Vegetation has long been acknowledged as having a major influence on wind erosion (Marshall, 1970, 1972). Vegetation achieves this by altering the roughness height of the surface (z_0) (Chepil and Woodruff, 1963), as illustrated in Figure 2.8. This figure also shows that the presence of a vegetation canopy not only increases the roughness height (z_0) of the surface, but also alters the wind velocity profile. The resulting change in the wind velocity profile can be related to the friction velocity ($u_\star$) and the roughness height (z_0) by Equation (2.1).

If however, the vegetation is not sparse as shown in Figure 2.8, but is tighly packed together, than the top of the vegetation elements appear to the flow to be like a solid surface. A good example of this is the canopy top of a dense forest. The height above the ground of this new pseudo-surface is called the zero plane displacement height (d). In such situations, Equation (2.1) becomes:

$$u = \frac{u_\star}{\mathcal{K}} \ln\left(\frac{z-d}{z_0}\right) \tag{2.2}$$

where $\mathcal{K}$ is von Kármán's constant, $u_\star$ is the friction velocity at the roughness interface, d is the zero plane displacement height, z_0 is the roughness height and u is the wind speed. Within the study site and the Channel Country, vegetation elements are not densely packed together, hence for most surfaces within the study site the displacement height (d) can be assumed to be zero.

Early work in Australia by Wasson and Nanninga (1986) suggested that the

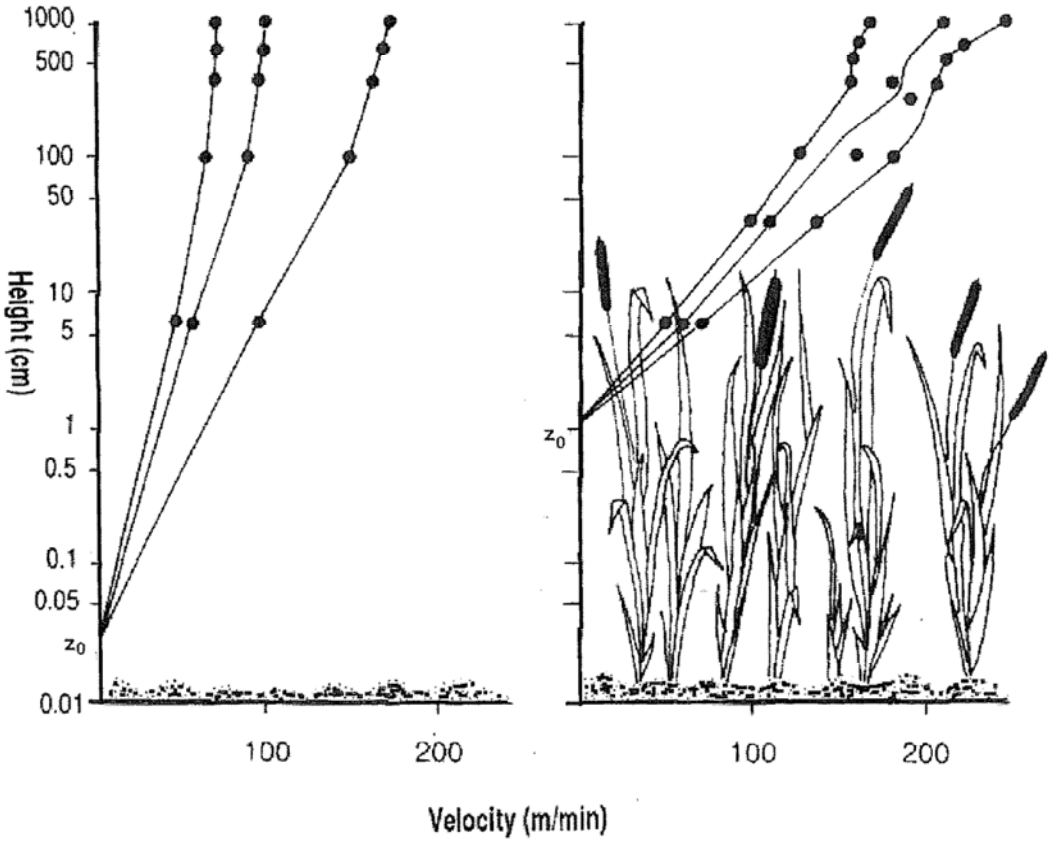

Figure 2.8: Wind velocity profile and roughness height in the absence/presence of vegetation. Note the increase in z_0 and dramatic alteration in the wind velocity profile in the presence of vegetation. Source: Chepil and Woodruff (1963).

density of the ground cover is a limiting factor upon wind erosion. This has been verified by a number of other studies, including Findlater et al. (1990) and Leys (1991b). Figure 2.9 illustrates two important points about how the percentage of ground cover effects sediment discharge rates. Firstly, as vegetation cover decreases below approximately 45%, the sediment discharge rate increases. Secondly, it suggests that as the erosivity of the wind increases, the sediment discharge rate increases.

Lyles (1977) showed that other features, such as rocks, have a similar effect to vegetation. The spacing of these features and the size of the frontal area presented to the wind, play an important role in determining the effective

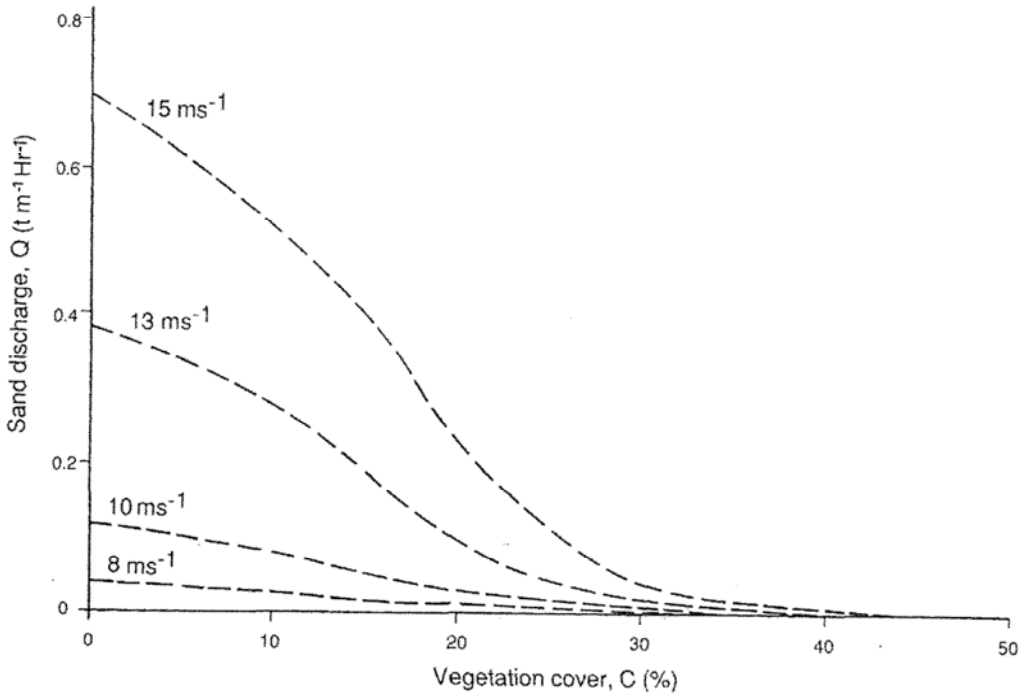

Figure 2.9: Influence of vegetation cover on sediment discharge rates for wind speeds of 8, 10, 13 and 15 ms^{-1}. Source: Wasson and Nanninga (1986).

roughness height (z_0). Other studies, such as Carter (1976); Gillette (1977), have suggested that sediment can become trapped behind features such as rocks and vegetation, as a result of several natural processes. On the claypan, flood deposition and aeolian deposition processes are in operation. The net result of this trapping is to alter the roughness height z_0 of the surface, thus altering the exposure of the deposited material to wind erosion. As this material is removed from between these features, z_0 increases as shown in Figure 2.10, and the rate of removal decreases (Carter, 1976; Gillette, 1977).

This trapping is likely to be particularly important; in areas of the claypan that are covered by gibber. During flooding and aeolian events, fine sand and silt are deposited between the gibber. Thus, these areas are likely to act as dust sources, during some wind erosion events and dust sinks in others. The above observations also suggest that if the amount of fine particles and sediment deposited, vary spatially within the gibber, the erodibility of the

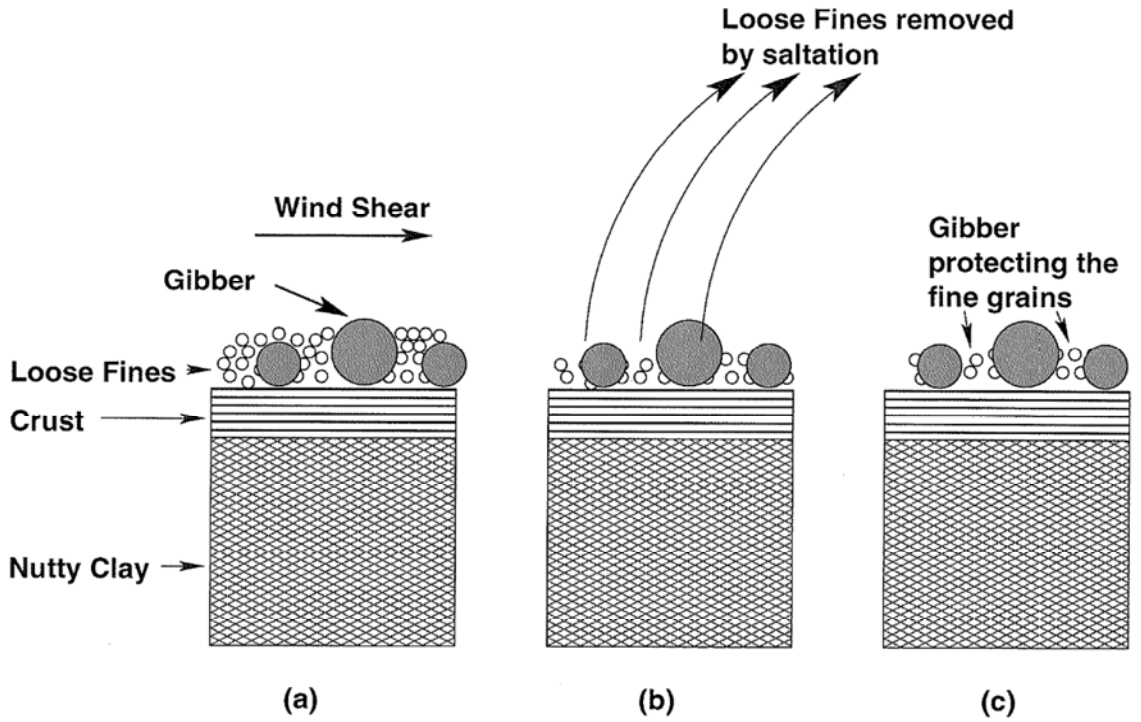

Figure 2.10: Schematic showing how large ironstone rocks (gibber) protect the fine silt and sand particles trapped between them from erosion. In (a) a large amount of fines are trapped between the large ironstone rocks. As the wind is applied across them some of the exposed fines are removed (b). After the wind ceases remaining fines are still trapped between the large ironstone rocks (c).

surface will also vary spatially across the gibber surface.

Another study by Gillette et al. (1982), which examined the relationship between threshold friction velocity (u_{*t}), and roughness height (z_0), suggests that roughness height (z_0) will vary between the surface conditions shown in Figure 2.4. This change in roughness height across the claypan suggests that the threshold friction velocity (u_{*t}) and erodibility will also vary across the claypan. Such changes in erodibility across the claypan indicate that the location and strength of these dust source areas, relative to each other, are likely to be important factors in determining not only how a dust plume evolves as it crosses the claypan, but also how wind erosion ultimately affects the claypan.

2.3.2.2 Crusts

Even without roughness and vegetation, certain other physical controls exist within the claypan that limit wind erosion. One such control is the formation of soil crusts. Formation of such crusts is quite common in the soils in arid inland Australia (McTainsh and Leys, 1993). This crusting occurs as a result of physical, chemical and/or biological processes (Leys, 1998; Strong, 2001, pers. comm.). Research by Gillette et al. (1980, 1982) suggests that there is a relationship between the strength of such crusts and the erodibility of the soil. In this research, they found that the stronger the crusts the higher the threshold friction velocity (u_{*t}) needed to initiate particle entrainment into the wind flow. Once this crust is broken, studies by Gillette et al. (1982) and Leys (1998) suggest that there is a significant reduction in the threshold friction velocity needed for particle entrainment to begin.

The above observations, when applied to the study site, suggest that areas where the crust has been disturbed, as a result of human or animal activity, will have significantly lower threshold velocity (u_{*t}) than the surrounding area. This suggests that wind erodibility will vary significantly in the neighbourhood of these disturbances.

As illustrated in Figure 2.4c, certain areas of the claypan are covered with fine sand and other sediment. In these areas the crust plays a very different role. The fine sediment sitting on the surface is easily removed by the wind, thus exposing the hard surface crust of the claypan (Fig. 2.11). While the fine sediment is still present on the surface, the threshold wind velocity (u_{*t}) will be lower than when the hard crust is exposed. Thus, areas of the claypan where fine sand and sediment still remain on the surface, will be more significant dust sources, than areas of the claypan where the hard surface crust has been exposed.

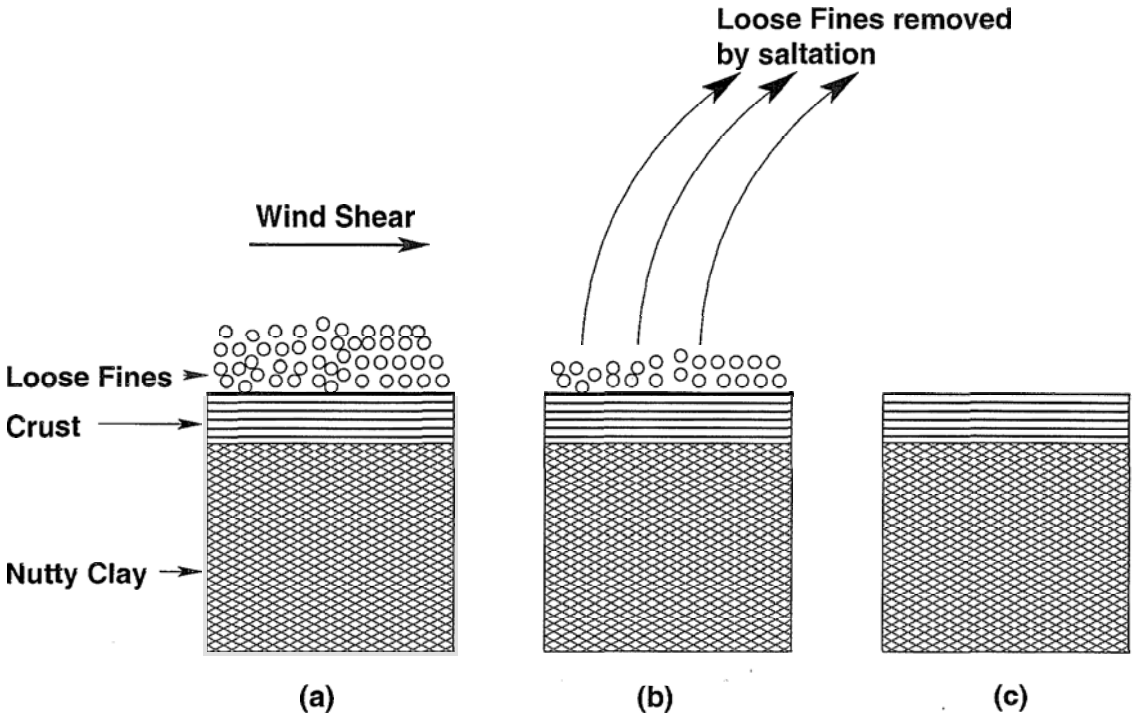

Figure 2.11: Schematic showing the typical soil structure of the areas of the claypan covered with fine sand and sediment. It also illustrates what happens to the soil structure once the fine sediment is removed by the wind. Fine sediment initially covers much of the crust present on the claypan (a), as wind shear increases much of these fines are removed (b), leaving only the exposed crust of the claypan (c).

2.3.2.3 Rainfall

Both vegetation and crust levels are sensitive to rainfall totals and rates. Dust storm occurrence is inversely proportional to average annual rainfall (McTainsh, 1989). The study of McTainsh (1989) on a continental scale showed there is a significant increase in dust storm occurrence once the average annual rainfall falls below 600mm (Fig. 2.12). This observation about average annual rainfall suggests that the Channel Country would be a significant dust source, as the long term average annual rainfall is 259mm (McTainsh et al., 1998). A more detailed examination of influence of rainfall within the Channel Country shows that some vegetation and crusts can respond quickly to even small amounts of rainfall. This response to rainfall, suggests that wind

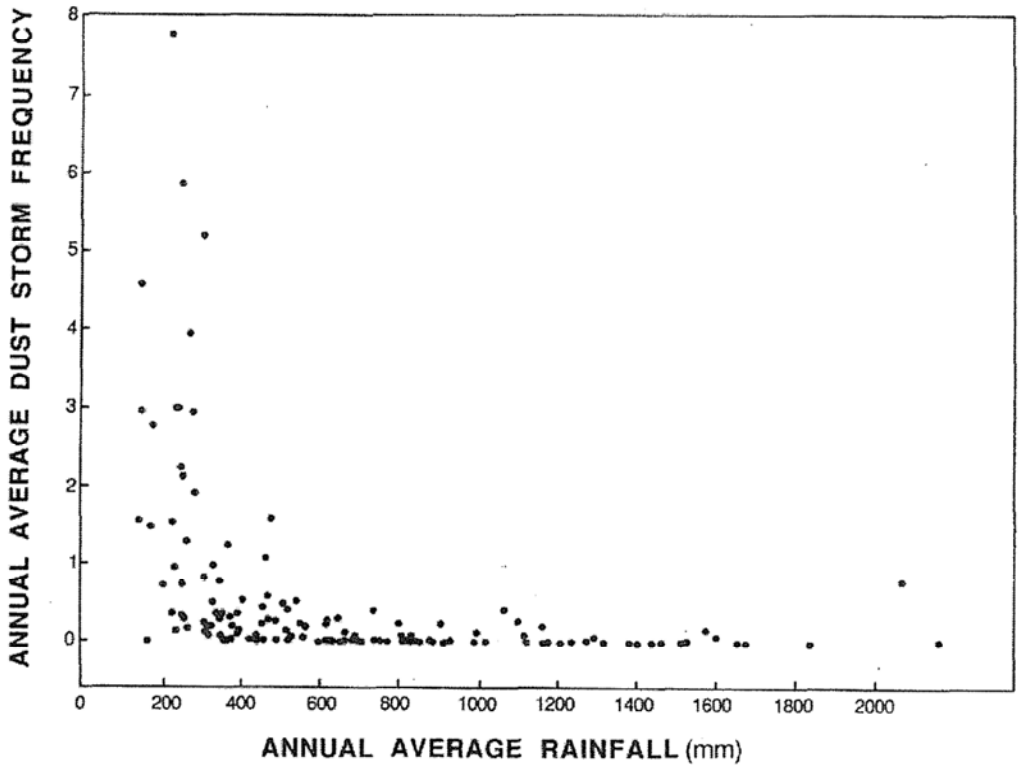

Figure 2.12: Average annual rainfall and its relationship to dust storm frequency within Australia. Source: McTainsh (1989).

erodibility will change spatially and temporally within the study site as a result of rainfall, in a complex manner. The extent of the effect upon wind erosion will depend upon among other things: the amount and intensity of rain that the surface is exposed to, and the type of vegetation/crusts present. Such a response to rainfall means that the vegetation and crusts present after a rainfall event are likely to be significantly different to those observed prior to the event. This implies that the spatial distribution of dust source areas following a rainfall event could be significantly different to that observed prior to the rainfall event.

The cohesive forces that exist between soil particles, also act as an important limiting factor on wind erosion, in the absence of vegetation. This bonding is enhanced by the amount of soil moisture present (Sherman, 1990; Cooke et al., 1993). Therefore, as soils dry out, the amount of erosion activity can

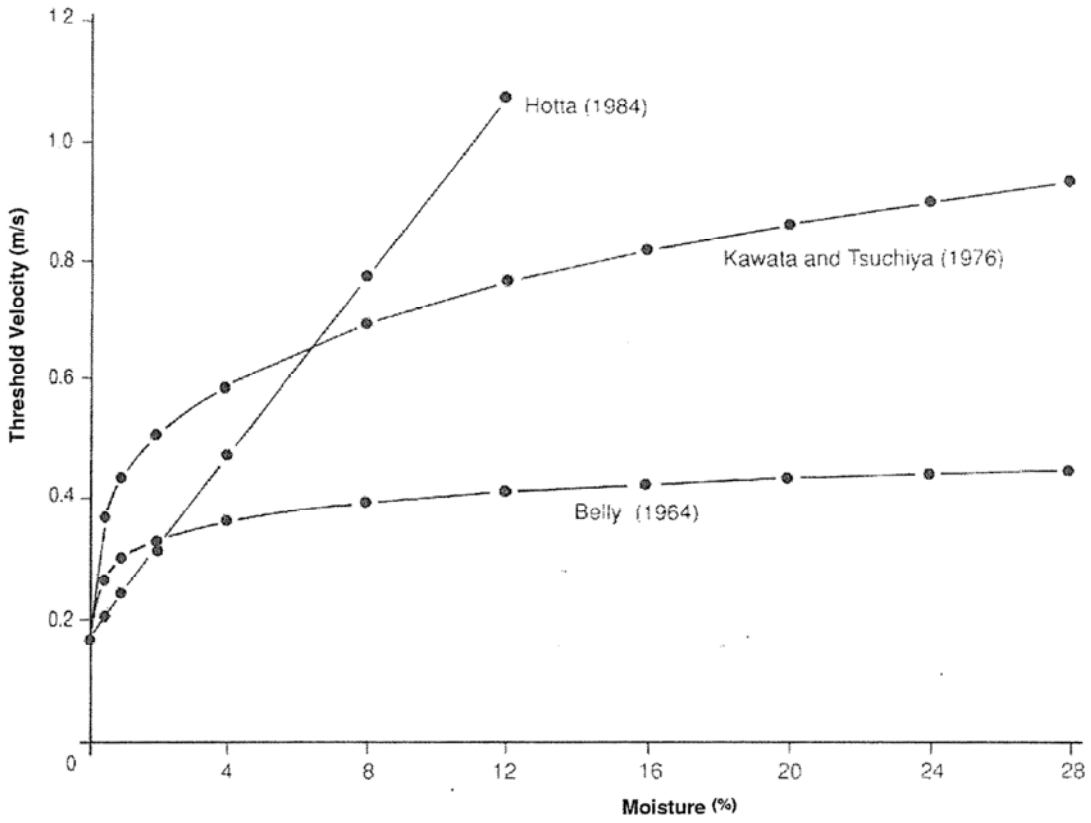

Figure 2.13: The variation in threshold velocities (u_{*t}) with soil moisture for three independent studies. Source: Sherman (1990).

increase. However, as Figure 2.13 shows there is no simple relationship between soil moisture and threshold velocity. But in all cases, the threshold velocity deceases as soil moisture decreases.

The drying process has major implications for the erodibility of the claypan used in this study. As mentioned in Section 2.2, the claypan is subjected to flooding. The result of this flooding has been to produce micro-channels and shallow depressions within the claypan that act as a natural water sink. These areas take a significantly longer time to dry out than the surrounding area, and thus retain a higher soil moisture content. Therefore, the erodibility of these areas will be substantially less than that of the drier surrounding areas. Thus the erodibility of the claypan will vary spatially, depending on the location of the micro-channels, and temporally as the drying process proceeds.

2.3.2.4 Saltation

One reason for the reduction in wind threshold velocity (u_{*t}) once the surface crust is disturbed is the effect that impacting soil particles have on the surface. To understand this effect, the role of saltation in the wind erosion process must be understood.

Bagnold (1941), originally classified saltation as the mode in which soil particles removed from the surface and travel only a short distance before impacting back on the surface. Anderson and Haff (1988) subdivided the saltation into two separate components based on energy, which they termed *reptation* and *saltation*. In their definition, saltation was defined as the high energy grains that made up Bagnold's 1941 original saltation mode, while reptation was used to refer to low energy grains present in Bagnold's 1941 original definition.

One implication of this energy breakup, is that when saltation particles impact back on the surface, a certain amount of energy will be transferred to the surface. If there is sufficient energy transferred to the surface to entrain two particles and this process gets repeated as the particles move downwind, the size of the dust plume will increase exponentially. Such a process forms the basis of the avalanche effect that was first noted by Bagnold (1941).

This also explains why disturbing the soil surface, reduces the wind speed threshold (u_{*t}) required for entrainment. The disturbance of the soil crust reduces the strength of the surface in the region of the disturbance, thus enabling the wind to erode particles from the surface. When these particles impact upon the surface they impart a significant amount of energy to the surface, thus reducing the amount of wind energy required for the removal of soil particles from the undisturbed surface.

As the saltation mode develops, the particles absorb energy from the wind. This absorption of energy by the particles results in a modification of the wind velocity profile, as shown in Figure 2.14. Such a modification in the wind velocity profile was first noted by Bagnold (1941). Since then these observations

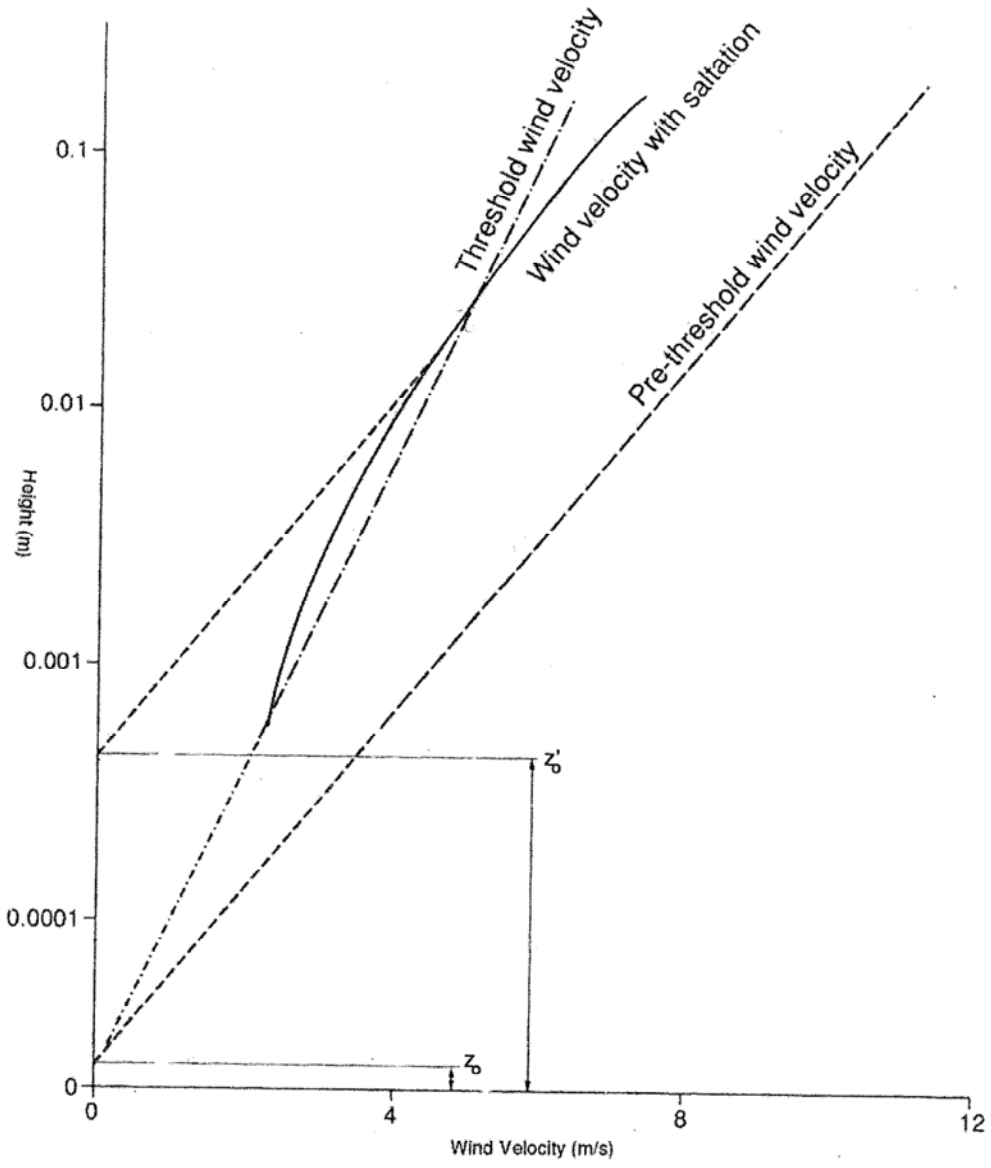

Figure 2.14: Wind velocity profiles: Pre-threshold (long dashed line), threshold (dash dotted line) and post threshold with saltation (solid). Also indicated is the original roughness height (z_0) and the roughness height as modified by the presence of saltation (z_0'). Source: Anderson and Haff (1988).

have been confirmed by Anderson and Haff (1988) and McEwan (1993). Other work by Owen (1964) has suggested that this modification can be thought of as an effective increase in roughness height. This increase in roughness height

is illustrated in Figure 2.14 by the extrapolation of the saltation wind velocity profile (the dashed line) to the point where it intersects the height axis (z_0'). Owen (1964) further found that this height was a function of the friction velocity of the wind ($u_\star$) and could be predicted by the following formula:

$$z_0' \approx \frac{C u_\star^2}{2g} \tag{2.3}$$

where g is the acceleration due to gravity and C is a constant, which Owen (1964) found to have the value 0.02. Such a modification of the wind profile, also suggests the presence of a feedback mechanism, which acts to limit the wind's capacity to move particles within the flow. This feedback mechanism along with the avalanche effect, has been referred to by Gillette (1999), as the "Owen effect".

At the field site, this suggests that emission rates of various dust source areas will alter depending on sediment loads. Thus, the spatial distribution and strength of these dust source areas is likely to be a distinct characteristic of each event.

2.3.2.5 Particle size

Spatial variations in the particle size of the claypan soils play an important role in determining the particle size distribution of the sediments in the resulting dust plume. The actual process by which this occurs is complex, and involves both entrainment and transportation processes.

Figure 2.6 shows that the wind speed threshold is dependent on particle size. It also shows the existence of a critical value of particle size, which minimises the threshold wind velocity for the surface. Therefore, if a soil consists of a mixture of particle sizes, particles of various sizes are likely to be emitted at different rates from the surface.

These particle size emission rates will also be dependent on how the particles of various sizes are arranged within the soil. For example, if the larger particles lay close to, or on the surface, then they will tend to increase the

roughness height (z_0), thus protecting the surface in a similar manner to that described in Section 2.3.2.1.

These particle size emission rates are also dependent on the size and number of particles that impact back on the surface. It is these particle size properties that ultimately determine how the momentum of the impacting particles is transferred to the surface, and therefore the final emission characteristics of the surface.

As dust plumes travel downwind, gravity acts on the particles within the plume. As a result, the dust plume will become finer the further it travels downwind. It also implies that the smaller particles will travel further from the source than the larger ones (Tsoar and Pye, 1987; Raupach et al., 1993).

In terms of the study site, this means that the final particle emission rates will be determined by: the particle size distribution of the surface, how the particles of different sizes are distributed within the soil, the number and size of particles that impact on the surface, the previous erosion-deposition history of the surface, and finally the value of friction velocity (u_*) (Gillette, 1979). These factors, along with distance the plume has travelled from the source, determine the final particle size distribution of the dust plume.

2.3.2.6 Particle shape

Since the arrangement of particles within the soil is to a certain extent, dependent on the shape of the particles, shape must therefore influence the particle size emission rates. For example, close fitting irregular grains have more contact points and take substantially more energy to entrain than other grains. Grain shape will also affect the deposition velocity of particles by altering their drag coefficient (Willetts and Rice, 1983), though the extent of this effect is as yet undetermined.

The aerodynamic properties of the particles are also affected by shape. As a result the trajectory of the particles within the saltation/suspension cloud will change depending on the aerodynamic properties of the particles. Such

change in the trajectory implies that the impact angle will also vary, since it is dependent on the trajectory of the particle. Thus, the amount of energy transferred to the surface, as result of the impact, will also alter as a result of the change in the aerodynamic properties of the particles. For example, particles with a shallow trajectory would transfer less energy on impact, than particles that have a higher trajectory (Fig. 2.15), and thus makes them far less likely to induce further impact entrainment. This is analogous to skimming a stone across a lake.

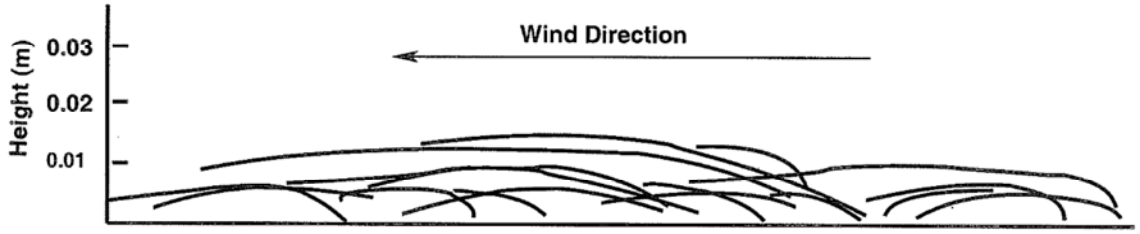

(a) Platey shell sand trajectories

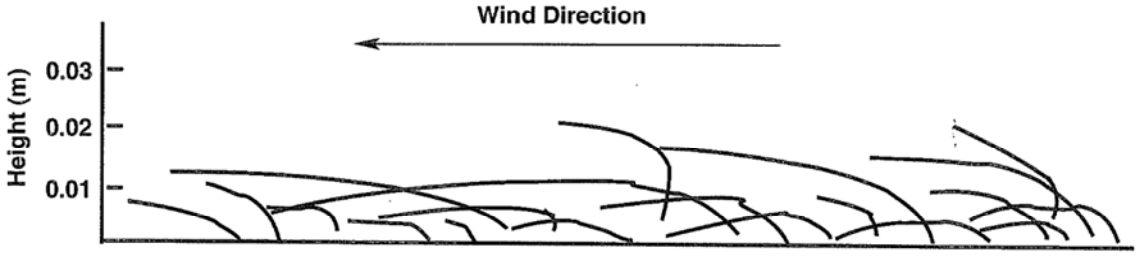

(b) Rounded quartz trajectories

Figure 2.15: Trajectory of different shaped particles. Note: The Platey shell sand (a) has much shallower trajectory than that of rounded quartz (b). Source: Willetts (1983).

Such a change in the trajectory of the particles is an important consideration on the erodibility within the claypan, since the erodible components of the surface mainly consists of sand grains, which have contrasting shape. It can be seen from the above discussion that the effectiveness of impact entrainment will vary considerably across the claypan, as a result of different aerodynamic

properties of the parent soil. It also reinforces the fact that there will be a significant spatial variation in emission rates across the claypan, as a result of the effect that shape has on both packing and aerodynamic properties of the particles.

2.4 Summary

This chapter provides an overview of the main characteristics of the Diamantina National Park field site. In addition it also details some of the environmental factors that are likely to affect wind erosion within the study site. While it is clear from the above discussion that much is understood about the various aspects of wind erosion, little is known about how these interact under field conditions. In particular, little is known about how spatial changes in erodibility may affect various aspects of the study site. It is this question, of how these various dust sources interact within the study site that will form the focus of the reminder of this thesis.

Chapter 3

Background II: Methods of modelling wind erosion

3.1 Introduction

Over the last thirty years numerous models have been developed to quantify various aspects of the wind erosion process. Many of these models examine wind erosion under ideal conditions and describe only a single aspect of the wind erosion process. In this discussion, only models that describe wind erosion at the local, regional and continental scale have been included. Thus models that describe wind erosion at the micro scale, have not been included in this discussion.

To facilitate discussion, the models have been broken up into four categories. The first, will be referred to as Climatic Index Wind Erosion Models. These models use an index calculated on various environmental and climatic factors to describe the risk of wind erosion on a regional or continental scale. The second class of models will be referred to as Empirical Wind Erosion Models. Such models use experimental data to predict wind erosion rates at the paddock (or local) scale. The third category will be referred to as Integrated Wind Erosion Models. These combine various models that describe a single environmental or climatic factor on wind erosion, into a single model which can be

used to predict wind erosion rates at the regional and continental scale. The remaining category will be referred to as Continental/Global Climate Models. These are designed to predict soil loss and soil transport on a continental or global scale.

In each category several types of models exist. Often these models are developments of a basic underlying algorithm. Rather than discuss all of the models, those described here have been selected to illustrate the differences between the various models available in each category. Readers should note that several generalised air pollution models also exist that deal with the movement of pollen and ash in the atmosphere. These models are not discussed separately in this review as they do not deal directly with the wind erosion problem. However, theory from such models is discussed as it is required throughout the remainder of this thesis.

The discussion of each model, is broken up into three sections. The first section details the background in which the model was developed. The next section details the operation of the model, while the final section presents a general discussion on the model and its relevance/relationship to this study.

3.2 Climatic index wind erosion models

This section examines the use of a climatic index to describe spatial and seasonal variations in wind erosion activity. In particular, the index developed by McTainsh et al. (1998), which has been used extensively in eastern Australia to describe climatic influences on wind erosion, is discussed in detail.

3.2.1 Background

One of the problems with modelling wind erosion is how to quantify the effect that climatic factors, such as wind speed and vegetation have on wind erosion. An early attempt to address this problem was made by Chepil et al.

(1963), when they derived a wind erosion index based on climatic considerations in the United States of America (USA). Similar indices have since been used in several countries (Yaalon and Ganor, 1966; Briggs and France, 1982; McTainsh et al., 1990) and have proved to be a successful means of identifying broad areas of wind erosion activity on a continental scale.

In Australia, Burgess et al. (1989) and McTainsh et al. (1990) successfully used a similar index to describe broad scale wind erosion activity using data from various meteorological stations in eastern Australia. This index was refined by McTainsh et al. (1998), to account for seasonal variations in the climatic influences that occur in eastern Australia. It is this form of the index that is discussed in the following sections.

3.2.2 Operation

The original wind erosion climatic index of Chepil et al. (1963), can be defined mathematically as:

$$C = \frac{U^3}{(P-E)^2} \tag{3.1}$$

where C is a wind erosion index, U is mean annual wind speed, and $(P-E)$ is the Thornthwaite (1931) climate moisture index. In index C, the values of U and $(P-E)$ are obtained by averaging wind speed, precipitation and temperature data on a yearly basis.

Initial work on adapting this index to Australian conditions was undertaken by Burgess et al. (1989). This study examined the relationship between effective soil moisture and dust storm occurrence in eastern Australia using the Effective Soil Moisture (Em) Index. This approach was extended by McTainsh et al. (1990) using wind run (the total distance resulting from an anemometer's rotation in a given period) as the measure of wind erosivity. McTainsh et al. (1998) also noted that changing the averaging from yearly to monthly, did make the index a good predictor of monthly dust storm frequency, as the yearly version did not adequately describe seasonal variations in climatic conditions and how these impact on wind erosion activity. To account for this

seasonal variation McTainsh et al. (1998) defined the following five indices:

$$E_w = \frac{W}{(P-E)^2}; \tag{3.2}$$

$$E_m = \frac{1}{(P-E)^2}; \tag{3.3}$$

$$E_{wt} = \frac{W}{(P-E)^2} + \left((P-E)^* \frac{W}{(P-E)^2}\right); \tag{3.4}$$

$$E_{wd} = \frac{W}{(P-E)^2} - \left(\frac{1}{(P-E)^*}\frac{W}{(P-E)^2}\right); \tag{3.5}$$

$$E_{md} = \frac{1}{(P-E)^2} - \left(\frac{1}{(P-E)^*}\frac{1}{(P-E)^2}\right); \tag{3.6}$$

where W is the average monthly wind run and $(P-E)^*$ the previous months value of $(P-E)$.

In these indices, McTainsh et al. (1998) used the subscript on the index to denote which index was to be used under given conditions. These indices therefore correspond to the following states:

E_w -- wind run is above threshold and the soil moisture is not changing,

E_m -- wind run is below threshold and the soil moisture is not changing,

E_{wt} -- wind run is above threshold and the soil moisture is increasing,

E_{wd} -- wind run is above threshold and the soil moisture is decreasing and

E_{md} -- wind run is below threshold and the soil moisture is decreasing.

Thus, for example if the wind run is below threshold and soil moisture has decreased from the previous month, then the E_{md} index would be used to determine dust storm activity. If the wind run was above threshold and soil moisture had increased than the E_{wt} index would be used to determine dust activity for that month. It is important to note, that these indices operate under the assumption that when wind run is below a certain threshold value, then soil moisture and the current state of the soil in the wetting/drying process is the major environmental factor preventing wind erosion from occurring.

3.2.3 General discussion

The use of such indices in Australia has proved to be an invaluable means of quantifying wind erosion activity on a regional scale for large areas of eastern Australia. The ability to identify these regions has enabled researchers to concentrate wind erosion research efforts in these areas, thus enabling detailed field experiments to be designed that enhance our understanding of the environmental and climatic factors that control wind erosion under Australian conditions.

A major advantage of Climatic Index Wind Erosion models is that they function with data that is readily available from meteorological stations throughout the country. At the time that Burgess et al. (1989) first proposed this style of model this was an important consideration as wind erosion research in Australia was in its infancy and detailed field data were not available. Since that time the work of Leys (1998) and others using portable wind tunnels, has significantly increased our understanding of which environmental and climatic factors play a critical role in determining wind erosion rates at the local scale. However, at present none of these additional features have been included in a climatic index style wind erosion model. Instead they have been included in the more advanced models presented in the remaining categories.

Unfortunately as well as being an advantage, the dependence of these models on meteorological data is also a limitation in that it controls the spatial resolution of the index. The reason for this spatial limitation is clearly illustrated in Figure 3.1. This figure shows the density of meteorological stations in Australia increase towards the south east corner of continent. Such a spatial distribution of meteorological stations implies that the spatial resolution of these models decreases with the decreasing density of the meteorological stations. Thus the ability of these models to describe local and regional spatial variations within the Channel Country of western Queensland (which in Figure 3.1 is bordered by: Winton, Boulia, Birdsville, Windorah, Quilpie and Longreach), and which is the subject of this study, is severely limited. It is

this limitation and the inability of these models to account for environmental/climatic factors other than soil moisture (as a surrogate for vegetation) and wind erosivity, that has led to the development of the other models that are described in the remainder of this chapter.

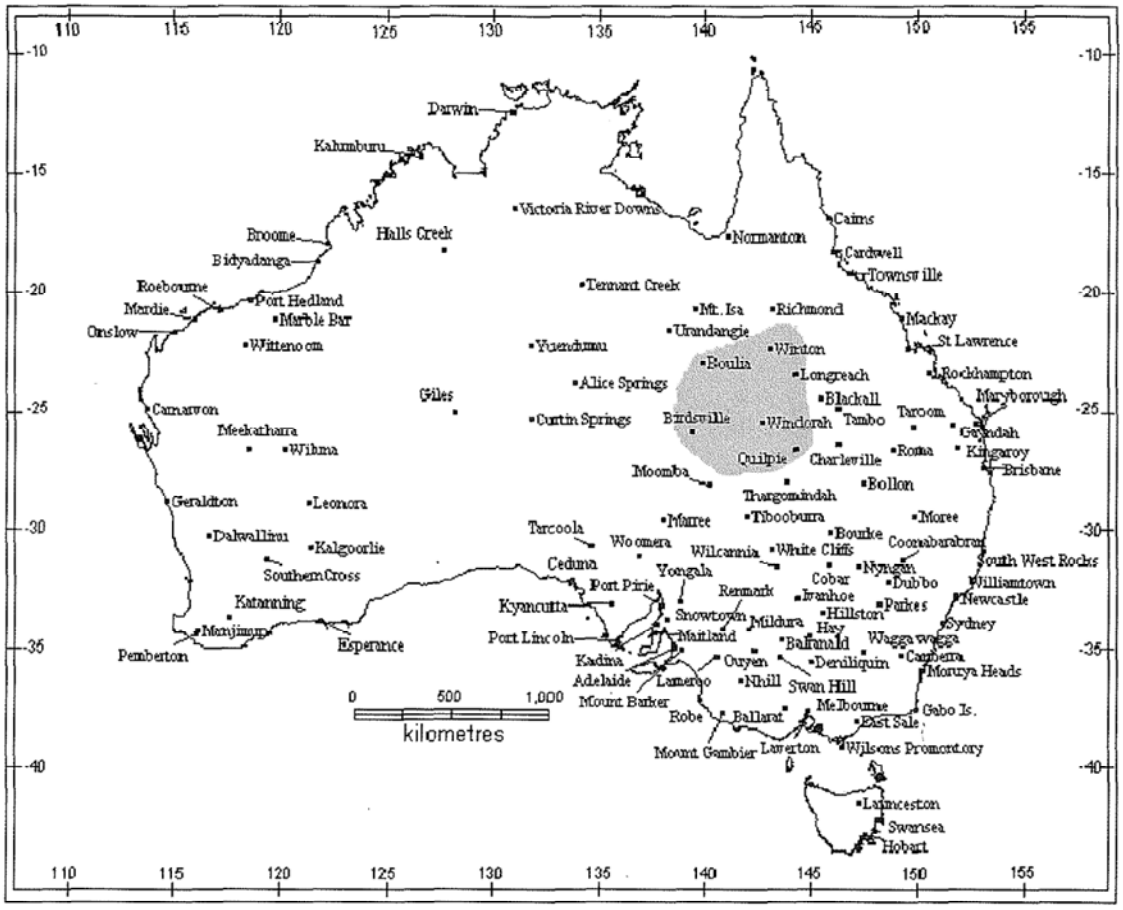

Figure 3.1: Meteorological station locations in Australia. Note the increase in density in the south east corner of the continent. The blue highlighted region illustrates the meteorological stations that border the Channel Country.

3.3 Empirical wind erosion prediction models

The index approach as used by Burgess et al. (1989); McTainsh et al. (1990) and McTainsh et al. (1998), has been able to distinguish regions of Australia that are subject to high levels of wind erosion activity. The models however,

were never designed to describe wind erosion activity at a finer scale. One of the problems with describing wind erosion at a local scale is that it is dependent on several environmental factors (see Chapter 2 for additional details on these). Thus, one of the greatest challenges that remain in wind erosion research is to understand how these factors interact under field conditions to determine wind erosion rates. Early work on linking these factors to produce an estimate of soil loss was undertaken by researchers working in the Great Plains of the USA. It is the empirical model that resulted from this research and its subsequent development that is discussed in the following section.

3.3.1 The wind erosion equation (WEQ) and related models

3.3.1.1 Background

The Wind Erosion Equation (WEQ) was the result of thirty years of research by W.S Chepil and colleagues in the Great Plains of the USA. A prototype of this equation was first released in 1961. However, it was not until 1965 that the equation was first published by Woodruff and Siddoway (1965). Since that time it has been modified several times to extend its functionality. However, it has seldom been applied to Australian conditions. This is partly due to the cost in obtaining sufficient experimental data on Australian conditions to make the equation useful and the fact that better physically–based models were becoming available by the time that research into wind erosion in Australia began to really develop in the early 1980's. It is still however, the most widely used method of accessing annual soil loss by wind from agricultural fields in the USA (Wind Erosion Research Unit, 2002).

3.3.1.2 Operation

The WEQ predicts annual soil loss on tilled agricultural fields by relating empirically derived dimensionless climatic and field factors to the annual soil

loss rate. Thus mathematically it can be expressed as:

$$E = f(I, K, C, L, V) \tag{3.7}$$

where E is the annual soil loss (t/ha/yr); I is soil loss erodibility; K is soil ridge roughness; C is a climatic factor; L is the width of the field; and V is the amount of vegetation cover. The final functional relationship is determined by using an empirical weighting of the contribution of each variable. These empirical weightings are determined from experimental field data.

The WEQ was modified by Bondy et al. (1980) and Cole et al. (1983) to adapt the wind erosion equation to estimate monthly or weekly wind erosion rates. In this procedure, factor values are used to describe successive wind erosion periods in which both the agricultural management and vegetation cover were nearly constant. The wind energy distribution is then used to obtain a weighted average of soil loss for each erosion period. Soil loss for each erosion period over a year can then be added to obtain an estimate of annual soil loss. More recently it has undergone a major revision to produce the Revised Wind Erosion Equation (RWEQ) (Comis and Gerrietts, 1994). This revision has added parameters for planting data, tillage method and crop residue to the equation. At the same time a stochastic weather generator was added to the equation. The addition of the weather generator enabled users of the RWEQ to simulate future weather conditions, based on previous climatic conditions, thus enabling the RWEQ to be used as a wind erosion prediction tool, instead of solely as a tool for quantifying the amount of wind erosion that has taken place over a given period.

3.3.1.3 General discussion

The original version of the WEQ provided the first feasible means of linking a variety of environmental factors mathematically to wind erosion rates on cultivated fields. Modifications since its introduction have improved the accuracy and range of problems to which the WEQ can be applied. However, despite these modifications the fundamental weakness of the original

approach remained; the application equation was still heavily data dependent. Such a heavy reliance on large amounts of experimental data, severely limited its adoption world wide and especially in areas like Australia. Gathering sufficient experimental data even to simply verify the equation under new conditions would involve a significant investment of research funds and time, which given the size of the continent and the population, are simply not available.

The other significant drawback in applying the WEQ and its derivatives to Australia is that it also requires a good historical record of meteorological data to function to a high degree of accuracy. Unfortunately large areas of Australia that are subject to wind erosion are located in remote areas of central Australia. Thus there is limited historical environmental and meteorological data for these areas (Fig. 3.1).

Another important issue when considering applying the WEQ to the Channel Country is that it was designed for cultivated land, where the surface conditions are largely controlled by human intervention. The Channel Country is primarily used for cattle grazing on a broadscale, and as such surface conditions are determined by grazing patterns and natural responses to prevailing environmental conditions. The net result of these differences is that surface conditions within the Channel Country can change substantially within a few hundred metres and there are often no well defined boundaries at which these changes occur. One of the implications is that for any given feature of Channel Country (e.g., the Lake Constance Claypan) it is hard to assign a single value for parameters such as soil moisture and roughness, as it is hard to clearly identify regions which are being eroded by the wind. Thus it is difficult to accurately apply models such as the WEQ to such areas without understanding of how wind erodibility varies spatially within these areas.

While the data issues outlined above limit the applicability of the WEQ and its derivatives to Australian conditions, it still provides important information on the role that certain environmental factors have on the wind erosion process. Such information is fundamental to our understanding of how the

wind erosion process functions under field conditions. It is therefore platforms like the WEQ that work in this thesis will draw upon.

3.4 Integrated wind erosion models

Since the initial research that resulted in the WEQ, a significant amount of research has been undertaken, which further details how individual environmental/climatic factors influence wind erosion under field conditions. As a result, several distinct models have been derived that describe how different individual environmental/climatic factors influence wind erosion rates. However, these models do not describe the interaction between these environmental factors. Thus, the next step in the modelling process is to begin combining these models into a single unified model of the wind erosion process. It is these unified or integrated models of wind erosion that are examined in this section.

3.4.1 The wind erosion prediction system (WEPS)

3.4.1.1 Background

The empirical nature of the WEQ and its derivatives has limited its adoption in many regions of the world. It also lacks the ability to fully account for how the complex interactions between environment factors alter wind erosion rates. To overcome these disadvantages the United States Department of Agriculture (USDA) began development of a new more process oriented model called the Wind Erosion Prediction System (WEPS) in the early to mid 1990's.

3.4.1.2 Operation

Based on information contained in Hagen (1991); Argabright (1991); Comis and Gerrietts (1994) and Wind Erosion Research Unit (2002), WEPS consists

of a number of distinct sub-models (Fig. 3.2). These sub-models include models for stochastic weather generation, crop growth, decomposition, soil type, hydrology and tillage (Hagen, 1991; Comis and Gerrietts, 1994; Wind Erosion Research Unit, 2002). Each of these sub-models is complex and therefore not discussed in detail here for two reasons. Firstly, the full details of each sub-model can be found on the Wind Erosion Research Unit (2002) web site. Secondly it is not necessary to describe the model in detail for the key points to be made.

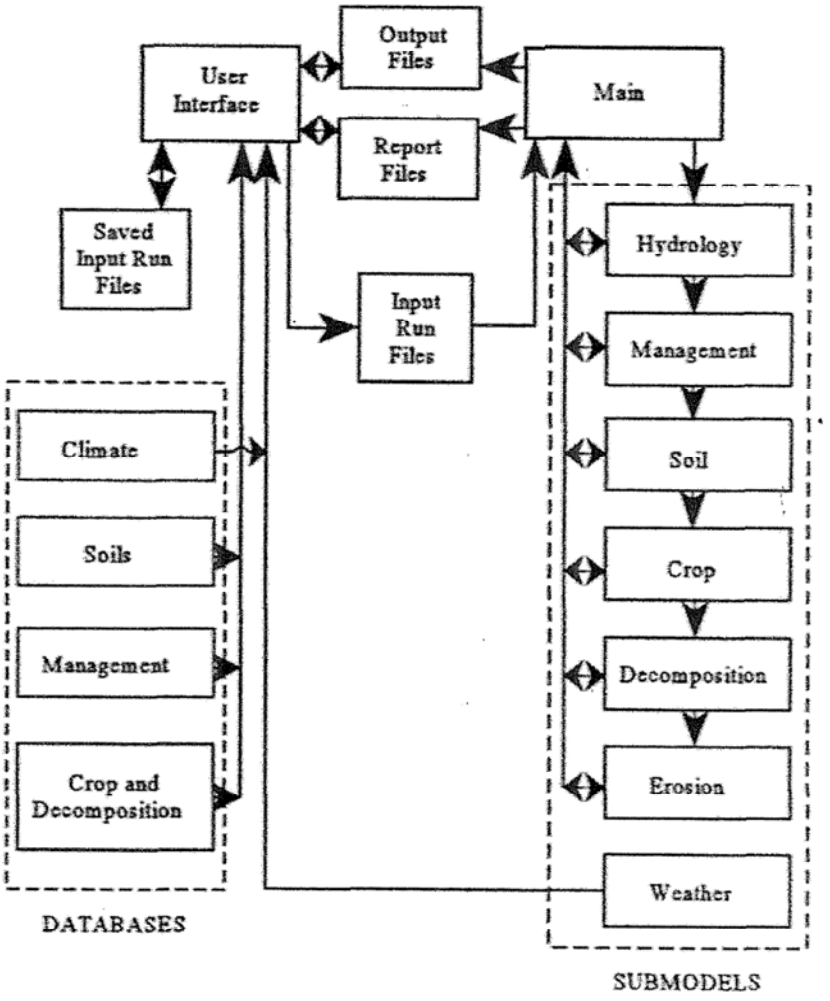

Figure 3.2: The structure of the WEPS model in terms of the sub-models which make up the final integrated model (Wind Erosion Research Unit, 2002).

In addition to the sub-models, a number of databases are required to run WEPS. These databases include detailed information on data on soils, farm

management practices, climate and crop growth and decomposition. The information from these databases are used to seed the various sub-models. During any given model run, updated information on current values of all the parameters (including predicted values of the values stored in the databases and erosion estimates), is passed between the various sub-models at regular intervals and also written to report files. Once the data run is completed the user can view these report files.

3.4.1.3 General discussion

It is important to note that WEPS has been developed as a *user management model* rather than a *research model* (Wind Erosion Research Unit, 2002). As a consequence numerous simplifications have been made in the various sub-models (Wind Erosion Research Unit, 2002). Such simplifications include assuming that the crop is a single height within a field and that soil and surface conditions are also uniform within the field. Such assumptions limit the applicability of WEPS to large areas of the Channel Country in similar fashion to that outlined for WEQ in Section 3.3.1.3.

Another important consideration, if we were to apply WEPS to the Channel Country is that detailed soil, vegetation, and climatic data would need to be available. In the case of the Lake Constance Claypan alone, this detailed information would need to include the effect flooding has on both vegetation and surface conditions. Unfortunately such information is not readily available and is not easy to collect for variety reasons. Firstly, as mentioned in Chapter 2, it is not easy to identify areas of the claypan that have been subject to erosion. Secondly, unlike cultivated fields there are no human controls on surface conditions. Thus surface conditions can vary greatly over the course of a season. As a result the spatial structure of dust source areas at the end of a season are likely be completely different from those observed at the start. It is this spatial variability in erodibility that is the key to understanding the role wind erosion plays within the Channel Country of western Queensland. One

of the key features of this project is therefore to determine if there is a physical link been observed dust concentration profiles and the spatial distribution of dust source areas within the claypan.

3.4.2 The Gillette and Passi model

3.4.2.1 Background

The model discussed in this section, is one of the early attempts to describe wind erosion rates based on physical theories developed from wind tunnel studies. It therefore represents an important stepping stone in the development of integrated wind erosion models.

The model described here was derived by Gillette and Passi (1988) to estimate the total dust production for the USA. It uses detailed soil and land data available from the USDA, wind data from the Wind Energy Resource Information Centre (WERIC), and a theoretically derived emission function Q. .Therefore while still using some empirical data, it is basically driven by the value of the physical parameters u_* and u_{*t}.

3.4.2.2 Operation

The dust emission scheme of Gillette and Passi (1988) is based around the following equation:

$$E = C \sum_{i=1}^{N} R_i g(L_i) A_i \Delta T \int_{U_{ti}}^{\infty} G(U) p_i(U)\, dU \tag{3.8}$$

where E is the mass of dust emitted in time ΔT, C is a constant, N is the number of different soils, R_i is the effect of roughness, $g(L_i)$ effect of the length of the field L_i, $G(U)$ is the vertical mass flux of dust as a function of wind speed, A_i is the area of the field being considered, $p_i(U)$ is the *Probability Density Function (pdf)* of wind during the period of interest and U_{ti} is the i'th threshold wind speed.

In Equation (3.8), $G(U)$ has the following form:

$$G(U) = C_2 c_d^2 U^4 \left(1 - \frac{U_t}{U}\right) \tag{3.9}$$

where C_2 is a constant, c_d is the coefficient of drag, U is the average wind speed and U_t the average threshold wind speed. This was weighted in Equation (3.8), by the pdf, which was assumed to follow the two-parameter Weibull distribution. This distribution can be written as:

$$p_i(U) = \left(\frac{k}{c}\right)\left(\frac{U}{c}\right)^{k-1} \exp\left[-\frac{U^k}{c}\right] \tag{3.10}$$

where c and k are parameters determined from the wind speed distribution data.

The threshold friction velocities (u_{*t}) were obtained from the experimental studies of Gillette et al. (1980, 1982), and Gillette (1988) and assigned to various regions of the USA depending on predominate type of land use in that region. The roughness was evaluated using the function derived by Armburst et al. (1964), since values of this function were listed in the USDA data set. The effect of field length was ignored, thus it was assumed that $g(L) \approx 1$.

Using these values the integral in Equation (3.8) was evaluated for all wind speed above threshold for each sub-area. The N sub-areas were then added together to obtain the total dust flux. The resulting dust flux was weighted by $g(L_i)$, Δt and the area A_i. C was obtained by calibration. It is also assumed that the soil parameters remained constant during the period Δt and that the effects of vegetation, roughness and moisture can be built into the U_t value.

3.4.2.3 General discussion

One of the key features of this approach is that this was one of the first models to formally relate U and U_t to dust flux (Equation (3.9)). This relationship has since been used in a number of other models, such as the Wind Erosion Assessment Model (WEAM) of Shao et al. (1996). It is this relationship therefore that has formed the basis of much of the modelling undertaken in the last 15 years.

Using this approach it is not possible to predict changes in the u_{*t} on an event basis or show how it changes within a given land type per event. Thus, values used are based either on long term averages or measured values taken at one point during the season. While the use of such estimates may provide reasonable estimates of wind erosion on a regional scale, they provide little information about any spatial changes in erodibility of the surface on a local scale. These spatial changes in erodibility are likely to be a distinguishing characteristic of individual events within the Channel Country. Thus it is extremely hard to make informed environmental management decisions for areas such as the Channel Country with little knowledge of how seasonal effects alter the spatial distribution of dust source areas.

This approach differs from DSism in that it provides estimates of the dust flux and mass of soil removed. In contrast, DSism provides information about how soil is being moved within rangeland environments and how this varies between events. The process information obtained from DSism can then be incorporated into models, such as Gillette and Passi (1988), to provide better estimates through space and time.

3.4.3 The wind erosion assessment model (WEAM)

3.4.3.1 Background

This model was one of the first integrated models to be applied specifically to Australian conditions. It was jointly developed by the CSIRO (Raupach) and the University of New South Wales (Shao) in the mid 1990's. The major purpose of the model was to provide a quantitative estimate of wind erosion rates in Australia. It has since been used as a basis for a continental dust transport model, which is discussed further in Section 3.5.2.

Essentially, this model combines many of the current theories relating to wind erosion into a single model by describing the influence that climate, soil, vegetation and land use have on wind erosion rates.

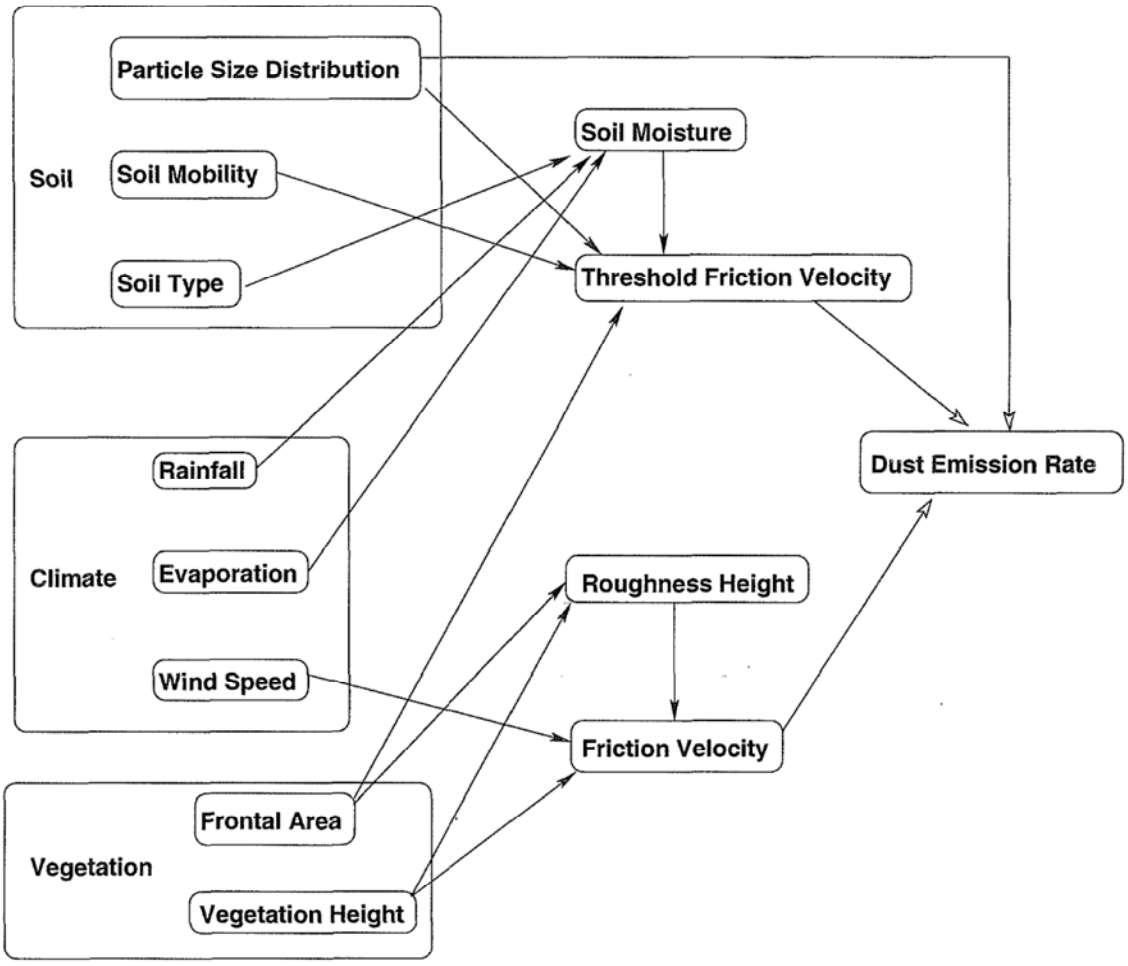

Figure 3.3: Schematic showing how various climatic and surface properties are included in the WEAM (Shao et al., 1996).

3.4.3.2 Operation

The fundamental concept that underpins WEAM is that the threshold friction velocity (u_{*t}) is determined by the soil surface conditions, land use and soil moisture, while the friction velocity (u_*) is determined by climatic conditions and the roughness height (Shao et al., 1996). This is shown schematically in Figure 3.3.

The model predicts streamwise dust flux Q and vertical dust flux F. In order to determine both these quantities the model is based around the sand transport equation of Owen (1964), which states that for soils of uniform particle

size d the streamwise transport rate is given by:

$$Q(u_\star, d) = \begin{cases} \frac{c\rho u_\star^3}{g}\left[1 - \left(\frac{u_{\star t}(d)}{u_\star}\right)^2\right] & u_\star \geq u_{\star t} \\ 0 & u_\star < u_{\star t} \end{cases} \tag{3.11}$$

where c is a constant (≈ 1), ρ is air density and g is acceleration due to gravity.

In WEAM, Equation (3.11) is used with multiple size distributions by assuming that the dependence of Q on $u_\star$ and $u_{\star t}$ is not significantly altered by the presence of other particle sizes. With this assumption Q can be estimated by:

$$Q = \int_{d_1}^{d_2} \tilde{Q}(d_s) p(d_s) \delta d_s \,, \tag{3.12}$$

where d_1 and d_2 are defined respectively as the lower and upper particle size limits of the saltation cloud, $\tilde{Q}$ is the transport rate of each particle size, and $p(d_s)$ is the pdf particle size distribution of the soil.

In order to predict F for multiple particle size soils, Shao et al. (1996) divided the particles into dust and sand at the size $d = d_1$, where d_1 was determined as the diameter in which the deposition velocity fell below a critical value. Thus the dust fraction d_d was defined as particles for which the size was between 0 and d_1 and the remaining particles were defined as saltation d_s. Based on the results of Shao et al. (1993b), the vertical dust flux $\tilde{F}$, of particles of size d_d induced by saltation bombardment of sand particles of size d_s can be approximated by:

$$\tilde{F}_d(d_d, d_s) = \frac{2\rho_p \beta \gamma g}{3\rho[u_{\star t}(d_d)]^2} \tilde{Q}_s \,, \tag{3.13}$$

where ρ_p is the density of the dust particles, ρ is the density of air, β is an empirical parameter determined from experiment, γ is the ratio of $\dfrac{U_0 + U_1}{2u_\star}$, where U_0 and U_1 are the takeoff and impact velocities of the saltating particles respectively, $\tilde{Q}_s$ is the saltation flux of particles of size d_s. Thus the total vertical flux is given by integrating over all particle sizes:

$$F = \int_{d_1}^{d_2} \int_{o}^{d_1} \tilde{F}(d_d, d_s) p(d_d) p(d_s) \, \delta d_d \delta d_s \,, \tag{3.14}$$

where $p(d_s)$ and $p(d_d)$ are the pdf's of the saltation and dust fractions respectively.

The threshold friction velocity (u_{*t}) is the key parameter in the model, as both Q and F depend directly on its value. WEAM assumes that the value of the threshold friction velocity (u_{*t}) is a function of the particle size (d_s), the frontal index of surface elements (λ) as defined by Raupach (1992), soil moisture (w) and the hardness of the surface crust (S_c). Therefore, the threshold friction velocity (u_{*t}) can be written mathematical as:

$$u_{*t}(d_s, \lambda, w, c) = \frac{u_{*t}(d_s, 0, 0, 0)}{R(\lambda)H(w)S_c} \tag{3.15}$$

where $u_{*t}(d_s, 0, 0, 0)$ was approximated from the model of Greeley and Iverson (1985), $R(\lambda)$ is the ratio of $\frac{u_{*tS}}{u_{*tR}}$ where u_{*tS} is the threshold velocity of the bare surface, and u_{*tR} is the threshold friction velocity of the rough surface, and $H(w)$ is the ratio of $\frac{u_{*tw}}{u_{*td}}$ where u_{*tw} is the threshold velocity of the wet surface, S_c is the hardness of the surface crust and u_{*td} the threshold friction velocity of the dry surface. The parameters $R(\lambda), H(w)$ and S_c are estimated based on the result of wind tunnel experiments carried out in the area.

3.4.3.3 General discussion

As with the Gillette and Passi (1988) model, this model relies on the prediction of u_{*t}, however in this case the value is determined by Equation (3.15). This approach has similar problems to the Gillette and Passi (1988) approach when considered in terms of the Channel Country. In particular, for areas such as the Lake Constance claypan, it is hard to determine values for R, H and S_c, as these can vary substantially across the claypan and through time. Thus for such models to work successfully in these areas it is necessary to understand how these values change between events.

It is this spatial and temporal variability in surface erodibility that Shao et al. (1996) alluded to as one of the possible reasons for WEAM's poor performance at certain periods of a field trial. This field trial was carried out on cultivated land in south-eastern Australia. In contrast to the Channel Country, the surface conditions of this cultivated field site were much more uniform. Given this difference between the locations, one would expect that spatial changes

in erodibility would play a more prominent role in the Channel Country. In order to understand the role of wind erosion in the Channel Country and if spatial variations in erodibility are in fact responsible for WEAM's poor performance at such times, it is crucial that we understand the effect that spatial variations have on dust measurements.

3.4.4 The fugitive dust model (FDM)

3.4.4.1 Background

The Fugitive Dust Model (FDM) was developed by the United States Environmental Protection Agency (USEPA) in the 1990's to predict the impact of rural dust on urban air quality. The model is essentially a modified version of the standard Gaussian Plume air pollution model (details of which can be found in Hanna et al. (1982) and Zannetti (1990)) in that it used a gradient-transfer deposition algorithm. It was also one of the early air pollution models designed to run on a desktop PC under the MS-DOS operating system. The details below are a summary of its operation, is largely based on the FDM user guide (Winges, 1992) supplied with the model by the USEPA.

3.4.4.2 Operation

The general equation governing the pollutant transport and dispersion of uniform particles in the atmosphere is given below:

$$\frac{\partial \chi}{\partial t} = \frac{\partial}{\partial x} K_x \frac{\partial \chi}{\partial x} + \frac{\partial}{\partial y} K_y \frac{\partial \chi}{\partial y} + \frac{\partial}{\partial z} K_z \frac{\partial \chi}{\partial z} - u \frac{\partial \chi}{\partial x} + v_g \frac{\partial \chi}{\partial z} \tag{3.16}$$

where χ is the concentration (g/m^3), x, y and z are the spatial coordinates, K_x, K_y, K_z are the eddy diffusivity in the x, y and z directions respectively, t is time, u is the wind speed and v_g the gravitational settling velocity.

The FDM makes a number of assumptions in order to achieve an analytical solution to Equation (3.16) (Winges, 1992). Firstly, the diffusion in the x direction is small compared to the advection by the wind in that direction.

Secondly K_x, K_y, K_z are assumed to be functions of downwind distance only. Thus Equation (3.16) simplifies to:

$$u\frac{\partial \chi}{\partial x} = K_y\frac{\partial^2 \chi}{\partial y^2} + K_z\frac{\partial^2 \chi}{\partial z^2} + v_g\frac{\partial \chi}{\partial z} \tag{3.17}$$

It is further assumed that $K = K_z = K_y$ is constant, and that $\sigma_z^2(x) = \frac{2}{u}\int_0^x K\,dx$, Thus, we get:

$$K = \frac{\sigma_z^2 u}{2x}. \tag{3.18}$$

Solving Equation (3.17) under these assumptions gives:

$$\begin{aligned}\chi \;=\; & \frac{Q}{2\pi\sigma_y\sigma_z u}\exp\left(-\frac{y^2}{2\sigma_y^2}\right)\exp\left(\frac{-v_g(z-h)\sqrt{2}\beta}{\sigma_z} - v_g^2\beta^2\right) \\ & \left[\exp\left(\frac{-(z-h)^2}{2\sigma_z^2}\right) + \exp\left(\frac{-(z+h)^2}{2\sigma_z^2}\right)\right. \\ & \left. - 4\sqrt{\pi}v_1\beta\exp\left(\frac{-(z+h)^2}{2\sigma_z^2}\right)\exp\gamma^2\mathrm{erfc}(\gamma)\right]\end{aligned} \tag{3.19}$$

where: Q is the emission rate, y is the crosswind distance, z is the vertical height, σ_y and σ_z are the dispersion parameters in the crosswind and vertical direction respectively, h is the release height, v_g is the gravitational settling velocity, $v_1 = u_d - \frac{v_g}{2}$, u_d is the deposition velocity, $\gamma = \frac{v_1\sqrt{2}x}{\sigma_z u} + \frac{z+h}{\sqrt{2}\sigma_z}, \beta = \frac{x}{\sqrt{2}\sigma_z u}$ and x is the downwind distance.

By assuming that K is constant and using the standard pasquill functions for σ_y and σ_z, then Equation (3.19) does not conserve mass. The resulting concentration is corrected by numerically calculating a correction term which is added or subtracted from the calculated concentration. However, this correction is not calculated for each case, but estimated using a least squares fit to the previously calculated values. These corrections are significant for particles larger than 10 μm in diameter.

The FDM also allows the user to specify emission rates as a function of wind speed, in two ways. Firstly emission rates can be specified as a simple power law:

$$Q = Q_0 u^s \tag{3.20}$$

where Q is the emission rate; Q_0 is a constant; u is the wind speed and s the wind speed dependence parameter. The second method allows the user to specify a threshold wind speed, by using the following equation:

$$Q = Q_1 + Q_2(u - u_0)^b \tag{3.21}$$

where Q_1 is the background emission parameter; Q_2 is a constant; u_0 is the wind speed threshold and b is the wind speed dependence parameter.

Sources are assumed to be either points, lines or areas. For lines the concentration is calculated using the integral version of Equation (3.19). Area sources are assumed to consist of a number of line sources. Two algorithms exist in the model for breaking these area sources up into line sources. The first simply divides the area up into 5 lines. The second uses a convergence criteria, in that it keeps adding lines until the calculated concentration is less than 1% of the previous value.

While the FDM calculates the concentration for a number of particle sizes, it only outputs the final bulk concentration (sum of all the particle size concentrations) and at a limited number of detector sites. This concentration is also assumed to be averaged over either a 1-hour, 3-hour, 8-hour or 24 hour period. In addition, it assumes that there is a significant reflection of the plume from the surface, and that there is no plume rise due to heating or topographical effects.

3.4.4.3 General discussion

The FDM approach shares several conceptual elements with the modelling approach described in this thesis, but there are also significant differences. In particular the approach taken here uses the Land Erodibility Index (LEI) developed by McTainsh et al. (1999) for the Diamantina National Park (DNP) site to adjust emission rates from a base value rather than requiring the user to define emission rates for each of the land systems as required by FDM. Another clear distinction between the two approaches is the time periods that dust concentrations are averaged over. In FDM the output dust concentration

represent the average concentration over either a 1-hour, 3-hour, 8-hours or 24 hour period, while in the approach taken in this thesis the dust concentration represent the average dust concentration over the event being considered.

In the approach taken by FDM, WEAM and Gillette and Passi (1988), the definition and allocation of source area properties is the key used to drive the models. This approach works when it is easy to identify and quantify the characteristics of source areas in the field or by satellite imagery. However, in cases like the Lake Constance claypan it is hard to identify source area boundaries and quantify source characteristics. The approach taken in this study, uses the information found in the dust concentration profile as a prediction of source characteristics and spatial patterns within the claypan.

Another significant difference between the FDM and the approach taken in this study is how particle size issues are handled. Here the user can set different emission rates for each particle size class in the model, in contrast FDM assumes that the emission rates are equal for each particle size. Thus, the approach used here allows the user to simulate the effect that different particle size emission rates would have on the resulting dust concentration and compare these to observed particle size affects.

3.5 Continental/Global climate models

In atmospheric studies, dust emissions have been the subject of research since the early 1990's. Early studies by Tegen and Fung (1994, 1995) were unsuccessful in reproducing the intensity of dust emissions and atmospheric dust concentrations. Part of the problem with these early attempts related to the simple dust emission scale used. These emission schemes assumed that the spatial-temporal variations in dust emission rates were due only to variability in wind velocity. They did not account for variations in surface features, which also play an important role in determining wind erosion rates. Several models have since been developed that have improved erosion schemes

that account for surface properties (Marticorena and Bergametti, 1995; Marticorena et al., 1997; Shao and Leslie, 1997). Due to the similarities in terms of processes between these models and the fact that few have been applied to Australian conditions, only the models of Knight et al. (1995) and Lu and Shao (2001) are discussed in detail in this review.

3.5.1 The Knight et al. model

3.5.1.1 Background

One of the major challenges in wind erosion research is estimating the dust loads that are associated with individual wind erosion events. These estimates of dust loads are particularly important if the impact/cost of dust events are to be accurately measured. Up until 1994, few estimates had been made of the amount of material transported in individual dust events in Australia. One of the first conservative estimates was completed by Raupach et al. (1994) for the dust plume that blanketed Melbourne in 1984 (Fig. 1.1). This study estimated that this event alone transported 2 ± 1 million tonnes of topsoil. The modelling of Knight et al. (1995) which is reported in this section, was designed to estimate the dust load of a single large dust event which occurred in the Simpson Desert–Channel Country region of western Queensland in 1987. It differs significantly from the Lu and Shao (2001) model reviewed in the next section, in that it used a different algorithm to determine the erosion area and the amount of material entrained.

3.5.1.2 Operation

Surface weather data from the Bureau of Meteorology were used to provide a first indication of the dust source regions and the dimensions of the resulting dust plume. Further information on the dust source and plume movements were obtained by back-trajectory analysis using 6 hourly meteorological data on wind speed and direction. This back-trajectory analysis traced parcels of

dust laden air back from the coast to the potential upwind source areas. These trajectories converged on an area near Birdsville (Fig. 3.4(a)).

The entrainment and transport of dust were modelled, using a series of linked boxes. The back-trajectories and surface weather data were used to define the locations and extent of the boxes, shown in Figure 3.4(b). The processes considered important in each of the boxes are as shown in Figure 3.5.

The model makes the following assumptions: (1) dust concentrations are homogeneous within each box; (2) the cross–wind and vertical dispersion is instantaneous within each time interval; (3) the source strength is constant over space and the time interval used, and this does not vary with height; (4) dust is not lost or gained through the ceiling of each box; (5) the deposition, advection and dust ceiling heights are constant; (6) the dust particles are chemically inert; and (7) losses occur only as result of washout, dry deposition and advection.

Based on these assumptions, the change in dust concentration (ΔX) in a box with entrainment rate S, volume V and basal area A over the time interval Δt can be written as:

$$\Delta X = \frac{\text{dust mass in - dust mass out} + SA\Delta t}{V}, \tag{3.22}$$

where dust mass consists of material entering from the previous box and dust mass out consisted of material leaving the box as a result of advection, dry and wet deposition.

As entrainment rates were not known for the Birdsville box, these were estimated by inverting the box equations to isolate the Birdsville entrainment term. Once estimated this data is used to solve the standard problem.

3.5.1.3 General discussion

The Knight et al. (1995) approach like FDM, WEAM and Gillette and Passi (1988) uses the source definition to drive the model. However, unlike these

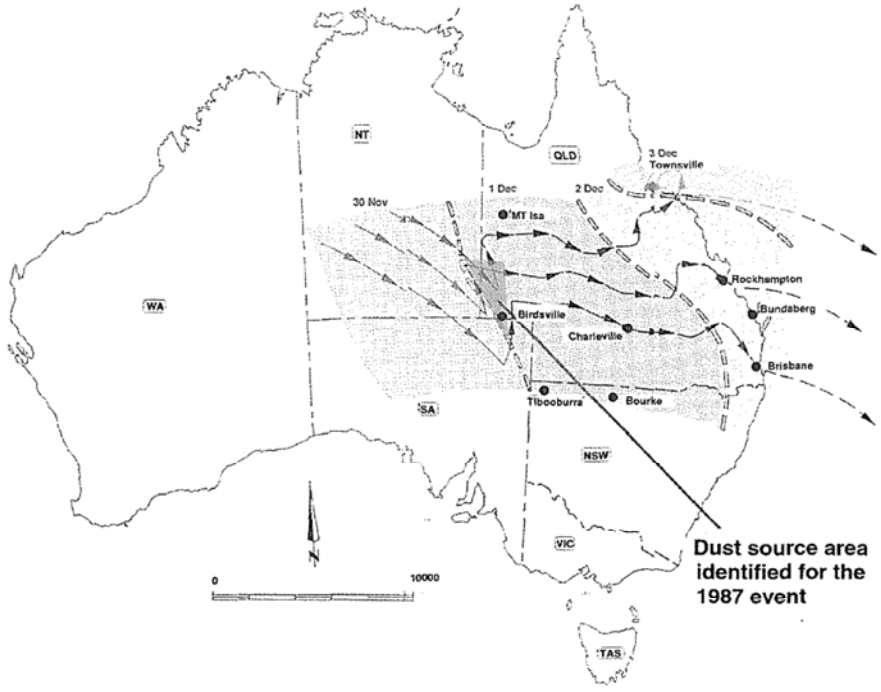

(a)

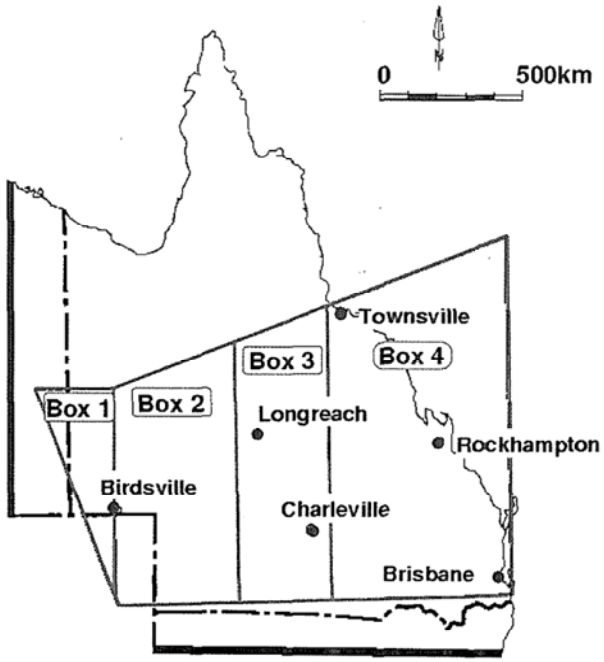

(b)

Figure 3.4: (a) The backtracked air parcel trajectories as calculated by Knight et al. (1995) for the 1987 event. The major source area identified by Knight et al. (1995) is shown in red. (b) The corresponding boxes used by Knight et al. (1995) to model the 1987 event.

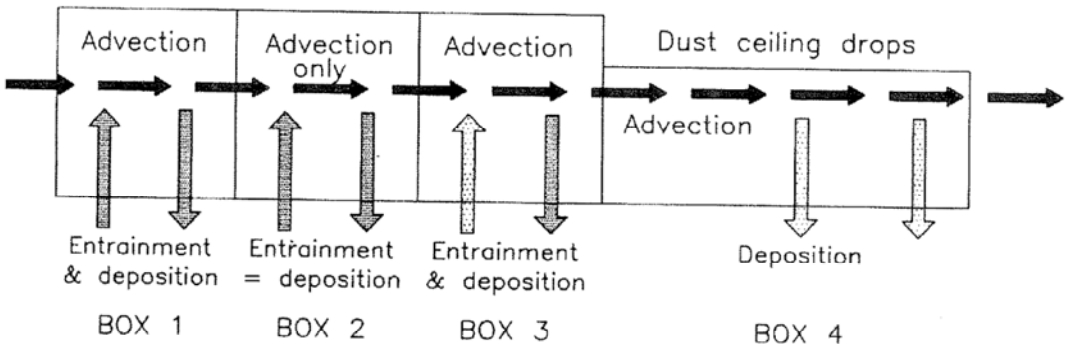

Figure 3.5: Processes included in the Knight et al. (1995) model on a per box basis.

other models the Knight et al. (1995) approach uses a recorded dust concentration to estimate the initial dust emission rates, instead of calculating it from values of roughness, and other soil conditions at the source. In order to simplify calculations, Knight et al. (1995) assumed that emission rates were constant throughout Box 1, however, surface conditions would have been far from uniform throughout Box 1. This raises the question of just how much do spatial variations in erodibility affect the predicted dust loads and dust concentrations downwind? Evidence presented by Lu and Shao (2001) suggests local spatial variations in erodibility can result in significant changes in these estimates. Thus, to achieve accurate predictions it is important to understand the local spatial characteristics of any given land type.

The importance of getting the spatial emission rates correct, is further illustrated in a study of land type erodibility for a single dust storm in the Channel Country, undertaken by McTainsh et al. (1996) (Table 3.1). This study considered three erodibility scenarios. In *Scenario I*, McTainsh et al. (1996) made the same assumption as Knight et al. (1995), that the erodibility of the source area was uniform. Under this assumption McTainsh et al. (1996) obtained a soil loss rate of 38·1 t/km^2. In reality (as *Scenario II* in McTainsh et al. (1996) describes) the main land types were eroding at significantly different rates. For example, the dunes land type was actually eroding at 100 times the rate assumed in *Scenario I*.

If the relative erodibilities and spatial coverage of the sources had been

Table 3.1: Estimated soil loss rates in t/km^2 under three scenarios for a dust storm in the Queensland Channel Country on 1 November, 1994. Source: McTainsh et al. (1996).

	Scenario		
Land Type	*I*	*II*	*III*
Dunes		389·2	124·4
Alluvium	38·1	151·2	208·8
Downs		1·9	1·9

known, then clearly Knight et al. (1995) could have made a much better estimate of the source strength. However, the Knight et al. (1995) model would not have been able to use this information to describe soil loss from the different land systems, as the model cannot handle more than one source area. It is often the case, however, that there are several dust source areas within a land type. DSism is designed to simulate the interaction of various sources, and their effect on the resulting dust concentration. This new simulation model also allows the user to do sensitivity testing, to determine the effect source strength and location have on downwind dust concentrations profiles.

Another result to come out of the McTainsh et al. (1996) study, is the sensitivity of soil loss to changes in land type area. In *Scenario III* the area of the dunes is increased over *Scenario II* by 5% points (i.e., that is from 18% to 23%), while the area of alluvium is decreased by 5%. This results in a large change in the soil loss rates from the two land types (Table 3.1). The Knight et al. (1995) model, would not be able to describe the effect of this change, whereas DSism is able to simulate the effect that such a change would have on downwind dust concentrations.

To summarise, the approach taken by Knight et al. (1995) cannot be easily adapted nor was it designed to explore the effect that such spatial changes in erodibility on the local scale has on the resulting dust cloud or dust loads. The

model/experimental approach taken in this thesis however uses the idea that the dust concentration profile can be viewed as a signal to provide a means of increasing the spatial resolution within a given land type. Using such an approach it has been possible to gain additional information about the role that spatial erodibility plays within a given land type and the likely processes that are occurring at the local scale within the Channel Country.

3.5.2 The Lu and Shao model

3.5.2.1 Background

The Lu and Shao (2001) model extends the Wind Erosion Assessment Model (WEAM) (Shao et al., 1996) to a continental scale by incorporating a transport component. It is essentially a more refined version of the original extension proposed by Shao and Leslie (1997). The differences between these models are now discussed.

3.5.2.2 Operation

The wind erosion emission scheme used in the model is an improved version of the WEAM, in that both the estimate of threshold friction velocity ($u_{*t}(d_s, 0, 0, 0)$) and Dust Flux (F) were improved, based on the experimental work of Lu and Shao (1999), and Shao and Lu (2000). In addition to this, the model uses Geographical Information System data to estimate the parameters in order to run the WEAM section of the model. The outputs from this model are then fed into the transport model that is outlined below.

The concentration of the i'th particle size is $c_i = c(d_i)$, and thus the total concentration is given by:

$$C_{\text{total}} = \sum_{i=1}^{N} c_i \,, \tag{3.23}$$

where N is the total number of particle size classes used in the model.

The concentration c_i is obtained by solving the dust concentration equation in

σ-coordinate system as defined by Phillips (1957):

$$\begin{aligned}&\frac{\partial p_s c_i}{\partial t}+\frac{\partial p_s u c_i}{\partial x}+\frac{\partial p_s v c_i}{\partial y}+\frac{\partial c_i}{\partial \sigma}(p_s\dot{\sigma}+g\rho w_{ti})\\&=p_s\frac{\partial}{\partial x}K_{ph}\rho\frac{\partial c_i/\rho}{\partial x}+p_s\frac{\partial}{\partial y}K_{ph}\rho\frac{\partial c_i/\rho}{\partial y}+\frac{g^2}{p_s}\frac{\partial}{\partial \sigma}K_{ph}\rho^3\frac{\partial c_i/\rho}{\partial \sigma}\end{aligned} \tag{3.24}$$

subject to the boundary conditions

$$c_i(p_s\dot{\sigma}+g\rho w_{ti})-\frac{g^2}{p_s}K_{pz}\rho^3 = g\rho F_i\,, \quad \text{at the surface, and} \tag{3.25}$$

$$\frac{\partial c_i/\rho}{\partial \sigma} = 0 \quad \text{at the top}\,, \tag{3.26}$$

where K_{ph} is the horizontal diffusivity which is assumed to be equal in the x and y directions, K_{pz} is the vertical diffusivity, w_{ti} is the settling velocity of the i'th particle size, F_i is vertical dust flux of the ith particle size, u, v and $\dot{\sigma}$ are the respective wind velocities, p_s is the surface pressure, g is the acceleration due to gravity and ρ the density of air.

3.5.2.3 General discussion

The Lu and Shao (2001) model is essentially a refinement of the Shao and Leslie (1997) model, and the comparison between these two approaches is significant in terms of this study. This fine tuning resulted in a total dust estimate of 1.2Mt compared to over 6Mt for the Shao and Leslie (1997) model for the same event.

There are two important implications of the above result. Firstly, that even minor spatial alterations in emission rates can cause significant variations in model estimates. Which is consistent with the conclusions of McTainsh et al. (1996). Secondly, if the total dust emission is to be estimated accurately, it is important to understand how erodibility varies spatially within each land type used in the model. This thesis uses the simulation/experimental relationship developed in the following chapters, to examine the affect that changes in erodibility within a land type has on the resulting dust concentration.

3.6 Summary and direction of this research

In the above discussion it should be apparent that the spatial variability in erodibility is a major factor in determining any reasonable dust estimate. Most models therefore have assumed that wind erosion within any given land type is uniform and varies little through time. These models also rely heavily on the user being able to clearly define boundaries for land types and provide sufficient information to define the emission rates for various land types. Unfortunately none of these models are able to describe spatial changes in erodibility within any land type, without large amounts of data, which often cannot be readily obtained for remote study sites.

The modelling/simulation approach taken in this thesis is different, in that it assumes that dust concentration profiles within the study site reflect the characteristics and spatial distribution of dust sources upwind. Thus, the model developed in the following chapters is designed to output detailed dust concentration profiles at any point within the study site. These modelled/simulated dust concentration profiles are then compared to actual dust concentration profiles observed within the study site.

The dust concentration profile is viewed as a signal, which is an amalgam of information about the dust sources and processes in operation during a specific event. By comparing the recreated signal against the actual signal, it is possible to confirm if the modelled signal has all the information contained in the original signal. If the simulation model does not successfully recreate the signal, then this shows that the simulation needs to be modified in some fashion to reproduce the information in the original signal. Such an approach enables the user to begin to understand how the characteristics and spatial variations in dust source areas interact with other processes in operation within the study site, to produce the observed dust concentration profiles.

Part II

Development of the dust source interaction simulation model (DSism)

Chapter 4

Experimental methods, model structure and sensitivity testing

4.1 Introduction

A key issue in the understanding of the spatial aspects of wind erosion is how spatial changes in erodibility affect wind erosion rates and the character of wind–eroded sediments. Neither experimental measurements nor modelling alone provide an adequate answer. The integration of modelling and experimental approaches needs to be considered. In taking this approach it is important to appreciate the limitations imposed by modelling and experimentation. This chapter outlines some of these limitations and provides some initial background to the simulation model developed for this study.

4.2 Experimental implications

A large amount of wind erosion data is available from the study site, as field studies have been undertaken since 1994. While this data has been used to study dust emissions and erodibility of various land types (Nickling et al., 1999; McTainsh et al., 1999), it has not been used to study any of the spatial aspects of wind erosion within the Channel Country. In order to use this data it is important to understand the experimental methods used in its collection and the limitations that these methods place on any simulation model developed for the Channel Country.

4.2.1 Two metre wind vane sampler towers

Wind vane samplers were set up at all Sites A to I, at Diamantina National Park (DNP), as shown in Figure 2.3. These samplers were modified from the original BSNE design of Fryrear (1986) by the addition of a rainhood. The dimension and design of these traps are shown in Figure 4.1. At each site these samplers were set up, as a single array, as shown in Figure 4.2. The heights of the samplers within the array were 0.07m, 0.5m and 2m at all sites except Site A and A1, where the heights were 0.07m, 0.25m, 0.5m, 1m and 2m. Sediments from these arrays were collected on a weekly basis.

A study of the efficiency of the five sampler arrays against three sampler arrays of wind vane samplers within the field site, was undertaken by Love (2001). This study showed less than a 2% difference in the total sediment flux between the two types of arrays. This result suggests that having more samplers does not significantly improve the calculation of sediment flux.

Wind vane samplers were used at this remote field site, since they do not require power to operate, and are easy to construct, repair and service in the field. These samplers have a sampling efficiency of between 86% and 95% under some conditions (Shao et al., 1993a; Fryrear, 1986). However, the efficiency decreases with particle size, with the efficiency dropping to under

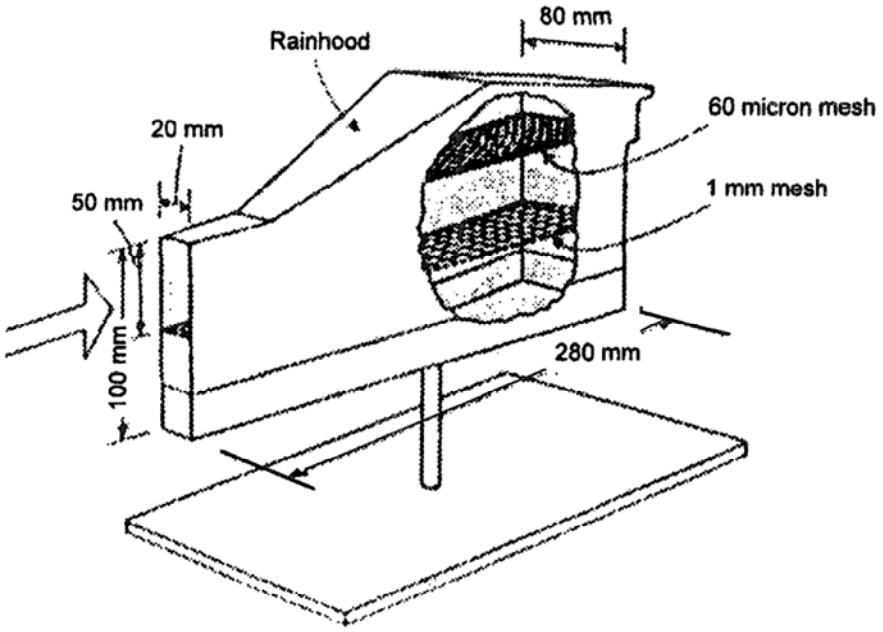

Figure 4.1: Wind vane sampler design used at the study site.

40% for particles less than 10μm (Goossens and Offer, 2000). This drop in efficiency with particle size, Goossens and Offer (2000) attribute to the divergence of flow around the wind vane sampler. Small particles tend to follow these diverted streamlines, rather than being collected by the sampler.

These wind vane samplers were in operation within the study site, during the periods shown in Table 4.1. Table 4.1 also shows what wind vane sampler sites were in operation during the various periods.

Table 4.1: Wind vane sampler operational periods

Start Date	End Date	Sites in operation
12/8/1995	6/11/1995	A,B,C,D,E,F,G
15/7/1996	28/10/1996	A,B,C,D,E,F,G,H,I
9/7/1996	21/7/1997	A,B,C,D,E,F,G,H,I
25/5/1998	17/5/1999	A,B,C,D,E,F,G,H,I
17/5/1999	26/5/2000	A,A1,B,C,D,E,F,G,H,I
26/5/2000	14/5/2001	A,A1,B,C,D,E,F,G,H,I
15/5/2001	29/4/2002	A,A1,B,C,D,E,F,G,H,I

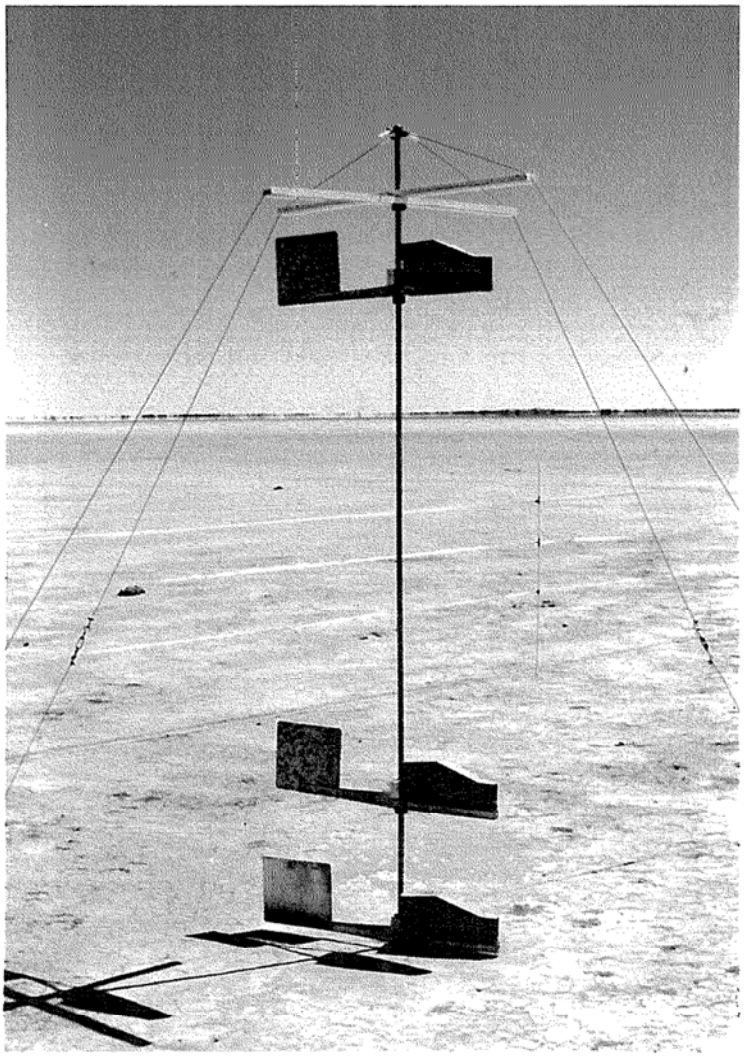

Figure 4.2: 2m tower containing 3 wind vane samplers, as set up at Site A.

4.2.2 Ten metre semi-isokinetic sampler towers

Semi-isokinetic sediment samplers partly overcome the sampling problems associated with the passive wind vane samplers, by providing active suction. This suction, was obtained by connecting a high volume vacuum pump to the sampler, via flow meters and a filter box. The power for the pump was supplied by a petrol generator. The system was automatically activated once the wind speed exceeded a pre-determined threshold for dust entrainment, since it was not possible to tend the equipment on a 24-hour basis. Details of this measurement system are provided by Nickling et al. (1999). These samplers were set up in tower arrays at heights of 2m, 3m, 5m and 10m. A

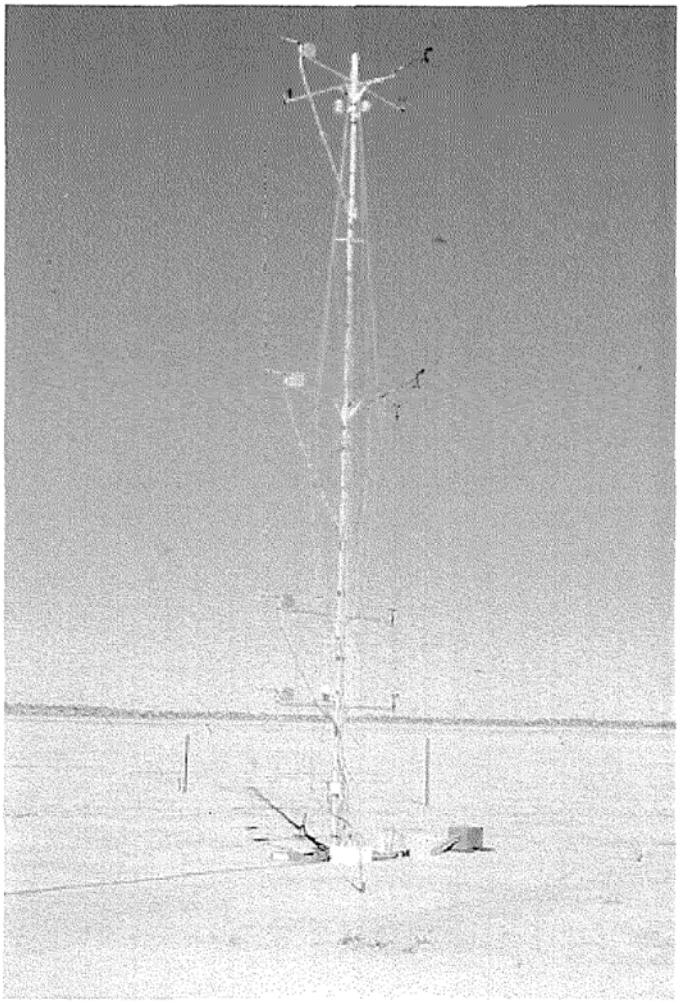

Figure 4.3: 10m tower containing 4 semi-isokinetic samplers, as set up at Site A.

maximum of two 10m sampling towers were set up on the Lake Constance claypan at any one time.

The pre-determined wind speed threshold for activating the sampling system was set to $8ms^{-1}$ (1 minute average), based on field observations. Once activated the samplers would run for a 15 minute period. After this period the wind speed was automatically checked again and if it was still above $8ms^{-1}$ the samplers would then run for a further 15 minutes. If the wind speed, however, was below $8ms^{-1}$ the samplers would shut down. Once shut down the wind speed was checked on a per minute basis and the process began again if the windspeed exceeded $8ms^{-1}$.

These 10m semi-isokinetic were run at the times and sites specified in the

Table 4.2. This table also details the number of events recorded during each of the sampling periods.

The 10m semi-isokinetic towers provide data on vertical dust concentration profiles within the Lake Constance Claypan on an event basis. Whereas the 2m wind vane towers were used extensively throughout the study site, and over the 7 years (1994 to 2000) provide a spatial picture of the wind erodibility of various land types within the study site. As such they are an important tool in establishing the wind erodibility of the various land types. By comparing these two data sets via a simulation model, new information about the spatial aspects of wind erosion was obtained.

4.2.3 Particle size analysis

Once collected, dust samples were analysed using the method of McTainsh et al. (1997) to determine the particle size distribution. This method requires the use of a Coulter Multisizer. Details of the operating principles of the Coulter Multisizer are described in Shao (2000), and therefore are not provided here. However it is important to note that, firstly this analysis can be performed on extremely small samples, which makes it ideal for analysing dust samples collected at the field site. Secondly, that it produces a high resolution particle size analysis of dust samples, since the particles are classified into 256 size classes.

Table 4.2: 10m semi-isokinetic samplers operational periods

Start Date	End Date	Sites in operation	Number of events collected
13/8/1995	25/9/1995	A	12
18/7/1996	1/10/1996	A	9
1997	*No 10m towers in operation*		
1998	*No 10m towers in operation*		
1999	*No events recorded*		
17/8/2000	26/9/2000	A,A1	8

4.2.4 Meteorological measurements

To track variations in wind speed, direction, temperature and pressure within the field site, a weather station was established at Site A. At this weather station, wind speed and direction were measured at each of the semi-isokinetic sampler heights (2m, 3.1m, 5.8m, and 10m), while pressure and temperature data were recorded at 2m and 10m. A data logger recorded the measurements at 1 second intervals for later analysis.

4.2.5 Vegetation and soil surface measurements

Over the monitoring period vegetation cover and surface conditions within the study site were observed to change dramatically on an annual basis (compare Figures 4.4 and 4.5). Similar changes have also been observed within a given season, though not on the same scale (Strong, 2001). It is also clear that vegetation cover and surface conditions on the Lake Constance Claypan can change spatially within a few metres (compare Figures 4.5 and 4.6). Such temporal and spatial changes in vegetation cover and surface conditions are more diverse within the Lake Constance claypan than in an equivalent sized cultivated field where the conditions would be more uniform due to human intervention. Consequently wind erosion within the study site is likely to exhibit quite complex spatial and temporal changes.

Ground surveys were undertaken at various stages during the 94-99 measurement seasons (see Table 4.3 for measurement periods). Initially these ground surveys consisted of taking four 300m transects due North, South, East and West of each wind vane sampler site and recording the frequency of various surface conditions using step points along each transect. These transects were permanently marked, so that the direction was consistent between surveys. Surface conditions were distingushed visually at each step point, and classified according to their surface morphology and vegetation type (if any). Photographic records were kept of each surface condition. The surface conditions were classified into the following broad categories: sealed clay, clay

Figure 4.4: Surface conditions and vegetation cover at Site A during the 1995 season.

Figure 4.5: Surface conditions and vegetation cover at Site A during the 2000 season. Note the dramatic increase in grass cover compared with Figure 4.4.

skins and curls, rippled clay, sand/silt deposits, gibber, wind sheeted, shrubs, standing plants and grass cover. Photographic examples of some of these surface types are given in Figure 4.7. These ground surveys provide a measure

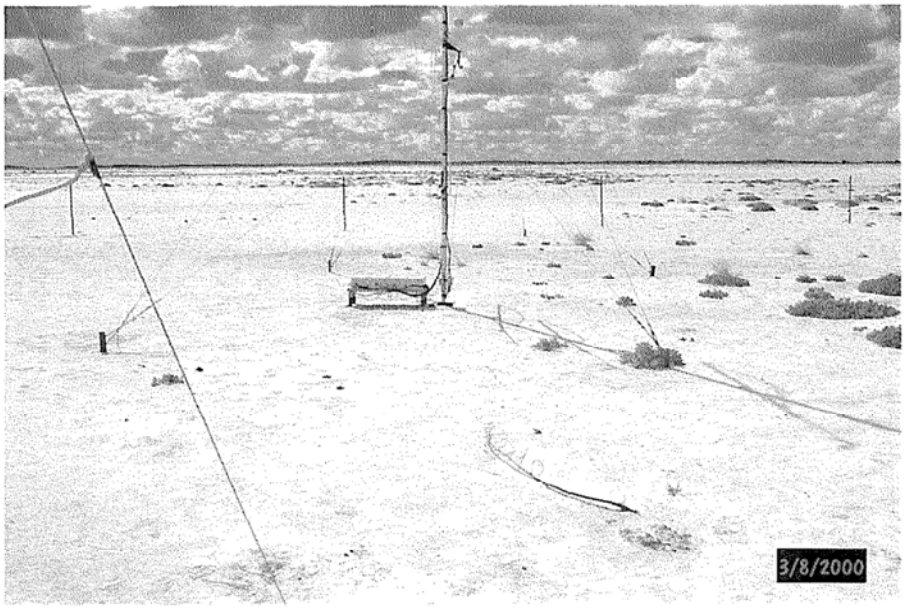

Figure 4.6: Surface conditions and vegetation cover (classified here as small standing plants) at Site A1 during the 2000 season. Note the difference in surface conditions compared with those at Site A (Fig. 4.5).

of the variability in surface conditions within a 300m radius of the wind vane sampler.

Table 4.3: Ground survey measurement dates

Dates over which surveys completed	Sites included in survey
12/8/1995–15/8/1995	A,B,C,D,E,F,G
2/11/1995–4/11/1995	A,B,C,D,E,F,G
14/7/1996–17/7/1996	A,B,C,D,E,F,G,I
26/10/1996–29/10/1996	A,B,C,D,E,F,G,I
21/7/1997–24/7/1997	A,B,C,D,E,F,G,I
24/11/1997–28/11/1997	A,B,C,D,E,F,G,I
11/5/1998–14/5/1998	A,B,C,D,E,F,G,H,I
8/7/2000-9/7/2000	A,B,C,D,E,F,G,H

In the 2000 field season, 500m upwind transects were measured and the surface conditions were recorded every metre after wind erosion events (i.e., they

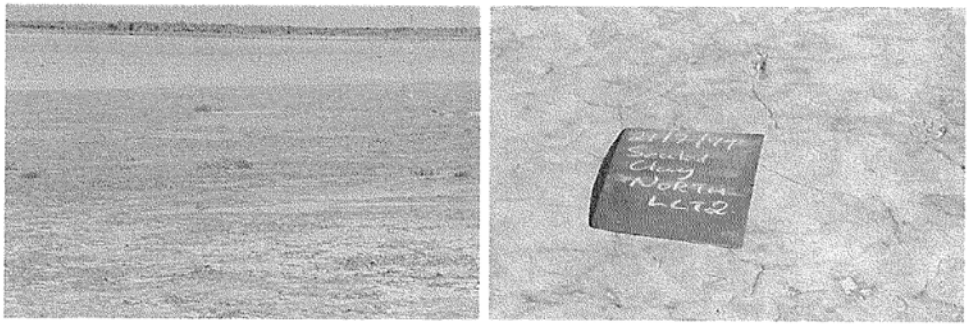

(a) Clay curls and skins surface

(b) Sealed clay surface

(c) Silt and sand deposit

(d) Rippled clay surface

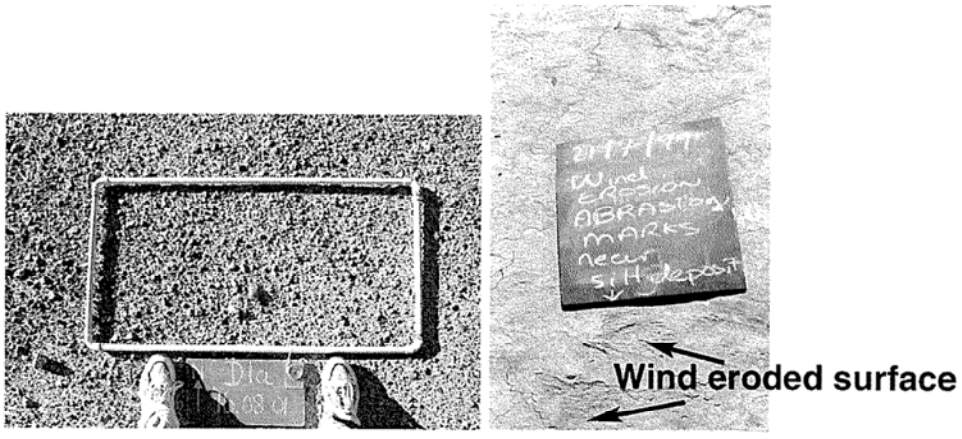

(e) Gibber surface

(f) Wind sheeted surface

Figure 4.7: Photographic examples of different surface classifications

provide **post event surface data**). The same methodology, as outlined previously for the ground surveys was used to classify surface conditions along these transects. The direction of these transect was determined from wind direction data recorded during the wind erosion event.

In contrast to the ground survey, these upwind transects provided useful information about upwind spatial changes in surface conditions between events. A major drawback with these transects is that they usually only provide information on vegetation and surface conditions after the dust event. However, if successive events had winds from the same direction then information would be available on pre and post upwind vegetation cover and surface conditions for one of the two events.

Measurements of Loose Erodible Material (LEM) were made on several of the surfaces identified in the ground surveys, during May 1995, July 1996 and July 2000, using a "Succo", which is shown in Figure 4.8. The "Succo" consisted of a portable vacuum pump connected to a loose material trap via a vacuum hose. The hose was held at 2.5cm above the soil surface as it was passed over a $1m^2$ area of the surface, at a constant rate. After passing over the whole sample area, the material was collected for weighing. Three repetitions were completed for each surface type. The LEM data collected was used as a measure of the relative erodibility of the soil surface.

4.3 Dust source interaction simulation model (DSism) – model structure and assumptions

The objective of the simulation model developed here was to encapsulate the environmental influences upon wind erosion outlined in Chapter 2. However, the ability of the simulation model to describe this behaviour is dependent on the availability of experimental data for any given site and other mathematical and computational considerations. This section details both the assumptions and structure of DSism in terms of the above considerations. In

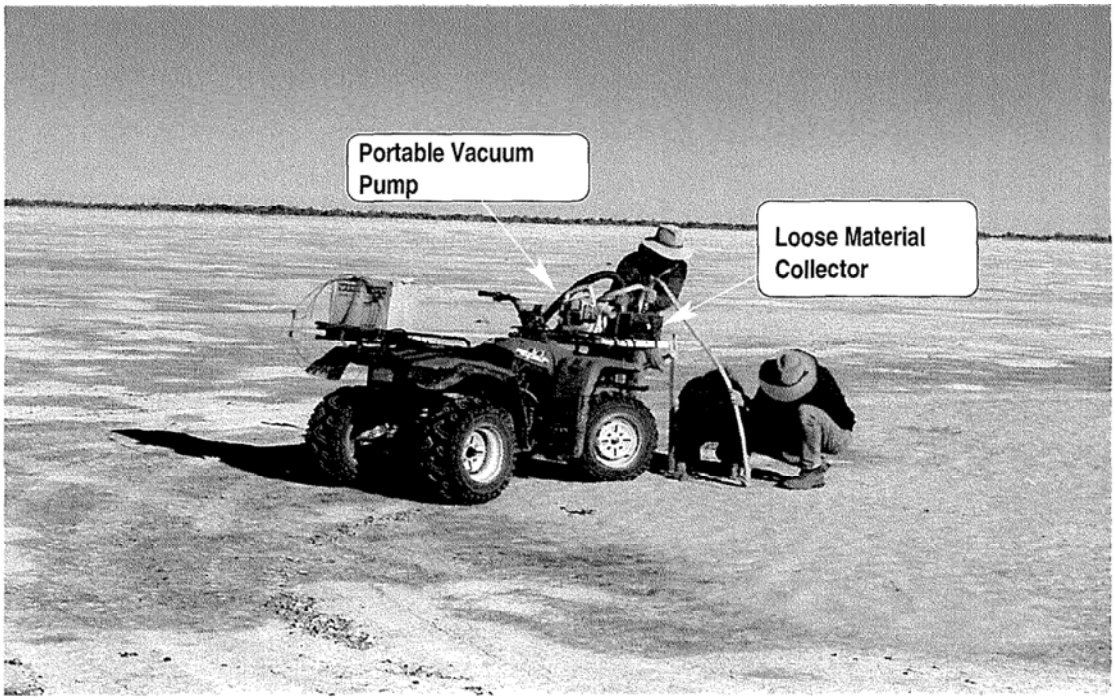

Figure 4.8: "Succo" in operation at the study site.

particular, it describes how DSism encapsulates dispersion/advection within the local area. As such it is largely based on the information presented by Butler et al. (1996).

One means of modelling the relationship between the various environmental influences is to solve the dispersion/advection equation:

$$\frac{\partial C}{\partial t} + u\frac{\partial C}{\partial x} + v\frac{\partial C}{\partial y} + w\frac{\partial C}{\partial z} = S + \frac{\partial}{\partial x}K_x\frac{\partial C}{\partial x} + \frac{\partial}{\partial y}K_y\frac{\partial C}{\partial y} + \frac{\partial}{\partial z}K_z\frac{\partial C}{\partial z}, \qquad (4.1)$$

where u, v, w are the wind components in the x, y, z directions respectively, $C = C(x, y, z, t)$ is the concentration at time t. Velocity fluctuations due to turbulence are included in the K's, while $S = S(x, y, z, t)$ is an emission term. To obtain analytical solutions to Equation (4.1) from a single point source requires a significant number of simplifying assumptions (Zannetti, 1990; Eltayeb and Hassan, 2000). Even numerical schemes designed to solve Equation (4.1) are subject to numerical instabilities (Hanna et al., 1982). The simplest analytical solution to Equation (4.1) is the Gaussian plume solution, which is achieved under the assumption that K, u, v, and w are constant (Hanna et al., 1982). This solution has been used in a number of air pollution

modelling applications, since it is conceptually simple, well understood; and extremely robust (*robust in the sense that accurate estimates can be achieved using a minimum of data and when some of the model assumptions have been violated*).

The Gaussian Plume dispersal model is therefore at the heart of the Dust Source Interaction Model (DSism) developed here. However in order to use this type of model at the study site, and make use of the experimental data available several assumptions are required.

As no data is available on real time changes in emission rates or dust concentrations from the study site, it was assumed that dust sources on any given land type within the study site had a constant emission rate (Q) within an event. This assumption has several implications for other aspects of DSism. Initially it implies that using real time data for wind speed and direction in the model would be difficult to justify, as it would not be possible to verify predicted changes in Q. Thus wind speed and direction values used in the model were averaged over the duration of any single dust event. In addition since wind speed and direction measurements were only recorded at one site, it was assumed that these were uniform throughout the study site. This assumes that small climatological changes in wind speed and direction are not a major factor within the study site.

By using a Gaussian Plume model, it is assumed that the dispersion of dust in the vertical and crosswind directions follow a Gaussian distribution and is independent of particle size or shape. This assumption is known to break down approximately 20km from the source (Hanna et al., 1982; Zannetti, 1990). However by confining DSism to the local study site (less than 20km) this issue is less important. Another consequence is that the effect of particle shape is not included in DSism. If at some future time data becomes available on how particle shape affects the dispersion, this could be built into the model by modifying the dispersion parameters used in DSism.

Initially several other assumptions were made to simplify DSism. The relaxation of some of these assumptions will be considered later in this thesis. These assumptions are now discussed in detail.

Since the Lake Constance Claypan forms the major part of the study site and has low relative topographic relief, it was initially assumed that the study site could be viewed as a flat surface. Thus in terms of the model, it can be assumed that the effective release height of the dust is 0m, that is, all sources are assumed to be ground based. It would be possible to relax this assumption in the future, should more detailed 3D temporal topographical data become available.

To further simplify the modelling, it was assumed that changes in erodibility due to vegetation, crusts, roughness, rainfall and saltation can all be accounted for by changes in Q. In addition, it was assumed that no material is re-entrained from the surface and that this effect can also be accounted for by spatial changes in Q. Initially it will also be assumed that there is no deposition. While deposition is obviously an important wind erosion process and is included later, its absence at this stage of the thesis will enable the spatial and dispersion aspects of DSism to be explored prior to the introduction of particle size affects. Its absence also makes it easier to verify that DSism conserves mass.

Given these assumptions, Hanna et al. (1982) state that the average concentration $C(\mu\text{gm}^{-3})$ at a point (x, y, z) downwind of a point source is given by:

$$C(x,y,z) = \frac{Q}{\pi\sigma_y\sigma_z u}\exp\left(\frac{-y^2}{2\sigma_y^2}\right)\exp\left(\frac{-z^2}{2\sigma_z^2}\right), \tag{4.2}$$

where z is the height above ground, y is the distance cross wind from the point source, u is the average wind speed, and σ_y and σ_z are the Pascal dispersion parameters in the y and z directions respectively.

The dispersion parameters (σ_y and σ_z) are assumed to be functions of downwind distance x and the turbulent stability of the system. Thus, the functional form of these parameters is based on the pasquil stability categories outlined

by Hanna et al. (1982). Initially, it is assumed that the dispersion parameters follow the functional form outlined by Zannetti (1990) for rural neutral stability conditions. Mathematically they take the form:

$$\sigma_y(x) = \frac{0.08x}{\sqrt{1+0.0001x}}, \quad \text{and} \tag{4.3}$$

$$\sigma_y(x) = \frac{0.06x}{\sqrt{1+0.0015x}}. \tag{4.4}$$

4.3.1 Dust source configuration used in DSism

There is a need in this project for DSism to be flexible in dealing with spatially discrete dust sources. This is illustrated by Figure 4.9 which provides an aerial view of a typical distribution of dust sources in the midwest of the USA during a dust event. In this figure, the dust sources are scattered and quite distinct, in addition they appear to be of variable size and strength.

To achieve flexibility a point source is used within DSism to represent the basic dust source. Other sources such as line sources, were modelled by packing these point sources together. By compressing/expanding this packing and also increasing/decreasing the emission rate Q, it is possible to simulate areas of high and low erodibility.

In applying this idea of point sources to field conditions, the field site was divided up into a number of crosswind lines (Fig. 4.10). Each of these lines is assumed to consist of a number of distinct point dust sources. This approach allowed the emission rate across any line to be easily varied by altering the emission rate of any of the point sources. DSism was then able to simulate the change in erodibility with changes in land type. It also allowed the density of source lines to be compressed or expanded, enabling the effective emission rate of any area to be altered. Thus, DSism can simulate areas of high and low erodibility within a given land type.

It is further assumed that the concentration of dust does not affect the emission rate of a source. In reality, this assumption, is simplistic, since the results of Bagnold (1941), McEwan et al. (1992) and Gillette (1999) suggest that

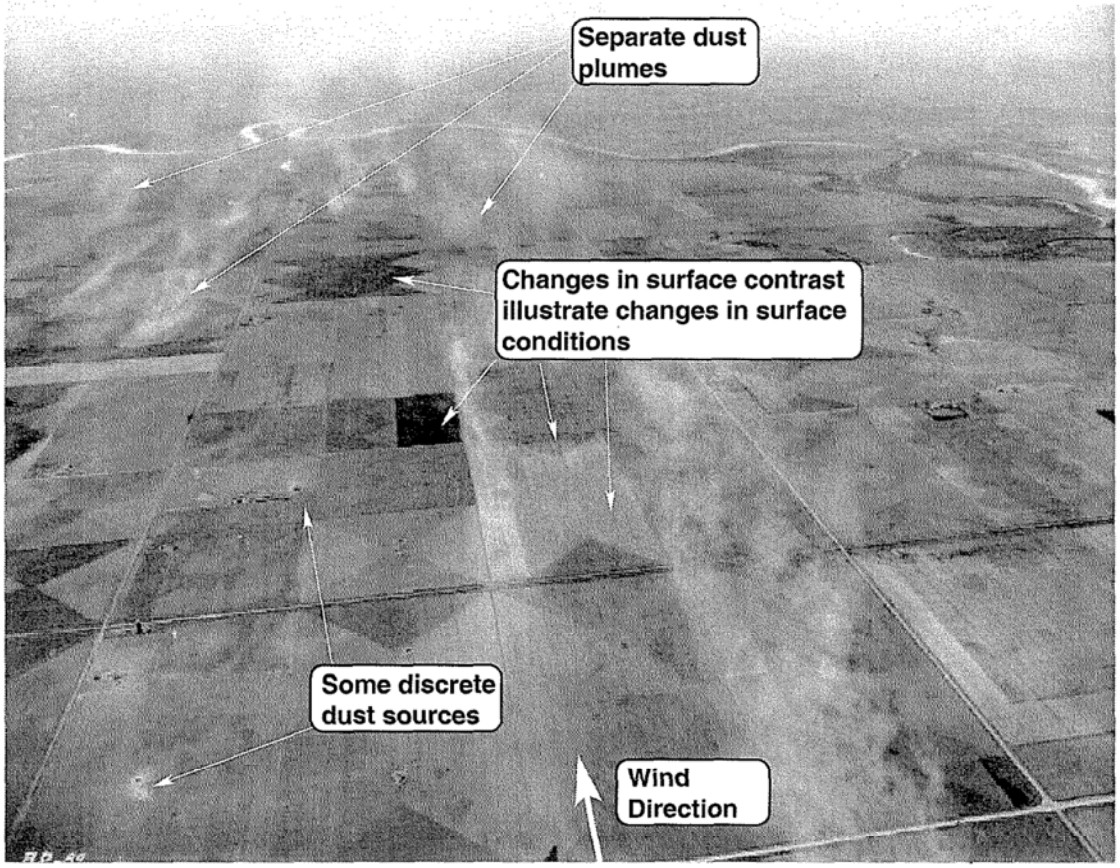

Figure 4.9: Aerial photo showing the spatial variation of wind erosion sources. (Photo: USDA).

a feedback mechanism operates between the dust plume and the wind to limit transport rates (see Section 2.3.2.4).

4.4 Sensitivity testing of DSism

To understand the influence that dust source area separation has on the distribution of dust within the local area, sensitivity testing is required. In this sensitivity testing a variety of different source structures were used. The following sections detail the results of this extensive sensitivity testing. In particular, it examines the effect that different source structures have on both the crosswind and downwind dust concentration profiles. The vertical dust concentration profile is not discussed here, but will be discussed once deposition

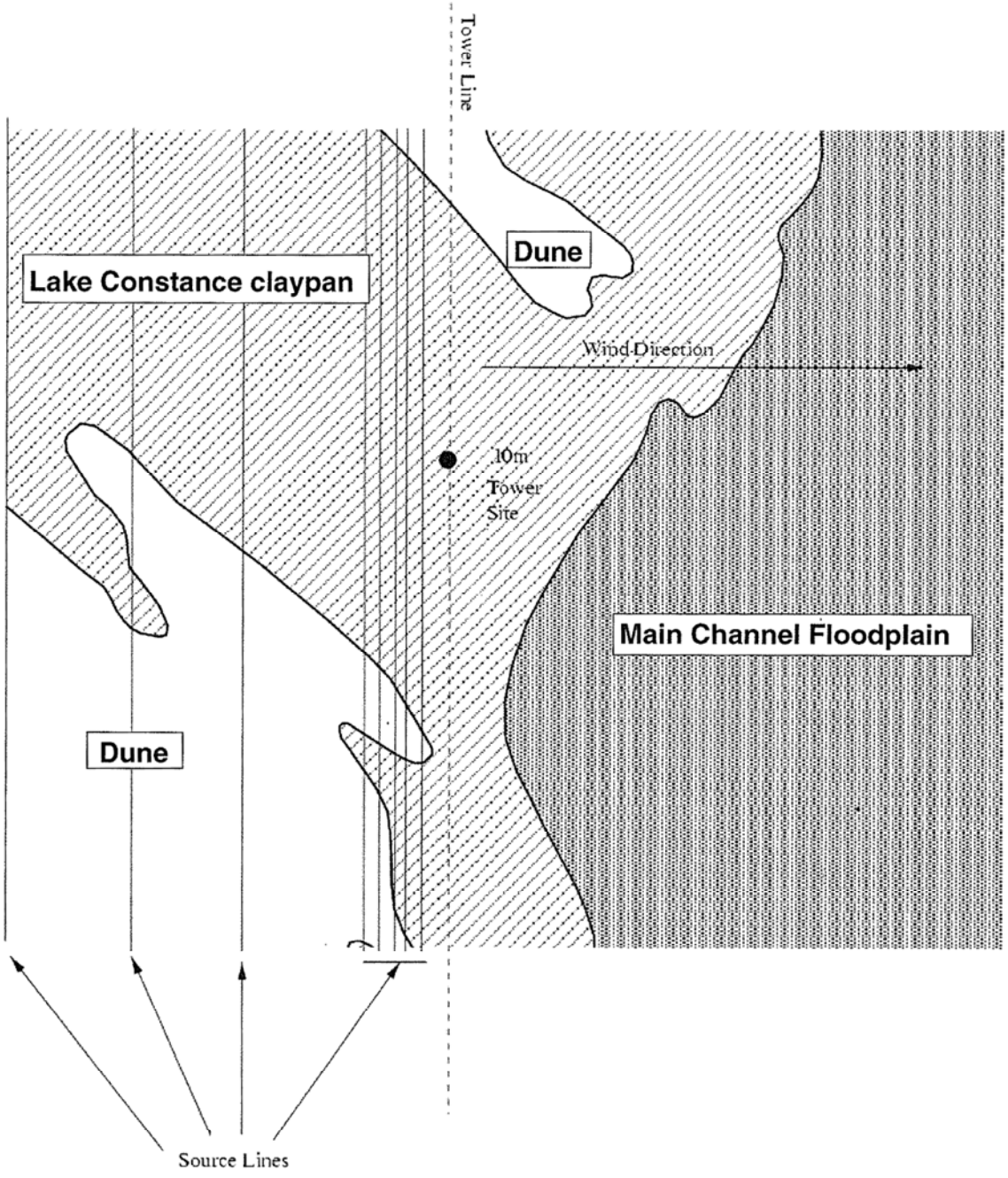

Figure 4.10: Plan layout of sources, showing how lines are used to approximate sources within the study site.

has been added to DSism in a later chapter.

4.4.1 Dust source area separation

To understand the effect that source area separation can have on simulated dust concentrations, the source structure shown in Figure 4.11(a) was used to seed DSism. The emission rate of the point sources that constitute the line was set to $10\mu gs^{-1}$. The separation of the source lines was varied and the predicted crosswind profiles recorded at various downwind distances. However, only the 10km downwind profiles are reported here (Fig. 4.11(b)), as they are indicative of the behaviour observed at the other distances.

Figure 4.11(b) shows the three distinct crosswind dust concentration profiles depending upon source area separation. These three distinct profiles are classified as:

Profile A – the dust plumes from each source has fully mixed producing a crosswind dust concentration profile that is essentially the same as a single source profile (the solid line in Figure 4.11(b)).

Profile B – dust plumes from each source have partially mixed producing the flat crosswind dust concentration profile (the dashed line in Figure 4.11(b)).

Profile C – the dust plumes from each source have just started to mix, thus producing two distinct dust concentration peaks (blue dotted line in Figure 4.11(b)).

Each of these crosswind profiles represents various levels of interaction between the dust source areas. In Profile C, each source produces distinct peaks. Thus, the dust sources are sufficiently far apart for the dust from each source to have only slightly mixed 10km downwind. This mixing increases as source separation is reduced, until Profile B is reached. As source separation is further reduced, the separate plumes completely combine and the final profile (Profile A) is indistinguishable from a single point source profile or simple Gaussian distribution.

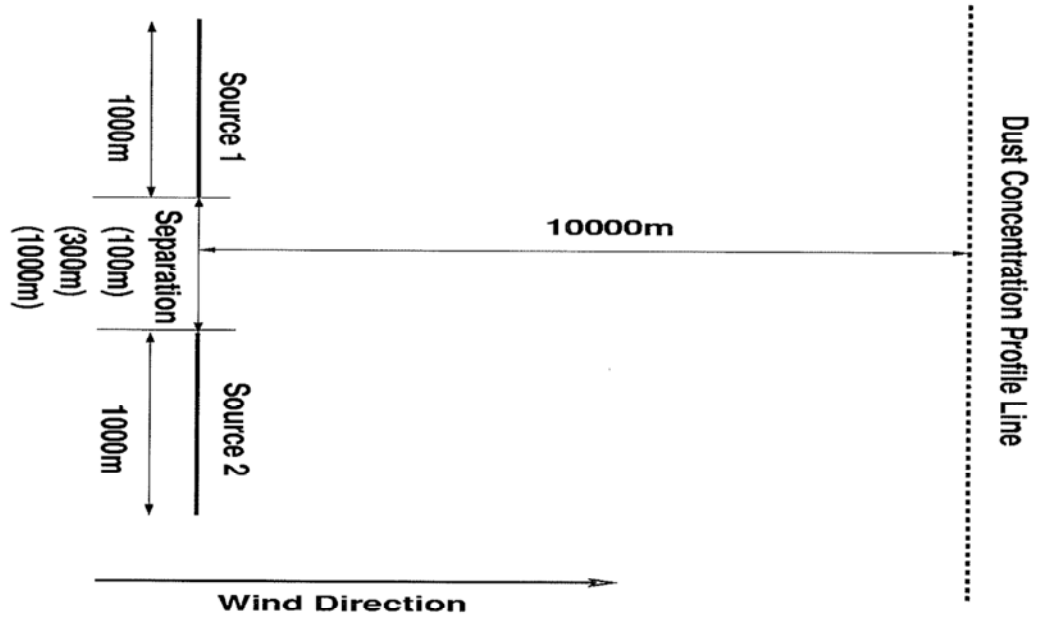

(a) Plan showing the dust source configuration used to produce the profiles shown in (b)

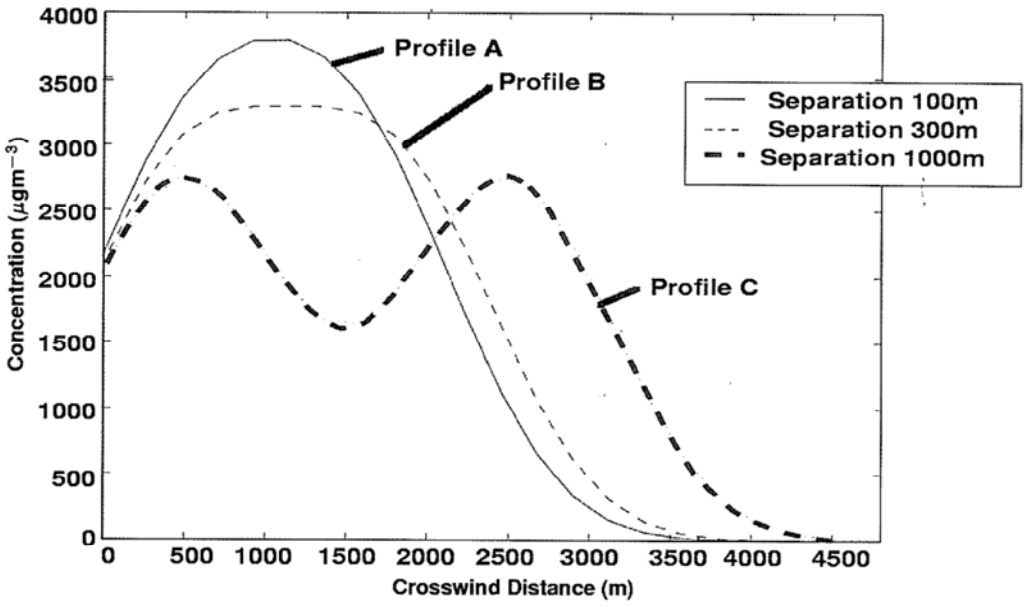

(b) Crosswind dust concentration profiles taken along the dotted line shown in (a) at a height of 10m.

Figure 4.11: Crosswind dust concentration profiles corresponding to the three different source separations shown in (a). These profiles are taken along the dust concentration profile line shown in (a), which is located 10km downwind of the sources.

The above simulations illustrate the limitations of the Knight et al. (1995) model. This model assumes that given land types or source areas are of uniformly erodibility. The simulations above indicate that this assumption is only valid if the sources have a small spatial separation in relation to the downwind distance of the monitoring point. This assumption of uniform erodibility is not likely to be valid for the Lake Constance claypan. It is only by using a simulation model, such as DSism, which can simulate the effect of spatial changes in erodibility on the resulting dust concentration profiles, that the spatial nature of wind erosion within the study site can be fully appreciated.

Lu and Shao (2001) claimed that the differences between their modelling results and those of Shao and Leslie (1997) (for the same event), could largely be accounted for by spatial variations in emission rates across each of the grids used in the model. The simulations presented here not only support this conclusion, but illustrate just how significant such variations can be. In particular, they show that the distribution of dust within the local area depends on the relative positioning of each source within it. Therefore, further illustrating why it is important to fully understand how spatial variation in dust source areas at the local scale propagate up to the continental scale.

Another advantage of using a Gaussian Plume model as the base for DSism is that it is able to produce 3 dimensional dust concentration profiles (Fig. 4.12(a)). This allows both the crosswind and vertical dust concentration to be modelled for any given dust source configuration.

4.4.2 Downwind changes in dust concentration

In this section, sensitivity testing is used to explore how dust concentration changes downwind as the plumes from various sources begin to mix. In undertaking these sensitivity tests, a variety of dust source configurations similar to those shown in Figures 4.13(a), 4.14(a), 4.15(a) and 4.16(a) were used. However, once again, only a small number of simulations are reported here, but these have been chosen as they are indicative of the behaviour observed

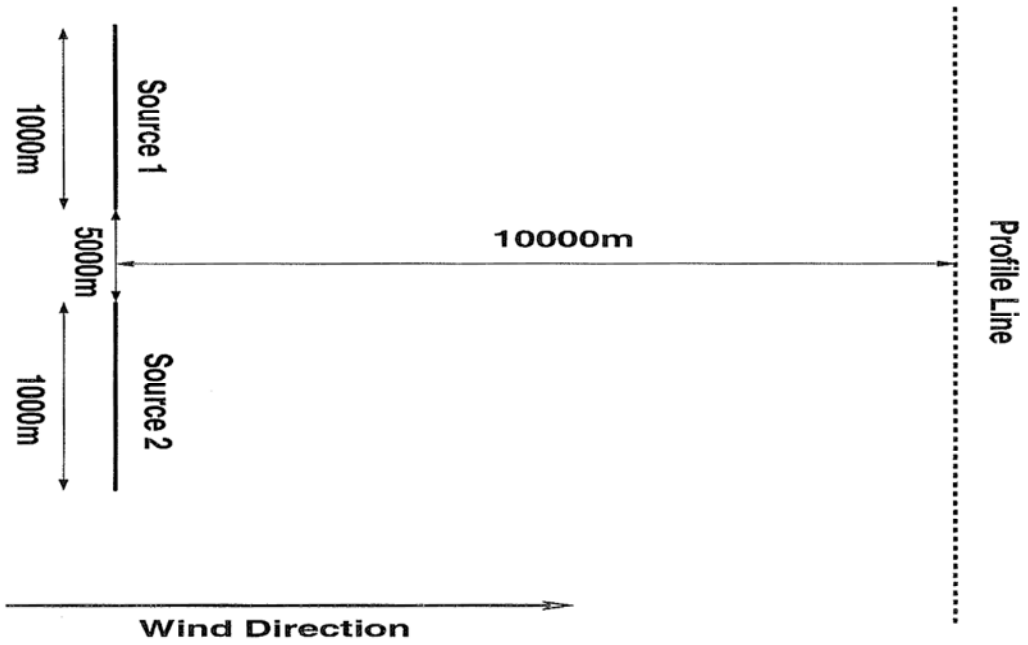

(a) Plan layout of the dust source configuration used to produce the 3D profile shown in (b).

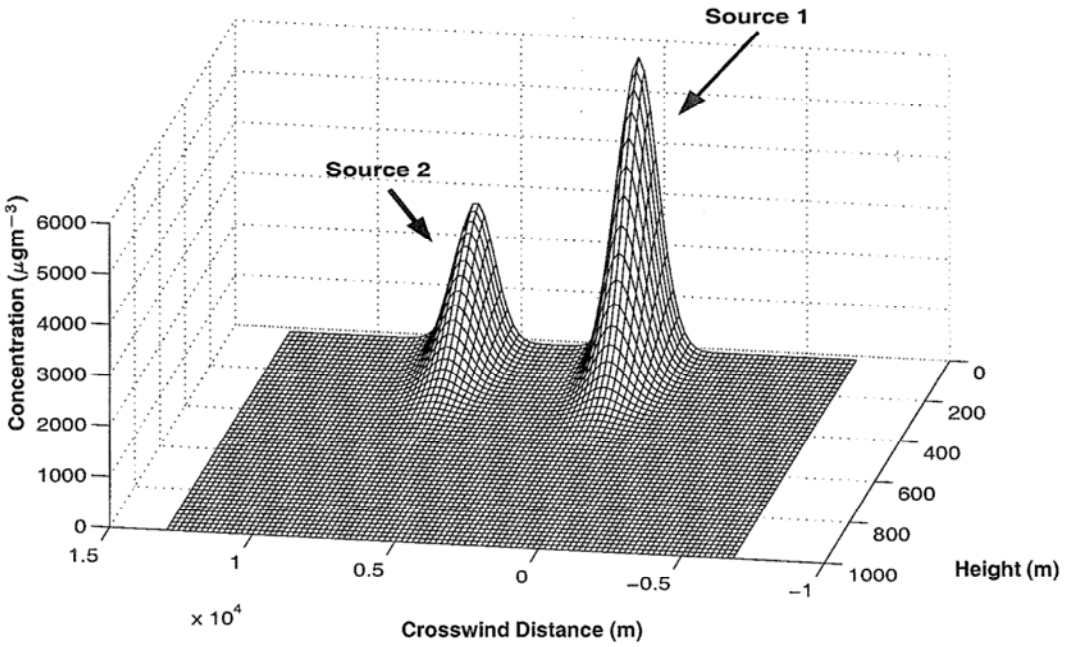

(b) 3D dust concentration profile taken along the dotted line shown in (a)

Figure 4.12: Three–dimensional dust concentration profile produced as a result of source layout shown in (a). Source 1 consists of point sources with emission rate $20\mu gs^{-1}$ and Source 2 consists of point sources with emission rate $10\mu gs^{-1}$.

in all simulations.

Figures 4.13 and 4.14, show the change in dust concentration with distance downwind, on different downwind profile lines. In Figure 4.13, the profile is measured between the two line sources, and there is a gradual increase in dust concentration as dust from the two source areas combine until a maximum concentration is reached. There is a gradual decrease as the plumes disperse and mix. In contrast, in Figure 4.14, the profile line is in the centre of a source, and the dust concentration decreases, until the dust from the second source begins to mix, producing a slight increase in the dust concentration before dust concentration decreases again.

This plume behaviour is consistent with how one might expect two dust sources to combine. In the centre of two sources one would expect an initial build up in concentration, as material is transported and dispersed into this region. This increase should continue, until dust from the two sources are well mixed. After this point is reached, dust is still being dispersed throughout the plume, so there should be a slow decrease in the concentration. In the centre of source 1 however, the concentration should initially decrease as dust is mixed and dispersed throughout the plume. This continues until dust from source 2 begins to mix in. At this point there should be a slight increase in the material present, thus causing the concentration to slow its rate of decrease (or to actually start increasing) at that point.

Figure 4.15 illustrates how dust plumes from sources at two different distances downwind mix in the crosswind direction as they travel downwind. Initially there is little mixing between the sources 5km downwind. However, when the plumes have travelled an extra 5km a substantial amount of mixing can be seen. It is also noticeable that the concentration peaks have been equalising out between the plumes, as more material is dispersed throughout the plume (crosswind and vertically). This continues until, approximately 20km downwind of the source, the crosswind concentration profile is much flatter. It is this point where the assumption of the broadscale model of Knight et al. (1995), regarding homogeneity of the plume, comes closer to being valid.

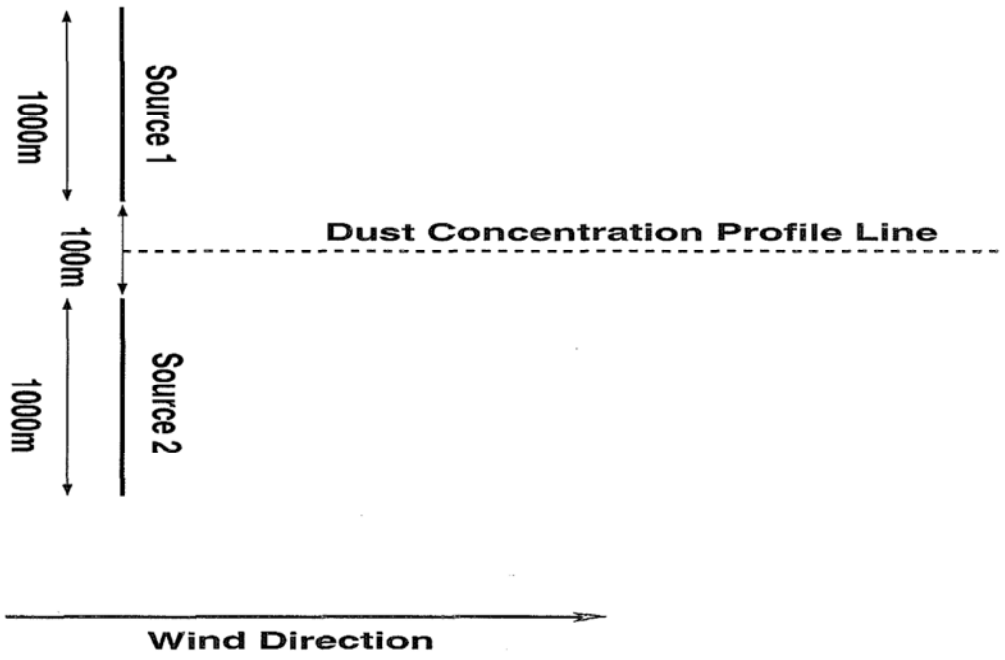

(a) Plan layout of the dust source configuration used to produce (b)

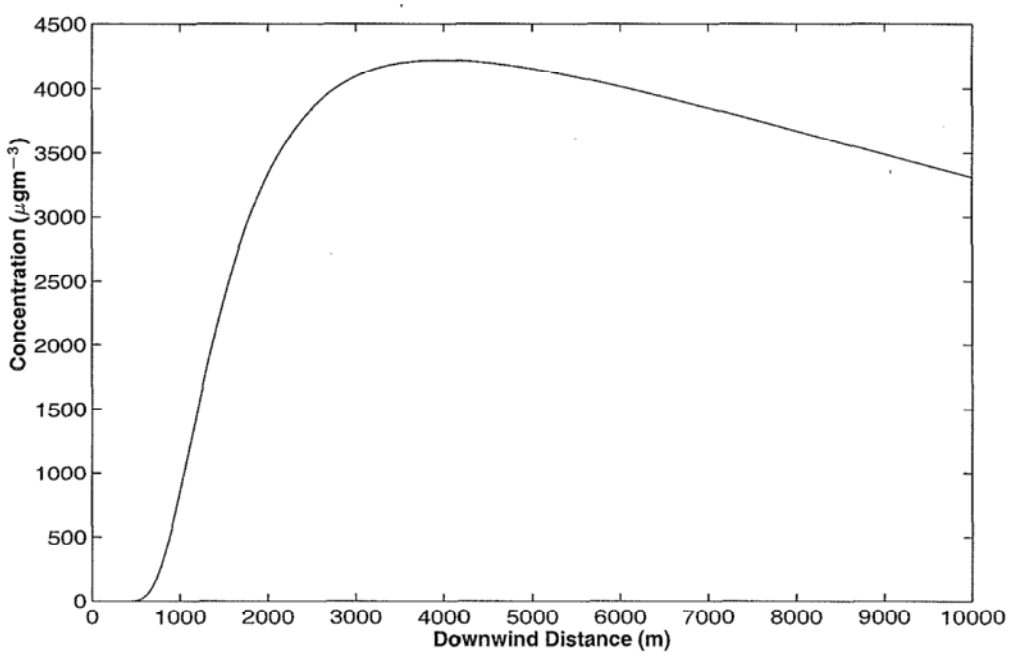

(b) Downwind dust concentration profile as taken along the dotted line shown in (a) at a height of 10m

Figure 4.13: Downwind concentration profile taken halfway between the two sources. Source details: two 1 km line sources where each of the point sources that make up the line are set to $10\mu gs^{-1}$.

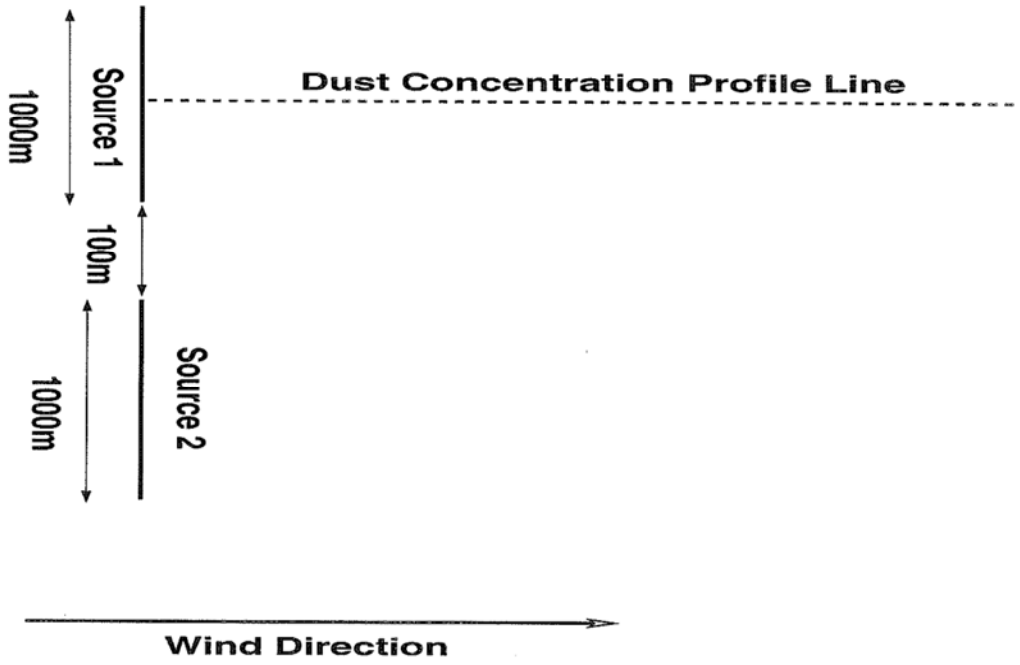

(a) Plan layout of the dust source configuration used to produce (b)

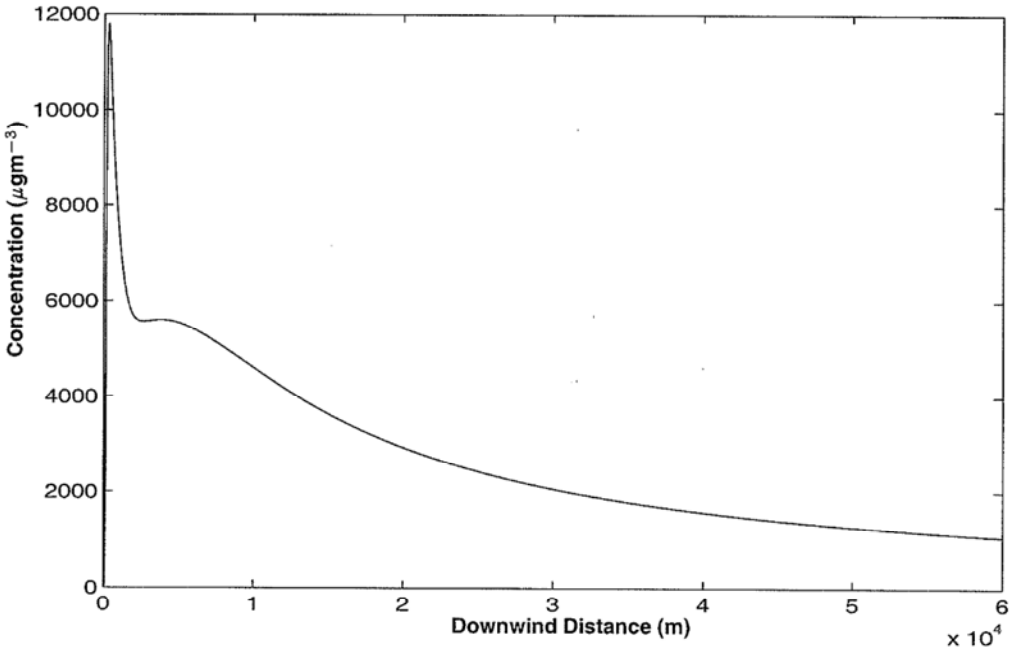

(b) Downwind dust concentration profile as taken along the dotted line shown in (a) at a height of 10m

Figure 4.14: Downwind concentration profile taken in the centre of the first source. Source details: two 1 km line sources where each of the point sources that make up the line are set to $10\mu gs^{-1}$.

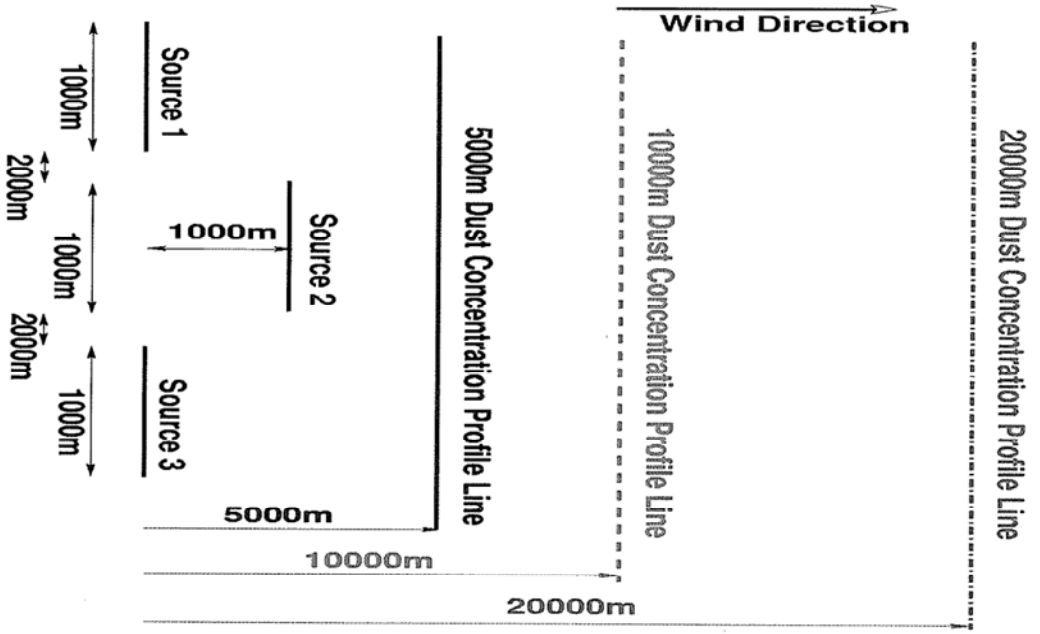

(a) Plan layout of the dust source configuration used to produce the crosswind profiles shown in (b).

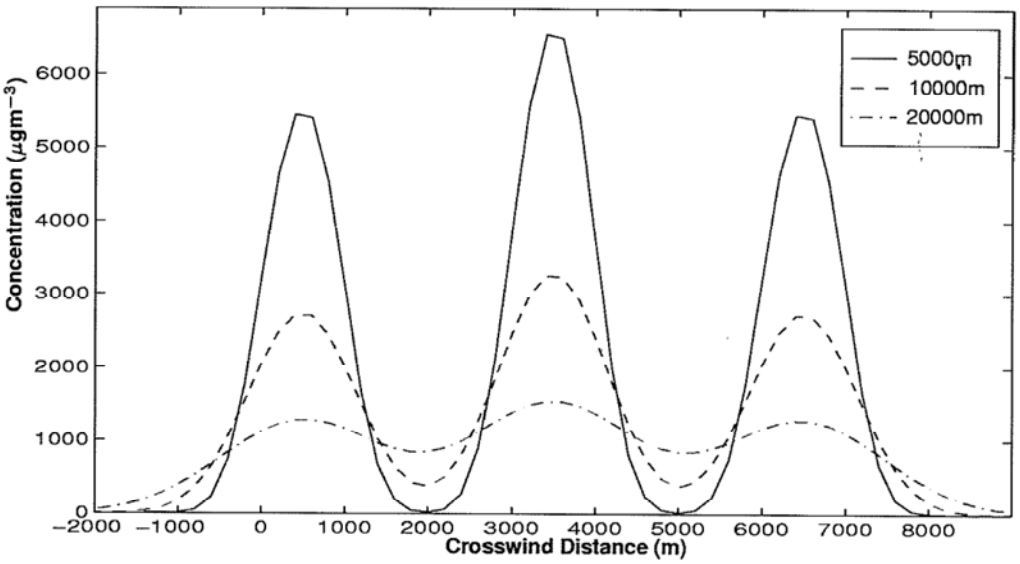

(b) Three crosswind dust concentration profiles taken along the dotted line shown in (a) at the distances indicated in (a) and a height of 10m.

Figure 4.15: Crosswind dust concentration profiles taken at three different downwind distances. Source details: each source is 1km in length and made up of point sources within an emission rate of $10\mu gs^{-1}$.

The addition of a third line source on a crosswind line downwind of the first set of sources, has little effect on the behaviour outlined above. However, by comparing the results achieved by adding this third source at different downwind distances (Fig. 4.16) from the initial two sources, one can clearly see the dispersion effects predicted by the model. In particular in the 5km case, it is noticeable that the material from the centre dust source has not dispersed as much as the 1km case.

4.4.3 Dust source area strength

The results presented so far, indicate that in DSism the separation of the sources and downwind distance are important factors in determining how and where the dust plumes from each dust source area merge. This information will be important in analysing the field data presented in Chapter 8. Another factor that will affect how the plumes merge is the emission strength Q of the various sources. To explore the effect that relative changes in emission rates have on the crosswind dust concentration profile, sensitivity testing was undertaken using dust source configurations similar to those shown in Figures 4.17 and 4.18.

If one source is significantly stronger than another, the weaker source has little effect on the dust plume from the major source, except to slightly skew the crosswind dust concentration profile. The amount of skewing depends upon the separation and relative strengths of the sources. This skewing almost disappears as the further mixing of the sources occurs. If however, the sources are of similar (but not equal) strength, the distinct profiles outlined in Section 4.4.1 can still be observed (Fig. 4.17). The major difference being that if the same separation is maintained that produced profile B in Section 4.4.1, but with different source strengths, the resulting profile no longer produces a large flat crosswind concentration, but rather a skewed crosswind concentration profile. The amount of skewing is dependent on the separation and relative strength of the two sources. However, if the source strength remains

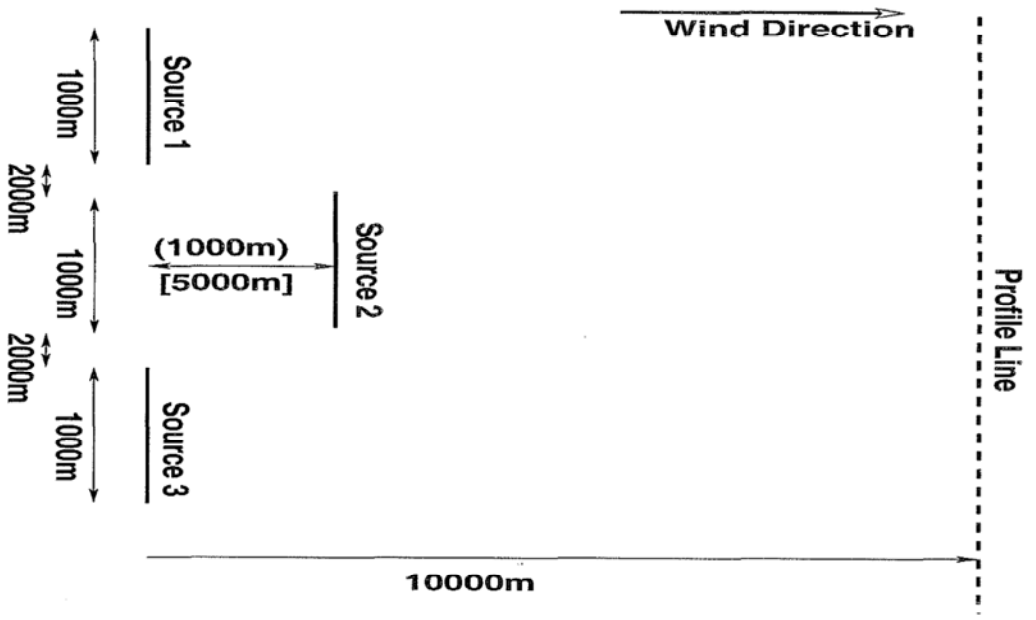

(a) Plan of the dust source configuration used to produce the profiles shown in (a)

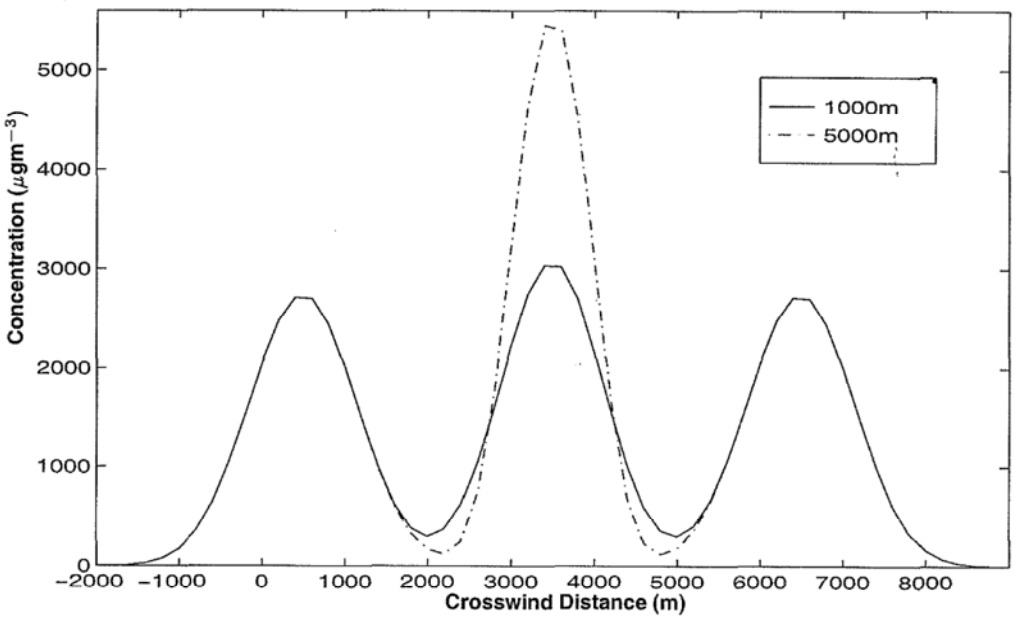

(b) Crosswind dust concentration profile showing the affect of moving source 2 in (a). Profile is taken along the dotted line at a height of 10m.

Figure 4.16: Crosswind dust concentration profiles taken 10 km downwind of sources 1 and 3. Source details: all sources 1km in length and have the constituent point sources emission rate set to $10\mu gs^{-1}$.

equal, but is increased (or decreased), the large flat crosswind concentration is maintained (Fig. 4.18). Such behaviour is consistent with Equation (4.2), as doubling Q in this equation will simply result in doubling C. Such a result indicates that the DSism is correctly implementing the Gaussian Plume model.

In DSism, it is assumed that crosswind dispersion remains constant, thus the two plumes merge at the same point, regardless of source strength. However, whether this merging actually occurs in nature, is open to question, as the dispersion rate maybe altered as the result of the increased particle interaction which would accompany any increase in source strength. Thus, if sufficient material is present in the plume, dispersion rates within the plume could be significantly larger than those modelled. The opposing argument is that inside the plume restoration forces, which act to limit the amount of material in the plume, will balance out any increase in the dispersion rate. Such interactions are not included in DSism, at present.

4.5 Summary

Information presented at the start of this chapter shows that the information contained in the Diamantina National Park wind erosion database is quite diverse and contains meteorological, 2m tower, 10m tower, and particle size data, with observations about the surface and vegetation conditions. Such information will be important in analysing the performance of DSism under field conditions. This chapter also detailed the basic structure and assumptions on which DSism is based.

The sensitivity results presented in this chapter, indicate that DSism can capture the important features of the dispersion process as dust from discrete sources merge into a single profile. DSism can use spatial and emission source data effectively to describe variations in dust plume concentration within the study site. The model is therefore able to predict changes in the local dust concentration profiles as a result of changes in environmental conditions. It

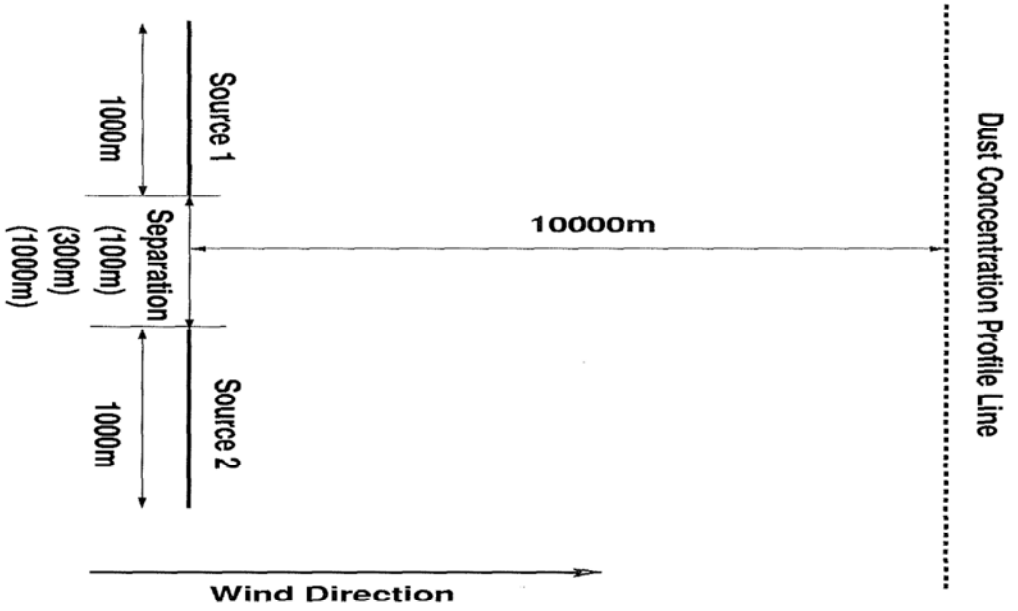

(a) Plan layout of the dust source configuration used to produce the profiles shown in (b)

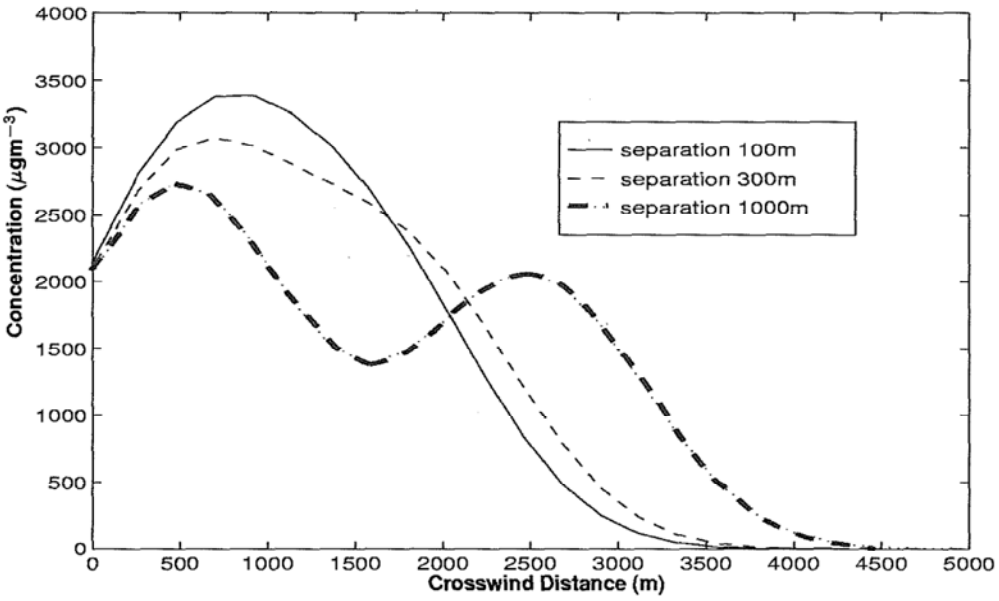

(b) Crosswind dust concentration profiles that correspond to the three different source separations shown in (a). Each profile is taken along the dotted line shown in (a) at a height of 10m.

Figure 4.17: Crosswind profiles corresponding to the three separations shown in (a). Source details: two 1km line sources, the first being made up of point sources emitting at a rate of $10\mu gs^{-1}$, while the second has point sources emitting at a rate of $7.5\mu gs^{-1}$.

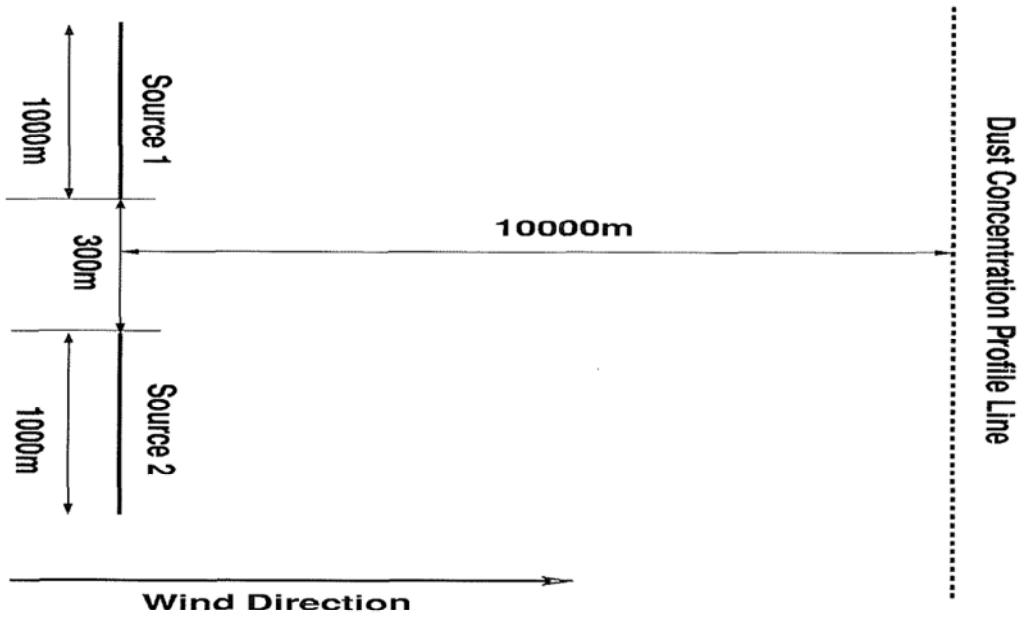

(a) Plan layout of the dust source configuration used to produce the profiles shown in (a)

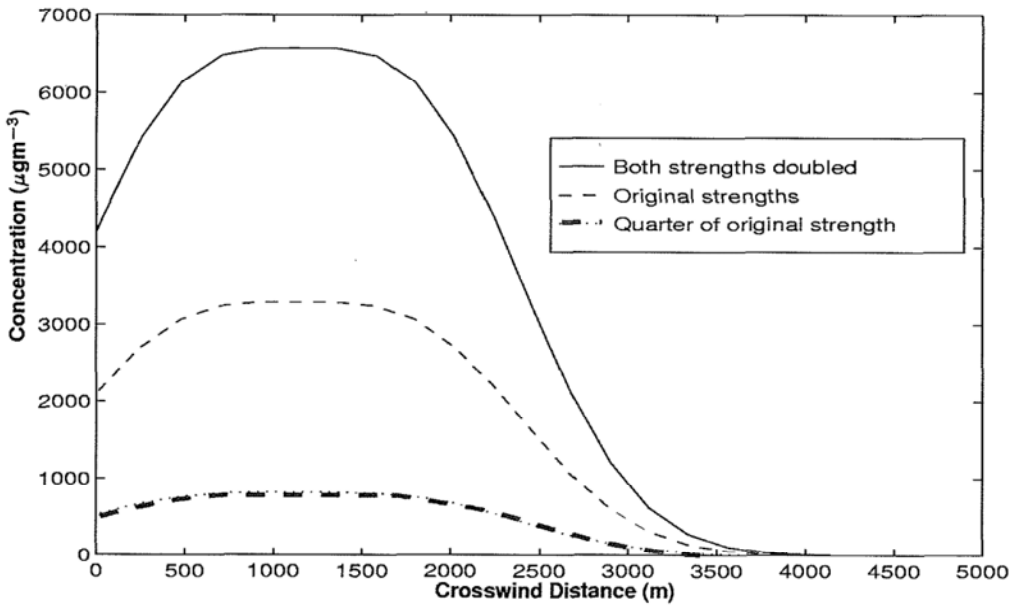

(b) Crosswind dust concentration profiles for each source combination used. Profiles taken along the dotted line shown in (a) at a height of 10m.

Figure 4.18: Three crosswind dust concentration profiles produce using three different source combinations. Source details: two 1 km line sources of equal strength. The original source lines were made of point sources emitting at $10\mu gs^{-1}$. These were than doubled and quartered to produce the other profiles.

also enables researchers to produce 3D visual images of how spatial changes in erodibility are likely to affect the spatial dust concentration within the study site.

The simulation results presented here represent a key step in conceptualising the signal analogy used in this thesis. It shows that the crosswind and downwind concentration profiles, clearly depend on the spatial distribution of upwind sources. This observation also suggests that the dust concentration profile contains information about the sources upwind. If it is possible to find a means (or a method) to unlock this information, vertical dust concentration profiles will become a rich source of information about the wind erosion process at the local scale. It is this concept that makes the ideas behind the DSism approach so useful.

It is important to note that the experimental data collected within the study site does not allow for field verification of DSism predicted crosswind and downwind profiles. However, the results presented in this chapter, will be important when analysing the results and observations presented in Chapters 5 and 8. In particular, these results are important in understanding the effect that crosswind distribution of dust sources has on the distribution of dust within the local area.

In the next chapter the DSism model is modified to incorporate deposition. The effect deposition has on the resulting vertical dust concentration profiles is explored through simulation.

Chapter 5

Modification of DSism to account for deposition and changes in erodibility

5.1 Introduction

The spatial distribution and emission rate (Q) of dust sources have a strong influence on dust concentration profiles within the study site (Butler et al. (1996) and Chapter 4). DSism in its current form is able to display these features, but it does not include deposition. As a result it is not able to accurately simulate differences in erodibility between the various land types within the study site and changes in the particle size distribution of the plume. This chapter extends DSism to include a deposition component and account for changes in erodibility between the various land types within the study site.

Chapter 5

Modification of DSism to account for deposition and changes in erodibility

5.1 Introduction

The spatial distribution and emission rate (Q) of dust sources have a strong influence on dust concentration profiles within the study site (Butler et al. (1996) and Chapter 4). DSism in its current form is able to display these features, but it does not include deposition. As a result it is not able to accurately simulate differences in erodibility between the various land types within the study site and changes in the particle size distribution of the plume. This chapter extends DSism to include a deposition component and account for changes in erodibility between the various land types within the study site.

5.2 Deposition

In Chapter 2 it was noted that the particle size of the source soil, is an important factor in the emission rate and the sorting that occurs as a result of gravitational settling within the plume. Thus, it is important that DSism be formulated so that emission rates (Q) can be defined on a particle size basis; as well as account for gravitational settling within the plume.

There are several ways to incorporate deposition into a Gaussian Plume model (Zannetti, 1990; Hanna et al., 1982). In DSism the classic "tilted plume" approach as described by Zannetti (1990) is used (Butler et al., 2003). To understand why the tilted plume approach was selected, it is necessary to consider it in relation to the other two popular approaches used in the air pollution literature. The first is called the "source deletion" approach. In this approach the emission rate Q is allowed to vary with downwind distance in order to account for the reduced amount of material remaining in suspended transport. One of the disadvantages of this approach is that deposition is allowed to occur over the whole depth of the plume. As a consequence the vertical dust concentration is invariant with distance (Hanna et al., 1982). Observations obtained by McTainsh et al. (1998), for the study site, have shown that when there is no entrainment on the claypan the vertical dust concentration is unchanging with height, and that exponential vertical dust concentration profiles occur if there is entrainment on the claypan. Such observations indicate that the dust concentration is not invariant with distance, within the study site, therefore the "source depletion" approach is less applicable.

Another approach to introducing deposition into a Gaussian Plume model, is termed the "partial reflection" approach. In this approach (which is really an extension of the "tilted plume" approach) an extra term is added into Equation (4.2) to account for material being reflected ("re-entrained") from the surface. Such a re-entrainment term, is important where there is a single well-defined, elevated source and most of the material is bounced back off the surface. However, for the claypan, where there are multiple ground based

dust sources, this re-entrainment can be accounted for by simply increasing the emission rate Q of sources in the appropriate region. By allowing any such re-entrainment to be simply viewed as an increase in emission rate Q for a given region, it is much easier to account for variations in the amount of retrainment, due to changes in surface conditions. Therefore, there is no practical advantage in incorporating an extra reflection term into DSism.

Since in the case of the study site, re-entrainment can be simulated in the above fashion, the standard "tilted plume" approach should be sufficient to produce an accurate simulation. In this approach, equation (4.2) is modified to include a deposition component, as follows

$$C(x,y,z) = \frac{Q}{\pi\sigma_y\sigma_z u}\exp\left(\frac{-y^2}{2\sigma_y^2}\right)\exp\left(\frac{-\left[z+\frac{v_t x}{u}\right]^2}{2\sigma_z^2}\right), \tag{5.1}$$

where z is the height above ground, y is the distance cross wind from the point source, x is the downwind distance from the dust source, σ_y and σ_z are the pascal dispersion parameters in the y and z directions respectively and v_t is the deposition velocity of the particles. This tilts the centre line of the plume as shown in Figure 5.1. Material below the "ground level" is then assumed to be deposited and removed from the calculation (Butler et al., 2003).

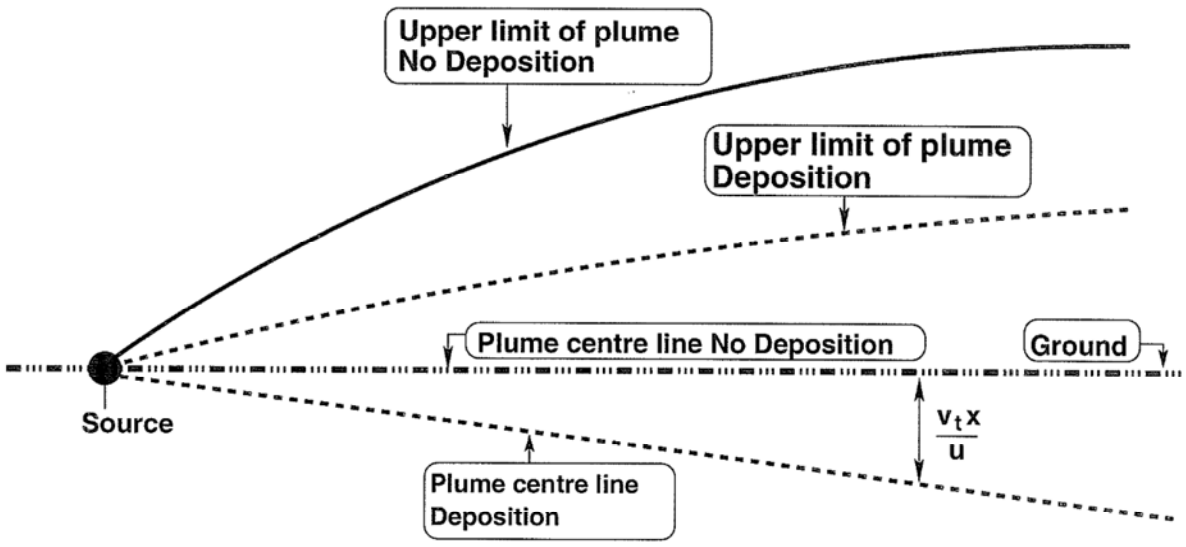

Figure 5.1: Schematic showing how gravitational settling is incorporated into DSism, using the "classic" tilted plume approach.

Ideally the calculation of deposition velocity (v_t) should account for the shape, size and drag of particles and change depending on the roughness and other surface properties (Hanna et al., 1982; Shao, 2000). As no field data is available on how all of these properties affect the deposition velocity (v_t), it was assumed in DSism that the entrained dust particles are spherical, with uniform density and have diameters between 10 and 60μm (Butler et al., 2003). Under these assumptions Stokes law states that v_t is given by

$$v_t = \frac{2\phi^2 g \rho_p}{36\mu}, \tag{5.2}$$

where ϕ is the diameter of the particle, ρ_p is the density of the particle, g is the acceleration of due to gravity and μ is the dynamic viscosity of air.

5.3 Particle size and emission rates

Since the deposition velocity v_t is dependent on particle size, it is assumed that the plume consists of N distinct particle size classes. Each particle size class used, is distinguished by the subscript j and will be represented in the model by the class centre. Therefore, the emission rate of the ith source upwind of a given point for a particle size class j is given by

$$Q_{ij} = K_{ij} Q_{bj}, \tag{5.3}$$

where Q_{bj} is a base source emission rate of the jth particle size and K_{ij} is a constant relating the ith source emission rate for particle size class j to the base emission rate (Q_{bj}). Assuming emission rates for each particle size class are equal, this can be simplified to

$$Q_{ij} = K_i Q_b, \tag{5.4}$$

where Q_b is a base source emission rate and K_i is a constant relating the ith source emission rate to the base emission rate (Q_b) (Butler et al., 2003). Thus, the emission rate Q_{ij} is independent of particle size class.

To determine K_i a Land Type Erodibility Index (LEI) is calculated as outlined by McTainsh et al. (1999) for each land type within the study site. The final

value of $\mathcal{K}_i$ for each land type within the study site is calculated by taking the ratio of the LEI for the ith land type to the largest value of LEI recorded within the study site. Thus, $\mathcal{K}$ for land type with the highest value of LEI, will have a value of one, while other land types within the study site will have values of $\mathcal{K}$ smaller than one (Table 5.1). Using such a structure means that the emission rates are simply a weighted approximation based on experimental field data for the DNP field site for a given month.

Table 5.1: Values of $\mathcal{K}$ calculated based on the LEI of McTainsh et al. (1999) for DNP in August 1996.

Land type	$\mathcal{K}$
Dunes	0.016
Downs	0.019
Main Channel Floodplain	0.001
High Floodplain	1.000

The concentration (C_{ij}) at a height z and a distance x downwind of the ith source for particles of size class j is

$$C_{ij} = \frac{Q_{ij}}{\pi u \sigma_y \sigma_z} \exp\left(-\frac{{y_i}^2}{2\sigma_y^2}\right) \exp\left(-\frac{\left[z + \frac{v_{tj}x}{u}\right]^2}{2\sigma_z^2}\right), \tag{5.5}$$

where v_{tj} is the terminal velocity of the jth particle size , and y_i is the line cross wind distance to the ith source.

The final concentration (C_f) at any point is then given by

$$C_f = \sum_{i=1}^{M} \sum_{j=1}^{N} C_{ij}, \tag{5.6}$$

where M is the total number of sources upwind and N is the number of particle size classes used in the model. Such a technique has been used in numerous models to calculate dust concentrations (Shao, 2000).

As outlined in chapter 4, dust sources are approximated by using a number of distinct point sources, lying along individual crosswind lines (Fig. 4.10).

These point sources can be arranged in a regular or random pattern along these lines. Using this approach different two-dimensional dust source configurations can be simulated for any given event. These dust source configurations can be superimposed on a land type map, as shown in Figure 4.10. The point source emission rate (Q_{ij}) is then determined by the land type on which the point source falls.

5.4 Effects of deposition upon predicted dust concentration profiles

5.4.1 Vertical dust concentration profile

To illustrate the effect of these changes to DSism, both non-deposition and deposition scenarios were simulated over the whole of the study area shown in Figure 5.2, using the source structure shown in Figure 5.3. In all of these simulations, Q_b was set to $17900\mu gs^{-1}$ for each particle size, and the values of K were set as per Table 5.1. Both vertical and crosswind concentration profiles were recorded for each scenario. The results of these simulations are shown in Figures 5.4 to 5.8.

Figures 5.4 to 5.7 show how calculated vertical dust concentration profiles at Site A are affected by the addition of deposition. Equation (5.2), indicates that the 20μm particles (this is the class centre of the 10-30μm class) have the smallest value of v_t in the DSism, thus one would expect the difference between the calculated deposition and non-deposition profiles to be a minimum for these particles. In contrast, the 60μm particles (this is the class centre of the the 50-70μm class) have the largest value of v_t and therefore should show the largest change. Comparing Figures 5.4 to 5.6, the above behaviour is clearly evident, in the DSism simulations. Note: 1) as is the case throughout the thesis the class centres have been used in DSism and 2) that the particle size classes are as follows 10-30μm, 30-50μm and 50-70μm unless

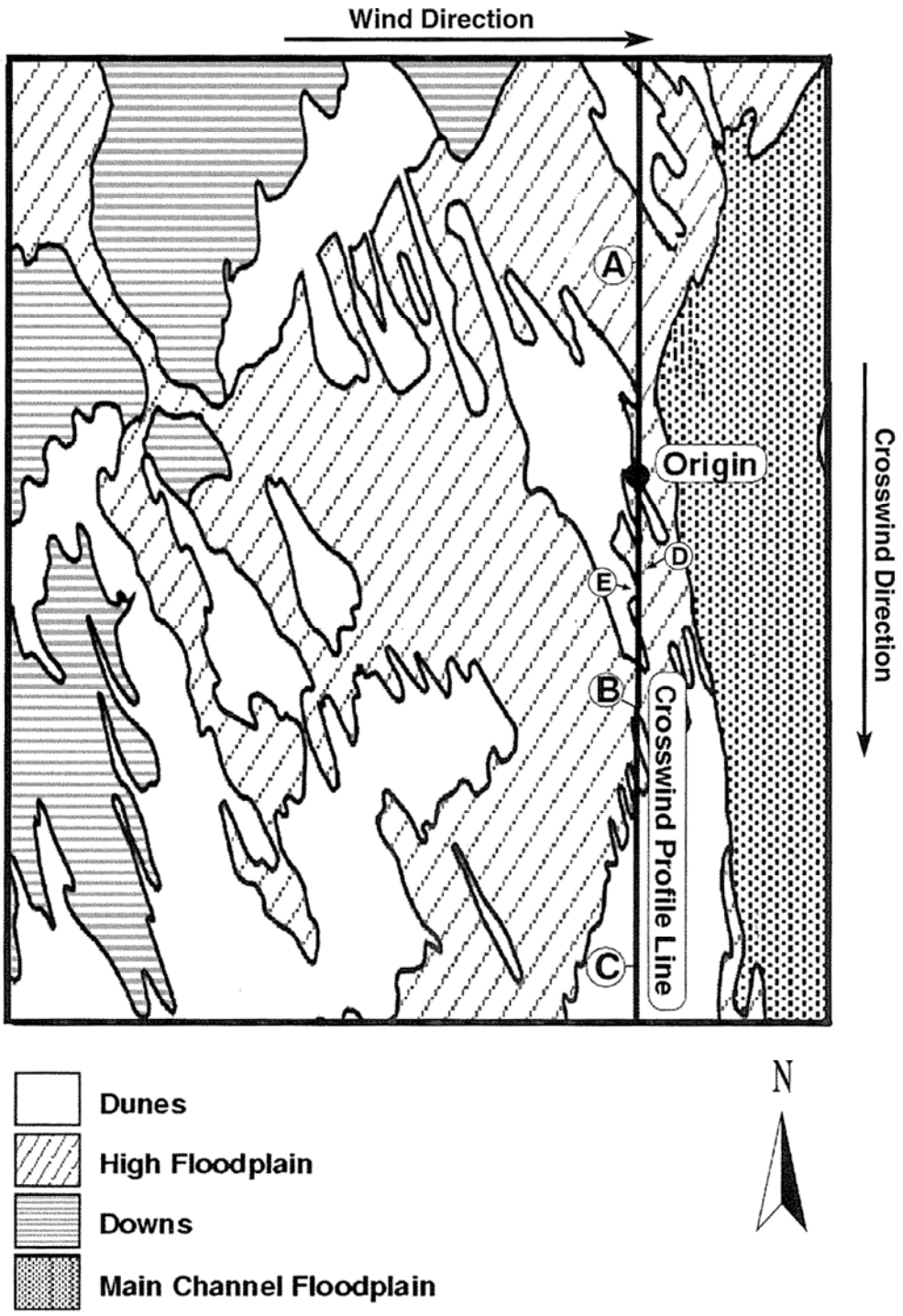

Figure 5.2: Map of study site used in the model. Points A, B, C, D and E are location markers and represent key points in the crosswind dust concentration profile, shown in Figure 5.8. The crosswind profile line (heavy solid line) in the figure, indicates the line on which the crosswind dust concentration profile shown in Figure 5.8 was calculated. The Origin marked in above figure, corresponds to a crosswind distance of 0 in Figure 5.8. NOT TO SCALE and measurement sites not shown.

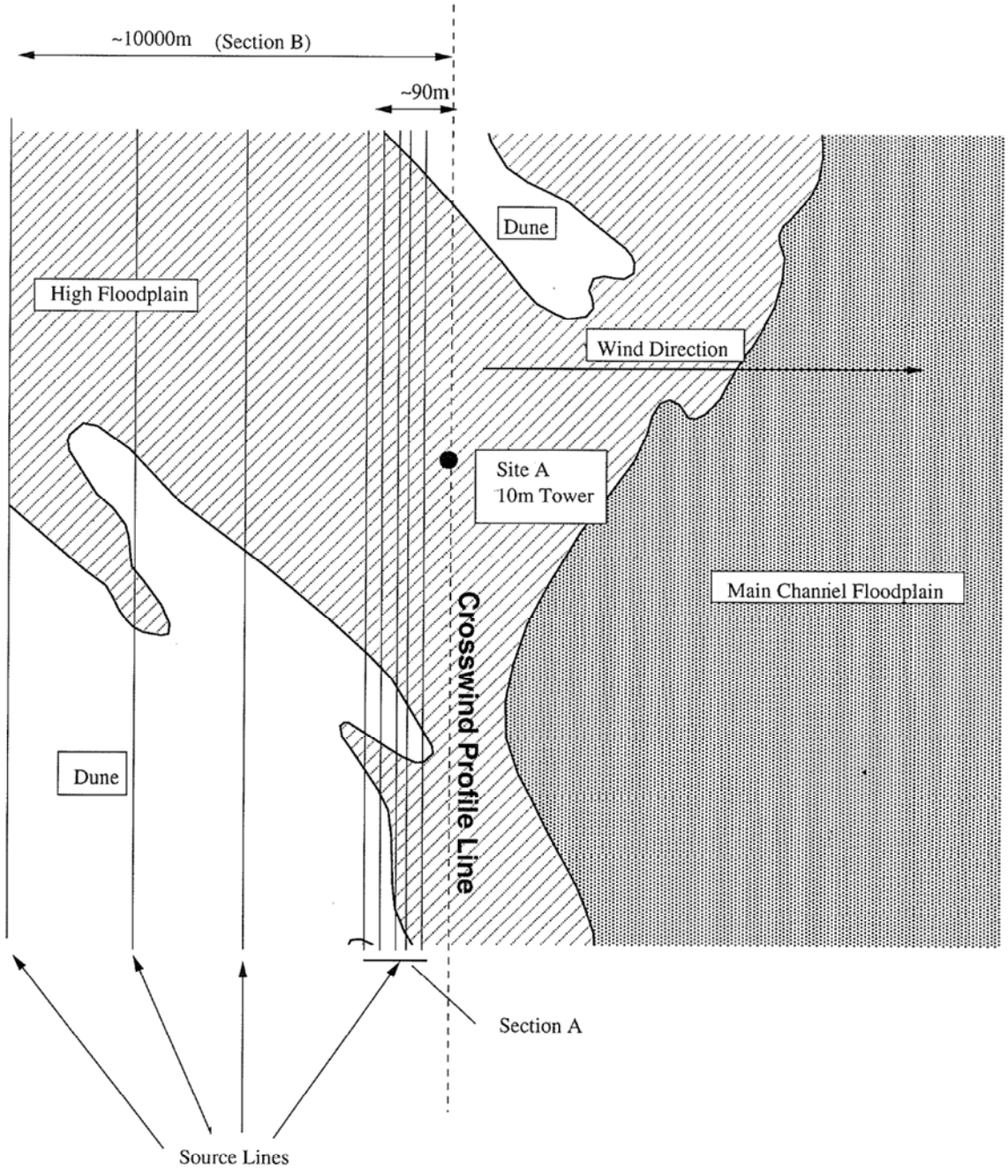

Figure 5.3: Spatial distribution of source lines used in all simulations in this chapter. Section A extends 90m upwind of the tower line and consists of source line every 10m for the first 90m. Section B consists of sources every 100m for 10km upwind. Note: The figure is NOT TO SCALE and that it has been simplified in that it only shows the line structure in the immediate neighbourhood of the claypan. Also Site A corresponds to point A in Figure 5.2.

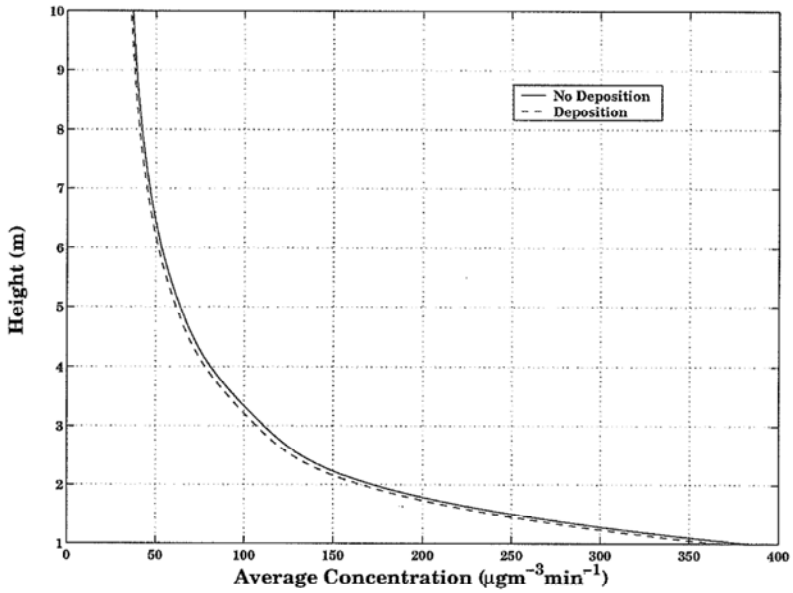

Figure 5.4: 20μm component of the deposition and non-deposition vertical dust concentrations calculated at Site A.

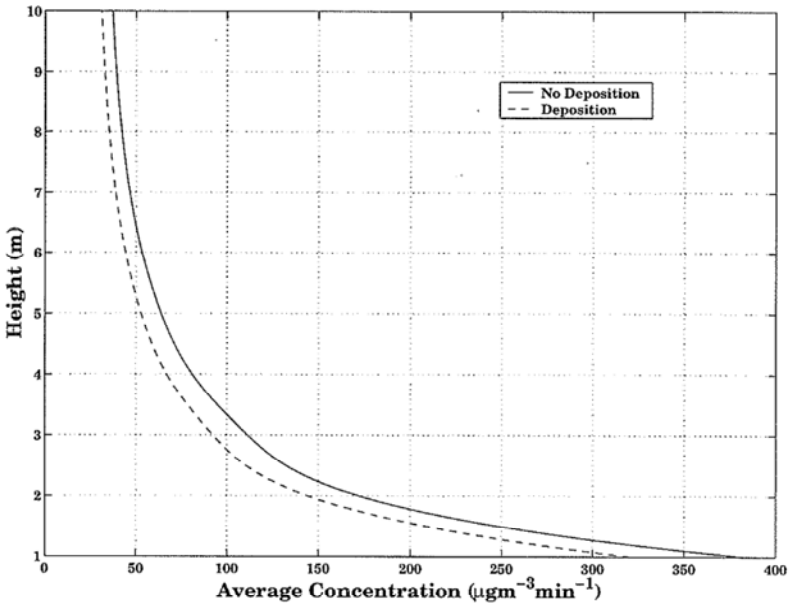

Figure 5.5: 40μm component of the deposition and non-deposition vertical dust concentrations calculated at Site A.

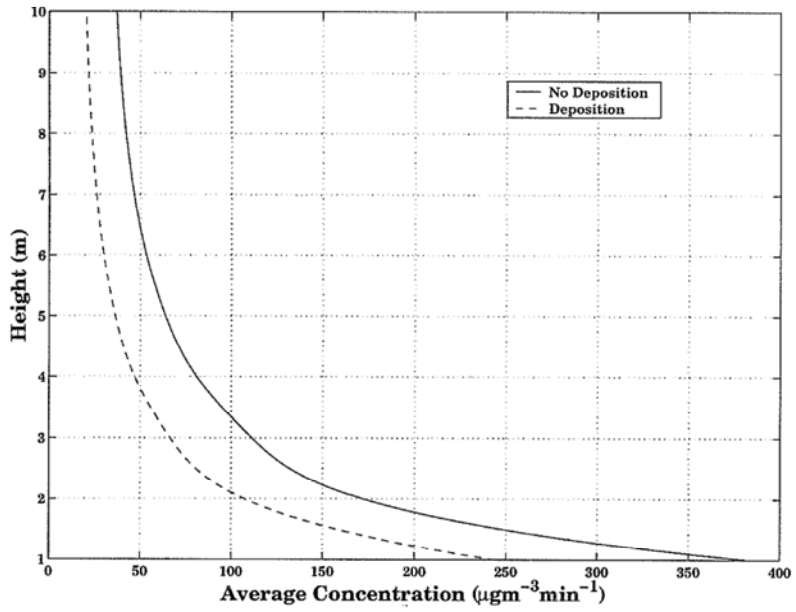

Figure 5.6: 60μm component of the deposition and non-deposition vertical dust concentrations calculated at Site A.

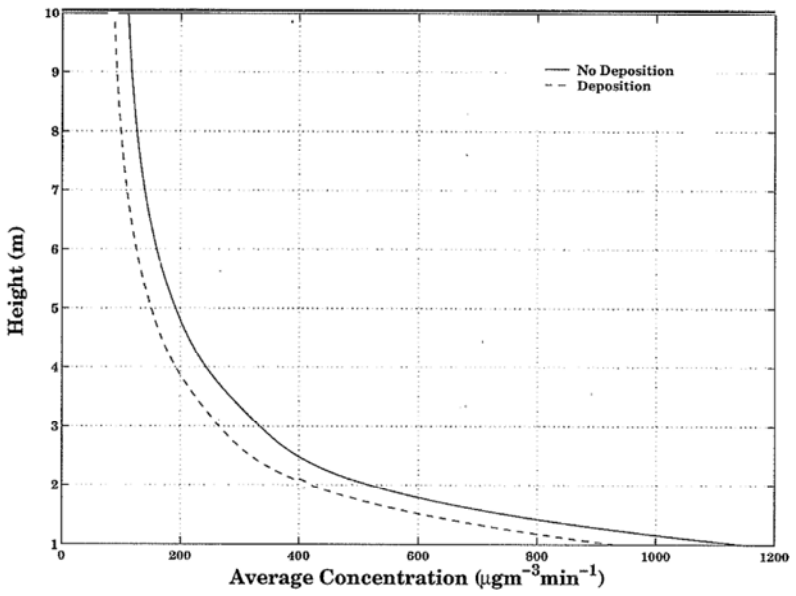

Figure 5.7: Total C_f deposition and non-deposition vertical dust concentration profiles produced by DSism at Site A.

otherwise specified.

The vertical dust concentration profile, shown in Figure 5.7 is achieved by adding the profiles shown in Figures 5.4 to 5.6, according to Equation (5.6). Since this profile is a direct addition of the 20μm, 40μm and 60μm profiles, it must simulate the change in the particle size distribution within the dust plume due to the preferential deposition of larger particles. As a consequence, in DSism the smaller particles will be transported the furthest from any given source. Such a preference in transport range, means that DSism is in agreement with theoretical predictions of Greeley and Iverson (1985), Raupach (1993) and Shao (2000) about the relative transport ranges of the different

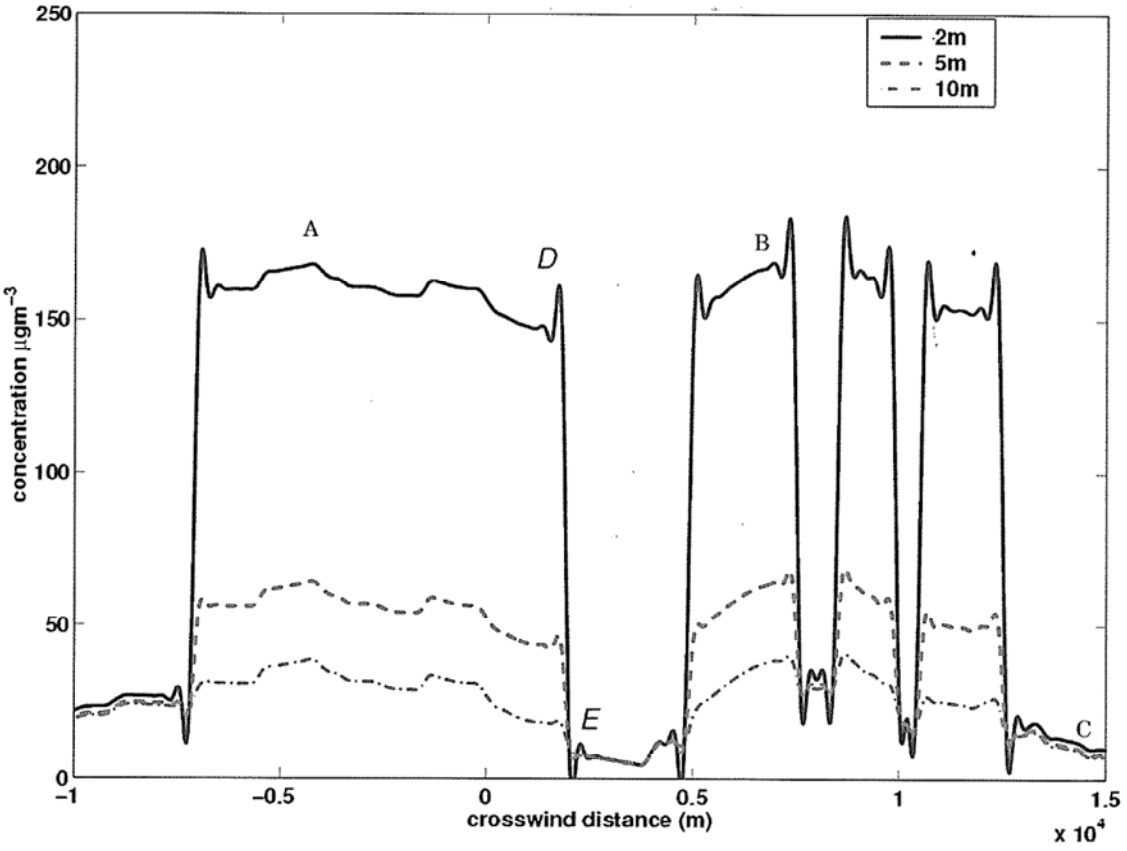

Figure 5.8: 20μm crosswind dust concentration profile produced by DSism when deposition is included, at 2m, 5m, and 10m above ground level, along the line shown in Figure 5.2. The labels A, B, and C refer to the location markers shown in Figure 5.2, while labels D and E mark another key feature of the profile.

particles.

5.4.2 Crosswind dust concentration profile

The 20μm crosswind concentration profile shown in Figure 5.8 was produced by the deposition version of DSism, along the line shown in Figure 5.2. Note that the: total, 40μm, 60μm and non-deposition profiles are not reported here, as they all produced similar characteristics to those shown in Figure 5.8, the only difference being the predicted dust concentration. In creating this crosswind profile, it was assumed in the simulation that the spatial distribution of source lines upwind of the line shown in Figure 5.2, did not alter between or within land types. While this is unlikely in reality, this simulation highlights the usefulness of DSism. It should be noted, that the assumption that the spatial distribution of source lines did not alter between or within land types, was not made due to any limitations inherit in DSism. The purpose of this assumption was purely to make the analysis of the crosswind and upwind variations easier to interpret.

A closer examination of the crosswind dust concentration shown in Figure 5.8 and matching A, B and C to their corresponding areas in Figure 5.2, illustrates several important characteristics of DSism. Both points A and B in Figure 5.2 are located on the claypan, which for this event has a high LEI, indicating that they are the most active wind erosion areas within the study site. Matching these to the corresponding points in Figure 5.8, it can be seen that these points correspond to areas where DSism predicts high dust concentrations. In addition, at these points DSism also predicts that the dust concentration will vary substantially with height (i.e., the purple line in Figure 5.8 is much lower in general than the blue line). Such behaviour is not surprising if one considers what is physically happening near an active dust source. In the immediate neighbourhood of an active dust plume, dust particles are being injected into the lower regions of the plume, thus increasing the dust concentration near the surface, whereas, very few dust particles will

have been dispersed into the upper levels of the plume. Thus, the vertical dust concentration will diminish substantially with height in the immediate neighbourhood of an active source.

In contrast, point C in Figure 5.2 is located near a dune which has a low LEI, thus indicating low erodibility. Matching this point to the corresponding location in Figure 5.8, indicates that it corresponds to a area which DSism predicts will have a very low dust concentration. This figure, also shows that there is very little variation in dust concentration with height in the region of point C. Such behaviour, further indicates that DSism is mirroring the behaviour observed by McTainsh (1998, pers. comm.) for actual events within the study site. In that, if only transported material is present in the plume, a near constant vertical dust profile is predicted, rather than the standard exponential profile.

The crosswind simulation results shown in Figure 5.8, illustrate a important feature of the wind erosion process in natural systems, such as the Diamantina National Park (DNP). Consider the points D and E shown in Figure 5.8. These two points lie along the same crosswind profile line shown in Figure 5.2. The only difference between the two points is that D lies on the high floodplain, while E lies on part of the dune system. Even though they are only separated by a hundred metres the simulated dust concentration is significantly different. Such a dramatic change in dust concentration prompts the question: What, in process terms, in the model could produce such a dramatic change in dust concentration? To answer this question, one needs to consider, how DSism simulates the wind erosion process.

In DSism the wind direction is assumed to be constant and dust is assumed to disperse as it travels downwind of the initial source. Under these conditions one possible scenario, for such a change in concentration is illustrated in Figure 5.9. In this scenario two different intensity dust sources exist and are separated spatially. Since the low intensity source area has a much lower emission rate the crosswind dust concentration predicted downwind (blue line in Figure 5.9) of this source is much lower than that downwind of the high

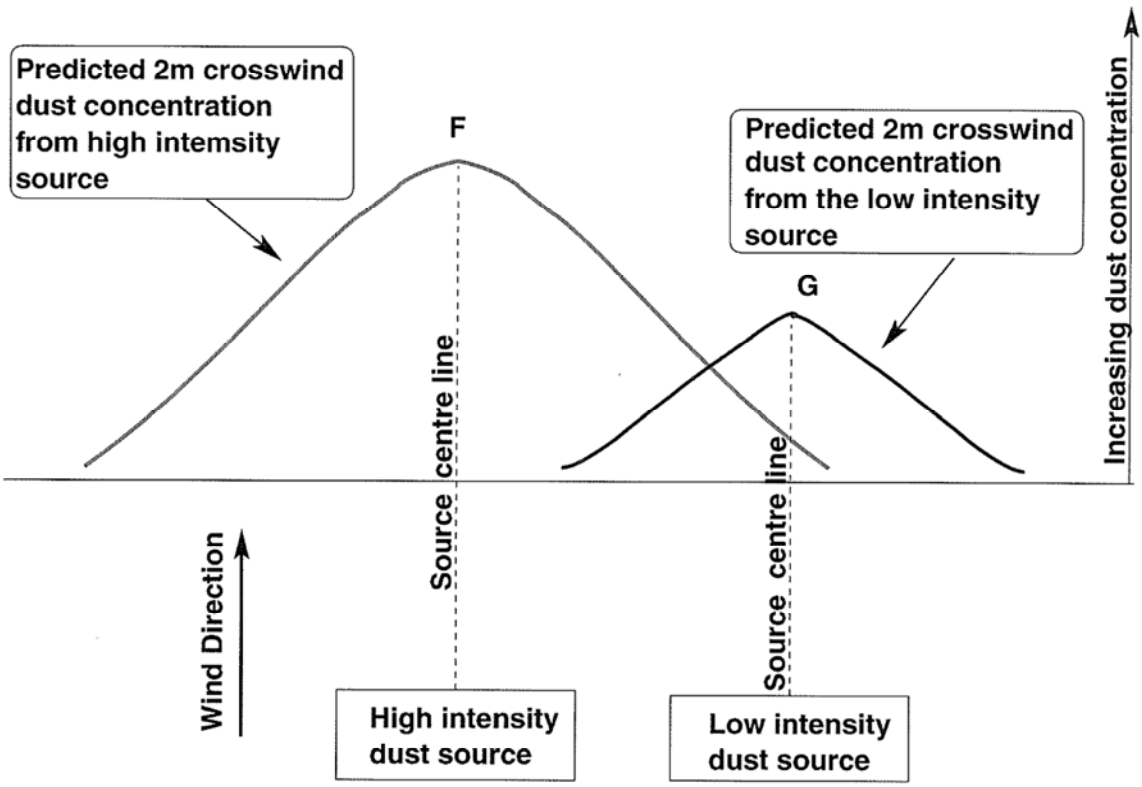

Figure 5.9: Schematic illustrating what the individual dust crosswind concentration profiles may look like at some point downwind. The red line corresponds to the predicted dust concentration from the high intensity source, while the blue line corresponds to predicted dust concentration from the low intensity source. The points F and G mark the peak concentration in each of the concentration profile.

intensity source (red line in Figure 5.9). As outlined in Chapter 4, the resulting crosswind dust concentration profile will depend on the separation of the sources and the downwind distance from each source. Thus, based on simulations run in Chapter 4, a point will exist downwind of these sources where the concentration recorded at F and G (Fig. 5.9) will be significantly different. The actual distance downwind where this occurs will depend on the separation of the two sources.

What does this imply in terms of points D and E on the crosswind profile? Since D is situated on the high floodplain which has a high erodibility and E is located on a dune which has a low erodibility, we have the situation shown in Figure 5.10. Material entrained on the high floodplain upwind of

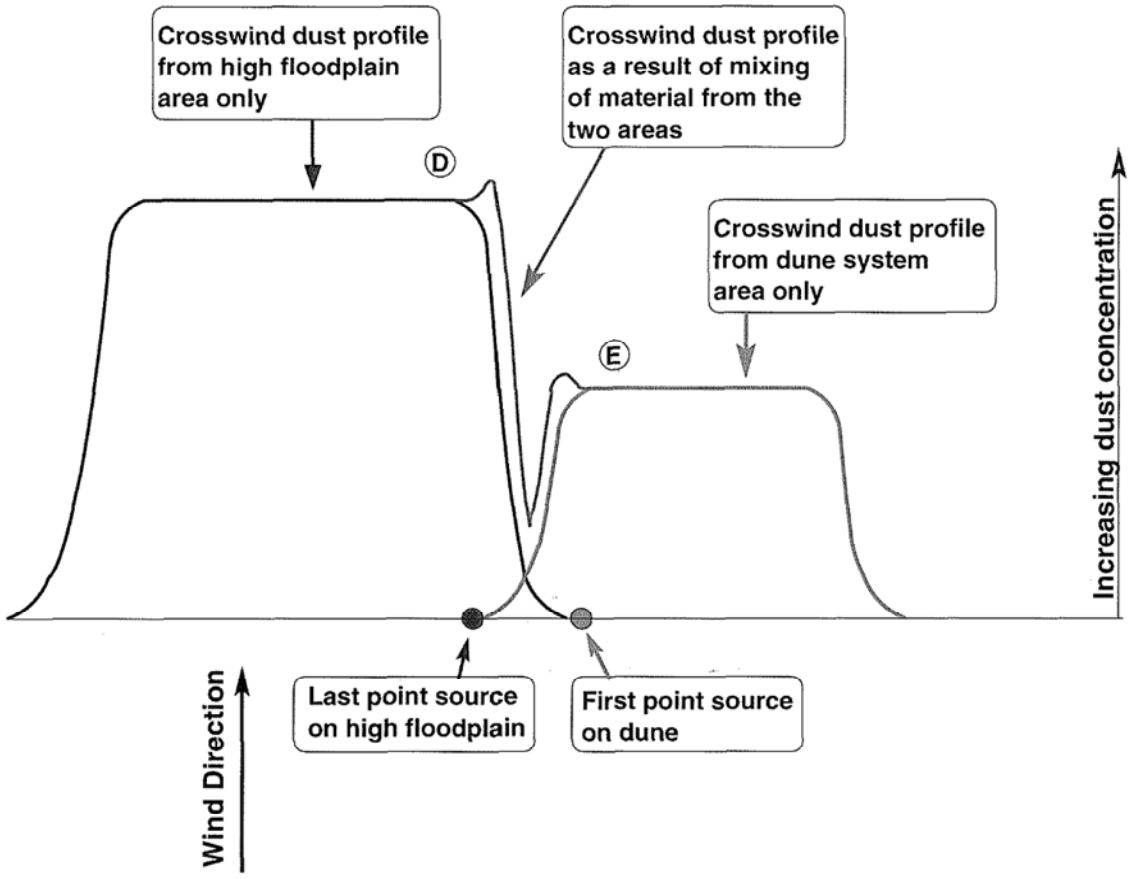

Figure 5.10: Schematic illustration of the processes occurring at D and E, which create the dip in the crosswind dust concentration profiles.

point D has only travelled a short distance, and therefore has only dispersed a small amount to the right of the last point source on the high floodplain land type. Similarly, the material upwind of E has only travelled a short distance, and therefore has only dispersed slightly to the right of the first point source on the dune. Material from the dune mixes with material from the high floodplain, thus reinforcing the crosswind high floodplain dust concentration profile (blue line in Figure 5.10). This causes a slight increase in the concentration of the mixed profile, before it decreases. Similar, this mixing reinforces the crosswind dune dust concentration (red line in Figure 5.10, thus causing a similar increase in the mixed profile at the edge of the original dune dust concentration profile. This processes is also responsible for the dips and troughs observed in Figure 5.8 between B–C and E–B.

Since DSism assumes that the line sources that make up each discrete source

areas are made up of discrete point sources, the extent of the drop at the change of land systems will depend on the distance between the last point source on one land type and the first point source on the other. While this is to some extent an artifact of DSism, it still is indicative of the real situation in which their is no guarantee that sources start and finish neatly at land type boundaries.

It is not surprising that the dips and troughs occur at the roughly the same places in the 5m and 10m profiles, as one would expect that the same effect is propagated through the vertical profile by the vertical dispersion process. These are also much smaller than the ones observed in the 2m crosswind concentration profile. This is not surprising as: 1) there is less material in the higher parts of the plume and 2) that material transported from further upwind tends to sustain the dust concentration at these heights.

The variation in the crosswind dust concentration observed between A and D, is due to the mixing of material from dust sources upwind. In this sense, the variations represents how discrete dust sources upwind reinforce each other at different crosswind locations. The resulting crosswind dust concentration profile can therefore be seen as the dust equivalent to an interference pattern.

5.4.3 Field implications

While the above scenario suggests that such changes in the simulated crosswind dust concentration are the result of upwind spatial variations in dust emission rates, it also implies that observed dust concentration values will depend on where the samplers are located relative to these upwind sources and the different land types. A consequence of this observation, is that for land types, such as the claypan, it is possible that two samplers which are only separated by 10m would record significantly different dust concentrations. Such an occurrence would be easy to prove if each site had two identical samplers installed side by side. However, this was not the case within the study site.

For example at Site A, a wind vane sampler is installed along side a 2m semi-isokinetic sampler. The only way to establish the possible existence of such behaviour is to compare the relative efficiency of the two types of samplers, and look for a change in this value.

To undertake this comparison between the 2m wind vane sampler and the 2m semi-isokinetic sampler at each site, the relative efficiency RE was calculated in the following manner:

$$RE = \frac{\text{Wind vane dust concentration 2m}}{\text{Semi-isokinetic dust concentration 2m}}, \tag{5.7}$$

where RE is the ratio of the two predicted concentrations expressed as a percentage. Using this formula the relative efficiency of the two samplers was calculated for the events and sites shown in Table 5.2. While ideally it would have been better to have more data points for this study than those shown in Table 5.2, these were the only events in the data set for which it could be guaranteed that both the semi-isokinetic and wind vane sampler were in operation for the same amount of time, and therefore recorded the same events. However, these are sufficient, when combined with other observations to provide evidence that two relatively close samplers on the claypan can record significantly different dust concentrations.

Efficiency studies undertaken in the field by Goossens and Offer (2000) indicated that for the types of samplers in question the relative efficiency as calculated above should be between 30 and 60 %. Other efficiency studies of Fryrear (1986) and Shao et al. (1993a), have indicated that under ideal conditions the relative efficiency of the two samplers should be around 80%, but this efficiency drops to around 40% for particles smaller than 10μm (Shao, 2000). As can be seen in Table 5.2 the site and event for which the value of RE is not close to this range coincides with event E2-2000 and Site A. Can this difference be related to the existence of a second source ?

Photographs taken during 2000 (Figs. 5.11 and 5.12), show that Site A was heavily vegetated, in contrast to Site A1 which was almost completely devoid

Table 5.2: Relative efficiency (*RE*) values for the four events, with associated average wind speed and direction data for each event. The 2000 events are dealt with first since they contain information at both Sites A and A1. N/A denotes that the site was not in operation during these periods and thus no results were available. Events in this thesis are labelled as follow: *EX–YYYY*. This notation indicates that it is the *x* event in the year *YYYY*.

Event label	Event Date	Wind Speed (ms^{-1})	Direction (°N)	*RE* (%) Site A	Site A1
E2–2000	25/09/2000	9	322	117	65
E1–2000	17/08/2000	9.53	170.6	53.5	68
E1–1996	19/07/1996	12.18	283.45	30.8	N/A
E2–1995	18/09/1995	10.85	67	49	N/A

of vegetation. In addition, field notes taken at the time show that a mini-nebkha field existed just north of Site A (Fig. 5.13). This mini-nebkha field was comprised of large amounts of unconsolidated sand, a large number of small vegetated mounds and had only 25% vegetation cover (Strong, 2001, pers. comm.). Other field observations made during the 2000 season by Leys (2001, pers. comm.), Strong (2001, pers. comm.) and McTainsh (2002, pers. comm.), all confirm that this mini-Nebkha field was an active wind erosion source during the 2000 season. Photographs taken during 1995 and 1996 (Figs 5.14 and 5.15), show that most of the claypan was devoid of vegetation and had similar surface conditions to those observed during the 2000 season.

The above observations suggest that the change in relative efficiency for E2-2000 at Site A, is associated with changes in surface conditions and the presence of the mini-nebkha field. To understand this conclusion, consider Figure 5.16 which shows the wind direction of E2-2000 and E1-2000, and the position of the two samplers relative to the mini-nebkha field. Figure 5.16 shows that the mini-nebkha field is located upwind of the Site A towers during E2-2000 and is downwind of the Site A towers during Event E1-2000. Given this spatial arrangement during the two events, it is likely that the mini-nebkha

Figure 5.11: Site A surface conditions during the 2000 wind erosion season.

Figure 5.12: Site A1 surface conditions during the 2000 wind erosion season.

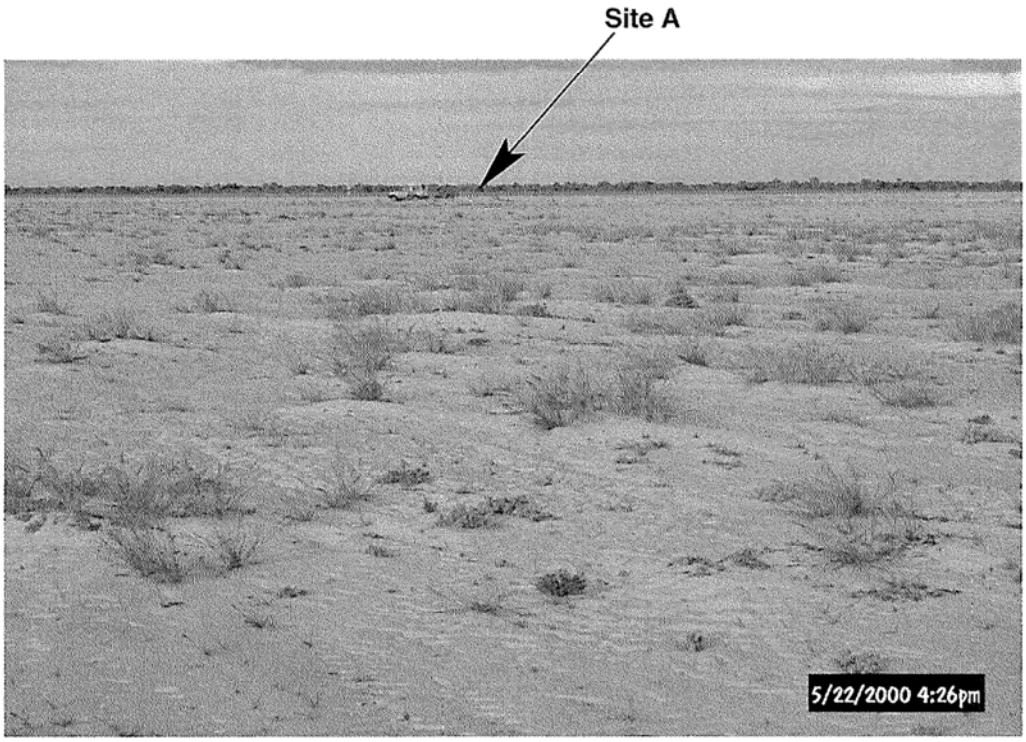

Figure 5.13: The location and depth of the mini-nebkha field in relation to Site A.

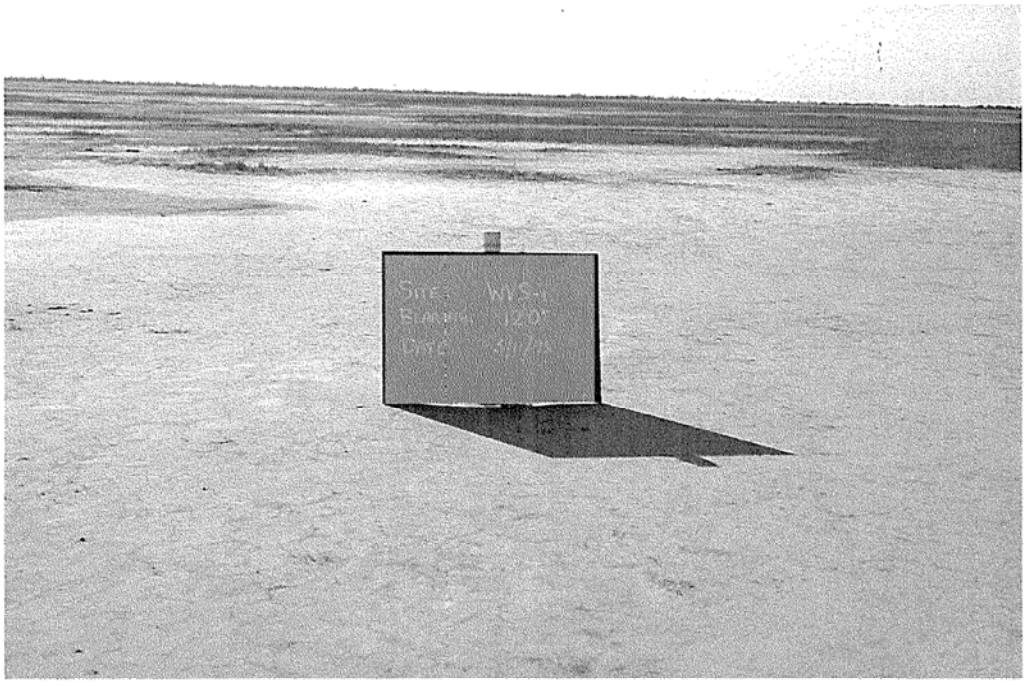

Figure 5.14: The surface condition of the claypan during the 1995 season.

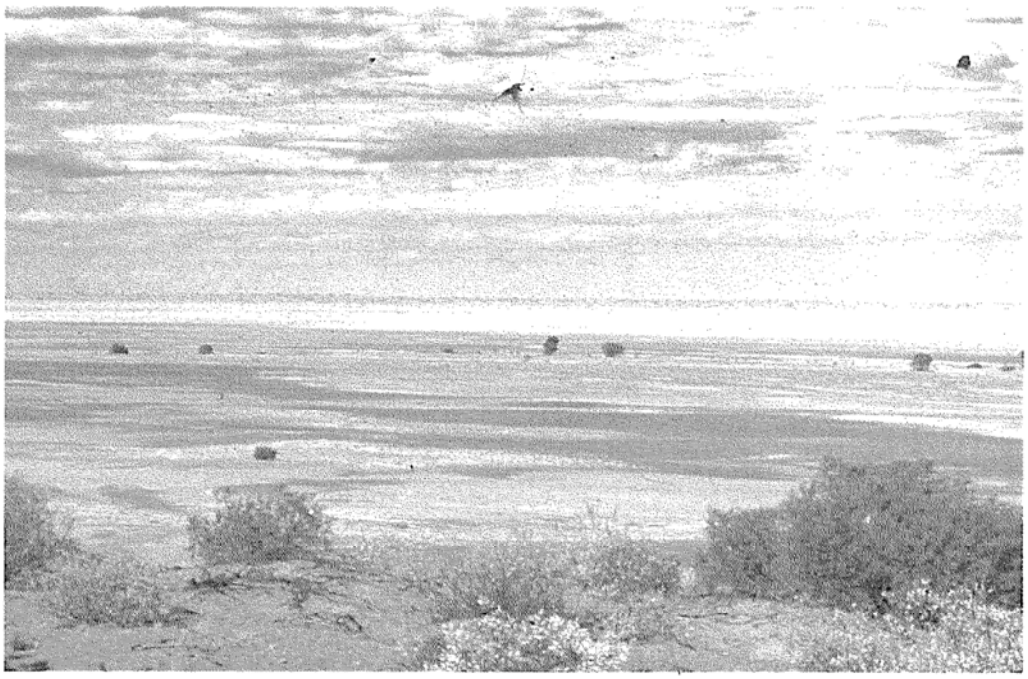

Figure 5.15: The surface condition of the claypan during the 1996 season.

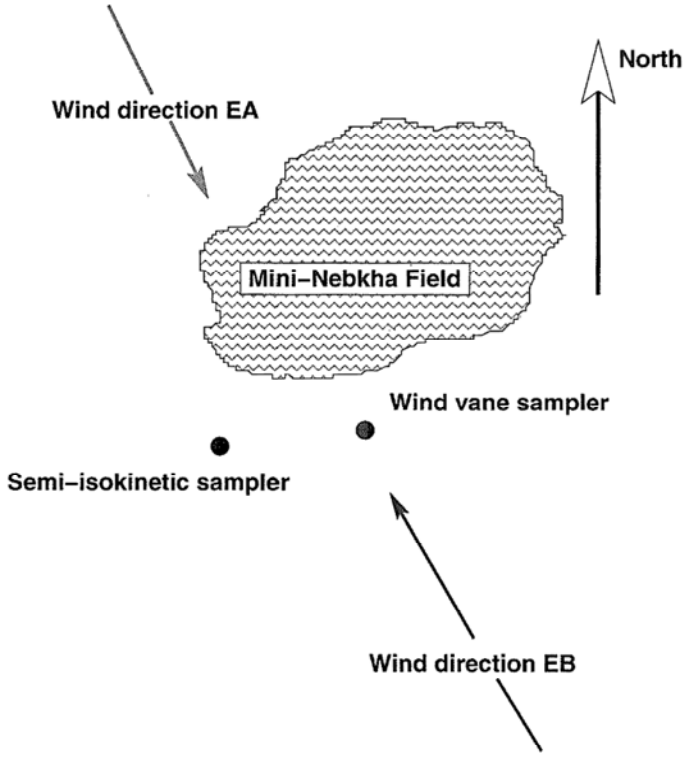

Figure 5.16: Schematic map illustrating the relative positions of the samplers in comparison to the mini-nebkha field. It also shows the wind direction of the E2-2000 and E1-2000.

field was a significant dust source during E2-2000 and that much of the entrained dust passed the wind vane sampler, rather than the semi-isokinetic sampler. The net result being that the actual dust concentration recorded by the wind sampler is much higher than that at the semi-isokinetic sampler, thus resulting in the higher relative efficiency being recorded at Site A. This issue will be discussed again in Chapter 8, where additional modelling and experimental evidence will be presented supporting the above conclusion.

5.5 Summary

The above results and discussion are important for several reasons. Firstly they indicate that DSism is capable of simulating the changes in the size distribution of the plume as a result of gravitational settling as the plume travels downwind. Secondly, they show that DSism can simulate the changes in the vertical dust concentration observed by McTainsh et al. (1998). The model simulates not only the dispersion of material, but also captures the changes in concentration and makeup of the plume on a spatial basis. Therefore, DSism can now be used to simulate any given dust event. It should now be possible to learn more about how spatial changes in surface erodibility are likely to affect the resulting dust concentration profiles within the study site.

In addition, the efficiency analysis presented here, while in general supporting the findings of Goossens and Offer (2000), also suggests that the positions of the samplers relative to any changes in surface conditions needs to be taken into account. In particular, it suggests for rangeland environments where surface conditions can vary substantially within several metres, that such changes will also be reflected in the dust concentration. The other important aspect of the crosswind simulations and the efficiency analysis is that they indicate that the dust concentration measured at any given point is dependent on the upwind source history. In particular it means that observed variations in the crosswind and vertical dust concentration provide information about

the spatial variations in source conditions upwind. Such an observation, suggests that if the measured dust concentrations are treated as a signal, made up of several components, it should be possible to deconstruct it into its base components, and thus obtain important process information about the upwind source conditions.

Part III

Source influences on the structure of dust plumes

Chapter 6

Effects of changes in dust source location and source strength during three wind erosion events

6.1 Introduction

The basic components of DSism have been described in the previous chapters. DSism will now be used to simulate three wind erosion events within the study site, using a variety of dust source area configurations. The results of these simulations, which are published in Butler et al. (2001) and described here, are then compared with observed vertical dust concentration profiles at Site A, to establish which source area configuration provides the best match to the actual profile. Several conclusions are then drawn about the spatial nature of the wind erosion process within the study site.

6.2 Details of wind erosion events simulated

Three wind erosion events were selected using the event definitions of Nickling et al. (1999) as basis for this selection. According to these definitions, local

dust events are those in which sediments are entrained only from the claypan. Regional events are wind erosion events where sediment is entrained upwind of the claypan, transported into the claypan and then combined with some locally entrained sediment. Three events were selected from the 1995–1996 wind erosion season to represent a range of these event types and for which good experimental field data is available. These events are labelled E1–1996, E11-1995 and E3-1995 respectively.

In order to be consistent when comparing the size of dust events generally in this thesis, the 2m dust concentration value on the 10m tower will always be used (unless otherwise stated). This is done for two reason. Firstly the 2m value gives the best estimate of local activity and secondly by using this value it is consistent with the concentrations reported in the Nickling et al. (1999) paper.

6.2.1 Wind erosion event:E1-1996

Event E1 occurred over three hours on the morning of 19 July 1996. This intense local event involved W–NW winds reaching $14 ms^{-1}$. Sediment entrained during this event resulted in a dust concentration (2m value on the 10m tower) at Site A (Fig. 2.3) of 85 $861 \mu g m^{-3}$. This represents one of the highest dust concentrations recorded in Australia. At the time of this event the claypan was in a highly erodible condition (McTainsh et al., 1999) with fine sands being released from low hummocks no longer stabilised by vegetation.

E1-1996 is examined first and in the most detail because more detailed experimental data is available for this event.

6.2.2 Wind erosion event: E11-1995

Event E11-1995 occurred over two hours on the morning of 18 September 1995. This was a local event of moderate intensity, which involved N–NE

winds reaching speeds up to $18ms^{-1}$. The sediment entrained during this event resulted in a dust concentration at Site A of 4 $761\mu gm^{-3}$. At the time of this event, the claypan was largely unvegetated, but had a relatively low erodibility.

6.2.3 Wind erosion event: E3-1995

Event E3-1995, was a composite of two small regional events each of less than two hours duration on the mornings of the 20 and 21 August 1995. These events involved N–NE winds reaching speeds of $14ms^{-1}$. Sediment entrained regionally and locally during these events resulted in a dust concentration at Site A of $578\mu gm^{-3}$. At the time of the event, the claypan was in a similar condition to that of Event E11-1995 in that it was largely unvegetated but had a low erodibility.

6.3 DSism modelling methodology

To determine which dust source configuration and strength combination best simulated each wind erosion event, the following methodology was used. The particle size date for sediments collected during four events within the study site (three of which are studied in this chapter), indicated that most of the sediments collected fell into the $20\mu m$ to $60\mu m$ range. Accordingly, $20\mu m$, $40\mu m$ and $60\mu m$ particle-size classes were used in DSism simulations. It was assumed that the emission rate Q_b was the same for each particle size class (for further discussion of this assumption see Chapter 9). To simulate the different dust source configurations, the study site was divided up into a number of crosswind lines, as described in Chapter 5. Several different combinations of these lines and emission rates Q_b were tried, until a combination was found where the simulated dust concentration profile approximated the measured vertical dust concentration profile at Site A.

To further verify that this combination was the optimum fit, the above process

was repeated but this time with small changes in the dust source configuration and emission rates, until the simulated vertical dust concentration profile closely approximated the measured vertical dust concentration at Site A. This process was repeated for each wind erosion event.

For each of the resulting dust source configurations, the following measures were used to determine how well DSism simulation fitted the experimental data. In each simulation run, R^2 (the non-linear correlation coefficient) and the standard deviation of the residual errors (σ_e) were calculated. The dust source emission combination that produced the best R^2 and σ_e (i.e., the one with the highest R^2 value and smallest value of σ_e) , was taken to be the optimum fit for that event.

Having thus determined the optimal dust source configuration and emission combination for each event, a number of sensitivity tests were carried out, in which the emission rate Q_b was held constant, while the upwind extent and the density of lines (a proxy measure of source strength) were varied. The purpose of these sensitivity tests was to determine the effect that such changes have on the vertical dust concentration profiles. Understanding these effects, is particularly important if we are to begin relating observed changes in dust concentration profiles back to changes in field conditions. The results of these sensitivity tests, and their relationship to field conditions occupy the remainder of this chapter.

6.4 Sensitivity testing results

The sensitivity testing undertaken for Events E11-1995 and E3-1995, produced similar results to Event E1-1996, so only the E1-1996 results are reported here. The dust source configuration and emission rate combination that was found to have the best value of R^2 and σ_e for Event E1-1996, is shown in Figure 6.1 as Case CA, and occurred when Q_b was set to 14 000μgs^{-1}. Cases CB to CL in Figure 6.1, correspond to various dust configurations used in the sensitivity studies undertaken for E1-1996. In these sensitivity studies, both

the upwind extent of the source area and density of lines were varied. Figures 6.2 to 6.5 show a comparison between the modelled and measured vertical dust concentrations for Cases CA to CF (Fig. 6.1).

Cases CA to CE (Figs. 6.1, 6.2 and 6.3) show that changing the source structure further than 5900m upwind has little effect on the predicted dust concentration profile at Site A. Thus DSism is predicting that most of the dust entrained a further 5900m upwind is deposited before it reaches Site A. This is consistent with the generalised predictions of Tsoar and Pye (1987) and Raupach (1993), which suggests that the transport distance for particles in the size range considered here, is of the order of a few kilometres. This result also suggests that the approximations used to include deposition into DSism in Chapter 5 are not unreasonable.

Case CF (Figs. 6.1, 6.3 and 6.4) indicates that increasing the number of lines between 90m and 5900m upwind of the tower, increased the dust concentration in the profile, with the greatest difference occurring at the top of the profile. This is not an unexpected result, since the number of sources DSism has in this region has increased significantly and hence more dust is released into the wind flow. Much of this additional dust has not travelled sufficiently far for it to be deposited by gravitational settling, so it is still airborne when it reaches the 10m tower at Site A, thus increasing the modelled dust concentration.

Cases CF to CH (Figs. 6.1 and 6.4) show that most of this modification in the vertical dust concentration profile at Site A can be accounted for by sources close to the tower. This is understandable since material introduced into the plume near the tower will not have had sufficient time to mix and settle out, thus producing a significant increase in sediment near the ground. The result is also consistent with the role played by saltation material in the dust concentration profile. Saltation particles are locally entrained and are concentrated in the bottom 1.5m of the profile (Pye, 1987), but they affect the shape of the dust concentration profile up to 3m. The remainder of the profile

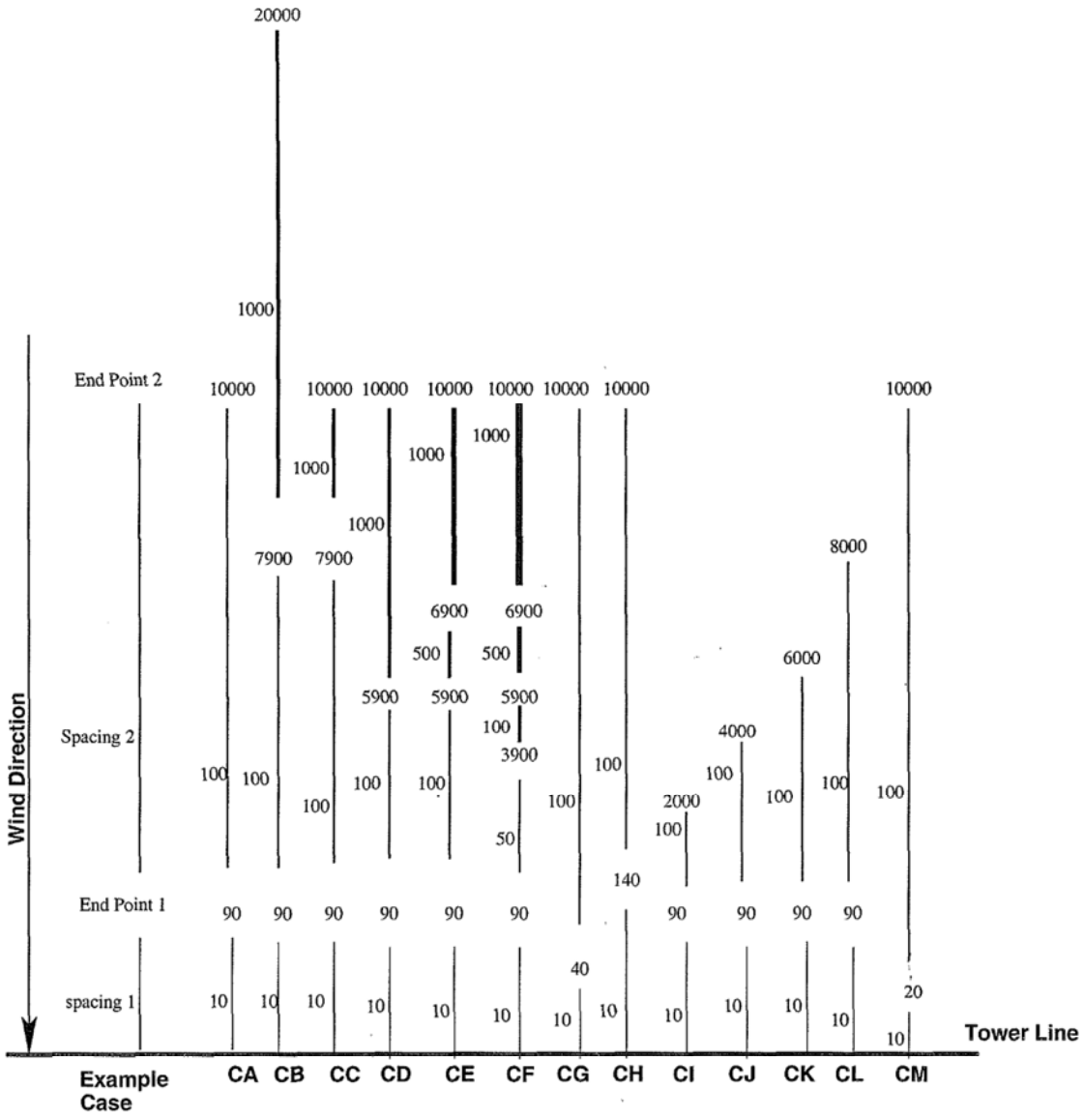

Figure 6.1: Different line spacings used to test the sensitivity of dust concentration profile (Cases CA to CM). All measurements are in metres. In the Example Case; spacing 1 is the initial spacing upwind of the Tower Line until end point 1 is reached. Spacing 2 is the source line spacing from end point 1 to end point 2 etc. In Case CA there are source lines every 10m for the first 90m and every 100m from 90m until 10000m, and no sources after 10000m. The different thickness of lines indicated where different line spacings are used.

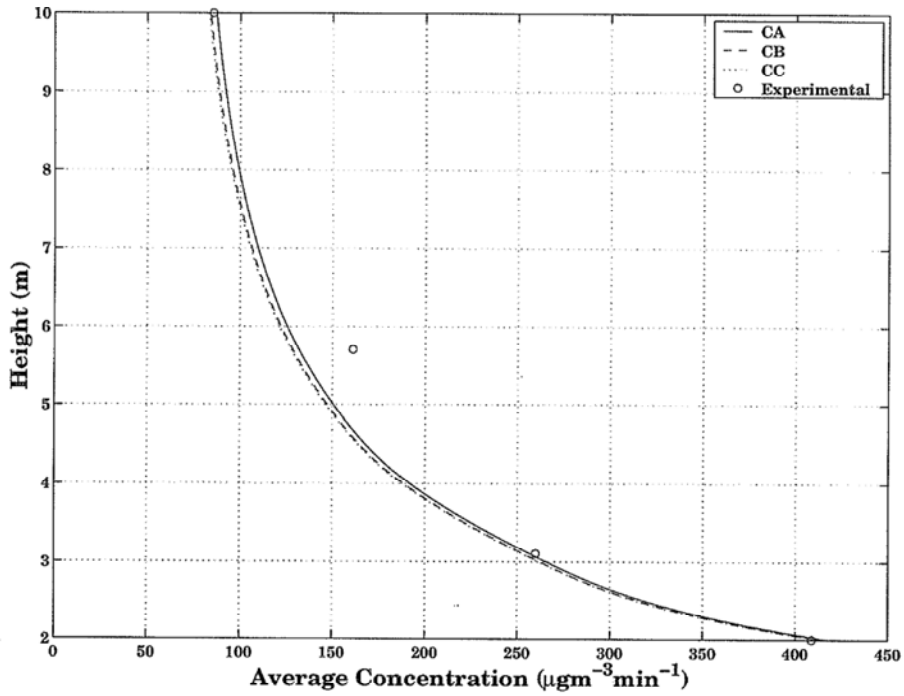

Figure 6.2: Modelled and measured vertical dust concentrations profiles at Site A for Cases CA to CC. Case CA gives the best fit with an $R^2 = 0.98$ and $\sigma_e = 15.3$. *Note: CB and CC overlap.*

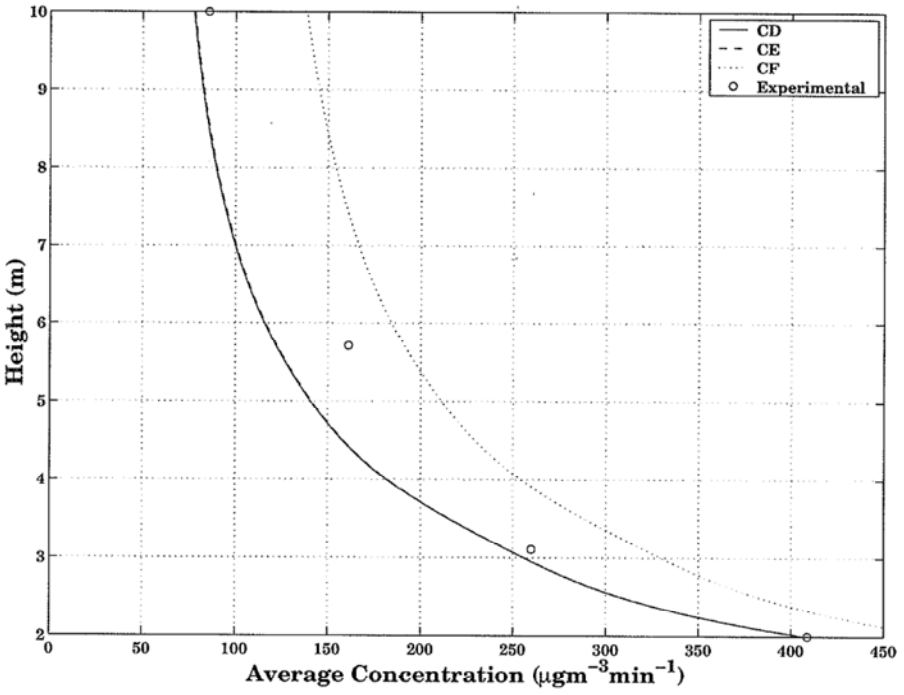

Figure 6.3: Modelled and measured vertical dust concentrations profiles at Site A for Cases CD to CF. Case CD gives the best fit with $R^2 = 0.95$ and $\sigma_e = 16$. *Note: CD and CE overlap.*

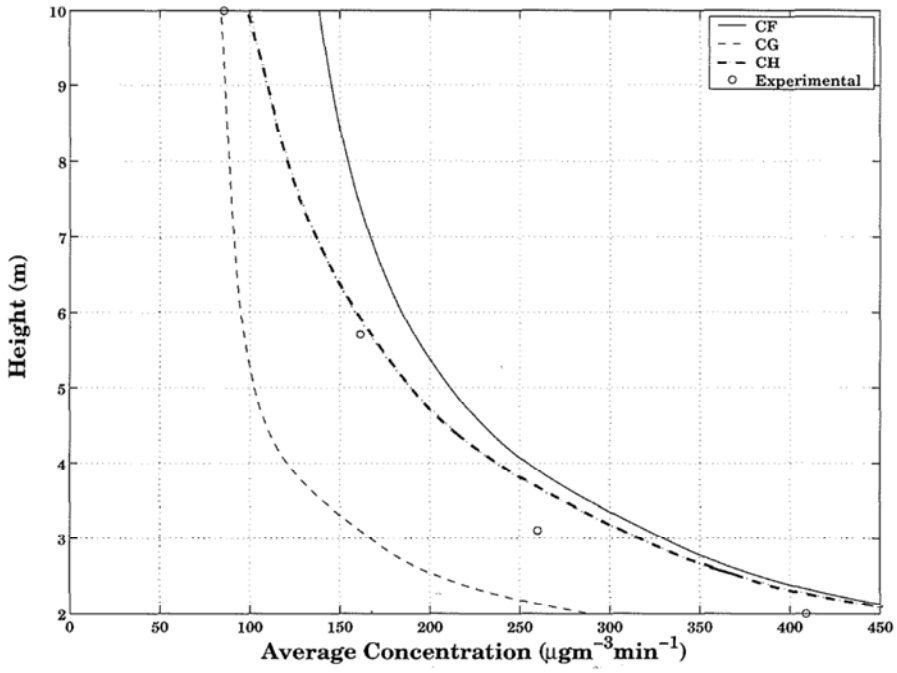

Figure 6.4: Modelled and measured vertical dust concentrations profiles at Site A for Cases CF to CH. Case CH gives the best fit with $R^2 = 0.92$ and $\sigma_e = 20.6$.

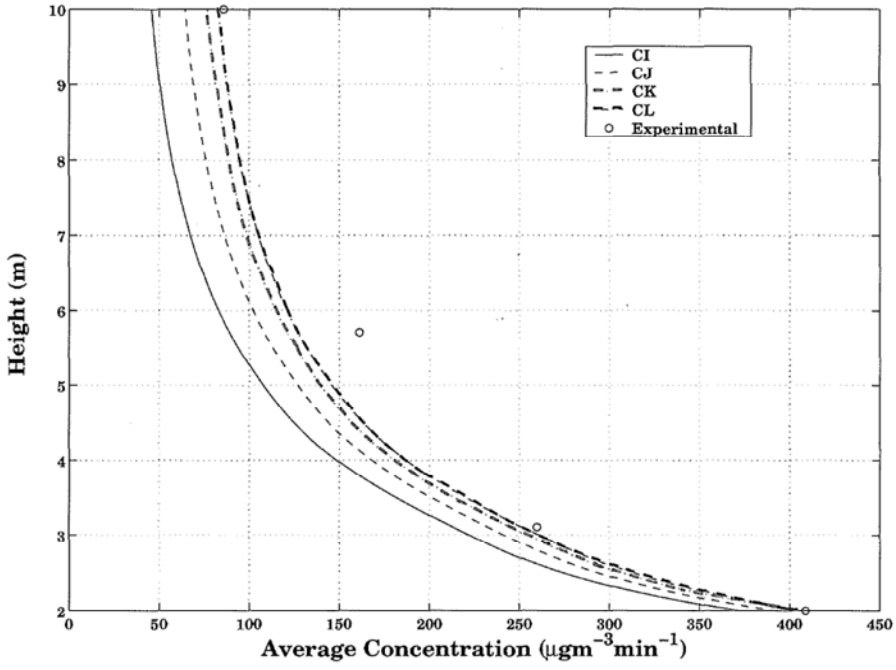

Figure 6.5: Modelled and measured vertical dust concentrations profiles at Site A for Cases CI to CL. Case CL gives the best fit with $R^2 = 0.96$ and $\sigma_e = 15.9$.

is most likely associated with the transport component of the process. It is apparent that the dust source configuration influences the interaction between the saltation and transport components, and therefore affects the shape of the dust concentration profile.

In Cases CI to CL (Figs. 6.1 and 6.5), the upwind limit of the erosion pattern is reduced, but the separation of sources in each section is held constant. These simulations, indicate that most of the dust concentration profile at Site A is made up of material originating within two kilometres upwind of the tower. This is consistent with Tsoar and Pye (1987) and Raupach et al. (1993), who indicate that the transport distance for particles of the size classes modelled here is of the order of a few kilometres. It also explains why there are marginal differences in the modelled concentration profile between Cases CA, CB, CC and CL.

In summary, the sensitivity testing undertaken above, suggests that the shape of the dust concentration profile at Site A is strongly dependent on the dust source configuration. This goes a long way to explaining why Nickling et al. (1999), fitting a power function to a number of Australian dust events, found that the exponent ranged from -0.14 to -1.89. Whereas other studies outside Australia found that the exponent ranged from -0.1 to -0.63 (Chepil and Woodruff, 1957; Gillette, 1977; Nickling, 1978; Nickling and Gillies, 1993; Nickling et al., 1999). Nickling et al. (1999) concluded that the dust concentrations in Australia decrease more rapidly with height, but our sensitivity studies indicate that the exponent of any power function fit, is dependent on the dust source configuration. Reinterpreting Nickling et al.'s data in the light of this implies that spatial changes in dust source configurations are extremely important in determining the vertical dust concentration profile in all wind erosion environments.

If this finding is correct, then the source structure for Events E11-1995 and E3-1995 should be different from that of E1-1996. Case CM (Fig. 6.1) shows the dust source configuration which gave the best fit to E11-1995 and E3-1995 (Figs. 6.6 and 6.7 respectively). The only difference between the two

fits is that Q_b was $1000\mu gs^{-1}$ for E11-1995, and $140\mu gs^{-1}$ for E3-1995, which is not surprising since E3-1995 was a more regional event, than E11-1995 and would therefore, have a smaller local emission rate. Comparing the dust source configuration CM (Fig. 6.1) with CA (Fig. 6.1), it is immediately apparent that both E11-1995 and E3-1995-1995, have smaller local components than E1-1996, as expected. A closer look at the results for E11-1995 and E3-1995 shows an apparent contradiction, in that, according to the Nickling et al. (1999) classification, E3-1995 was a regional event, and E11-1995 was a moderate local event. DSism required both events to have sources *placed near Site A*. This can be explained by noting that disturbance at Site A, during the construction of the 2m and 10m towers and fences, would have ruptured the surface crusts, hence lowering the wind erosion threshold. Thus DSism correctly indicates that this disturbance was an actual erosion source during both events, but in E3-1995 the disturbed region was nowhere near as active as in Event E11-1995.

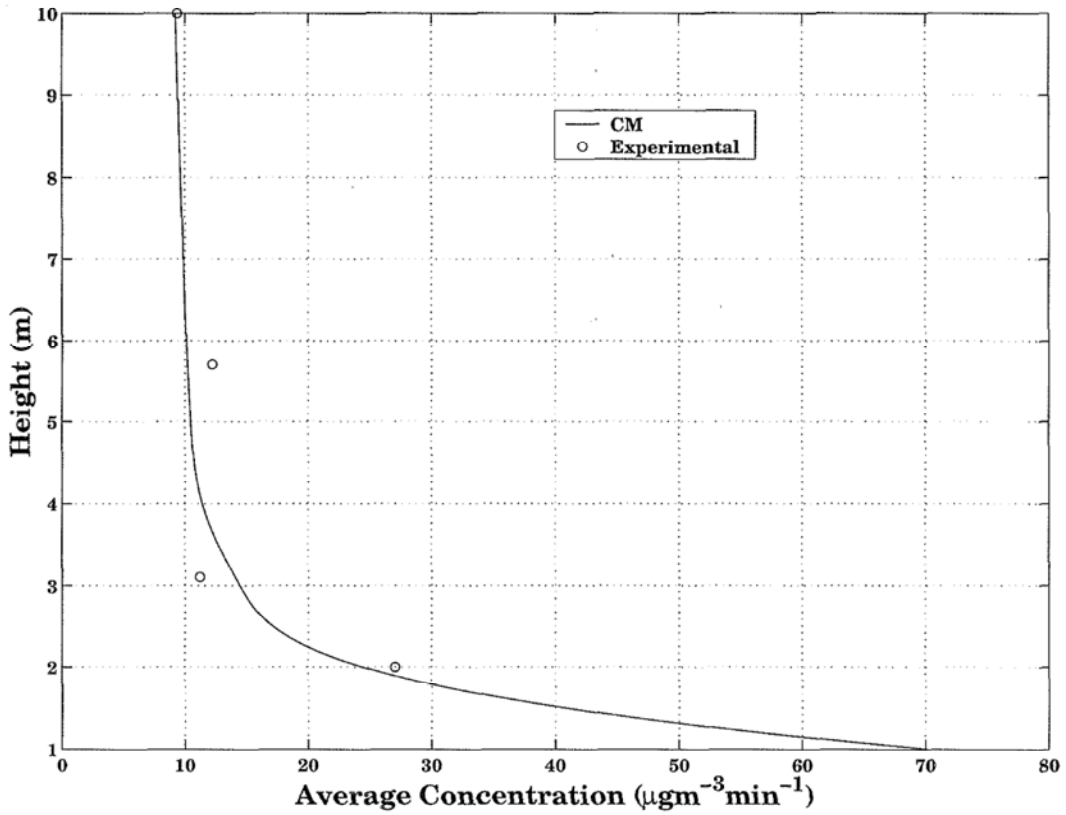

Figure 6.6: Modelled and measured vertical dust concentrations profiles at Site A for E11-1995. $R^2 = 0.90$, $\sigma_e = 2.3$.

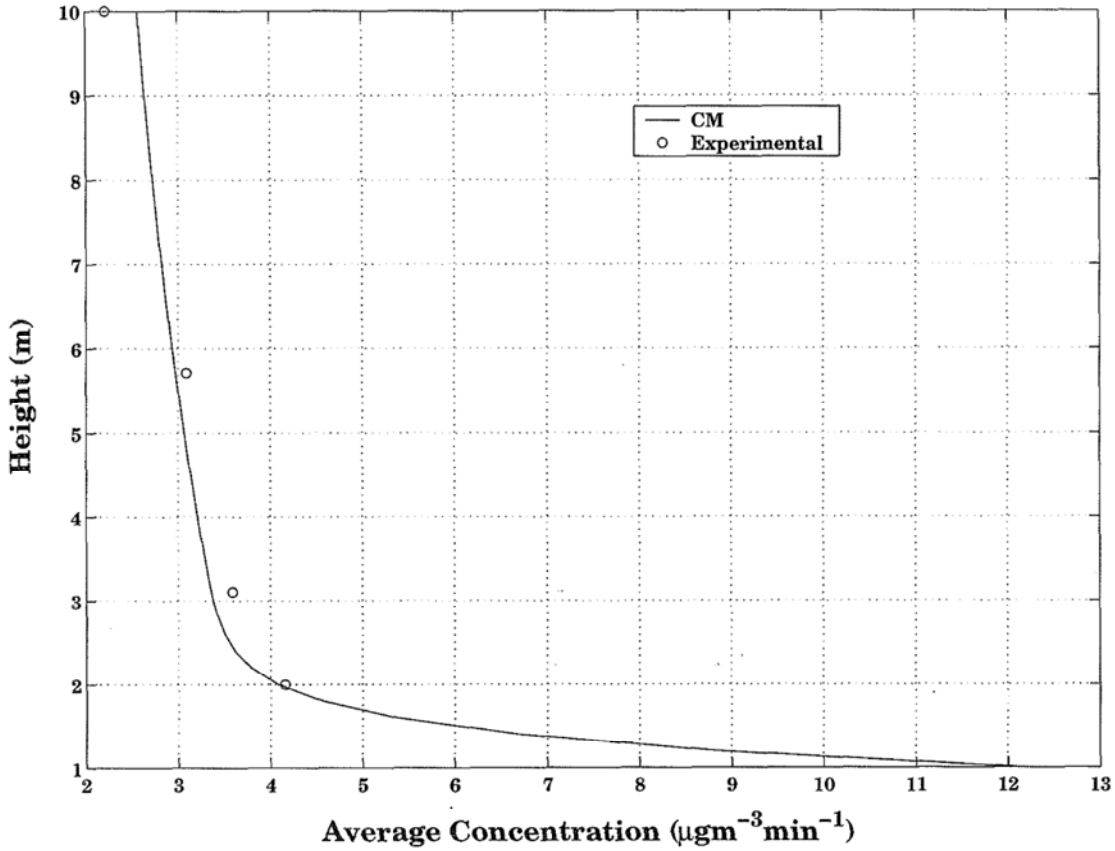

Figure 6.7: Modelled and measured vertical dust concentrations profiles at Site A for E3-1995. $R^2 = 0.92$, $\sigma_e = 0.23$.

6.5 Conclusion

The model simulations presented in this chapter show that the location of the sources within a given source region has a significant effect on the shape of the dust concentration profile. During large local wind erosion events the most important sources of material are within a hundred metres of the tower and the saltation and low level suspended material has an important influence on the dust concentration profile up to the height of 3m. During regional and minor local erosion events local erosion was less important, though, soil disturbances close to the tower were still a significant factor.

Another important result, is that using a given dust source configuration, with DSism, it is possible to reproduce the vertical dust concentration profile at any given point within the study site. The three separate events modelled here indicate that DSism, is correctly simulating wind erosion processes in

these events. This observation will be further tested in later chapters.

These simulations indicate that dust concentration profiles are extremely dependent upon the dust source configuration, which explains why the exponent of power function fits to the measured vertical dust concentration at the same site may have a wide variety of values (Nickling et al., 1999). The exponent may simply be quantifying the separation and location of dust sources with different erodibilities. This will be considered further in the next chapter.

Finally, these simulations illustrate nicely that, by treating the dust concentration profile as a signal and understanding the physical processes by which that signal can be reconstructed, it is possible to gain a significant new insight into the wind erosion process. Looking at more events in this fashion, will cause this insight to grow rapidly.

Chapter 7

Effects of topography, surface roughness and heating upon vertical dust concentration profiles

7.1 Introduction

As outlined in Chapter 2, wind erosion rates are affected by numerous environmental factors, such as vegetation, roughness and land type, acting both individually, (Gillette, 1977; Iversen et al., 1991; Lancaster and Baas, 1998; Lancaster et al., 1991; Leys, 1991a) and collectively (summaries in Greeley and Iverson, 1985; McTainsh and Boughton, 1993; and Shao, 2000). Less is known, however, on the individual or collective effect of these factors upon dust concentration profiles and in particular the role of different spatial patterns of these factors.

7.2 Measurements of the characteristics of vertical dust concentration profiles

Most vertical dust concentration profiles measured during wind erosion events were fitted to the function

$$C(z) = az^b\,, \tag{7.1}$$

where $C(z)$ is the mass flux at height z, and a and b are regression coefficients (Chepil and Woodruff, 1957; Nickling et al., 1999). Such a fit is illustrated in Figure 7.1. The exponent b in Equation (7.1) was found by (Nickling et al., 1999) to range between $-1{\cdot}89$ and $-0{\cdot}14$ for Australian conditions. This contrasts with field studies outside of Australia that found the exponent b to range from $-0{\cdot}63$ to $-0{\cdot}1$ (Chepil and Woodruff, 1957; Gillette, 1977; Nickling, 1978; Nickling and Gillies, 1993; Nickling et al., 1999). However, Nickling et al. (1999), found that the Australian values of b were similar to intense dust events in the Yukon Territory of Canada. Thus both in Australia and for intense dust events in the Yukon, the dust concentration tends to decrease more rapidly with height than elsewhere.

Since the early 1990's a number of attempts have been made to find a function that gives a significantly improved fit to the vertical dust concentration profile. Vories and Fryrear (1991) and Fryrear and Saleh (1993) reported that using the form described in Equation (7.1), was only strictly valid for dust transported in suspension. In order to improve the fit, Vories and Fryrear (1991) added an exponential term to the power function to describe the creep and saltation component and thus described the variation of mass flux with height as

$$q(z) = az^{-b} + \exp(-dz)\,, \tag{7.2}$$

where $q(z)$ is the mass flux at height z and a, b, c and d are regression coefficients. As reported by Sterk and Raats (1996) the use of Equation (7.2) is not appropriate if only a few data points are available. Instead they suggested

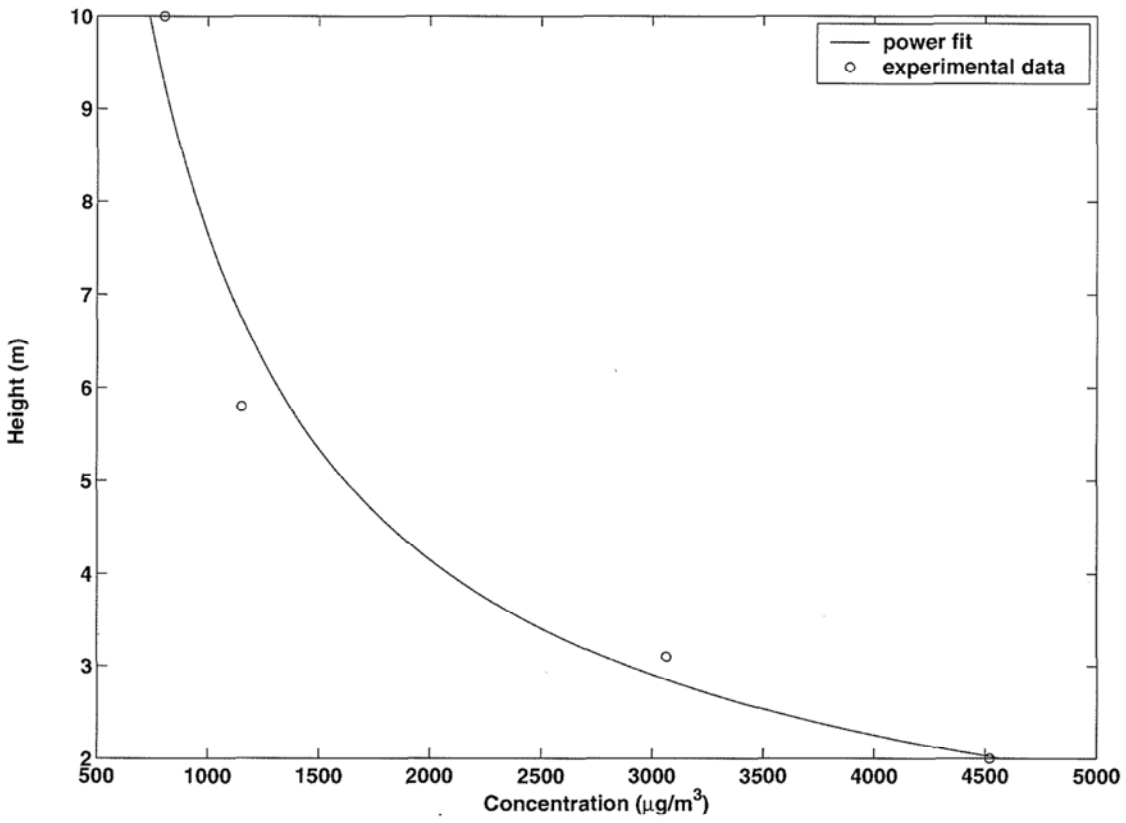

Figure 7.1: Example of a power function as described in Equation (7.1) providing a "good" fit to the vertical dust concentration data recorded at Site A for the dust event that occur on the 6 September 1995. Fitting this function produced an R^2 value of 0.97 and $\sigma_e = 95.7$.

the use of a modified power function of the form:

$$q(z) = q_0 \left(\frac{z}{\alpha} + 1\right)^{-p}, \tag{7.3}$$

where q_0 is a constant, α and p regression coefficients. Leys (1998) however, found that there was little difference in the performance of these different fitting techniques under Australian conditions.

The results presented in the previous chapter suggest that the exponent b in Equation (7.1) might be reflecting the location and separation of dust sources within a given land type. Although this explains the change in exponent b on a event basis due to variation in field conditions, it fails to explain why several events have been recorded in the Channel Country, that have distinct "kinks" in the profile (Fig. 7.2). In these cases a power/exponential vertical

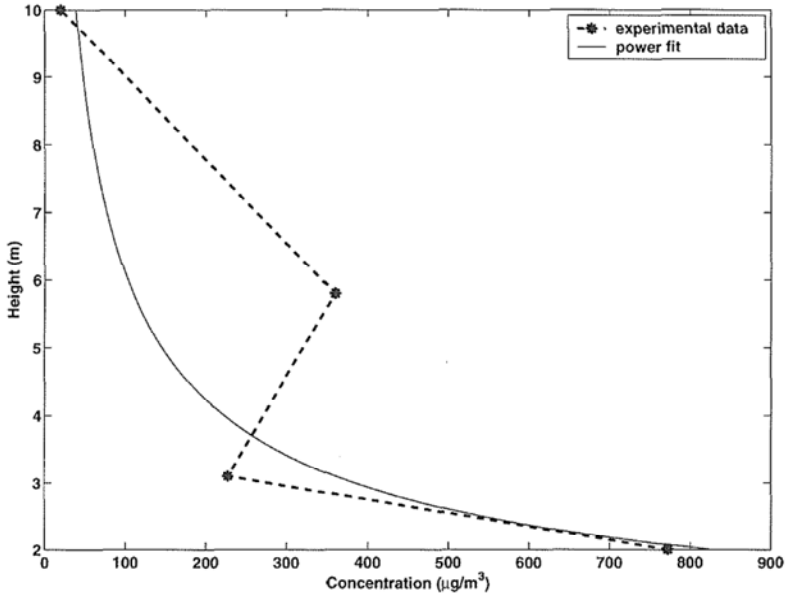

Figure 7.2: A typical "kink" recorded in the vertical dust concentration profile during the E2-1995 wind erosion event. A linear spline has been used to illustrate the extent of the variation. Fitting a power function as in Equation (7.1) produced in $R^2 = 0.72$, $\sigma_e = 146.6$.

profile model does not adequately describe the variation in concentration with height.

The non-linear regression coefficient (R^2) (and the standard deviation of the residuals (σ_e)) values for the fits shown in Figures 7.1 and 7.2, also show something interesting in terms of processes. In particular, the dramatic reduction in R^2 value (from 0.97 to 0.72) when the "kink" is present, suggests that another process may be in operation during such events. This observation is particularly important in terms of the signal versus noise view of dust concentration profiles being developed in this thesis. It supports the view that process signal (variation) degrades an otherwise reasonable regression fit. The remainder of this chapter considers possible process differences between "Kinky" profiles and "normal" profiles and searches for field evidence to support the existence of such processes. If the existence of such processes can be accounted for by field data, it would strongly support the view taken in this thesis, that the dust concentration profile can be viewed as a signal. If so, then the vertical dust concentration profile must contain information about

wind erosion processes and sources within the local area.

7.3 Field conditions

"Kinks" in the vertical dust concentration profile have been recorded on a regular basis by the 10m dust monitoring towers with semi-isokinetic samplers (Fig. 7.2) within the study site. They have also recently been simulated by vehicle induced entrainment at different distances upwind of the tower using DustTraks (Leys, 2001, pers. comm.).

Twelve dust events were recorded during the 1995 wind erosion season. Eight of these (or 66%) show "kinks" in the recorded dust concentration profile (Table 7.1). The position of this "kink" also varied from one event to another. To understand these processes, DSism was used to simulate the 1995 wind erosion events (Chapters 4 to 6 and Butler et al. (1996) and Butler et al. (2001) for additional details). The Site A data was selected for this study, since during 1995, the claypan was almost completely devoid of vegetation, thus simplifying the analysis.

7.4 Possible natural process explanations

Possible explanations for the appearance of the "kinks" in the vertical dust concentration profile include thermal heating, topographical and spatial effects. These are discussed below.

Initially, it was thought that separation of, and spatial variations in dust sources created the "kink". To see if DSism could reproduce these kinks by simply varying the dust source configuration, several different simulations were undertaken using the dust source configuration shown in Figure 7.3. Sensitivity testing was then used to determine the effect that S_1 (source line separation in Source Area A), S_2 (source line separation in Source Area B), SW_1 (upwind width of Source Area A), SW_2 (upwind width of source area B)

Table 7.1: Wind speed and direction, and temperature data, for wind erosion events in the Channel Country of western Queensland, 1995.

Event No.	Mean Wind Speed (ms^{-1})	Wind Direction °T	Temperature °C		Kink (yes/no)
			2m	10m	
E1-1995	12.62	29.65	21.65	20.62	yes
E2-1995	10.85	67	24.01	23.27	yes
E3-1995	11.79	23.66	26.6	25.5	yes
E4-1995	13.46	32.21	26.0	25.55	no
E5-1995	12.31	297.43	25.84	24.98	yes
E6-1995	12.39	25.76	24.26	23.24	yes
E7-1995	11.01	291.14	26.78	26.76	no
E8-1995	13.63	219.02	28.01	27.69	no
E9-1995	11.47	89.73	23.48	22.76	yes
E10-1995	14.85	27.98	26.81	25.83	yes
E11-1995	14.6	31.7	30.98	29.91	no
E12-1995	11.45	339.89	22.69	21.77	yes

and D (the separation between Source A and B) have on the vertical dust concentration profile. Four of the five parameters were held constant and the remaining parameter varied, and results compared. In all, over 200 simulations were undertaken with the different combinations of S_1, S_2, SW_1, SW_2 and D. In each of these, the emission rate across each source line was assumed to be constant (Figure 7.4 and Table 7.2).

Figure 7.4 shows that altering the source locations and strength, clearly affects the shape (curvature) of the vertical dust concentration profile. In Simulations 1 and 2 (Table 7.2), the distance between Source Area 1 and 2 was increased by 10m. This change produced a significant alteration in the shape of the vertical dust concentration profile (Fig. 7.4). Simulations 3 and 4 (Table 7.2) show that simple changes in the dust source configuration (i.e., the distribution of the various source lines in each source area) can produce further dramatic changes in the dust concentration profile (Fig. 7.4). Thus, the rate of decrease in dust concentration with height is altered by spatial variations in the source areas. While these results support the claims of Butler et al. (2001) that the exponent in a power function fit is an indirect measure of

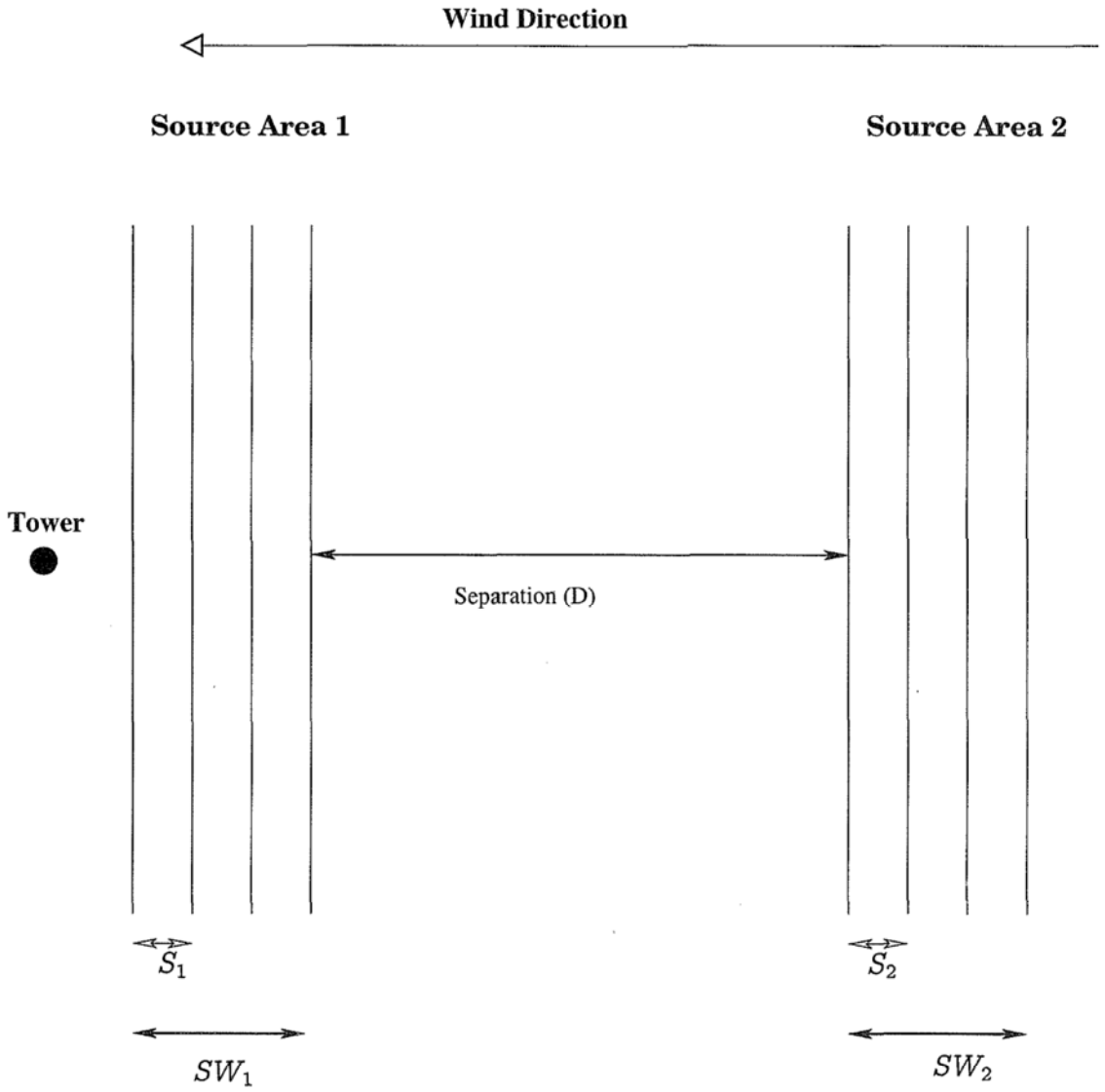

Figure 7.3: Schematic of how dust sources areas 1 and 2 are represented in the simulations. Based on the dust source distribution required to simulate Event 2.

the spatial variation in dust sources, none of the simulations above produced a "kink", in the vertical dust concentration profile.

The above simulations, assumed that wind flow did not change during each event. No allowance was made for possible variations in the wind profile, which cause changes in the buoyancy of the dust plume. A number of environmental factors can affect wind flow, some of which have already been outlined in Chapter 2. The most important are: topography, surface roughness, and heating.

Table 7.2: Data used in simulations 1–4 for the source structure described in Figure 7.3).

simulation	Source Area 1			Separation	Source Area 2		
No.	S_1	Strength	SW_1		S_2	Strength	SW_2
	(m)	(μgs^{-1})	(m)	(m)	(m)	(μgs^{-1})	(m)
1	2	6	10	35	2	36	10
2	2	6	10	45	2	36	10
3	2	6	10	45	2	6	10
4	2	36	10	65	2	6	10

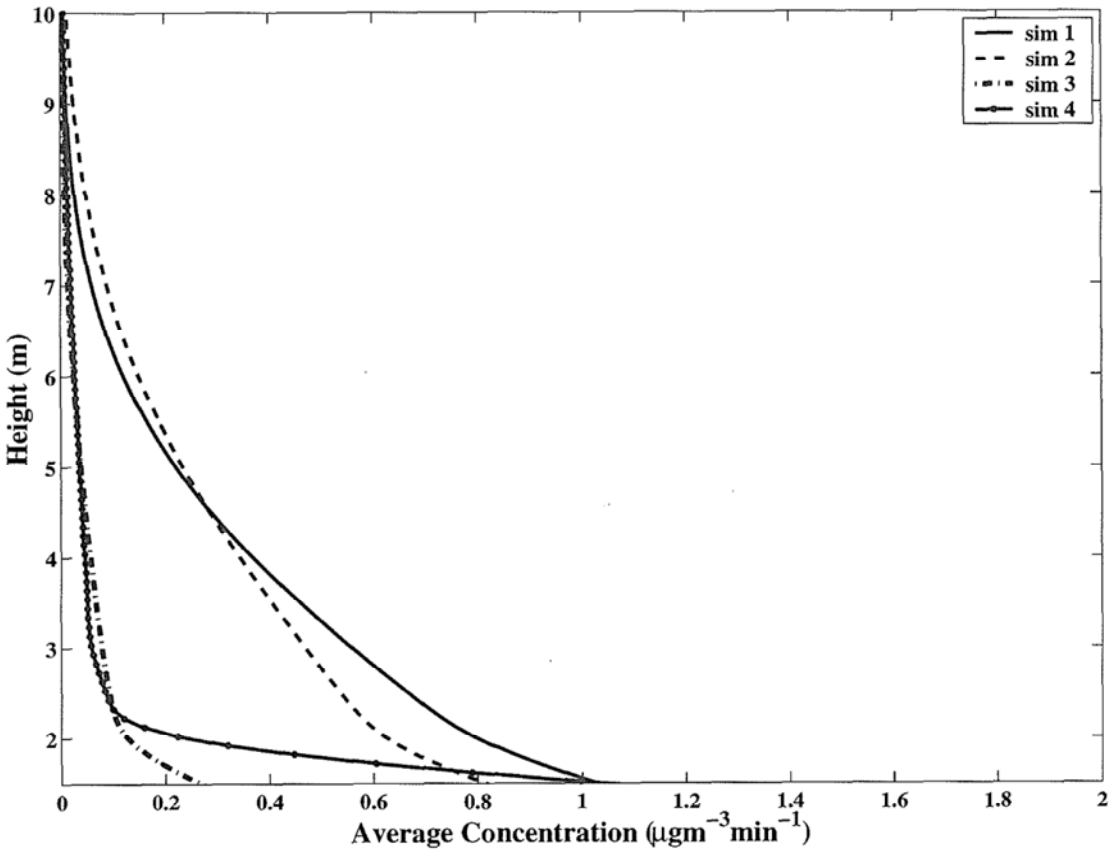

Figure 7.4: The dust concentration profiles resulting from source variation simulations, using that data in Table 7.2.

7.4.1 Topography

Topographic effects upon wind flow (Fig. 2.7), have been well studied (Walmsley et al. (1982); Baines and Hoinka (1985) and Baines (1995)) (see Figure 2.7). These studies show that the magnitude of the disturbance to the wind flow is dependent on the wind speed and the relative height of the topography. In the wind erosion events considered here, topography is unlikely to be a major cause of the "kinks", since the claypan has a relative relief of less than 1.5m over more than 1km (Fig. 7.5) and it is unlikely to have a significant effect on the wind profile.

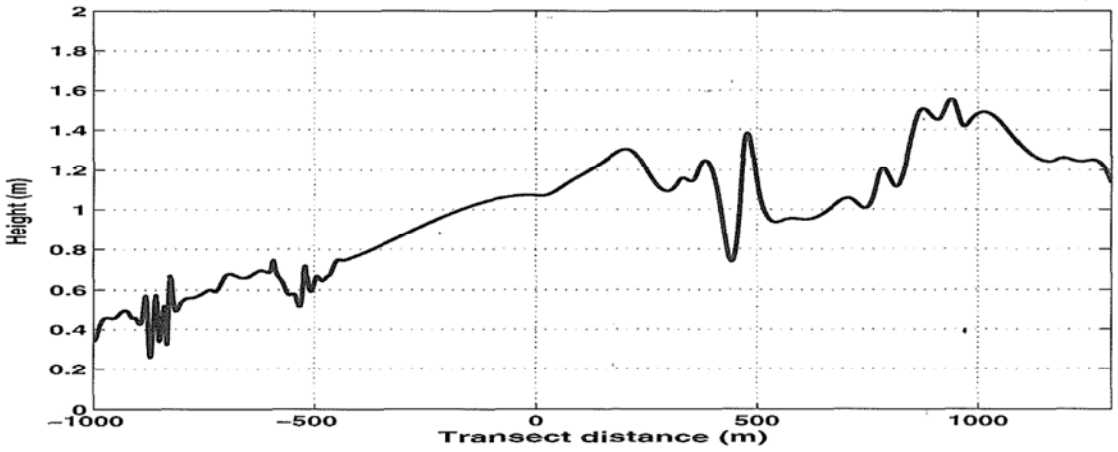

Figure 7.5: Topography of the claypan. The transect for this diagram was taken along the line of Event 10 in Figure 7.9. Zero represents the centre of the wind rose in Figure 7.9, with the positive direction being to the NE.

7.4.2 Vegetation and surface roughness

During 1995, there were only very small pockets of vegetation on the claypan (Fig. 7.6), the maximum height of which was less than 10cm. Vegetation is therefore unlikely to have had a significant effect on the wind flow. It is more likely that these small pockets of vegetation alter the turbulence structure in the immediate neighbourhood of the surface (Brookshaw, 2001, pers. comm.). Such turbulence does not significantly affect the streamlines of the air flow, but does alter the momentum of particles within the dust plume. This

changes the dispersal rate in these regions, and could possibly account for the structure of the dust plume, shown in Figure 7.7. But is unlikely to produce the "kink", since the flow structure in not significantly disturbed.

While roughness and vegetation cover did not vary much within the claypan in the 1995 season, easterly winds pass over the main channel of the Diamantina River, which had a large number of River Red Gums (Fig. 2.3). These can reach a height of 20m, and act as a natural shelter belt, so that events coming from the east are likely to have a much more complicated wind flow pattern.

7.4.3 Soil surface heating

Yoshida (1991) showed that buoyancy rise due to thermal heating in urban areas, affects the dispersion air pollutants and other air pollution studies have shown that plume buoyancy effects need to be taken into account (Hanna et al., 1982; Zannetti, 1990). Since temperatures are high on the claypan, the thermal convection there is likely to be important. Figure 7.6 shows that during the 1995 season there were a range of light and dark areas on the claypan, which would have had quite different thermal radiation and absorption properties, thus producing different temperature gradients across the claypan. In addition the meagre vegetation on the claypan at the time, meant that changes in thermal radiation were mainly due to changes in soil surface conditions. Of the three factors examined, surface heating is the most likely cause of the "kinks" in the vertical dust concentration profile.

A possible mechanism by which the "kinks" are created is shown in Figure 7.8. Material entrained at Source 2, is picked up in Air Parcel B, and transported downwind. As the air heats up it becomes more buoyant and thus rises as it travels. In contrast, material entrained at Source 1 is transported in Air Parcel A. Since Air Parcel A hasn't travelled as far, the rise due to buoyancy is much smaller. Hence material from Source 2 is recorded higher up the tower than that of Source 1, therefore creating the "kink" in the dust concentration

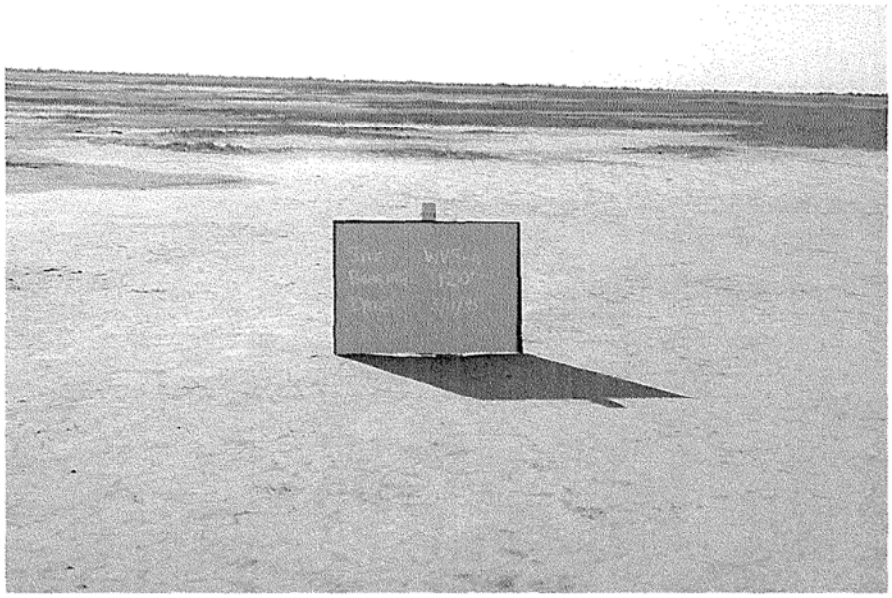

Figure 7.6: The surface condition of the claypan during the 1995 season. Note: The light and dark areas are clearly visible and that the claypan is almost devoid of vegetation.

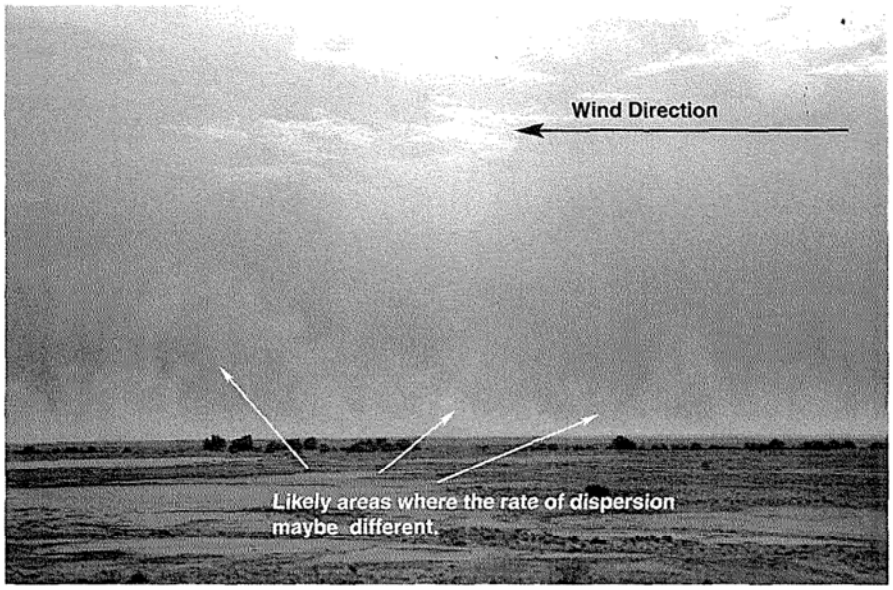

Figure 7.7: This dust event, which occurred on 12th February 2000, illustrates that variations in roughness due to vegetation or surface heating of the claypan might cause dust within the plume to be dispersed at different rates.

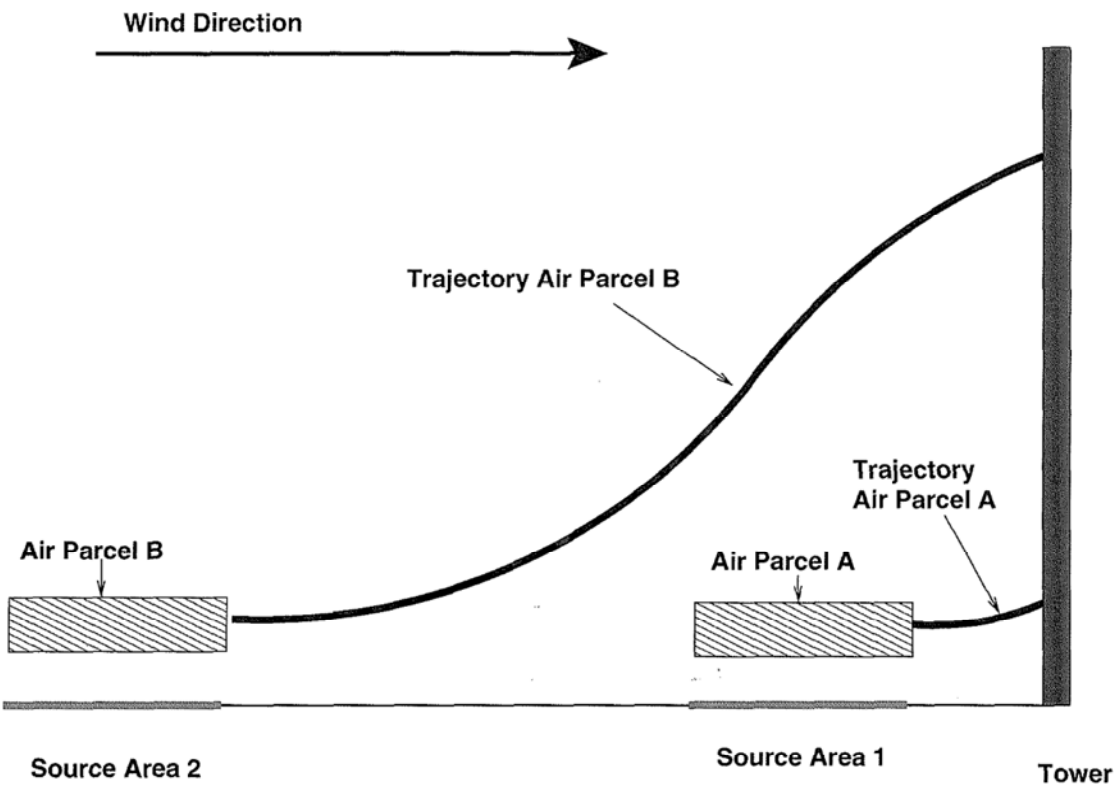

Figure 7.8: Schematic showing the most likely mechanism by which the "kinks" in the dust concentration profile are generated.

profile.

The thermal stability conditions during each event were classified by Richardson's number (Ri), which is the ratio of the vertical thermal gradient to the vertical velocity gradient. Ri was calculated at 2m using the formula given below:

$$Ri|_{z=2\mathrm{m}} = -\frac{g\,\frac{dT}{dz}\Big|_{z=2\mathrm{m}}}{T|_{z=2\mathrm{m}}\left(\frac{du}{dz}\Big|_{z=2\mathrm{m}}\right)^2}, \tag{7.4}$$

where g is the acceleration due to gravity, T is the temperature and u is the wind velocity (Sutton, 1953). This formula assumes that air behaves as an ideal gas, with

$$\frac{PV}{T} = \text{constant}, \tag{7.5}$$

where P is the pressure, V is the volume and T is the temperature. The

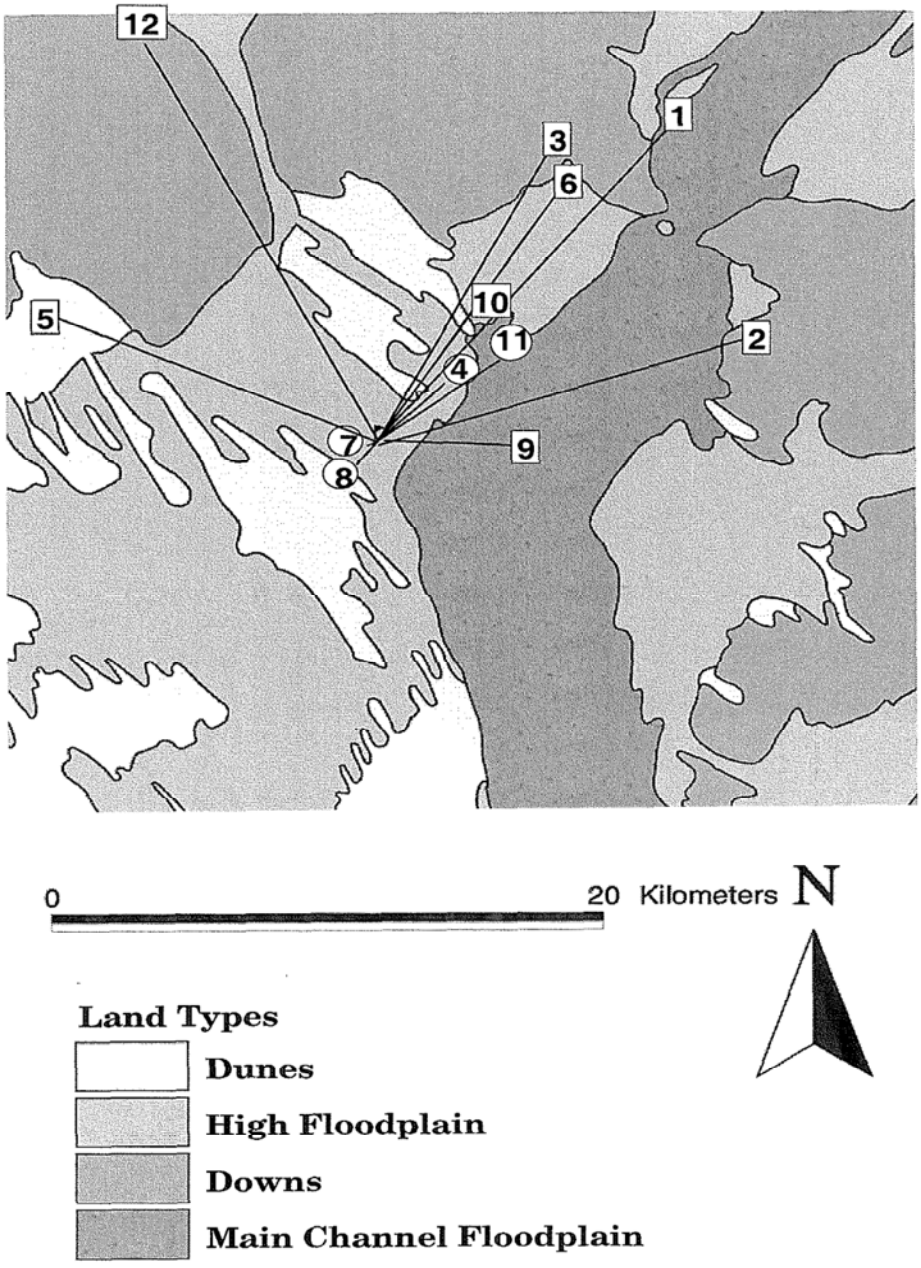

Figure 7.9: Wind rose for the events shown in Table 7.3. The centre of the wind rose corresponds to the location of the 10m tower at Site A (Fig. 5.2). The longer the line the greater the magnitude of the Richardson's number, $|Ri|$. Events with a "kink" in the dust concentration profile are marked using a square box, while those without are marked by a round box. Note: 1 and 10 lie along the same line.

gradients $\frac{dT}{dz}$ and $\frac{du}{dz}$, were calculated using the forward difference formulas:

$$\left.\frac{dT}{dz}\right|_{z=2\text{m}} = \frac{T(10\text{m}) - T(2\text{m})}{8}, \tag{7.6}$$

$$\left.\frac{du}{dz}\right|_{z=2\text{m}} = \frac{u(10\text{m}) - u(2\text{m})}{8}, \tag{7.7}$$

where $T(10\text{m})$ is the average temperature at 10m, $T(2\text{m})$ is the average temperature at 2m, $u(10\text{m})$ is the average wind speed at 10m and $u(2\text{m})$ is the average wind speed at 2m.

Events E1-1995, E3-1995, E4-1995, E6-1995, E8-1995 and E12-1995 (Table 7.3), actually consisted of a number of smaller events (or sub-events), each of which varied in terms of wind speed, direction and temperature, but for which only one dust concentration profile was recorded. It was therefore, necessary to distinguish which event contributed most to the resulting dust concentration profile, by using an Event Strength Index (ESI) for each sub-event. The ESI must incorporate both the wind speed and duration of the event, since the final concentration is proportional to both these factors. The simplest ESI, was the product of event duration and wind speed.

The ESI was calculated for each sub-event Table 7.3, and it was assumed that the sub-event that contributed the most to the dust concentration profile was the one which had the largest value of ESI. Figure 7.9 shows the magnitude of Richardson's number $|Ri|$, wind direction and whether the dust concentration profile has a kink. This figure also shows that the events which had "Kinky" profiles did not come from any one direction. Therefore, further indicating that topography is an unlikely cause of the "kinks".

Table 7.3, shows that for single Events E2-1995, E5-1995, E9-1995, and E10-1995, events which has a moderately large $|Ri|$ had a "kink" in the vertical dust concentration profile, while Event E7-1995 which has a small $|Ri|$ did not have a "kink". An exception to this is Event E11-1995, which has a large value of $|Ri|$ (ie $|Ri| \gtrsim 1$), but no "kink". During the period of highest wind speeds recorded in Event E11-1995, the generator powering the vacuum pump ran out of fuel, which brings into question the validity of this data. Excluding Event E11-1995, the evidence points to a threshold value for $|Ri|$ of around 1,

Table 7.3: Events and sub-event data for 1995 season.

Event	Sub-event	Wind Speed (ms^{-1})	Wind Direction (°T)	Duration (hrs)	Event Strength Index (ESI)	*Ri*	Kink
E1-1995	a	10.89	55.13	1.67	18.15	4.59	yes
	b	12.62	29.65	2.5	31.55	3.7	
	c	10.95	345.46	1	10.95	-0.36	
E2-1995	–	10.86	67	3.58	38.92	2.58	yes
E3-1995	a	11.79	23.66	2.83	33.41	2.99	yes
	b	12.14	25.81	1.25	15.71	1.92	
E4-1995	a	11.25	46.61	9.25	104.06	2.17	
	b	13.46	32.21	8.5	114.41	0.78	no
	c	12.14	53.09	3.58	43.5	2.49	
E5-1995	–	12.31	297.43	3.33	41.03	2.37	yes
E6-1995	a	11.13	38.39	1.42	15.77	4.08	yes
	b	12.39	25.76	3.67	45.43	2.64	
	c	12.11	30.41	2.33	28.26	2.89	
E7-1995	–	11.01	291.14	1.08	11.93	0.03	no
E8-1995	a	11.79	21.48	2.0	23.58	4.5	
	b	13.63	219.02	4.67	63.61	0.3	no
E9-1995	–	11.47	89.73	1.17	13.42	0.93	yes
E10-1995	–	14.85	27.98	4.75	70.53	1.23	yes
E11-1995	–	14.6	31.7	2.17	31.6	1.337	no
E12-1995	a	11.45	339.89	3.83	43.89	4.38	yes
	b	11.61	333.23	2.08	24.19	1.15	

when these "kinks" begin to appear. This is consistent with Sutton (1953) and Shao (2000), who state that for given surface, a critical value of Ri exists, at which the thermal gradient becomes an important physical consideration.

For Events E7-1995 and E8-1995, which have values of $|Ri| < 0.5$, a power law fit (Fig. 7.10), similar to Nickling et al. (1999) produced a $R^2 > 0.94$. The standard deviation of the error (σ_e) confirms how well this model fitted this data. Thus, under stable thermal conditions, when $|Ri|$ is small, the power law provides an extremely good approximation of the dust concentration profile and thermal processes have little impact. However, the majority of events in 1995 had an $|Ri| > 1$, so thermal heating is likely to play a much more important role. As shown in Figure 7.11, the R^2 value in these cases decreases to around 0.7–0.8. The standard derivative of the error (σ_e) in these fits suggests that these data points are much more scattered about the fitted line.

While a power fit still describes the basic vertical dust concentration profile, thermal heating is scattering these data points. In these cases, when $|Ri| > 1$, the thermal gradient dominates the vertical velocity gradient. Thus, suggesting that surface heating and resulting buoyancy effects are the most likely cause of the "kinks" in the vertical dust concentration profile.

The lowest positive value of Ri occurred during Event E7-1995. This not a surprising result, since 2.2mm of rainfall was recorded between Events E6-1995 and E7-1995. This rainfall, would have reduced the amount of reflected radiation from the claypan, resulting in an almost uniform temperature profile ($\frac{dT}{dz} \approx 0$, see Table 7.1), thus producing the low value of Ri.

Events E3-1995, E6-1995 and E12-1995 all have dominant sub-events, with $|Ri|$ values greater 1. The remaining multiple events consist of a high and low $|Ri|$ value. In Event E1-1995, sub-events a and b, clearly contribute the most to the final vertical dust concentration profile. Since each of these has an $|Ri|$ of greater than 1, a "kink" would be expected in the vertical dust concentration profile for Event E1-1995. Table 7.3 shows that this was indeed the case. Event E8-1995 is clearly dominated by sub-event b, which has an

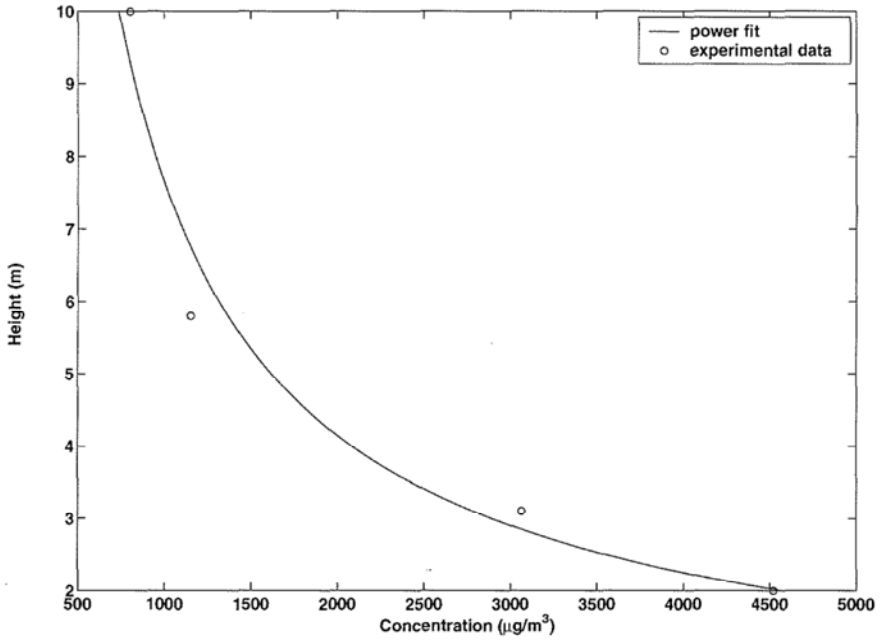

(a) Power law fit to Event E7-1995, giving an R^2 value of 0.97, and $\sigma_e = 114$.

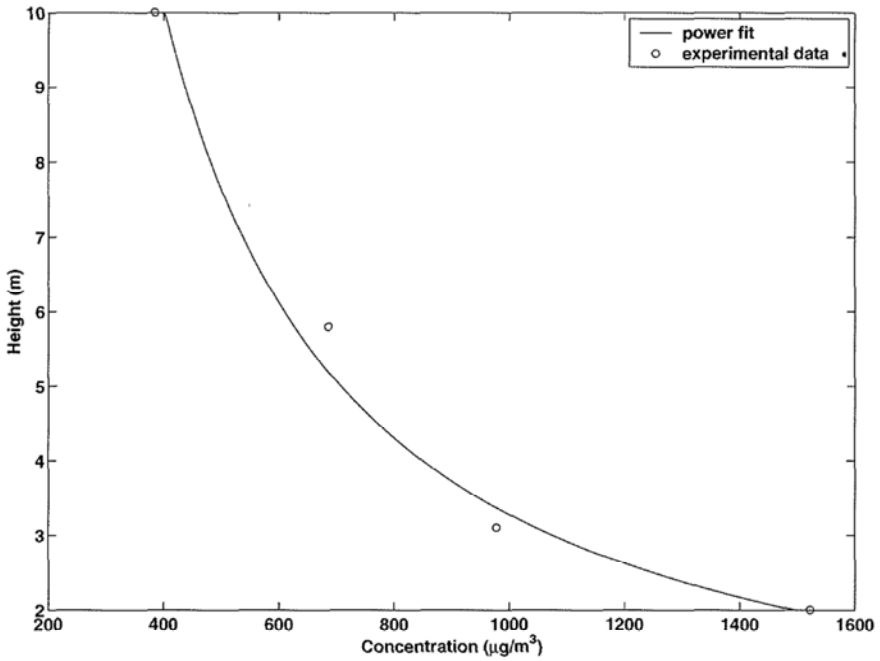

(b) Power law fit to Event E8-1995, giving an R^2 value of 0.99, with $\sigma_e = 24.7$.

Figure 7.10: Power law fits for Events E7-1995 and E8-1995 which have a low value of $|Ri|$.

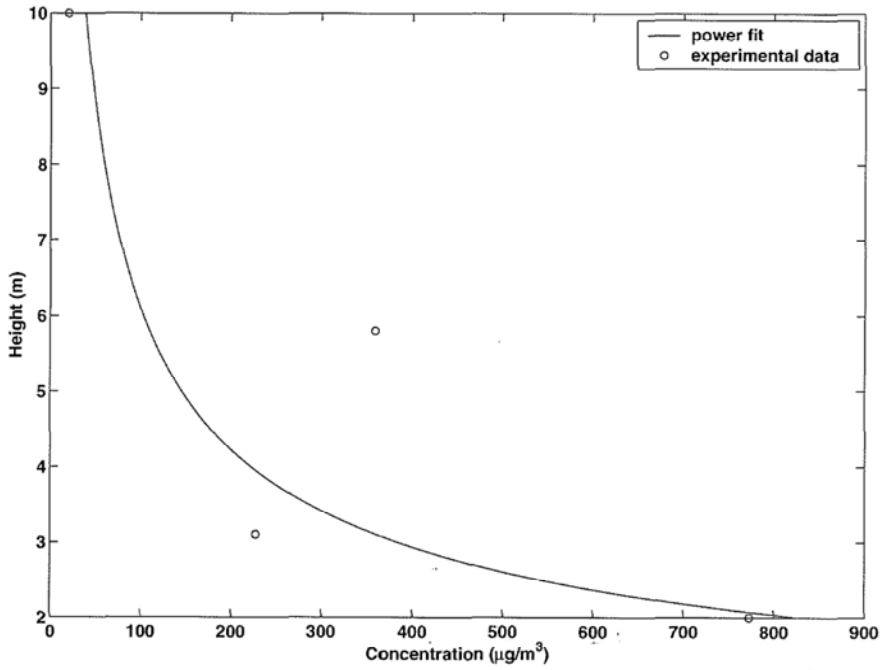

(a) Power law fit to Event E2-1995, giving an R^2 value of 0.72, σ_e = 100.

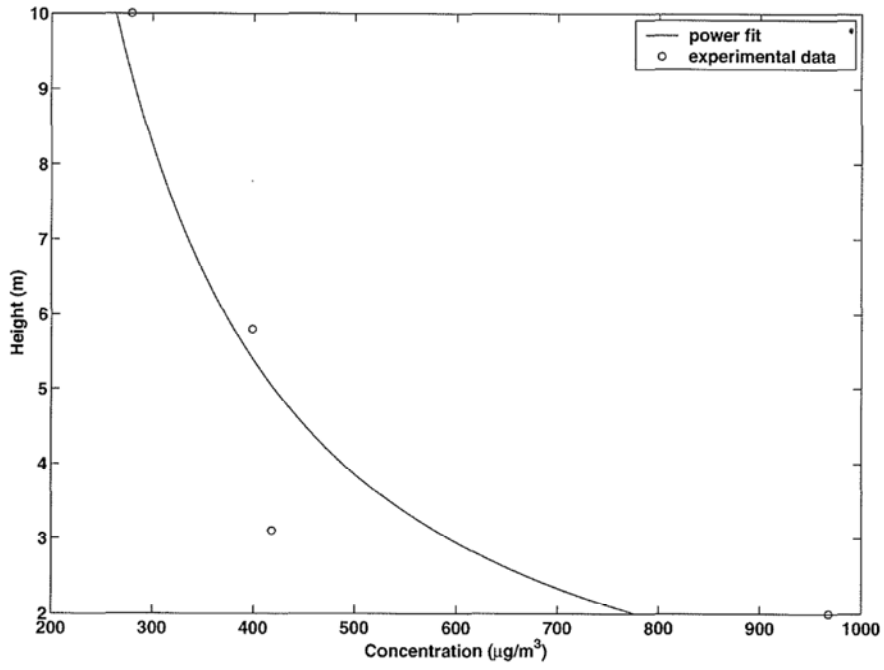

(b) Power law fit to Event E5-1995, giving an R^2 value of 0.80, σ_e = 92.7.

Figure 7.11: Power law fits for Events E2-1995 and E5-1995 which have a high value of $|Ri|$.

ESI approximately three times that of sub-event a. Since sub-event b has an extremely low value of *Ri* and contributes the most to the final concentration profile, it is reasonable to assume that it would contribute most to the final dust concentration profile. Thus Event E8-1995 would not have a "kink". In Event E4-1995, there are two large sub-events (a and b), contributing to the final profile. In calculating the ESI, it is assumed that erosivity is directly proportional to wind speed. In fact, erosivity increases exponentially with wind speed. This means that sub-event b will clearly dominate the concentration profile for Event E4-1995, thus dominating any contribution from the other sub-events. Therefore, Event E4-1995 should not have a "kink".

7.4.4 Model simulations of surface heating affects

It is not possible at this stage to build a component into DSism to simulate the buoyancy rise due to thermal heating because temperature data is only available at a single location. One can indirectly simulate the effect that buoyancy would have by introducing different release heights for Source Areas 1 and 2 (Figs. 7.12 and 7.13). Hanna et al. (1982) used a similar technique to describe the effective release height due to plume rise in urban areas . Thermal buoyancy is simulated by releasing particles into a linear air flow line corresponding to the flow line from the heated surface (Fig. 7.12). Thus, if the thermal buoyancy effects are causing the "kinks", it should be possible to simulate the position and location of an "kink" for a given event by altering the angle (α) of the simulated release line in Figure 7.12. To test this hypothesis Simulations 5 to 10 were run using data shown in Table 7.4. The amount of plume rise, was assumed to increase as distance from the tower increases (Fig. 7.13). Increasing the value of α, therefore simulates the effect of increasing the amount of plume rise.

The effect of varying the angle α can be seen in (Fig. 7.14). The more α increases the higher the "kink" will appear in the dust concentration profile. It is particularly interesting to note that the "kink" is produced for a relatively

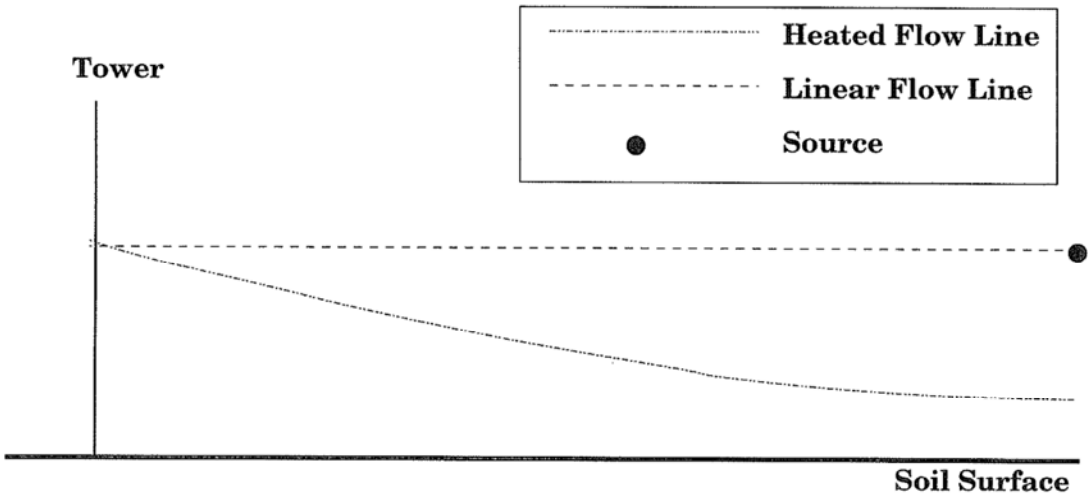

Figure 7.12: Schematic of how DSism simulates heated plume rise.

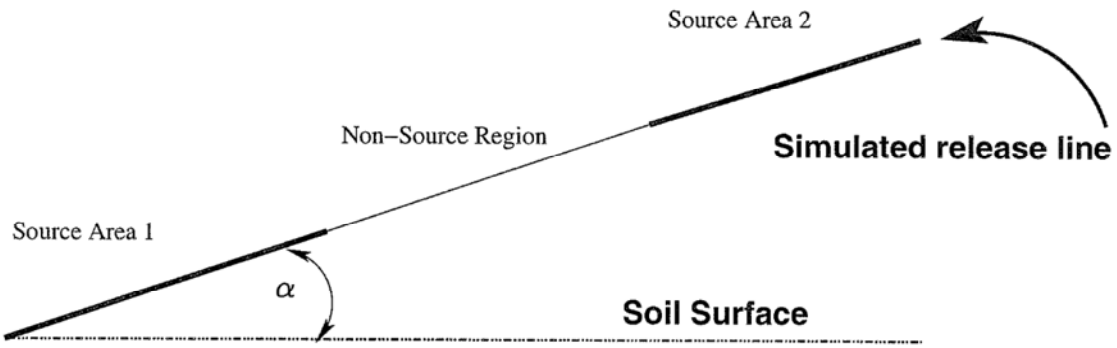

Figure 7.13: Schematic of how elevation is included in the simulation.

small value of α (i.e., around 0.15 radians or 8.6°). Such a small value, suggests that very little heating is required to produce a buoyancy effect sufficient to cause the "kink" to appear.

It is also important to note, that fitting a power law to the experimental data shown in Figure 7.14 produced an R^2 of 0.72 and a σ_e of 100. The R^2 value in this case is a good 0.2 lower than is typical of events shown in Figure 7.10, which have a low Ri value. In contrast, using DSism and accounting for thermal buoyancy, produced a R^2 value of 0.8 and a σ_e of 84.2. The R^2 value in the DSism case is approximately 0.1 lower than for events which have a small Ri. Such an improvement clearly suggests that by adding thermal buoyancy into DSism, much of the observed variability in vertical dust concentration profiles for events which have large Ri is accounted for.

Frank and Kocurek (1994) observed that changes in thermal stability have a strong influence on the wind velocity profiles. The fact that DSism is able to produce such good fits to the vertical dust concentration profiles for all Ri's, indicates that DSism is correctly accounting for the affect that changes in thermal conditions have on the wind velocity profile. If this was not the case then the DSism fit would be much worse for events which have a large Ri.

While the above results suggests that thermal heating is a likely cause of the "kink", it does not necessary imply that the larger the value of Ri at the tower, the higher the kink will appear. The reason for this, is that the actual rise is dependent on the thermal properties of the surface upwind of the tower (for which there is no data). Thus, without knowing the thermal properties upwind of the tower it is not possible to truly relate the position of the "kink" to the Ri values for the event.

7.5 Conclusions

Until now, most researchers have used some type of power function to model how vertical dust concentration varies with height. However, many vertical

Table 7.4: Data used in simulations 5–8 for the source structure described in Figure 7.3), including the angle α used to describe the buoyancy effect of thermal heating.

No.	Source Area 1			Separation	Source Area 2			α
	S_1 (m)	Strength (μgs^{-1})	SW_1 (m)		S_2 (m)	Strength (μgs^{-1})	SW_2 (m)	
5	2	6	10	35	2	36	10	0.0
6	2	6	10	35	2	36	10	0.1
7	2	6	10	35	2	36	10	0.12
8	2	6	10	35	2	36	10	0.15

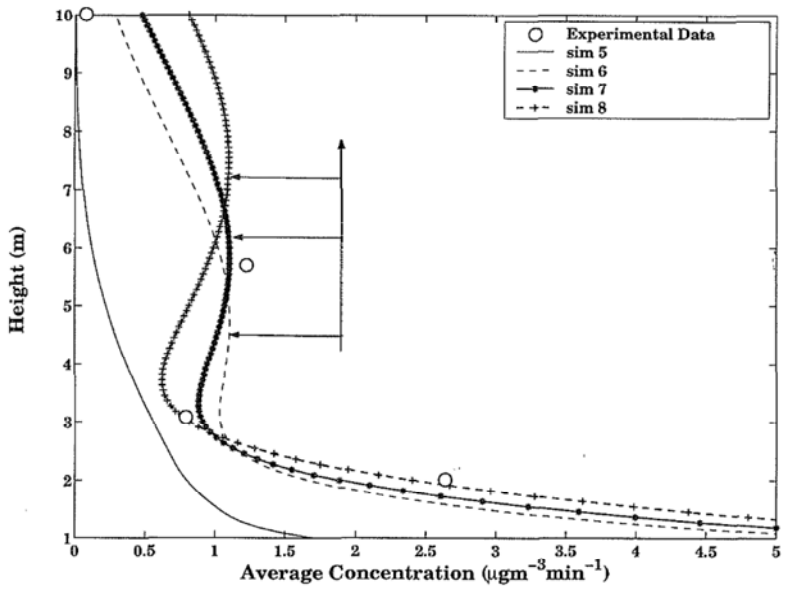

Figure 7.14: The effect that varying the angle α in Figure 7.13 has on the resulting dust concentration profile (Event E2-1995). The horizontal arrows illustrate the position of each "kink", while the vertical arrow is the direction of movement of the "kink" with increasing α. Simulation 7 produced an $R^2 = 0.8$ and $\sigma_e = 84.2$. The power law fit to this data (Fig. 7.11) in contrast had an $R^2 = 0.72$ and $\sigma_e = 100$.

dust concentration profiles have been recorded within the study site by Leys (2001, pers. comm.) and McTainsh (2002, pers. comm.) which show evidence of a distinct "kink" in their profile. It was first thought that these were a measurement artifact. However, similar "kinks" have been simulated in the field by Leys (2001, pers. comm.), using the independent DustTrak system, implying that the "kink" is not a measurement artifact.

A possible explanation is that it is due to spatial variations in dust sources within the claypan. To test this scenario, several simulation were undertaken using DSism. The results of these simulations (simulations 1 to 4) suggest that while changes in the dust source configuration do alter the curvature of the dust concentration profile, it alone cannot produce a "kink" similar to those observed in the measured dust concentration profiles. This suggests that the "kinks" must be the result of another process operating within the plume.

Another possible explanation for the presence of the "kinks", is that an additional process is in operation. Field conditions during the 1995 season suggests that kinking is most likely related to the thermal buoyancy of the plume. In particular, there appears to exist a critical value of Richardson's number, $|Ri|$ above which these kinks appear. For the 1995 season this critical value appeared to be around 1. However, the lack of vegetation on the claypan during 1995, means that, it is impossible to say whether this number is constant or depends on the roughness of the surface as suggested by Sutton (1953).

While the "kinks" may occur as the result of the thermal buoyancy within the study site, they also imply that what might have been regarded as natural variation in the experimental data, is in fact important process information and therefore should not be ignored. In particular, such variation in the vertical dust concentration profile, formerly thought to be noise, may contain important information about the erodibility of the surface and how this changes upwind. If the vertical dust concentration profile is viewed as a signal, it should be possible to analyse its individual components to obtain information

about the spatial erodibility properties of the surface and the thermal buoyancy.

Chapter 8

Upwind changes in surface conditions: model prediction against field observations

8.1 Introduction

The results of the simulations presented in Chapters 6 and 7, suggest that there is significant spatial variation in the location and strength of dust sources within the claypan and that the vertical dust concentration profile at any point is dependent on the spatial pattern of dust sources. While spatial variability in erodibility and emission rates has been observed on the claypan (Love, 2001), its relationship to the vertical dust concentration profile has not been experimentally measured. Moreover it is difficult simulate, since most approaches rely on identifying fixed dust sources and then modelling the resulting dust cloud (see Chapter 3). The problem with this approach is that the spatial pattern of dust sources changes both between, and within wind erosion events. Butler et al. (2001) suggested that the vertical dust concentration profile can be viewed as a composite signal from different dust source areas. If this 'dust signal' for any given event could be separated into its constituent dust sources then it would be possible to understand how dust

sources vary spatially and temporally for an event.

In this chapter, DSism is used to deconstruct a dust concentration profile for a given event into a spatial pattern of dust source areas, in order to further validate its underlying assumptions. The resulting pattern should not, however, be viewed as unique as it is quite possible that a different spatial pattern of dust sources could produce a similar concentration profile. The results reported in Section 8.4 confirm that a recorded dust concentration profile can be deconstructed into constituent dust sources and that these can be related to observed surface conditions if field data is available.

8.2 Field methodology

To verify that DSism source area predictions for a given wind erosion event, are representative of surface conditions upwind, it is first necessary to obtain field data on the surface and vegetation cover upwind of the measurement site on an event basis. Prior to 1998, data collected on vegetation and surface conditions around the tower sites did not provide an accurate map of surface conditions within the study site. After 1998, 500m transects were surveyed in the upwind direction from each of the two 10m towers at Site A and A1 (Fig. 8.1), **after** significant dust events (i.e., the transects were taken post event and in the direction the event had come). Along each transect, vegetation and surface conditions were recorded every metre, using the classifications outlined in Chapter 4. Thus each surface was classified according to morphology and structural formation. In addition a photographic record was quite of surface condition which was morphologically different. Thus, it was possible to use these transects to identify upwind changes in surface conditions. However, as initial test of DSism, these surface conditions were classified into the broad categories: sealed clay, rippled clay, clay skins and curls, sand/silt deposits, gibber, wind sheeted, shrubs, small standing plants and grass cover.

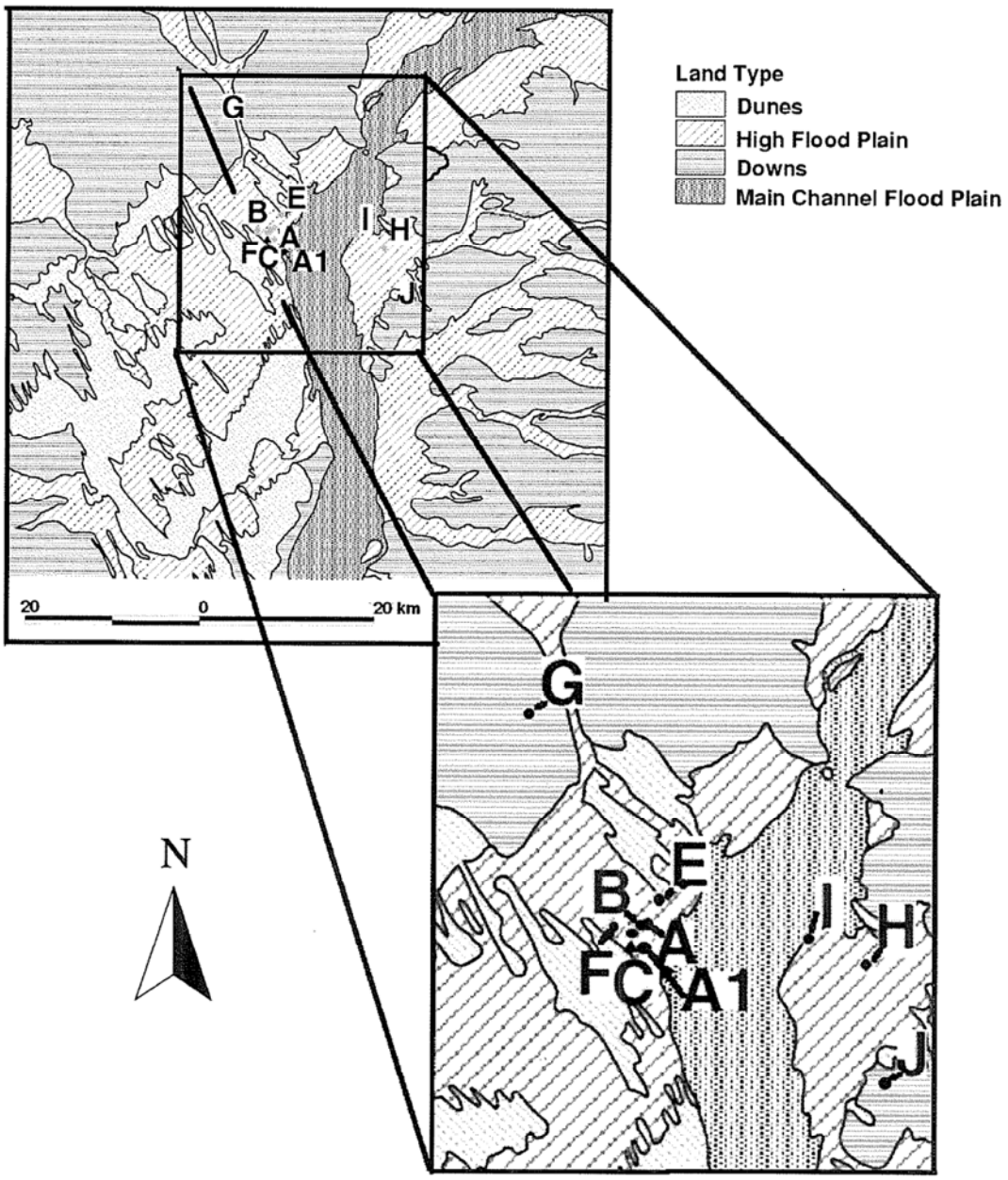

Figure 8.1: Map showing the locations of Site A and A1 within the claypan.

A disadvantage of these surveys is that the post-event erodibility of the surface is not necessarily the same as the pre-event erodibility, especially if removal of erodible material exposes a low-erodibility surface or creates a surface lag. However these transects do provide useful information on the source structure upwind of the 10m towers and allow relative erodibilities to be estimated. Also, a fortunate coincidence occurred when winds for two consecutive events blew from the same direction, thus providing pre- and post-event data for one event. Since it is the pre-event surface conditions that are mostly of interest, this data will be used in the remainder of the chapter.

The post-event data while available for another two events in the 2000 season, did not prove to be conclusive, and therefore is not discussed here. The reason for this was that it was difficult to establish from post event observations the condition of the surface prior to the event. For example a wind sheeted surface observed post event, could imply that a) it was an active source during the event or b) that it was sheeted prior to event and therefore not an active source during the event. Without additional field information, it is not possible to distinguish which of these scenarios is correct. Therefore, there is a need to gather further information to confirm the results presented in this chapter. However, the results presented in this chapter, are still important in that they provide an important insight into how powerful the methodology used in this thesis is.

To assess the performance of DSism it was first used to simulate the conditions that produced the dust concentration profiles at Sites A and A1, as previously described in Chapters 5 and 6, then the spatial erodibility pattern, produced from these simulations, was compared to the 500m survey data collected at each site.

8.3 Dust event details

The meteorological conditions, associated with the test event, are summarised in Table 8.1. While this was the only event recorded for which pre-event, upwind ground-survey, data was available, it turned out to be ideal, since the surface conditions at Sites A and A1 were completely different (Figs. 8.2 and 8.3). At Site A1, there was little vegetation cover in the immediate upwind area of the tower, while Site A was heavily vegetated upwind of the tower, and the only bare areas were significant distances from the tower. Not surprisingly, the vertical dust concentration profiles were quite different (Figs. 8.4 and 8.5). The profile at Site A is very different from events simulated in previous chapters, while the profile observed at Site A1 is similar to those previously simulated. In Chapters 6 and 7, it was shown that changes in dust concentration can be simulated in DSism by changing the spatial pattern of dust sources in the neighbourhood of the site and by accounting for thermal buoyancy of the plume. By comparing the predicted spatial pattern of dust sources with the observed surface conditions and vegetation cover upwind of each site, it should be possible to verify if DSism is accurately simulating the wind erosion processes and sources on the claypan.

Table 8.1: Environmental conditions of the test dust event which occurred on the 26/9/2000 (E2-2000).

Average Wind speed (ms^{-1})	Average wind direction (°N)	Extreme Wind Directions(°N)	Temperature (°C)	Duration (hrs)
9	322	326 316	29	4

Figure 8.2: Site A surface condition during the 2000 wind erosion season.

Figure 8.3: Site A1 surface condition during the 2000 wind erosion season.

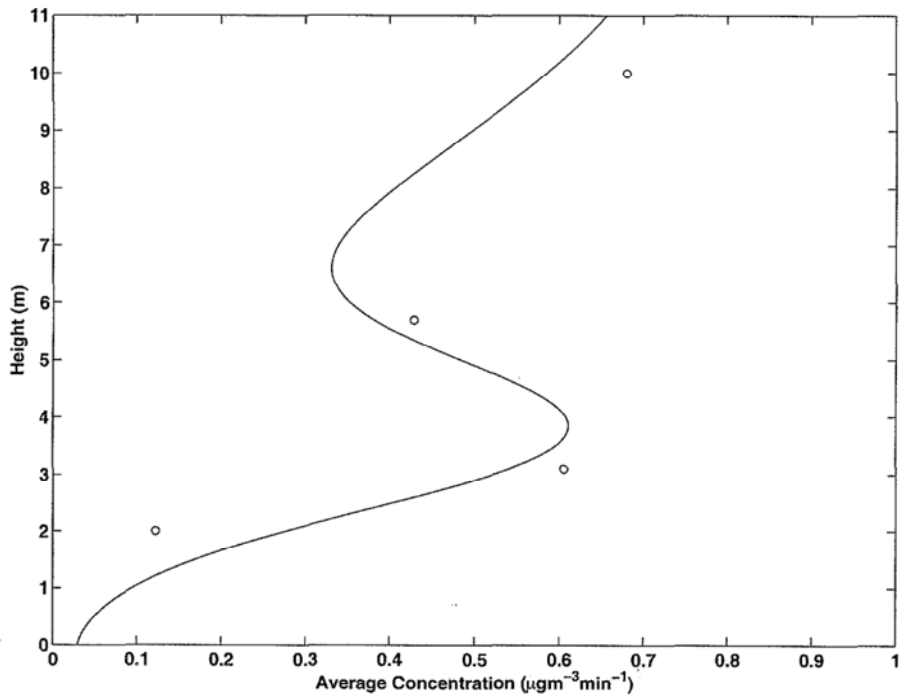

Figure 8.4: Comparison of the DSism predicted (–) and measured (o) vertical dust concentration profile at Site A. $R^2 = 0.91, \sigma_e = 0.08$.

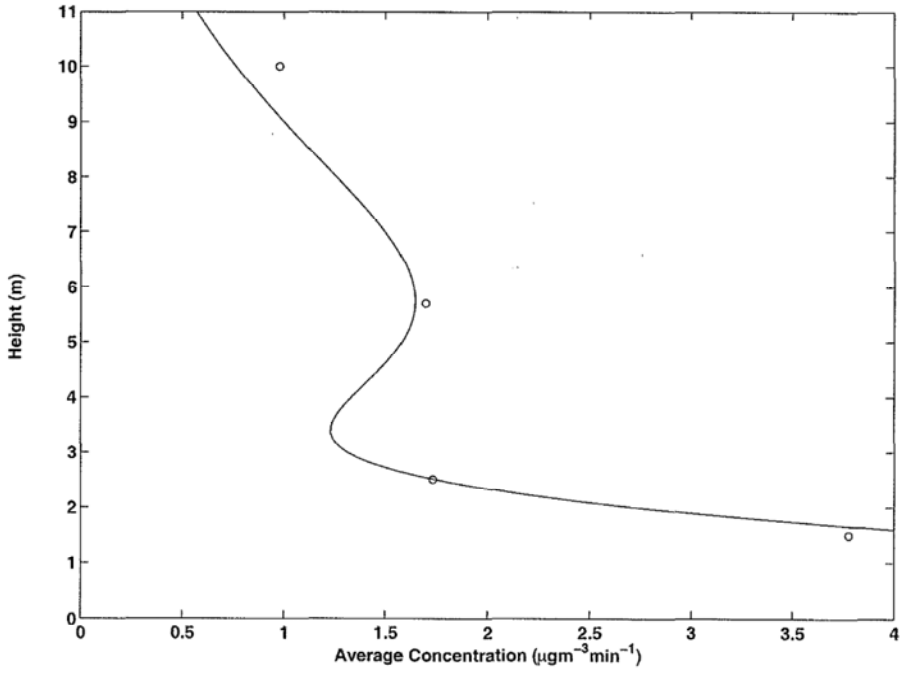

Figure 8.5: Comparison of the DSism predicted (–) and measured (o) vertical dust concentration profile at Site A1. $R^2 = 0.96, \sigma_e = 0.14$.

8.4 Results

8.4.1 The DSism simulation process

First the best fit to the measured vertical dust concentration profile profiles at Site A and A1 was determined, using the method outlined in Chapter 6. For Site A, the complex nature of the vertical dust concentration profile (Fig. 8.4) required testing over a hundred different dust source area layouts, while for Site A1 only fifty-three were required. Once an initial source area layout was found, it was optimised by repeating the process with finer changes to both the dust source configuration and emission rates, until only minor improvements were observed in R^2 and σ_e. In total, over 250 combinations were tested to provide a satisfactory fit to the dust concentration profile at Site A, while 150 were required for Site A1.

Figures 8.4 and 8.5, show the best DSism fits to the measured dust concentration profiles at Sites A and A1. The dust source configurations that correspond to these fits are shown in Figures 8.6 and 8.7. At each site, DSism required two intense dust source areas to accurately reproduce the measured dust concentration profiles. (The area closest to the tower will be referred to in the following text as Area 1, while the second of these source areas will be referred to as Area 2.) In the case of Site A, this resulted in Area 1 having an emission rate, Q, of $1\mu gs^{-1}$, while Area 2 had an emission rate of $22\mu gs^{-1}$ and an angle of 10° to account for thermal buoyancy, while Site A1 required Area 1 to have an emission rate of $160\mu gs^{-1}$, Area 2 an emission rate of $320\mu gs^{-1}$ and an angle of 9° to account for thermal buoyancy.

8.4.2 General discussion

The results suggest that the vegetation around Site A during the 2000 season significantly reduced the emission rate there. This confirms the observations of Wasson and Nanninga (1986), Findlater et al. (1990) and Leys (1991b), that

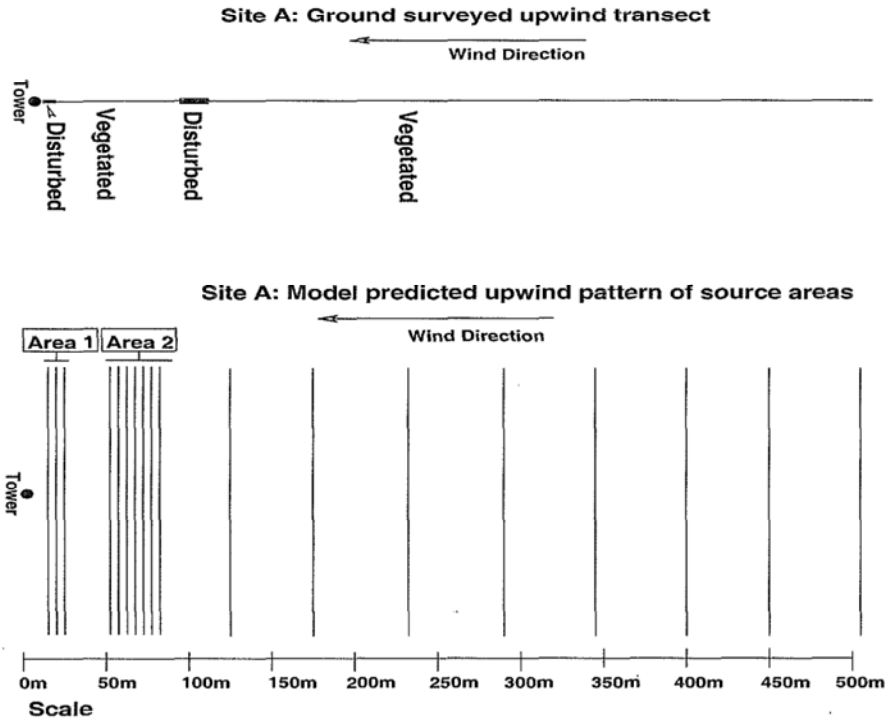

Figure 8.6: Comparison of DSism predicted source structure to 500m transect ground survey data at Site A.

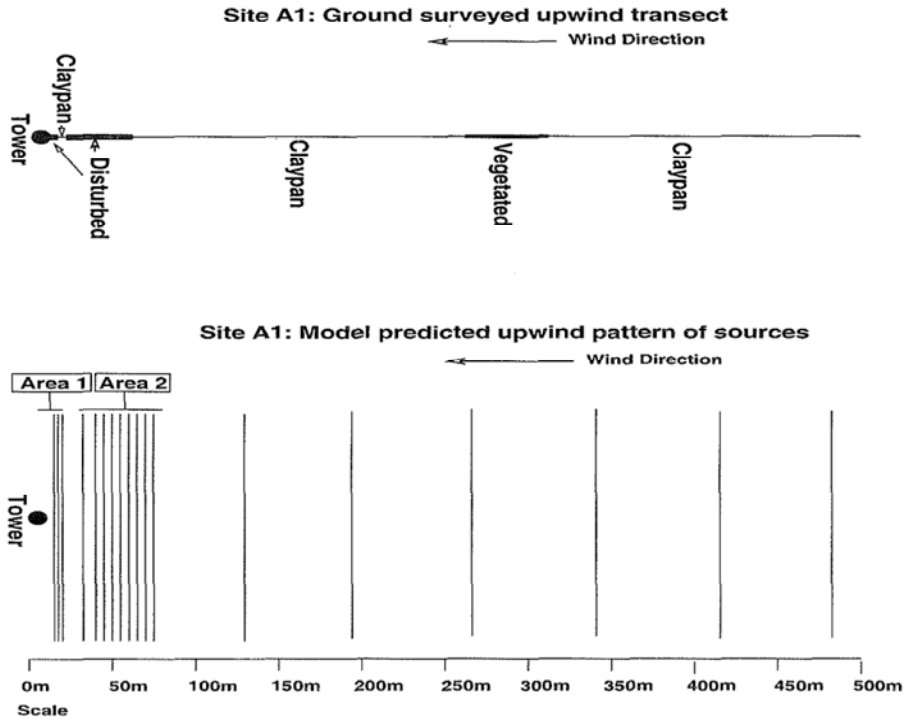

Figure 8.7: Comparison of DSism predicted source structure to 500m transect ground survey data at Site A1.

vegetation significantly reduces the erodibility of the surface. The similarity of the dust emission angle at each site, simulating the thermal buoyancy, suggests that the thermal conditions were similar at both sites during this event. One would have expected the thermal conditions at the two sites to be significantly different since one is vegetated, and the other is almost completely devoid of vegetation. However, since the angle used by DSism, takes into account the thermal properties upwind of the site, it may be better to interpret the result as implying that the surfaces upwind of each site had similar thermal properties.

It was important that DSism was able to reproduce the dust concentration profile at Site A, even though it was extremely complex. This is very useful because vertical dust concentration profiles in nature, may deviate significantly in form from the conventional power function. Hence, variation in the vertical dust concentration profile, yields significant information about erodibility upwind of the point where the profile was measured.

8.4.3 Surface conditions

To verify that the upwind dust source configurations predicted by DSism (Figs. 8.4 and 8.5) were an accurate representation of the actual spatial erodibility the predictions were compared to the 500m transect data collected prior to this event. An initial comparison is shown in Figures 8.4 and 8.5, showed model predictions are apparently much better for site A1. This is not surprising since the surface conditions and vegetation cover were more uniform at Site A1, than at Site A. The predictions at Site A1 are discussed in detail first, followed by those at Site A.

8.4.3.1 Site A1

Figure 8.7 shows the predicted dust source configuration compared to the measured transect. In this case the two source areas required by DSism to

accurately recreate the profile correspond nicely to the disturbed areas. Loose Erodible Material (LEM) surveys (see Chapter 4 for details on how these surveys were undertaken), taken at the time (Fig. 8.8) indicate that there was little loose erodible material on the claypan, and that much of the claypan had low erodibility. The LEM surveys also indicate that there was little loose erodible material present in the vegetated areas of the claypan, confirming that these areas too would have had low erodibility. Hence, the disturbed areas observed in the transects are the most likely dust sources during this event.

Unfortunately, no LEM data was available on how surface disturbances affected the amount of loose erodible material during the 2000 season. However, such data was available for 1996 (Fig. 8.9). The 1996 data shows that once

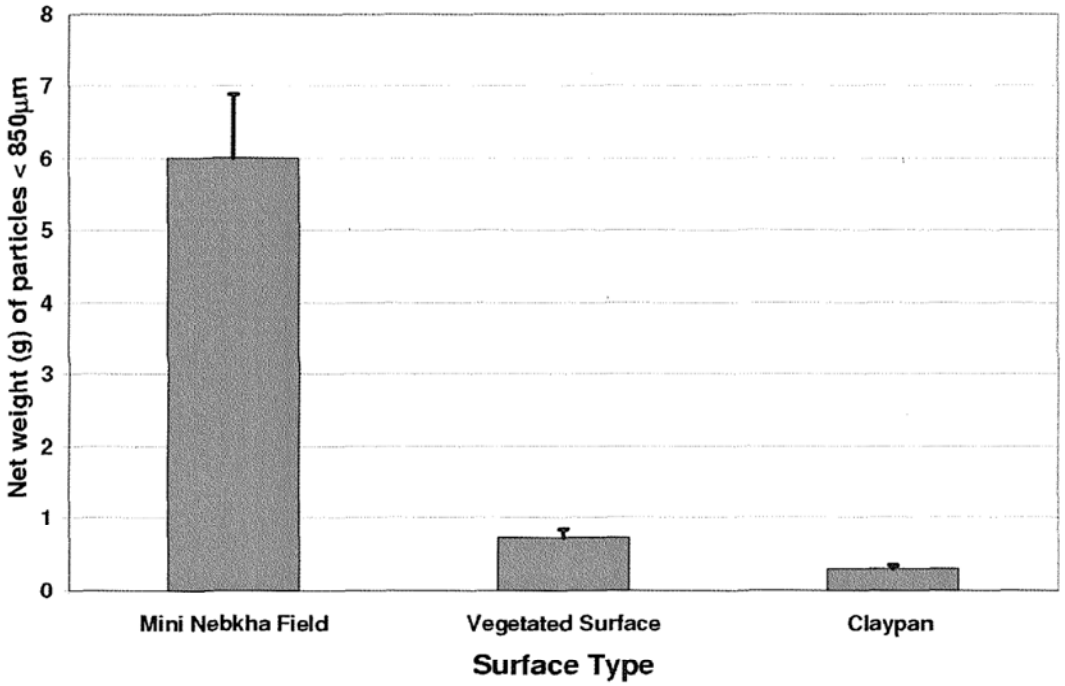

Figure 8.8: The amount of loose erodible material (LEM) present on different surfaces during the 2000 wind erosion event.

disturbed, the amount of loose erodible material on the claypan increases substantially. These observations are supported by wind tunnel studies undertaken by Gillette et al. (1982). They found that for many different clay based soils in the United States, there was a significant reduction in the threshold velocity (u_{*t}) once the surface was disturbed. Thus, the erodibility of the disturbed areas in the transect is likely to be much higher than the undisturbed areas. The two disturbed areas in transect are most likely to be the only dust sources in operation during this event. Hence, the DSism deconstruction of the dust concentration profile at Site A1 is very plausible in the light of field evidence.

8.4.3.2 Site A

Figure 8.6, shows that DSism predicted two quite distinct and highly erodible source areas upwind of Site A. Comparing these source areas with the observed transect data at Site A, shows the predicted Area 1 corresponds well to the observed disturbed area close to the tower, but Area 2 does not match any feature of the transect data. Field notes, taken at the time, report that the second disturbance observed in the transect was only minor and extremely patchy (Strong, 2001, pers. comm.). This region of the transect is unlikely to correspond to the second source area (Area 2) predicted by DSism. One must assume that there was a second dust source area that was not picked up in the transect survey. Field notes, loose erodible material analysis, and the efficiency analysis, all support this conclusion.

Field notes taken at the time of the event, indicate that there was a mini-nebkha field, just to the north of Site A (Fig. 8.10). This mini-nebkha field, consisted of a large number of small vegetated mounds and large amounts of unconsolidated sand. The analysis undertaken in Chapter 5 suggest strongly that there was a second source upwind of Site A. LEM observations taken at the time (Fig. 8.8), show that the largest amount of loose erodible material within the claypan was in this mini-nebkha field during the 2000 season. Other field observations made at the time by Leys (2001, pers. comm.), Strong

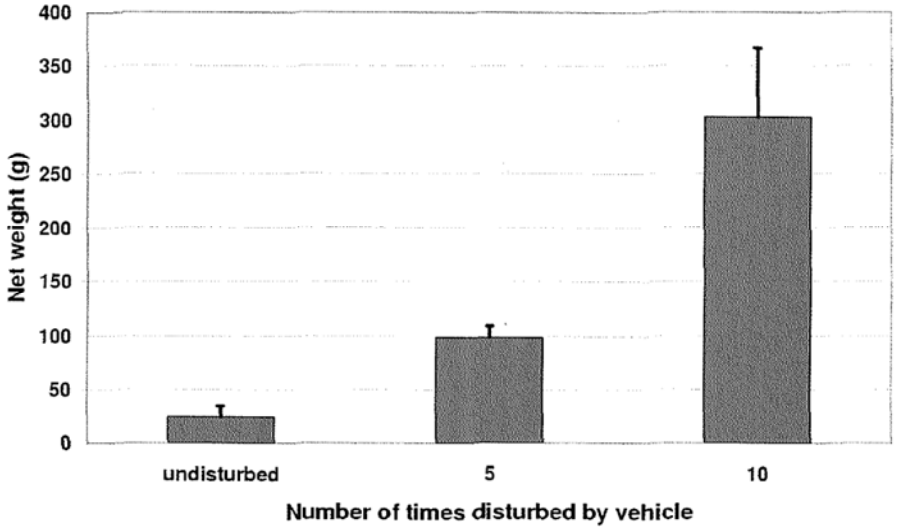

(a) Unvegetated claypan

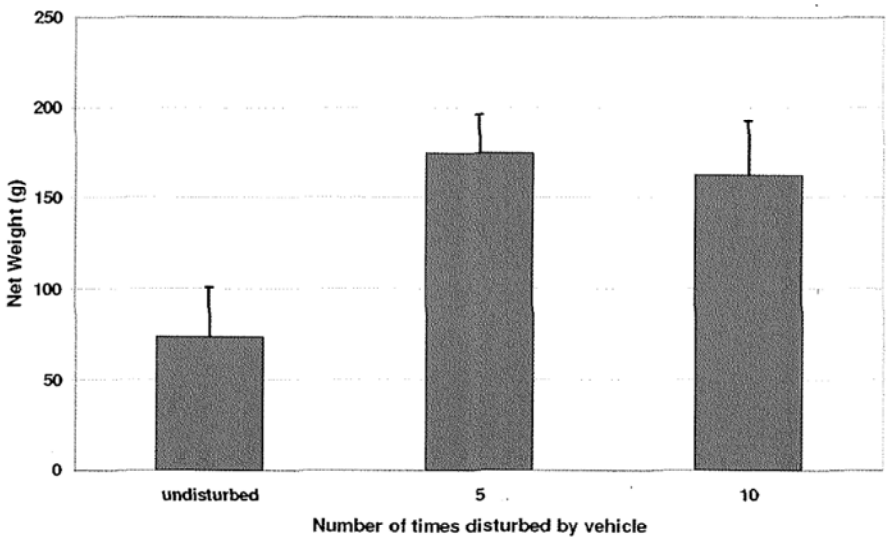

(b) Vegetated surface

Figure 8.9: Loose erodible material (LEM) measurements for a variety of surfaces within the study site during the 1996 season. These illustrate the affect on LEM of disturbing the surface. Source: Strong (2001, pers. comm.).

(2001, pers. comm.) and McTainsh (2002, pers. comm.), confirm that dust was indeed being entrained from the mini-nebkha field during the 2000 season.

There are two possible process scenarios for dust from this mini-nebkha field

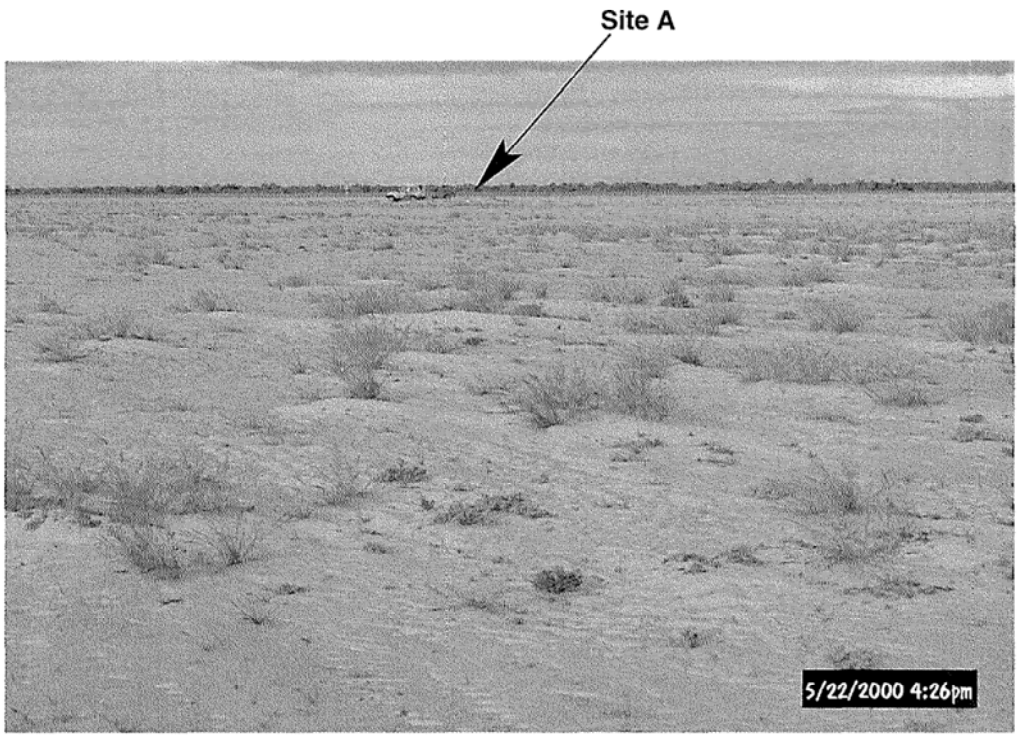

Figure 8.10: The mini-nebkha field located just to the north of Site A.

to be transported to the Site A tower. In the first scenario (Scenario 1) fluctuations in the wind direction would allow material entrained in the mini-nebkha field to be transported to Site A (Fig. 8.11). For the event considered here, meteorological observations show that, the wind only blew from the direction of this mini-nebkha field 16% of the time. This implies that much of the material entrained in this field did not arrive at Site A, but rather was transported past it. Since the predicted emission rate from Area 2 is based on the profile recorded at Site A, it is likely that this emission rate estimate is much lower than the actual rate from the mini-nebkha field.

In the second scenario (Scenario 2), dust is transported by lateral dispersion from the mini-nebkha field to the towers at Site A (Fig. 8.12).The crosswind dust source simulations undertaken in Chapter 4, suggest that, given the location, size and distance of the mini-nebkha field from Site A, the dispersion would be approximately 10m. This would mean that only a small fraction of the sediment entrained in the mini-nebkha field would have arrived at the Site A tower. Again since the emission rate used in DSism is based on the

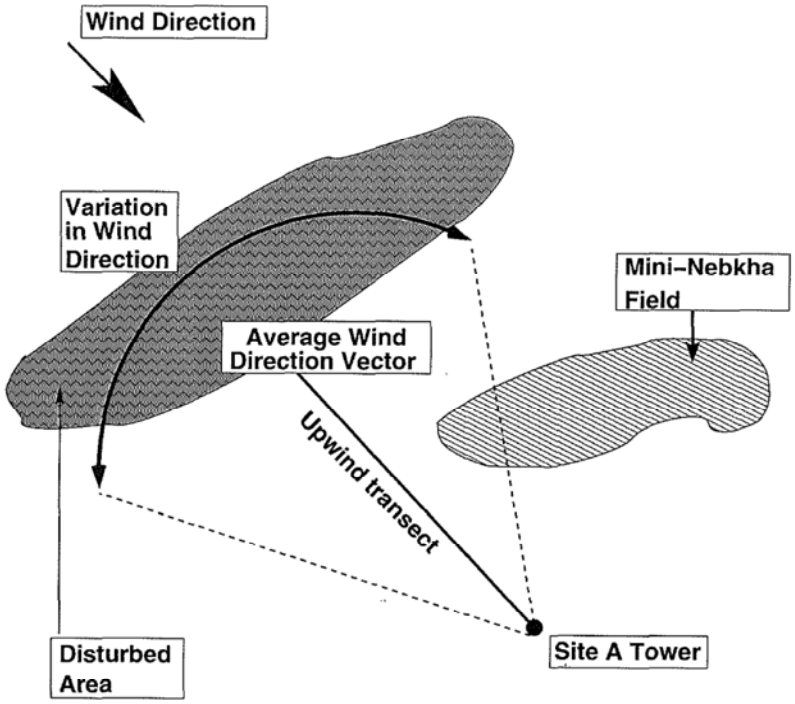

Figure 8.11: Schematic illustrating how Scenerio 1 would transport material from the mini-nebkha field to Site A.

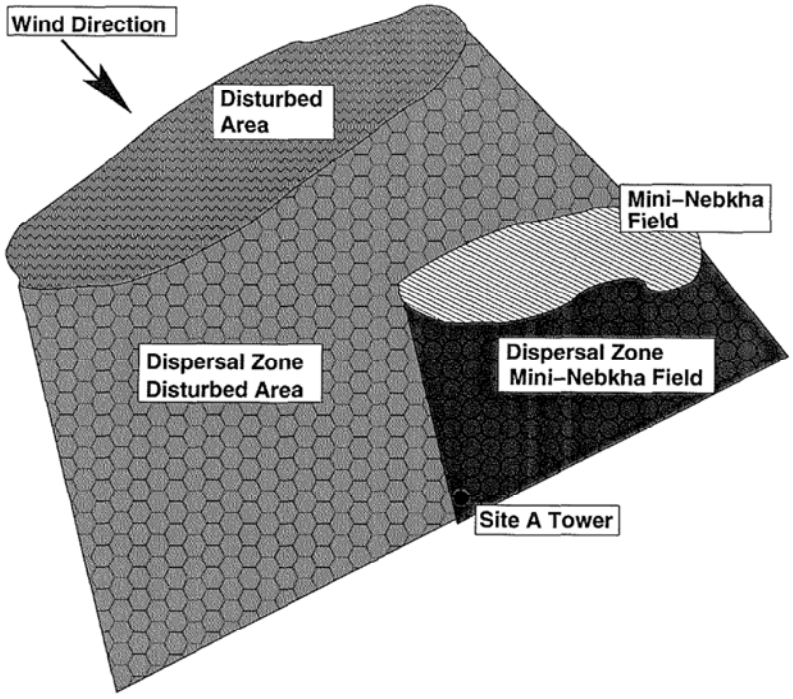

Figure 8.12: Schematic illustrating how Scenerio 2 would transport material from the mini-nebkha field to Site A.

material that arrives at Site A, it is likely that this emission rate will be lower than the actual emission rate of the mini-nebkha field.

While DSism can simulate both scenarios, it does not provide an effective means of choosing between them. DSism cannot distinguish between these scenarios because it assumes that the wind speed and direction are constant, taking the average of these during the event, as its estimate. Coupled with the additional assumption that the emission rate is uniform along the crosswind lines, implies that DSism simulates these two scenarios by placing crosswind lines at the appropriate distance upwind. Nonetheless, the simulations still imply that measured vertical dust concentration profiles contain significant information about where dust sources are located upwind.

8.5 Conclusion

This chapter, shows that DSism can accurately predict upwind source locations. However, the modelling methodology involved cannot produce accurate erodibility estimates for sources not directly upwind of the recording tower. Thus to be able to accurately resolve the crosswind contributions of the various dust sources, additional data will be needed on crosswind variations in dust concentration. A possible experimental scenario for gathering this additional crosswind data, is presented in Chapter 11. Such experimental data would also play an important role, in further verifying the observations and results presented in this chapter.

The results suggest that there is sufficient information contained in the vertical dust concentration profile to distinguish upwind variations in surface conditions. They also support the claim, presented in Chapter 6, that spatial variations in dust source locations within the claypan are responsible for the final shape of the vertical dust concentration profile.

Chapter 9

The effects of particle-size upon the vertical dust concentration profile

9.1 Introduction

Experimental studies have shown that particle-size plays an important role in wind erosion. The particle-size contribution to soil erodibility is well known (Bagnold, 1941; Gillette, 1979) and dust transport studies suggest that smaller particles are transported further than larger particles (Greeley and Iverson, 1985; Raupach, 1993). However, few studies have looked at spatial variations in the particle-size emission characteristics of dust sources and the resulting effects upon dust concentration profiles. One reason for this is that, not only are discrete dust source areas difficult to identify accurately in the field, but also the emission rates of these sources cannot be measured directly (Shao, 2000). Most studies have used portable wind tunnels to infer the relationship between the particle-size distribution of the soil and emission rate of particles from a given surface.

Most wind erosion models, such as WEAM (Shao et al., 1996), assume that the dependence of the emission rate (Q), on the friction velocity ($v_\star$) and threshold

friction velocity (v_{*t}) is not significantly altered by the presence of other particles. Thus, Q can be expressed simply as a function of the particle-size distribution of soil, and both the friction velocity (v_*), and threshold friction velocity (v_{*t}) as in Equations (3.11) and (3.12). In rangeland environments, such as the claypan, where erodibility varies spatially within a given land type, this implies that the particle-size distribution of the particles being emitted is also likely to vary spatially. Therefore, the final particle-size composition of a vertical dust concentration profile, will depend on both the distance material has travelled (due to gravitational settling), and any spatial variations in the rate at which particles of a particular size are being emitted from the surface (particle-size emission rate).

Results, presented in Chapter 7, show that dust concentration profiles are related to not only the spatial pattern of erodibility, but also other environmental processes, such as surface heating. Taken together, with the particle-size sorting that occurs as a result of deposition, and the likely spatial variation in particle-size emission rates, the final particle-size distribution of any vertical dust concentration profile will also depend on the processes in operation during a particular wind erosion event. In this chapter, DSism is used to examine how variations in particle-size emissions and other environmental processes, affect the particle-size distribution of a vertical dust concentration profile.

9.2 Altering the emission rate, Q, for different particle-size classes in DSism

One of the most difficult parameters to estimate in wind erosion is the surface emission rate. It cannot be directly measured, but is inferred indirectly. Most wind erosion models make some kind of assumption about particle-size emissions. For example, WEAM assumes that the emission rate (Q) is not altered significantly by the presence of other particles. Other models assume that emission rates are independent of particle-size. Neither assumption reflects

the real situation. The WEAM assumption fails because of the presence of different sized particles, which influence how the particles bond and are packed within the soil. This, in turn changes the rate at which particles are surrendered to the wind. Nonetheless, it is difficult to improve upon this assumption until there is a better understanding of how wind erosion process are affected by changes in particle emission rates. The following DSism simulations, make a contribution to this understanding.

Until now, DSism has assumed that each particle-size class is emitted at an equal rate, which was necessary because there was little reliable field data or experimental data available, on specific particle-size emission rates. One of the key design features of DSism, is the capacity to assign different emission rates to each particle-size class. In this chapter, the emission rate assumption is relaxed to some extent. The lack of experimental data however, means that the simulations described in this chapter, are the outcome of a theoretical study into particle-size emission effects.

For this study, two monitored events from the 1995-1996 wind erosion season were selected (Table 9.1), because of the different nature of their vertical dust concentration profiles (Fig. 9.1). Event E1-1996 (is event E1 in Chapter 6) occurred on 19 July 1996, and had a smooth vertical dust concentration profile, while Event E2-1995 (is Event 2 in Chapter 7) occurred on 17 August 1995, and had a "kink" in the vertical dust concentration (Chapters 6 and 7). The thermal buoyancy of the air, as measured by Richardsons number ($|Ri| < 1$) was low, in the case of Event E1-1996, so its effect on the vertical dust concentration was likely to be small (according to the results presented in Chapter 7). In Event E2-1995, the thermal buoyancy was much higher ($|Ri| > 1$), resulting in a "kink" in the vertical dust concentration profile (see Chapter 7). Altering the particle-size emission rates in simulations of these events should demonstrate how different particle-sizes are transported under different thermal conditions.

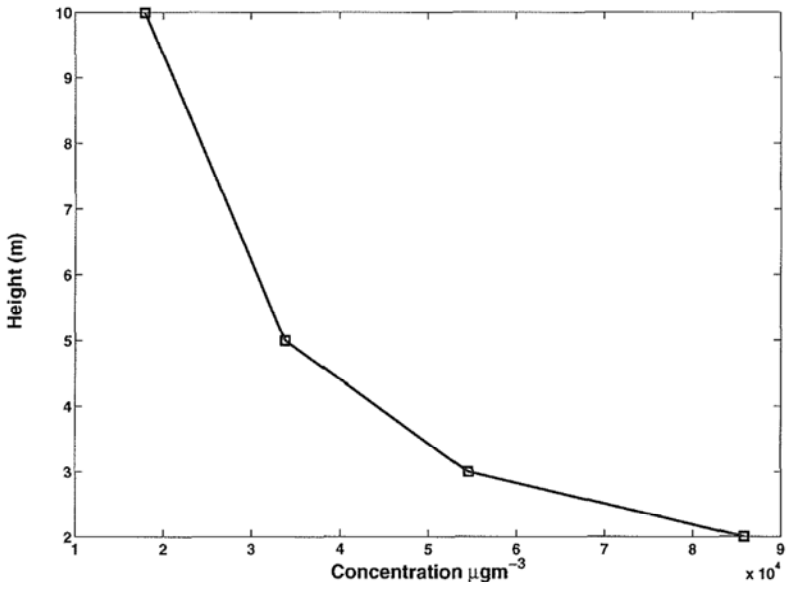

(a) Dust concentration profile for Event E1-1996.

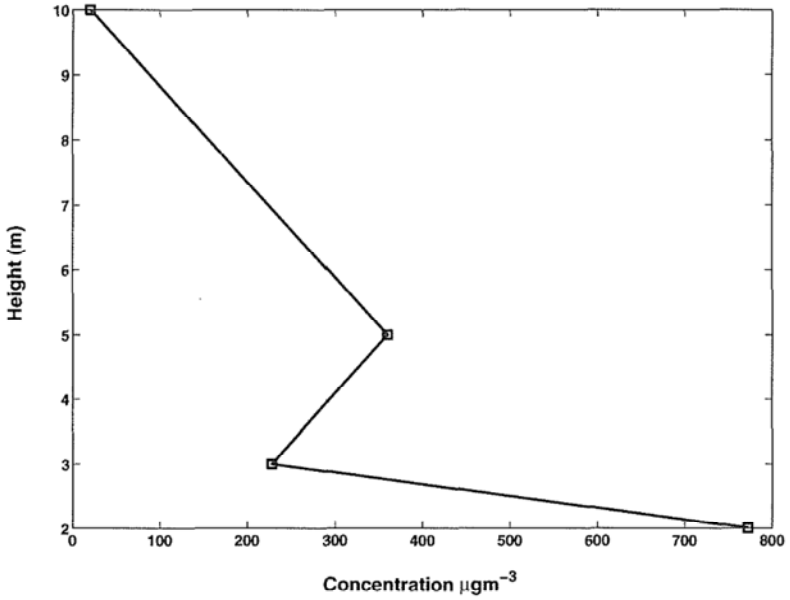

(b) Dust concentration profile for Event E2-1995.

Figure 9.1: Dust concentration profiles for Events E1-1996 and E2-1995 under conditions shown in Table 9.1. Lines have been used to connect the data points to illustrate the shape of each profile.

Table 9.1: Summary of the wind speed, direction and temperature for Events E1-1996 and E2-1995.

Event E1-1996

Date	Mean Wind Speed ms^{-1}	Mean Wind Direction °T	Temp (°C) 2m	Temp (°C) 10m	2m Dust Concentration μgm^{-3}	Ri 2m
19th July 1996	12.18	283.45	25.51	25.01	85,861	0.83

Event E2-1995

Date	Wind Speed ms^{-1}	Wind Direction °T	Temp (°C) 2m	Temp (°C) 10m	2m Dust Concentration μgm^{-3}	Ri 2m
17th August 1995	10.85	67	24.01	23.27	772.59	2.58

9.2.1 Initial fitting of DSism to Events E1-1996 and E2-1995

The initial fit to the vertical dust concentration profile, was obtained as outlined in previous chapters, except that, instead of the three particle-size classes used in Chapter 4 DSism simulations (20μm, 40μm and 60μm), six particle-size classes (10-20μm centre 15μ, 20-30μm centre 25μm, 30-40μm centre 35μm, 40-50μm centre 45μm, 50-60μm centre 55μm and 60-70μm centre 65μm) were used to provide more detailed particle-size information. In both events, several different spatial dust source configurations were tried. These were compared using the R^2 and σ_e (as described in Chapter 5), and the best combination selected. Once an initial source combination was found, it was adjusted to the optimum fit, by making minor corrections to the spatial configuration and emission rates, until R^2 and σ_e showed only minor changes between the simulation runs. Figure 9.2 shows the final DSism fits.

Figure 9.3 shows the dust source configuration corresponding to the optimum

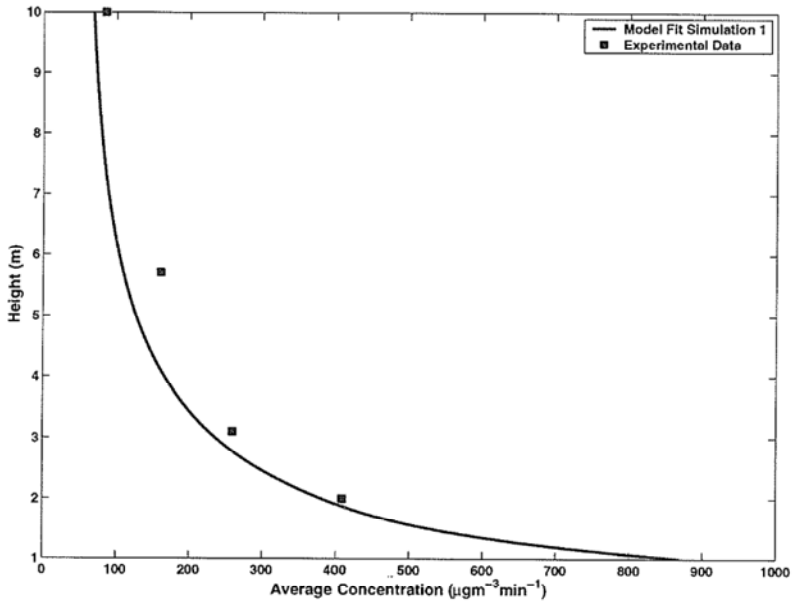

(a) Event E1-1996 $R^2 = 0.85, \sigma_e = 41$

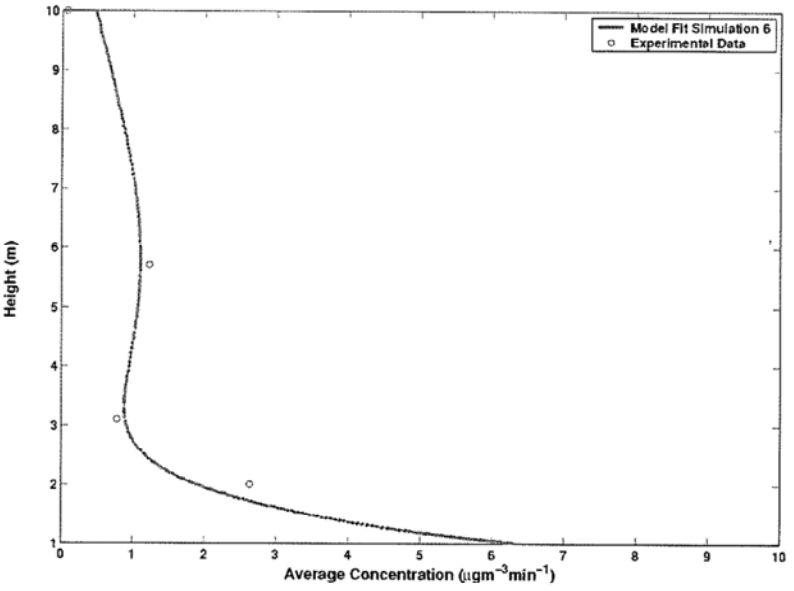

(b) Event E2-1995 $R^2 = 0.88, \sigma_e = 0.38$

Figure 9.2: Initial model fits for Event E1-1996 and B as described in Table 9.2 and Figure 9.3.

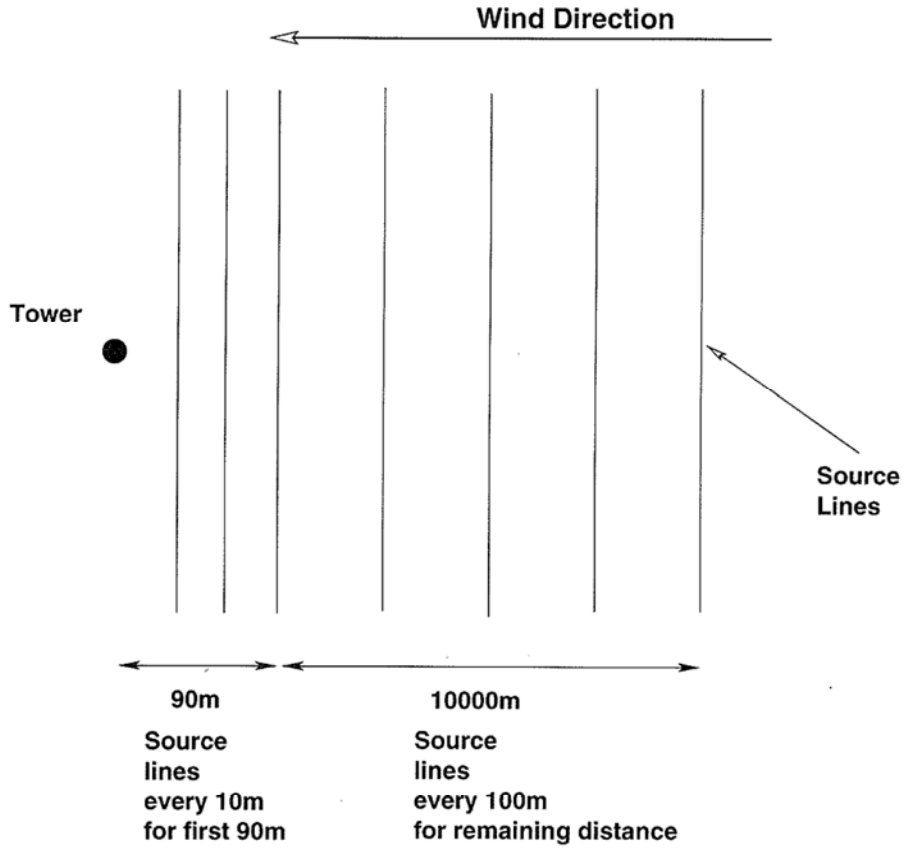

(a) Event E1-1996 dust source configuration

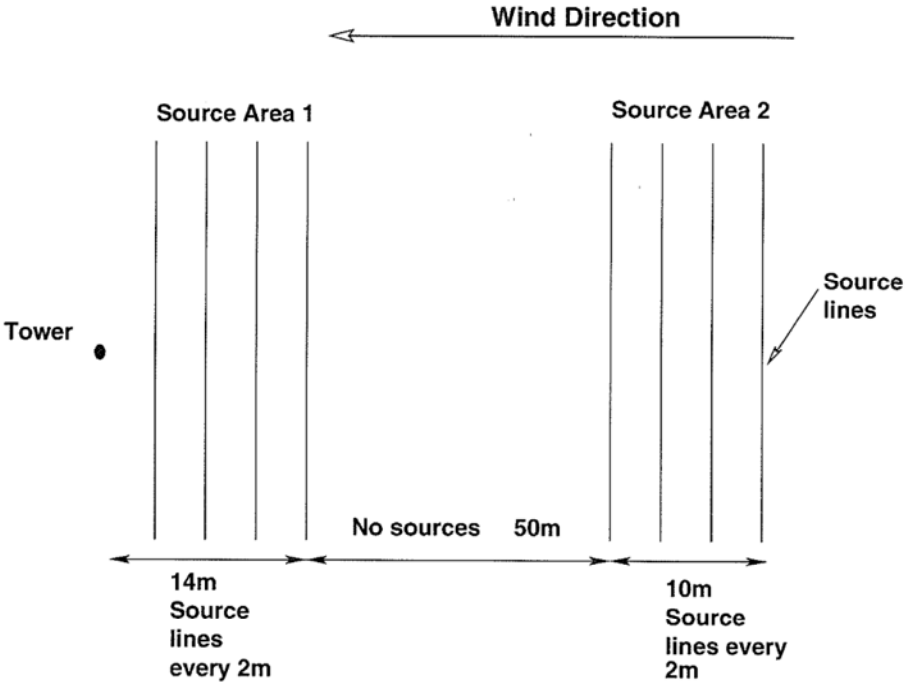

(b) Event E2-1995 dust source configuration

Figure 9.3: Dust source configurations used in all simulations under taken in this chapter.

DSism fit for each event. These spatial configurations were used for all other simulations undertaken in this chapter. The emission rates and other parameters associated with these source configurations are listed in Table 9.2. The optimum fit for Event E1-1996 is listed in the table as Simulation 1, while the Event E2-1995 parameters are listed as Simulation 6. The values of the emission rates in these two simulations were used as a basis to construct several new simulations. These new simulations used to study how changes in particle-size emission rates affect the vertical dust concentration profile.

9.2.2 Initial particle-size simulations

Table 9.2 also shows how the emission rates were modified in Simulations 2 to 5 and 7 to 10. For example, in Simulation 2 the emission rate of the 15μm particle-size class was doubled, while emission rates of the other classes were held constant. In Simulations 7 to 10, where there were two source areas, the particle-size class emission rates were altered identically in both areas. For example, in Simulation 7, the 15μm rate is doubled in both Source Area 1 and 2. Only the 15μm and the 65μm particle-size class emission rates were altered in the simulations reported here. Other simulations were run for these particle-size classes but the results are not presented here as they did not contribute any new information.

9.3 Results

As mentioned earlier, the two-metre dust concentration readings from the 10m towers were used to classify the relative size of events. Two metres is the lowest height measured on the tower and therefore should contain the most information about erodibility at the site. Comparing the emission rates for Simulations 1 and 6 (Table 9.2) to the dust concentrations observed at two metres (Table 9.1) offers an insight into the wind erosion process. Event E1-1996 had a dust concentration at 2m of 85, 861μgm^{-3}, while Event E2-1995

Table 9.2: Emission rate (μgs^{-1}) by particle-size class for each simulation. Simulation 1 was used as a base for Simulations 2–5. Simulations 2–5 differed in the particle-size emission rate for a single particle-size class. Similarly Simulation 6 was used as a base to construct Simulations 7–10.

Event E1-1996

Simulation	Particle-Size (μm)						Buoyancy Angle
Number	15	25	35	45	55	65	
1	14000	14000	14000	14000	14000	14000	0°
2	28000	14000	14000	14000	14000	14000	0°
3	7000	14000	14000	14000	14000	14000	0°
4	14000	14000	14000	14000	14000	28000	0°
5	14000	14000	14000	14000	14000	7000	0°

Event E2-1995

Source Area 1

Simulation	Particle-Size (μm)						Buoyancy Angle
Number	15	25	35	45	55	65	9°
6	6	6	6	6	6	6	9°
7	12	6	6	6	6	6	9°
8	3	6	6	6	6	6	9°
9	6	6	6	6	6	12	9°
10	6	6	6	6	6	3	9°

Source Area 2

Simulation	Particle-Size (μm)						Buoyancy Angle
Number	15	25	35	45	55	65	
6	36	36	36	36	36	36	9°
7	72	36	36	36	36	36	9°
8	18	36	36	36	36	36	9°
9	36	36	36	36	36	72	9°
10	36	36	36	36	36	18	9°

had a dust concentration at 2m of 772.59μgm^{-3}, a difference of two orders of magnitude. Table 9.2 shows that the emission rate required to simulate Event E1-1996 was 14000μgs^{-1}, while Event E2-1995 only required an maximum emission rate of 36μgs^{-1}. Thus, the emission rate increased by almost three orders of magnitude, in contrast to the two-order increase in dust concentration. So a small increase in dust concentration occurs as a result of a much larger increase in emission rate.

This is significant because emission rates cannot be measured directly. Most observations on emission rates in the field have been made either using portable wind tunnels, or observational data collected over a season (Raupach and Leys, 1992; Leys and McTainsh, 1996; McTainsh et al., 1999). Such data constitute either a brief snapshot of emission rates, or a seasonal average. Very few studies have tried to link variations in observed dust concentrations to actual changes in emission rates on an event basis. Thus, the result presented here is quite significant. A small increase in measured dust concentration, is associated with a much larger increase in emission rates. There is also a significant temporal change in the emission rates between these two events. One implication of this is that the claypan is in a much more erodible condition during Event E1-1996, than it was during Event E2-1995.

9.3.1 Event E1-1996 simulations

Figure 9.4 shows how the various particle-size dust concentrations varied with height for Simulation 1. The smallest particles (15μm) had the highest concentration over the whole 10m, while the largest particles (65μm) had the lowest concentration. Given that larger particles have the higher deposition velocity, this result is not surprising.

The results of Simulation 2 (Table 9.2) are shown in figure 9.5. This figure shows how the vertical dust concentration profile is affected by altering the

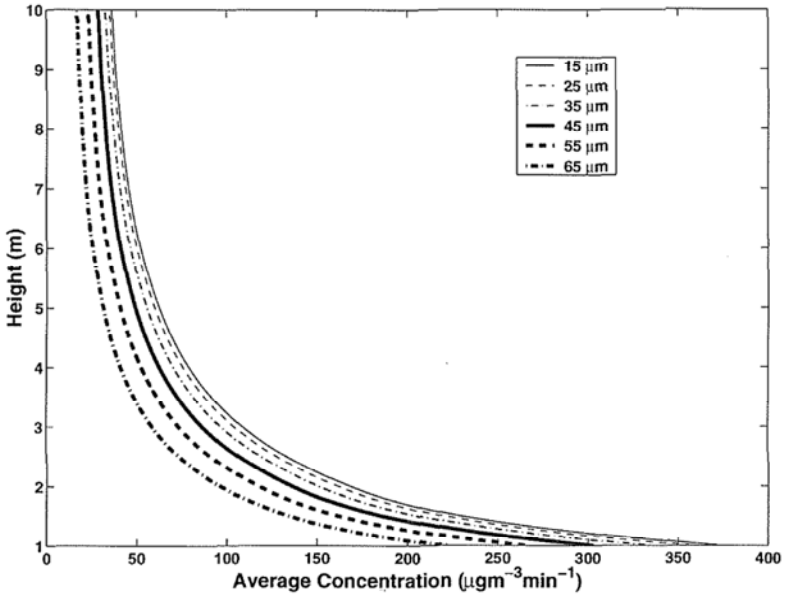

Figure 9.4: Particle-size concentration for Event E1-1996 under the assumption that all particle-sizes are emitted equally (Simulation 1).

emission rate of 15μm particles. As expected, doubling the emission rate increased the dust concentration by a small percentage (5%), while a corresponding decrease in emission rate reduced the dust concentration by a similar amount. Changing the emission rate of a single particle-size class had a minimal affect on the total vertical dust concentration profile (Fig. 9.5(a)). In Figure 9.5(b), the change in dust concentration is small in relation to the actual change in emission rate. Figure 9.6 shows that increasing the emission rate of the 65μm particles has increased the dust concentration, and that dust concentration decreased when the emission rate was decreased. Once again any actual change in concentration was small when compared to the change in emission rate. In Figures 9.5 and 9.6, the greatest change in dust concentration occurred in the lower part of the profile and decreased with height. Physically this means that only a very small percentage of the particles emitted are dispersed into the upper reaches of the profile, that is, increasing the emission rate only adds a relatively small number of particles in these upper regions. So the overall change in dust concentration is very small.

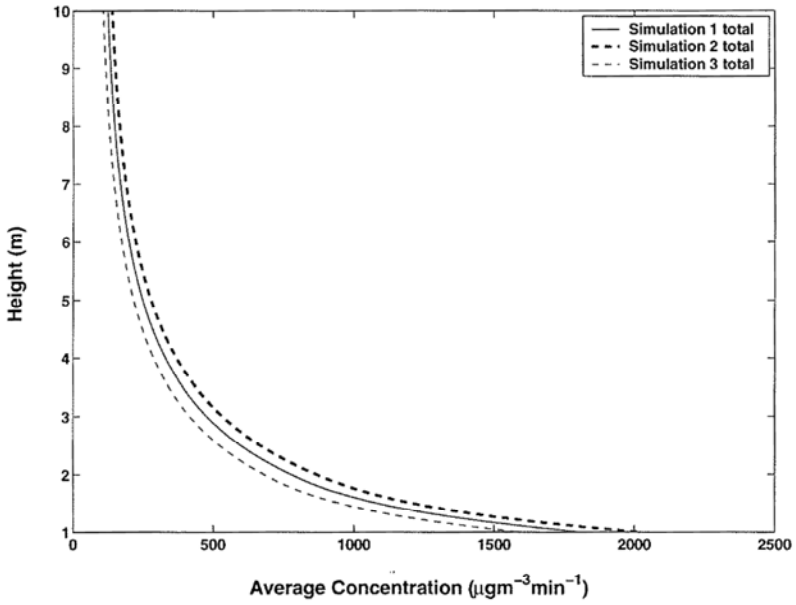

(a) Total vertical dust concentration for Simulations 1–3.

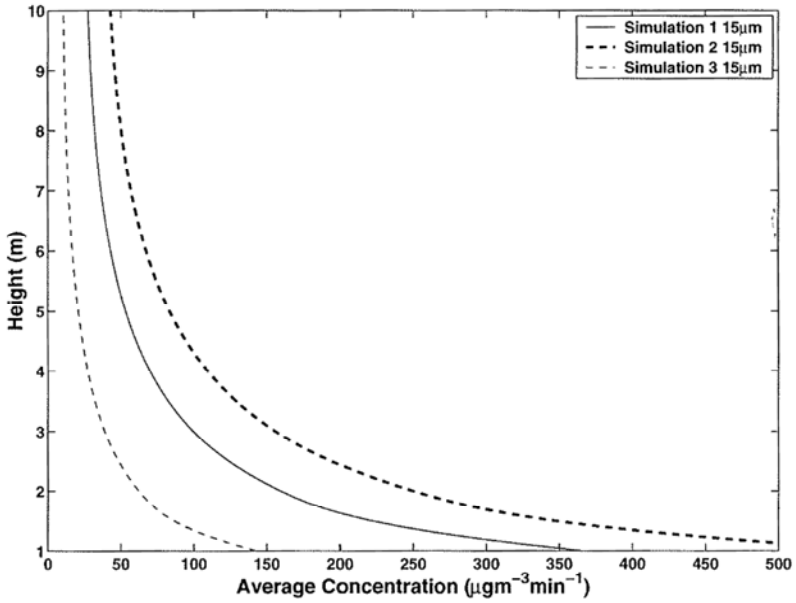

(b) 15μm vertical dust concentration for Simulations 1–3.

Figure 9.5: The effect of altering the emission rates for 15 μm particles, as in Table 9.2, for Event E1-1996.

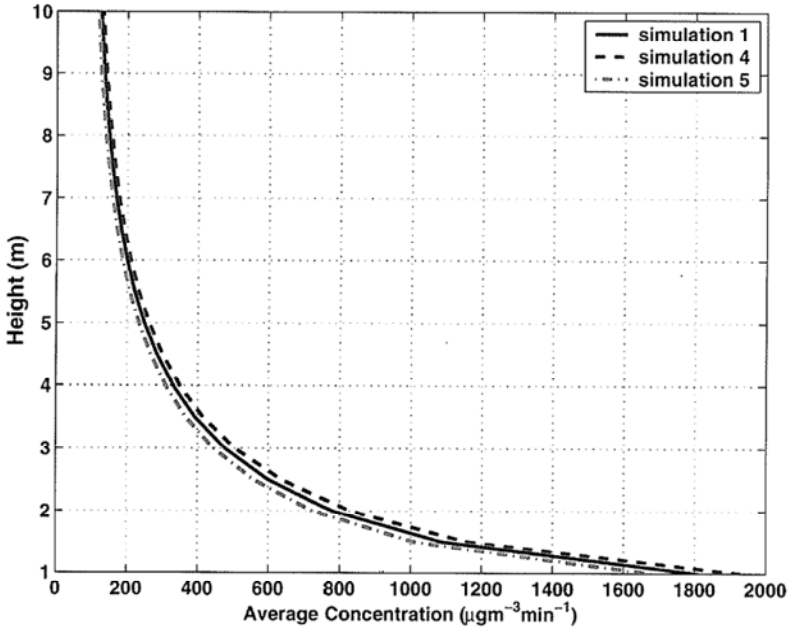

(a) Total vertical dust concentration for Simulations 1, 4 and 5.

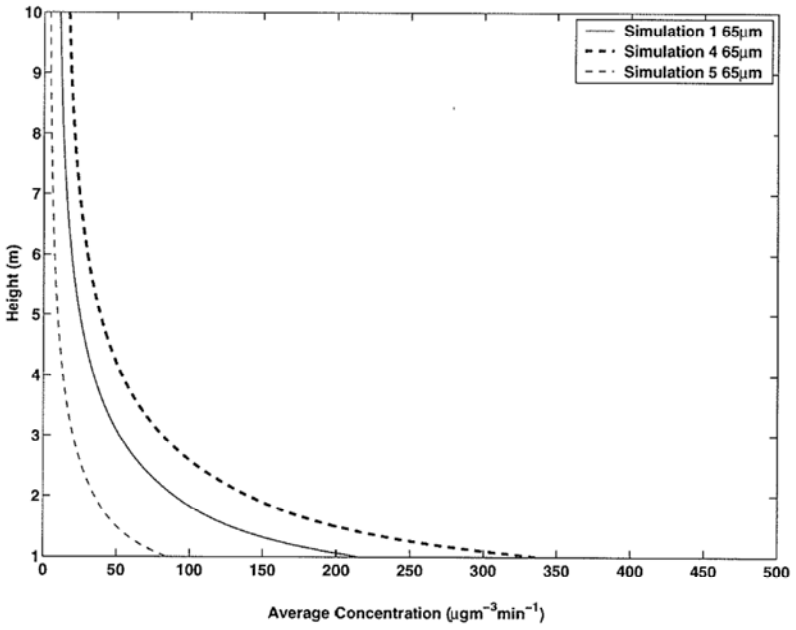

(b) 65μm vertical dust concentration for Simulations 1, 4 and 5.

Figure 9.6: The effect of altering the emission rates for 65 μm particles, as in Table 9.2, for Event E1-1996.

9.3.2 Event E2-1995 simulations

The various particle-size dust concentrations resulting from Simulation 6 are shown in Figure 9.7. In contrast to Figure 9.4, the 15μm particles do not have the highest dust concentration throughout the profile, but only above 6m and below 2.6m. Figure 9.8 shows that the "kink" occurs approximately a metre lower for the 65μm particles than for 15μm particles. This behaviour is associated with the way deposition and thermal buoyancy of the plume interact. As particles entrained in Source Area 2 travel downwind, the thermal buoyancy of the air lifts these particles away from the soil surface (Fig. 9.9), but gravity also acts to return the particles to the surface (Fig. 9.9). Since the 65μm particles have the highest deposition velocity, they would settle out significantly faster than the smaller 15μm particles. Therefore, 65μm particles from Source Area 2 are concentrated lower in the profile, causing the increase in the 65μm concentration in the 2.6 to 6m range. Below 2.6m insufficient particles from Source Area 2 are presented to dominate material being introduced into the profile from Source Area 1. Thus it is material from Source Area 1 that dominates the profile under 2.6m. The larger 65μm particles from Source Area 1 are removed first, causing the 65μm particle concentration to dip below that of the 15μm particles.

Simulations 7 and 8 in which the emission rate of the 15μm particles have been altered according to Table 9.2 are shown in Figure 9.10. Increasing the emission rate (Simulation 7) did result in an increase in dust concentration throughout the profile, but this effect did not decrease with height, as observed in Simulation 2, but rather altered with height, with the greatest increase coinciding with the middle of the "kink" at 7m. Up to 7m, there was a gradual increase in concentration as a result of the change in emission rate. After that point, the concentration decreased to its original value. Similarly, decreasing the emission rate in Simulation 8, produced the expected decrease in concentration, but unlike Simulation 3 (Fig. 9.5), did not continue to decrease with height. As in Simulation 7, Simulation 8 produced a significant decrease in the concentration around 7m. Simulations 9 and 10 (Fig. 9.11)

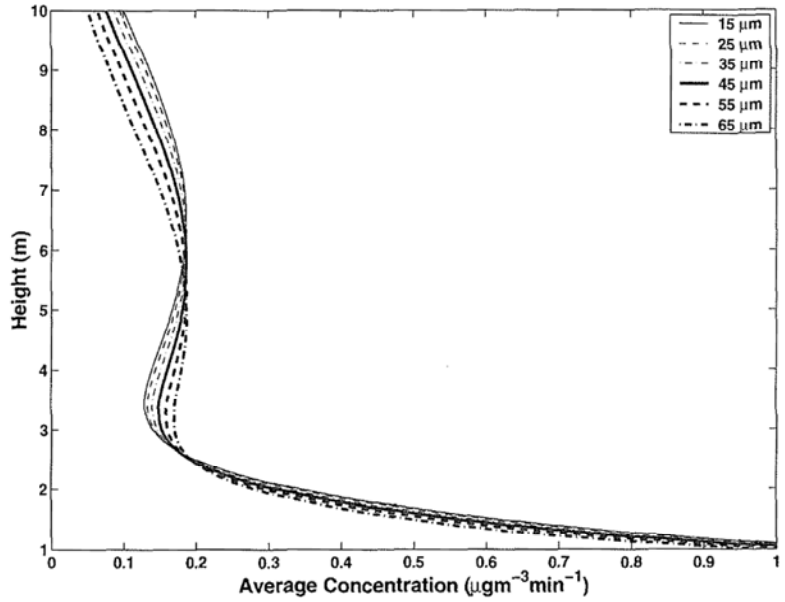

Figure 9.7: Particle-size concentration for Event E2-1995 assuming all particle-sizes are emitted equally (Simulation 6).

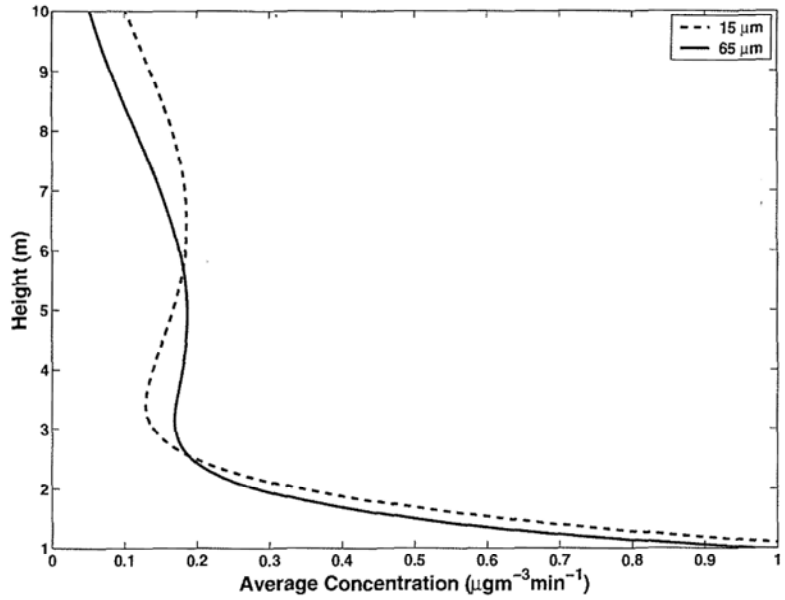

Figure 9.8: Contrast in dust concentration profiles for the 15 μm and 65 μm particles in Event E2-1995.

produce similar results, the only significant difference being that the peak change, that occurred around 7m in the 15μm, case now occurs at approximately 5m.

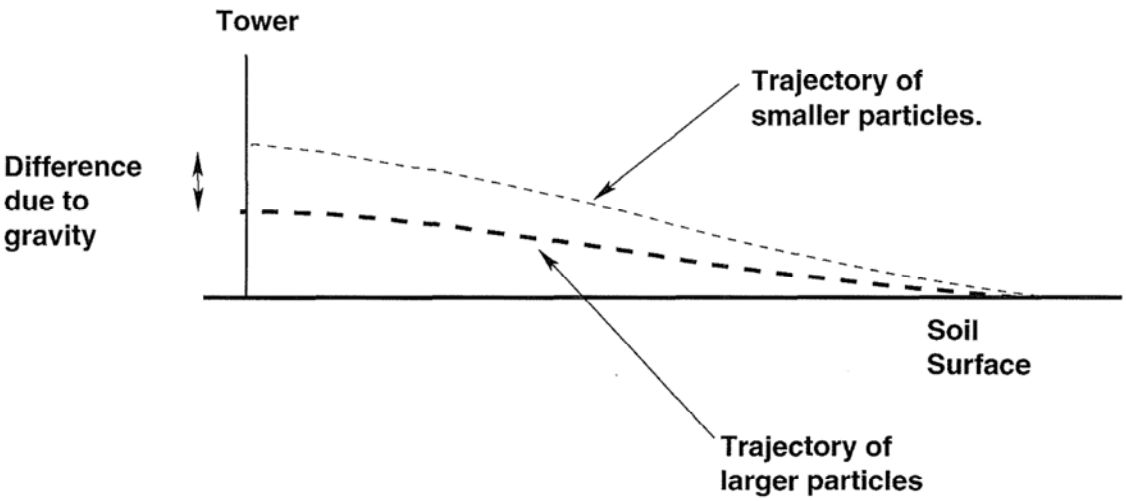

Figure 9.9: Schematic showing the effect of gravity with regards to particle-size on the "kink" in Event E2-1995.

These two heights can be explained by considering how material from Source Area 2 arrives at the tower. After being entrained, dust is taken away from the surface by the thermal buoyancy of the air (Fig. 9.9), arriving at the tower at a height determined both by the thermal buoyancy and the particle-size. In particular, most of the 15μm particles from Source Area 2 arrived at 7m, while the bulk of the 65μm particles arrived at 5m. The difference is due to the larger deposition velocity of the 65μm particles. This implies that the height of the "kink" decreases with increasing particle-size (Fig. 9.12).

It is important to consider how dust concentrations would alter if, for example, Source Area 1 began emitting finer particles. The simulations so far undertaken for Event E2-1995 (i.e. Simulation 6–10) assumed that an increase in emission rate for Source Area 1 is accompanied by a similar change to the emission rates in Source Area 2. Four additional simulations for Event E2-1995 were run (Table 9.3), to explore this scenario. These were constructed in a similar fashion to the earlier simulations in Table 9.2, except that only one particle-size emission rate was altered. For example, in Simulation 11 only the 15μm emission rate in source Area 2 was altered.

Figure 9.13(a) shows the resulting vertical dust concentration profiles. Note that this only produced a signification change in the dust concentration above

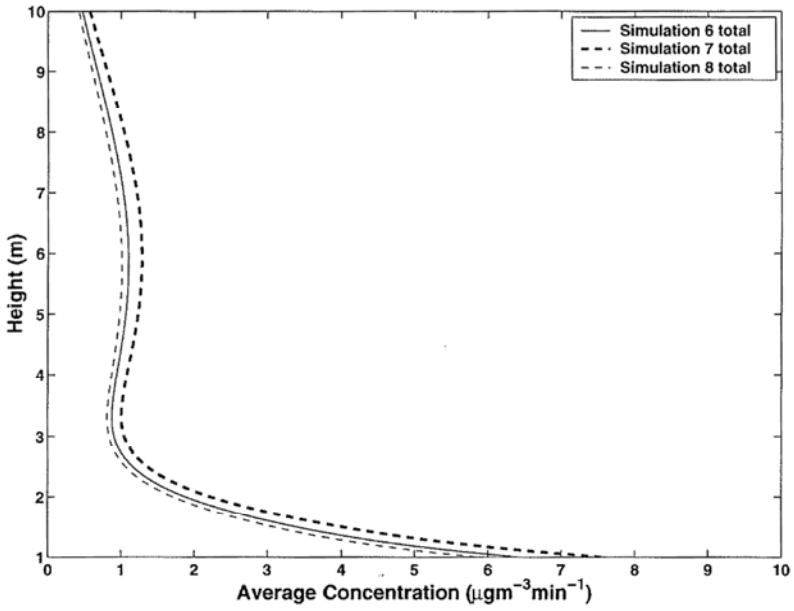

(a) Total vertical dust concentration for Simulations 6, 7 and 8.

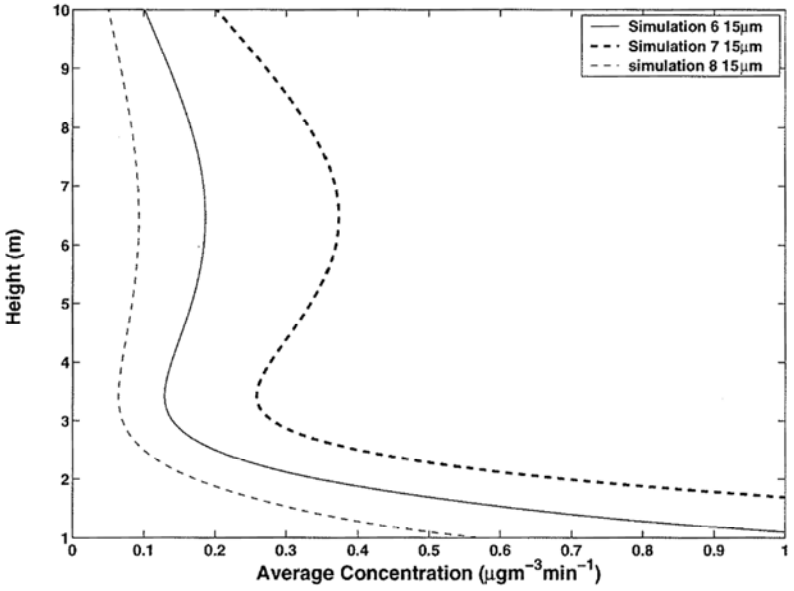

(b) 15μm vertical dust concentration for Simulations 6, 7 and 8.

Figure 9.10: The effect of altering the emission rates for 15 μm particles as per Table 9.2 for Event E2-1995.

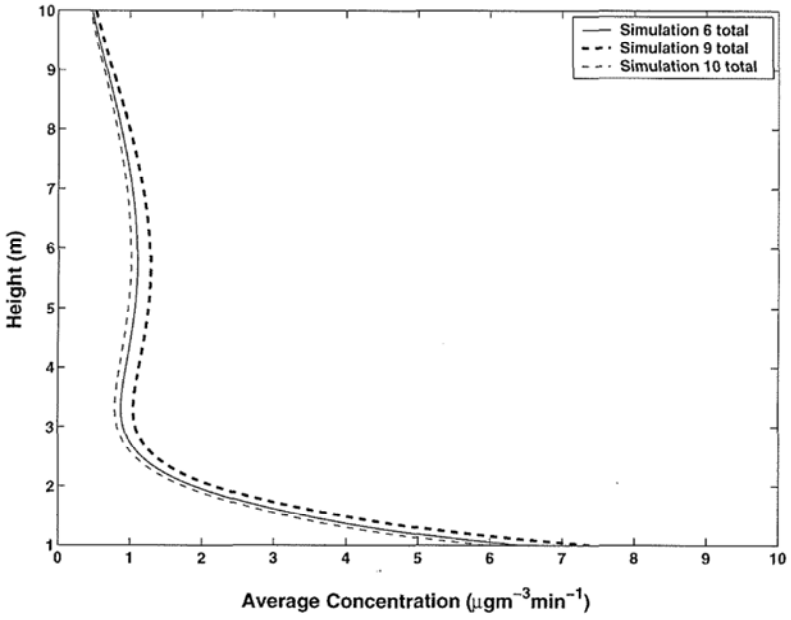

(a) Total vertical dust concentration for Simulations 6, 9 and 10.

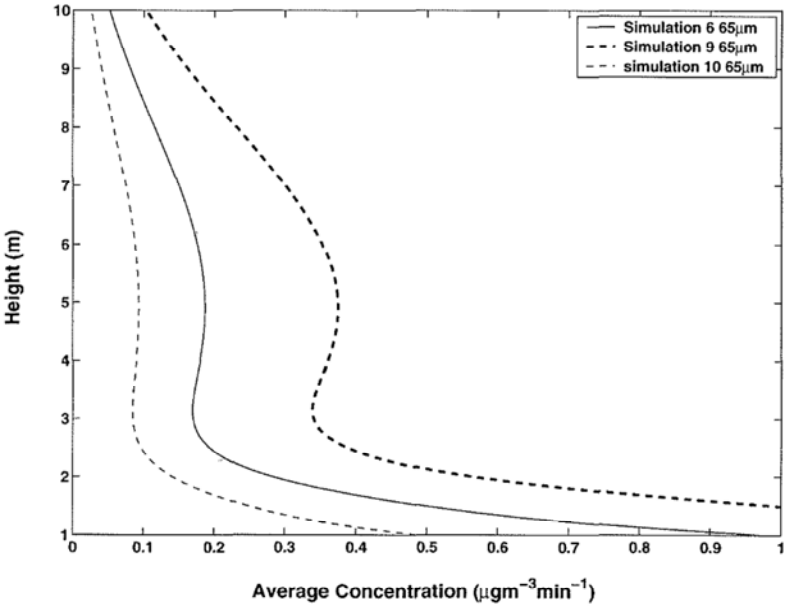

(b) 65μm vertical dust concentration for Simulations 6, 9 and 10.

Figure 9.11: The effect of altering the emission rates for 65 μm particles as per Table 9.2 for Event E2-1995.

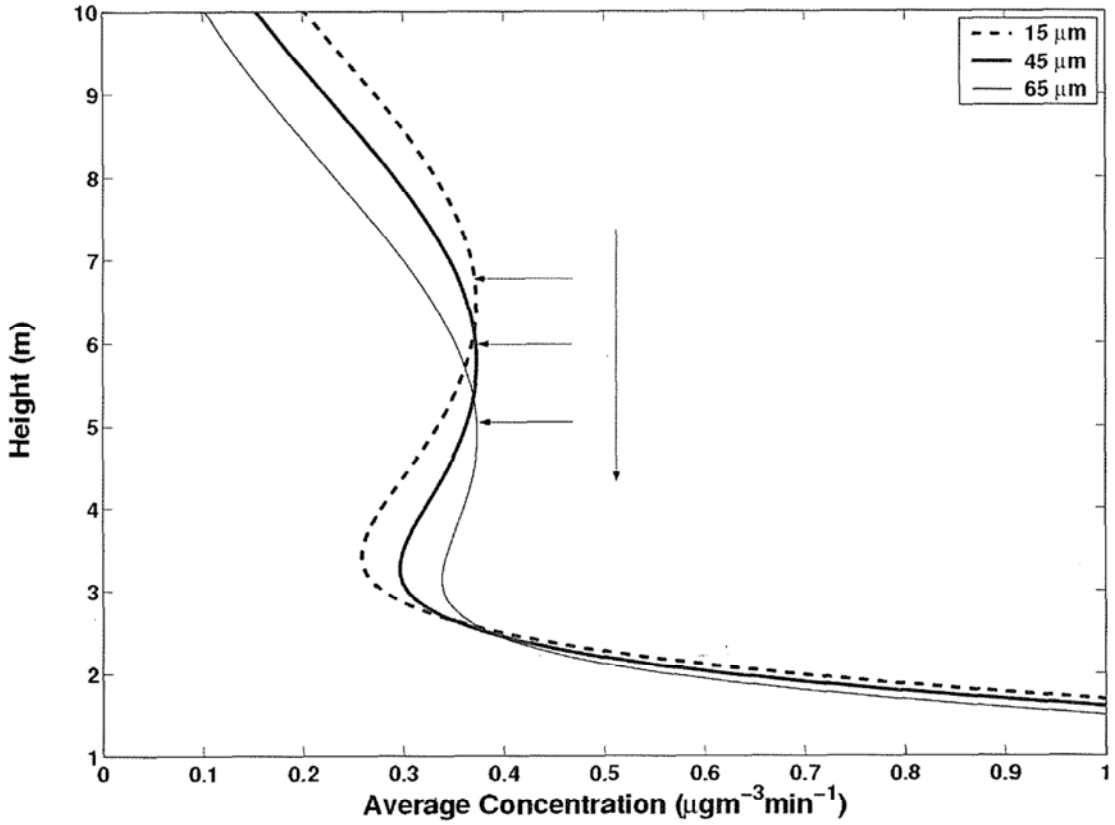

Figure 9.12: Contrast in vertical dust concentration profile for the 15 μm, 45 μm and 65 μm particles in Event E2-1995, under the assumption of equal emission rates. The horizontal arrows indicate the position of the "kink", while the vertical arrow indicates the direction of movement of the "kink" as particle size is increased.

2.6m. Similarly, in Simulation 12, (which only altered the 45μm emission rate in Source Area 2), there was a slight offset from that observed in Simulation 11, due to the faster deposition velocity of the 45μm particles. Changes in emissions from Source Area 2 affect the middle to upper reaches of the profile. In contrast, Simulations 13 and 14 (Table 9.3) show that altering the emission rates in Source Area 1 only affects the profile below approximately 3m.

These results are interpreted as follows. Since Source Area 1 is closer to the tower, dust from it has only had a short amount of time to disperse. Hence, most of this dust is confined to a small area near the surface (<2m), increasing the concentration in the bottom half of the profile. Dust being transported

Table 9.3: Emission rates (μgs^{-1}) per particle class size for additional simulations simulation of Event E2-1995.

Source Area 1						
Simulation	Particle-Size (μm)					
Number	15	25	35	45	55	65
11	6	6	6	6	6	6
12	6	6	6	6	6	6
13	12	6	6	6	6	6
14	6	6	6	12	6	6
Source Area 2						
Simulation	Particle-Size (μm)					
Number	15	25	35	45	55	65
11	72	36	36	36	36	36
12	36	36	36	72	36	36
13	36	36	36	36	36	36
14	36	36	36	36	36	36

from Source Area 2 is affected by the thermal buoyancy, gravity and has had more time to disperse. This means that the larger particles from Source Area 2 have settled out and that the remaining particles are fairly evenly distributed throughout the profile. Hence, this dust has the greatest impact on the dust concentration in the upper part (>2m) of the profile. Much of the dust from Source Area 1 makes up the saltation material, while dust from Source Area 2 makes up most of the suspended component.

DSism can resolve the effects that particles moving in both the saltation and suspension mode, have on the vertical dust concentration profile. This suggests that particles moving in both modes are governed by the same physical processes. Another feature of the results is that above 2m, the Event E2-1995 concentration profile is dominated by transported dust, while the lower half (<2m) is dominated by dust entrained in the immediate neighbourhood of the

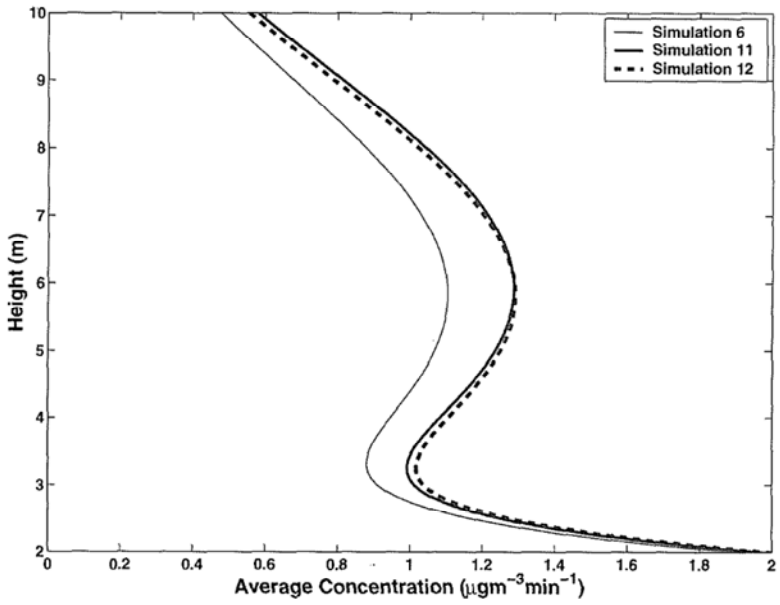

(a) Source Area 2 effects

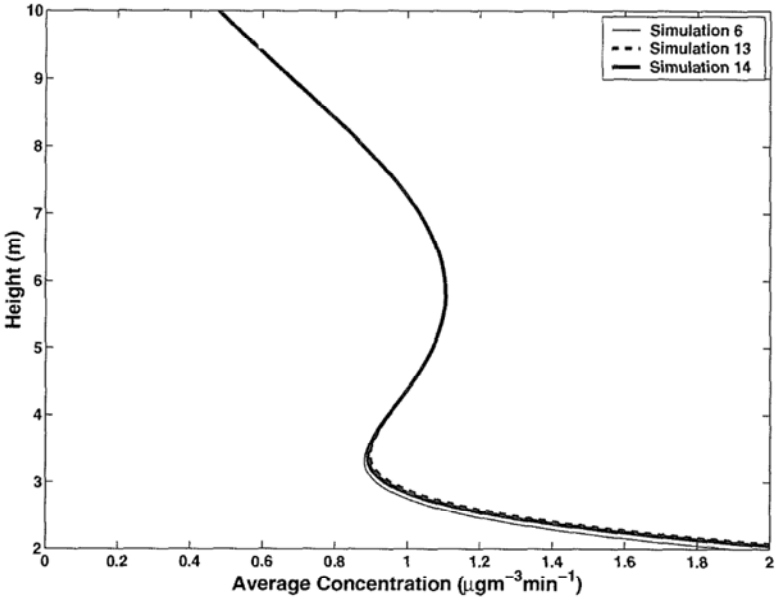

(b) Source Area 1 effects

Figure 9.13: The effect on total dust concentration of altering the source emission characteristics in Source Area 1 and 2 individually as per Table 9.3.

tower. This scenario agrees with the Vories and Fryrear (1991) regression model of how dust flux varies with height (Equation (7.2)), but here the same

result has been obtained by simulating physical processes. The advantage of this approach is that no assumptions are made about the shape of the vertical dust concentration profile, unlike the Vories and Fryrear (1991) model which forces the dust concentration into a given functional form, and assumes that any variation from this is the result of experimental "noise". The DSism approach, has shown instead that this variation ("noise") contains significant process information.

9.4 Conclusion

This chapter shows that changes in particle-size emission rates have a significant affect on the vertical dust concentration profile. The shape of the vertical dust concentration profile depends not only on how these particle-size emission rates vary spatially within the site, but also on the types of processes in operation. To truly understand how the particle-size distribution varies throughout the plume, it is first necessary to understand the effect that spatial variations in emissions has on the profile.

These results also show that there is significant variation in dust emissions between discrete dust events. In particular, a small increase in dust concentration, is associated with a much larger increase in emission rate.

Lastly, the position of the "kink" depends not only on the thermal buoyancy of air, but also on deposition processes within the plume. In practice, the position of a "kink" will depend on factors, such as the emission rates, thermal heating and spatial variation in the surface and vegetation conditions within the site. Much more work needs to be done to understand how all these factors interact before we can fully understand the mechanism that is producing these "kinks" in the vertical dust concentration profiles.

Part IV

Concluding comments

Chapter 10

Comparison of the DSism approach to existing models

10.1 Introduction

In Chapter 3, several different approaches to modelling wind erosion were discussed in detail. Now that DSism has been described it is worthwhile comparing it with each of these modelling approaches. This chapter discusses the features and limitations of each of these approaches in rangeland environments. Included in this discussion is a comparison of each approach to DSism in terms of their applicability to rangeland environments.

10.2 Climatic index wind erosion models

In Section 3.2, the basic ideas and methodology behind climatic index wind erosion models were discussed. These models are designed to provide information about the seasonal occurrence of dust events at a regional scale using meteorological information. In Australia, these models were verified using the Australian Dust Event Database (ADEDB). This database contains information on event frequency and intensity of dust events, at the various

meteorological stations shown in Figure 10.1. The ADEDB does not contain information on dust flux/emission rates (and therefore soil loss) of the various regions.

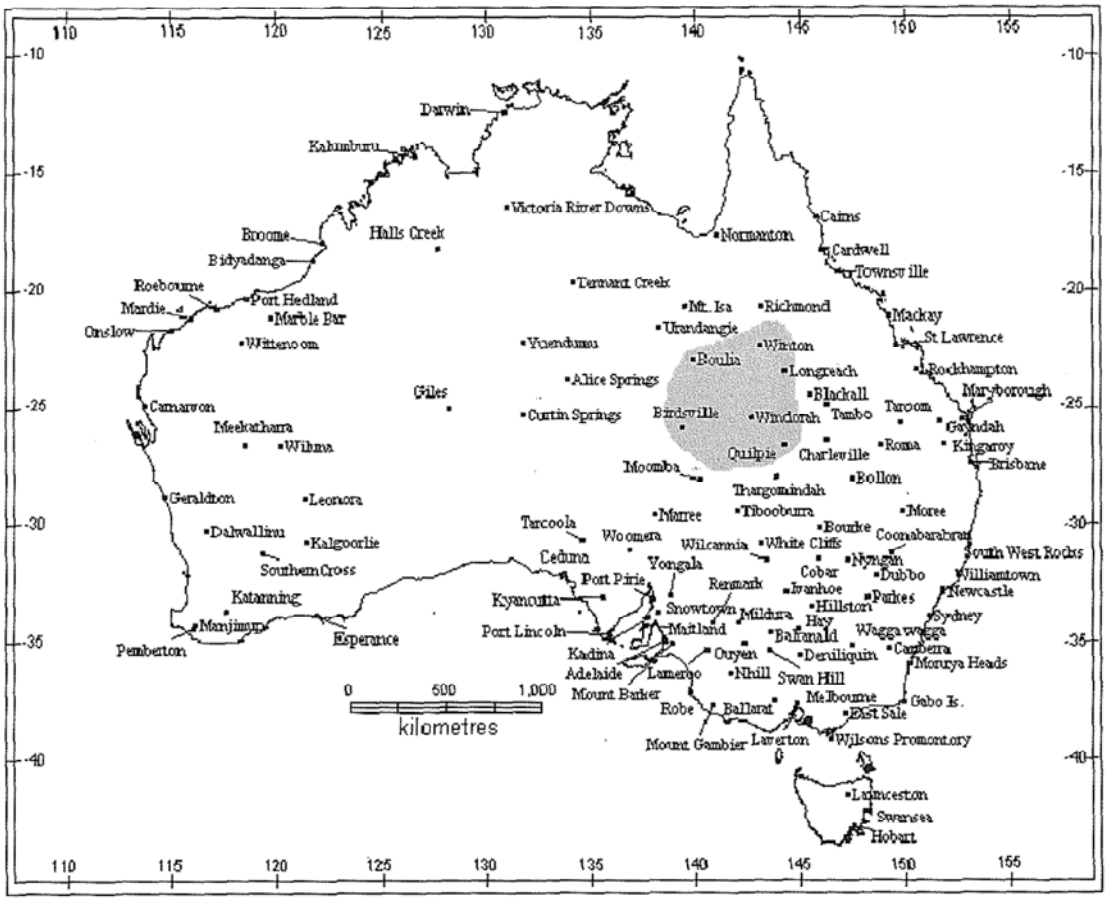

Figure 10.1: Meteorological station locations in Australia. Note the increase in density in the south east corner of the continent. The blue highlighted region illustrates the meteorological stations that border the Channel Country. (This figure is the same as Figure 3.1 and has been repeated for convenience.)

The dependency on meteorological data has the disadvantage that it controls the resolution of these models. In particular, in the case of the Channel Country, only 6 meteorological stations (Winton, Boulia, Birdsville, Windorah, Quilpie and Longreach) provide data to calculate the wind erosion index (Fig. 10.1). Since these are separated by hundreds of kilometres, the spatial resolution of the index within the Channel Country is extremely limited.

As the climatic index models focus on the frequency of dust events in specific regions and how these vary with seasonal changes in climatic conditions, they do not provide information on how one wind erosion event differs from the next. Consequently, these models give little information about soil loss or what processes are in operation during each event at the local scale. DSism, in contrast, has been designed to investigate the effect that spatial/temporal changes in dust source areas and processes at the local scale, have on the distribution of dust within rangeland environments. This implies that DSism provides more detailed, process-specific information about wind erosion within rangeland environments.

10.3 Empirical wind erosion prediction models

As stated in Chapter 2, wind erosion rates are dependent on a complex mixture of vegetation cover, surface and atmospheric conditions. Empirical wind erosion models, such as the Wind Erosion Equation (WEQ) and Revised Wind Erosion Equation (RWEQ) described in Section 3.3, were designed to link observed values of vegetation cover, surface and atmospheric conditions to wind erosion rates via an empirical relationship. While these models provide a quantitative link between various factors influencing wind erosion rates, they provide little information about the processes in operation spatially and temporally within the local area, as they are not based on physical process considerations. Additionally, since these relationships were developed for cultivated fields (where surface conditions and vegetation cover were uniform) they do not adequately account for spatial and temporal variation in surface conditions and vegetation cover commonly associated with the Australian rangelands.

DSism, in contrast, is not designed with the primary goal of estimating wind erosion rates. Rather, it was designed to simulate spatial and physical processes in operation during wind erosion events within rangeland environments. By taking a simulation approach DSism provides more detailed

information about spatial/temporal aspects of dust transportation processes in rangeland environments. In addition, by simulating actual physical processes rather than using an empirical relationship DSism can be more readily adapted to other sites and locations. The additional spatial and process information obtained via DSism can be then used to improve either empirical or physical based emission rate models for the rangeland environments, such as the Channel Country.

10.4 Integrated wind erosion models

DSism is to some extent similar in operation to the Fugitive Dust Model (FDM) and is quite different from the Wind Erosion Prediction System (WEPS), Wind Erosion Assessment Model (WEAM) and the Gillette and Passi (1988) model. This section looks at these differences and similarities and places DSism in the context of these models.

10.4.1 Differences between DSism and WEAM/WEPS

The key difference between DSism and WEAM (or WEPS) is that DSism does not relate surface conditions, vegetation cover and atmospheric conditions to emission rates. In the DSism case the required emission estimates are obtained using sensitivity analysis and the fitting procedure outlined in Chapter 5. Unlike WEAM (or WEPS) which are emission models and therefore designed to link observed conditions to emission rates/erodibility of the surface, DSism is a transport model designed to provide dust concentration estimates at various points downwind.

The ideal modelling situation would be to use a model, such as WEAM (or WEPS) to seed a transport model, such as DSism. However, there are several reasons why this should not be done. The most obvious is that it is difficult to identify which dust source areas are in fact active during specific wind erosion events within rangeland environments (especially within a given land type).

This means that it is hard to: 1) verify emission models in the field and 2) identify the actual processes in operation within the local area or study site. It also means that without an effective means of identifying emission areas in the field, it is hard to fully appreciate the role that spatial and temporal changes in dust source areas and processes, have on the wind erosion within rangeland environments.

The other important reason for not using WEAM (or WEPS) to seed DSism relates to the need for both models to have detailed descriptions of soil surface properties and vegetation conditions in order to make accurate predictions of emission rates. The problem with this approach in rangeland environments is that unlike cultivated fields where surface and vegetation conditions are fairly uniform and each field has distinct boundaries, they can change several times within a single land type and the actual boundaries are not distinct. Therefore, spatial changes in surface and vegetation conditions within land types are likely to be more important in rangeland environments.

Combining the two observations above indicates that it would be 1) difficult to collect accurate field measures to use an emission model such as WEAM, at the resolution required for this study, 2) if WEAM (or WEPS) was used to seed DSism then there would not be sufficient data in the Diamantina National Park data set to run the model for any of the events in the data set and 3) adding a model like WEAM would have added an additional source of error to the model. By using the sensitivity/simulation approach and matching it against experimental observations, DSism avoids some of these data issues and thus, enables us to analyse the Diamantina National Park data and to extract process and spatial information from it.

10.4.2 Differences between DSism and the Gillette and Passi Model

In the Gillette and Passi (1988) model, the mass of soil loss is linked to various surface properties. The surface property values used in this model are

based on either long term averages or on measured values taken at one point during the season. Such estimates provide a reasonable approximation to assess the damage done by wind erosion at a regional scale. However, without a better understanding of how these properties vary though time and space at the local scale, it is not possible to fully appreciate the damage incurred locally on an event basis. In particular, this means that for much of the Australia rangelands, where there is substantial spatial and temporal diversity in surface conditions, little is known about the damage incurred on an event basis.

DSism, unlike the Gillette and Passi (1988) model, is not designed to estimate the amount of soil lost during a given period. Rather, it is designed to understand how spatial and temporal changes within the local area affect the dust concentration. Thus, it enables the investigator to explore whether observed changes in dust concentration within rangelands, can be simply related to spatial changes in erodibility. By understanding how the processes that control the distribution of dust within rangelands vary from event to event, then this will enable us to determine what spatial and temporal resolution is necessary to accurately estimate wind erosion damage on an event basis.

10.4.3 Differences between DSism and FDM

Many of the differences between FDM and DSism discussed in the following text, reflect the different applications of these two models. In particular they highlight that FDM is designed to estimate urban pollution levels and the effect that rural dust has on urban air quality, while DSism is designed to study how spatial/temporal changes in dust source areas and processes in rangeland environments affect observed dust concentration profiles. The outputs of the FDM and DSism strongly reflect these different applications. The output from FDM only produces dust concentration estimates at single points (Winges, 1992) and is in fact limited in the computer coding to providing these estimates at 100 points. In contrast, DSism output provides both vertical and

crosswind dust concentration profiles (or a combination of these profiles) at any point downwind. The advantage of using vertical dust concentration profiles rather than individual points, is that it enables detailed comparisons to be made against observed dust concentration profiles. Such comparisons allowed DSism to show that surface heating in rangeland environments is an important consideration in wind erosion processes.

The differences between FDM and DSism are further highlighted by considering how crosswind source lines are used to model dust source areas in each model. In FDM only two options exist. The first option places five equally spaced crosswind source lines throughout the dust source area. In the second option crosswind source lines are added to the source area one at a time, until the predicted dust concentration downwind does not alter between successive additions. In contrast, DSism allows such lines to be placed in much more complex patterns. Thus enabling the areas of high/low erodibility within these areas to be linked to the dust concentration profile. Thus, it is possible for the investigator to use DSism to test several different spatial source combinations in the simulation, in order to see which combinations best match the observed dust concentration profiles.

A further difference between FDM and DSism can be found in the dust source emission rate input required by each model. In FDM, the user has to specify the actual emission rates and how they vary with wind speed (see Section 3.4.4). This approach is taken for two reasons. The first relates to the fact that unlike DSism which actually estimates dust concentration over a single event, FDM provides a value of the dust concentration over a 1, 3, 8 or 24 hour period. To do this FDM has to account for periods in which no erosion was taking place. The second, is to allow FDM to account for sources that may not erode until a specific wind speed is reached.

Provided the source areas can be readily identified there are no difficulties with this approach. However, in rangeland environments, it is difficult to identify the source area boundaries for each event, as the wind direction and active sources may change between events. For example, in the case of the

Lake Constance claypan, it is hard to identify the boundaries of the different surfaces shown in Figure 4.7. This makes it extreamly difficult to classify the changes in emission within a given land type. In addition, data is not readily available for each of the events to account for changes in erodibility of the surface. Thus, DSism was designed to overcome this lack of data. DSism therefore, has several modes of operation. If the source areas could be clearly defined and emission data was available DSism can operate in a similar fashion to FDM. However, if this data is not available, DSism was designed to have a different mode of operation. In this mode, the Land Erodibility Index (LEI) (McTainsh et al., 1999), is used to specify the relative erodibility of each land type. Once this is determined the base emission rate (Q_b) is obtained by sensitivity testing and comparing modelled dust concentration profiles to the observed profiles. A side benefit of setting the base emission rate in this way, is that DSism does not assume that (a) the same sources are in operation for each event and (b) that the emission rate (Q_b) can vary substantially between events.

The final difference between FDM and DSism, once again concerns how the emission rates are specified. In DSism, the user is also allowed to specify emission rates on a particle-size basis and to add new particle-size classes as required. Thus, it is possible in DSism to change the distribution of particles being emitted from any dust source area. This feature enables DSism to simulate dust source areas, which have different particle-size characteristics and are therefore likely to have different particle-size emission characteristics. In contrast, FDM does not allow the emission rate to be specified on a particle-size basis. Thus, there is no mechanism in the FDM to model the effect that particle-size characteristics of the parent soil has on dust concentration profiles downwind.

The use of particle-size emission rates enables DSism to estimate dust concentration profiles downwind for each particle-size. This feature is important in a wind erosion model as wind erosion processes are extremely particle-size selective. Being able to provide estimates of dust concentration profiles on a

particle-size basis is extremely useful, since it provides process information on how changes in particle-size emission rates propagate through the dust plume. Such process information is important to be able to understand the impact that changes in the particle-size characteristics of the parent soil have on the resulting dust plumes.

10.5 Continental/Global climate models

Two models were discussed in Section 3.5, that modelled wind erosion at the continental scale in Australia. The first of these is the Knight et al. (1995) model, while the second is the Lu and Shao (2001) model. The following discussion considers DSism relative to these two models.

10.5.1 The Knight et al. model

The goal of the Knight et al. (1995) model was to quantify the amount of dust moved in a single dust storm that occurred in 1987 in western Queensland. In the Knight et al. (1995) model, back–trajectory analysis was used to identify the dust source areas. As the entrainment rate was not known for their Birdsville source area box (Fig. 3.4), Equation (3.22) was inverted to isolate the Birdsville entrainment term. Once estimated this data was used to solve the standard forward transport problem and estimate dust loads within the plume.

To simplify calculations Knight et al. (1995) assumed that emission rates were uniform in the Birdsville box and that the dust concentration was uniform within each box (Fig. 3.4). However, during the 1987 event the surface conditions were far from uniform in the Birdsville source box. These assumptions raise the question of just how much does spatial and temporal variations in dust source areas and processes within the Birdsville and other boxes affect dust concentrations downwind. Evidence presented by McTainsh et al. (1996)

and Lu and Shao (2001) suggests that local spatial variations in soil erodibility can result in significant changes in both estimates of dust loads and soil loss rates (see Section 3.5 for additional details). The results of the DSism simulations presented in this thesis, not only support these claims, but go further, by suggesting that the spatial and temporal variations in dust source areas and processes determine the shape of the dust concentration profiles at the local scale.

Knight et al. (1995) could have achieved a more accurate estimate of dust loads if they had more accurately estimated the emissions in the Birdsville source area box. However, even if better spatial erodibility estimates were available to Knight et al. (1995), the model could not have fully utilised them as their model is not designed to distinguish variations in crosswind or vertical dust concentration profiles within each box. To fully appreciate the effect that spatial and temporal variations in dust source areas within the Birdsville box has on dust loads at the continental scale, it is first necessary to understand how such variations affect the dust concentrations within each box.

By simulating spatial and temporal changes in dust source areas and processes at the local scale, DSism is able to provide information on how the distribution of airborne dust within the local area is affected by such spatial and temporal changes. While DSism is able to provide this information in its current form, it does not provide information about how these changes are propagated beyond the local area, since it has a 20km limit imposed by the Gaussian approximation. Overcoming this limitation is a longer term research goal.

10.5.2 The Lu and Shao model

As mentioned in Section 3.5.2, the Lu and Shao (2001) model extends the original Wind Erosion Assessment Model (WEAM) of Shao et al. (1996) to the continental scale by incorporating a transport process and GIS data. By using GIS data on vegetation cover and land types, Lu and Shao (2001) are able

to predict wind erodibility and dust transport at the continental scale. However as mentioned in Section 3.5.2 when they compared their results to that of Shao and Leslie (1997) their total dust estimate was significantly different (i.e., 1.2Mt compared to 6Mt estimated by Shao and Leslie (1997)). This difference Lu and Shao (2001) put down to the spatial variability in dust emissions within each grid element used in the model. In particular, this result suggests that averaging the emissions over such a spatial element results in a significant change in the amount of airborne dust predicted in the model.

The ideal solution is to increase the spatial resolution of the model. However, there are some problems inherent in increasing the spatial resolution. The first problem relates directly to the GIS information in that the spatial and temporal resolution of the GIS data is not sufficient to resolve differences in erodibility within individual land types. Secondly, it assumes that spatial variations in erodibility and processes within each cell do not have a significant effect on the spatial distribution of airborne dust downwind. Thirdly, it is very expensive in computer time.

What these observations suggest is that at present it is impossible to say what spatial resolution is necessary to accurately predict downwind dust concentrations. It is this spatial resolution question that DSism is designed to address at the local scale. Thus, while DSism may at present be limited to 20km, it provides essential information on how spatial/temporal and variations in processes within the local source area affects dust concentrations downwind. Such information will be crucial in understanding how spatial and temporal changes within rangeland environments influence dust concentrations at the regional and continental scale.

10.6 Summary

This chapter illustrates where DSism fits within the spectrum of the other wind erosion models discussed in Chapter 3. In particular, it highlights that DSism was designed to investigate the effect that spatial/temporal changes in

emissions have on dust concentration within the local area. It also shows that DSism was designed to study how various physical processes interact with different spatial source area distributions. All this implies that DSism fits well between the local emission models and continental scale models. Thus, it is well placed to provide an insight into: 1) what physical processes influence dust concentrations within the local area and 2) the importance of spatial source variations within land types in determining dust concentration within the local area. Consequently, the results from DSism are likely to prove an important stepping stone in understanding how local changes in dust emissions influence dust concentrations at the local, regional and continental scales.

Chapter 11

Summary and concluding comments

11.1 Summary of research outcomes

The major aim of this research was to improve our understanding of how spatial and temporal variations in dust source areas and physical processes in rangeland environments influence how dust is vertically and laterally distributed during wind erosion events. Most studies and models, have assumed that emission rates are uniform within a given land type. One of the reasons for this assumption, is that spatial and temporal changes in emission rates within a land type cannot be easily identified in the field. In addition, since most experimental work in Australia has been done on cultivated fields where surface conditions are relatively uniform and the spatial variability is less important, the spatial issue at the local scale has been largely ignored. However, in rangeland areas (such as the Channel Country), it is argued that spatial and temporal variations in source area erodibility are likely to play a much more significant role in the wind erosion process. This observation, is supported by the study of Lu and Shao (2001), which suggest that local changes in emission rates can have a significant impact on dust loads at the regional and continental scales.

To investigate these issues, the Dust Source Interaction Simulation Model (DSism) was constructed using a robust air pollution model as its basis, to

simulate wind erosion events within the study site. The basic model is robust in that accurate estimates can be achieved using a minimum of data and even when some of the model assumptions have been violated. DSism represents a departure from the conventional approaches to modelling wind erosion in that it uses vertical dust concentration profile data and sensitivity testing to identify spatial dust source areas. Other models, such as FDM (see Chapters 3 and 10) require the user to have identified the actual emission areas in the field, which is often not possible in rangelands. Thus, most wind erosion models assume that the emission rates are constant within a given land type. The advantage of the DSism approach is that the additional information contained in measured dust concentration profiles is used to seed the simulation. Thus, unlike regression models, such as Fryrear and Saleh (1993), DSism is able to provide a greater insight into how the physical processes and spatial changes in surface and vegetation condition interact at the local scale to produce recorded vertical and crosswind dust concentration profiles.

The resulting model (DSism) is not limited to rangeland environments. The only limitation on DSism is the 20km downwind limit. The crosswind extent is not limited at present. Thus, DSism can be applied to any region where surface conditions and vegetation cover vary. This means that DSism can also be used to simulate wind erosion processes within areas, such as the Klondike in Canada or cultivated fields where conditions vary from plot to plot.

11.1.1 Discussion of findings

The results of the simulations examined in Chapters 4 to 6, show that dust source area configurations and the emission rates of such dust source areas are important factors in determining the shape of the vertical dust concentration profile downwind. There are three important implications of this result. These are: 1) dust sources at different distances from the monitoring tower influence different parts of the dust concentration profile, 2) the effects of spatial changes in dust source areas upon dust concentration profiles are not

site specific, but rather the result of universal processes and 3) the "kinks" in observed vertical dust concentration profiles cannot be simply the result of spatial variations in dust emission rates.

The DSism simulations in Chapters 4 to 6, show that sources close to the tower have the greatest impact on the saltation and lower suspension component (i.e., the lower half of the dust concentration profile ($\leq$3m)), while dust sources further away influence the shape of the whole profile.

These simulations also provide an insight into how the coefficients used in the dust concentration-height regression models described in Chapter 7, relate to physical processes. In particular, it explains why Nickling et al. (1999) observed that the values of the exponent (b) in Equation (7.1) varied over so great a range. Analysis of other simulation results in this thesis suggests that the variation in parameter (b) is the result of the interaction between various dispersion processes and the spatial and temporal variability in dust source areas. These simulations and the variability observed by Nickling et al. (1999) suggest that the effects of spatial changes in dust source areas upon vertical dust concentration profiles are not site specific processes within the Channel, but are the result of universal processes. The results in Chapter 7, also suggest that by using regression models that smooth out the data, much of the important process information contained in the vertical dust concentration profile is lost.

Finally these simulations indicate that the "kinks" in the vertical dust concentration profiles within the study site cannot be simply the result of spatial variations in emission rates. Further examination of environmental conditions observed during a number of events, suggests that such "kinks" occur as the result of changes in thermal conditions within the study site. Additional simulations, which include a method to simulate the thermal buoyancy of the plume, further support this conclusion. Once the thermal buoyancy term is added, DSism is able to accurately recreate the observed dust concentration profiles. This is important in that it implies that these "kinks" are most likely the result of actual physical processes occurring within the study

site. Therefore, fitting regression models to vertical dust concentration profiles may smooth out and remove important information about wind erosion processes and upwind dust source areas.

The importance of this observation, can be visualised by thinking of the dust concentration profile, as a radio signal. Using this analogue, it is possible to view the vertical dust concentration profile as a composite radio signal, which is composed of several signals (input signals) from different sources. These input signals, would add variation to the resulting signal. Contained in this variation would be information about each individual input signal. In terms of wind erosion, this composite signal contains valuable information about the processes and dust sources in operation during any given dust event.

In Chapter 8, DSism, is used to deconstruct two vertical dust concentration profiles into their component dust source configurations. The predicted dust source configurations were then compared to surface and vegetation conditions observed upwind of the appropriate tower prior to the event. In both cases, DSism predictions compared favourably with the transect and field observations. However, this approach did not accurately resolve the crosswind locations of the various dust sources. This result suggests that a single vertical dust concentration profile contains significant information about the upwind boundaries of dust source areas. However, it also implies that additional information may be required to improve the crosswind resolution. The importance of understanding this crosswind variability is illustrated by the crosswind simulation undertaken in Chapter 5. The results of these crosswind simulations are shown in Figure 5.8 on page 115. This, figure shows that at lateral dust source boundaries, there is often a significant change in dust concentration across the boundary. Together, the above results suggest that a detailed analysis of vertical and lateral dust concentration profiles can provide significant information of the dust source areas and processes operating during any given event. This information adds significantly to our understanding of how wind erosion varies both spatially and temporally within rangeland environments.

Further investigation of how particle size emission affects the structure of the dust concentration profiles under various conditions (Chapter 9), indicates that particle size sorting within the plume also plays an important role in determining the final shape of the plume. In particular, these simulations show that the position of the "kink" in the vertical dust concentration profile (if present) will depend on the different particle size emission rates of the various dust source areas. Other simulations undertaken in Chapter 9, show that the shape of the resulting dust concentration profile will also depend on the particle size emission rates of the various dust source areas. These simulations indicate that altering the emission rates of sources close to the tower affects the lower half of the profile ($\leq$3m), while altering the emission rates of sources further from the tower affects the whole profile. These results demonstrate that measured dust concentration profiles contain information about the dust sources and the emission rates upwind of a monitoring tower.

11.2 Future research directions

The results presented here also show that more research is needed before it is possible to have an accurate picture of wind erosion within such rangeland environments. There are three directions in which the research presented in this thesis, can be readily extended. One is to extend DSism by exploring its usefulness as a predictive tool. Another is improving the resolution of dust source areas used in DSism. While the last is to further explore the effect that temporal and spatial variations in dust emissions have on crosswind dust concentration profiles. How this research can be extended in these directions, is discussed in detail below.

11.2.1 Testing the predictive power of DSism

The predictive ability of DSism under field conditions has not been fully explored in this thesis due to insufficient field data. Rather, DSism has been

used as an analytical tool to understand how the various processes and spatial variations in dust source emissions affect dust concentrations within the rangeland environments, such as the Channel Country.

To explore the predictive power of the DSism, additional field data needs to be collected in such away that the vertical dust concentration profile predicted by DSism, can be directly compared to one collected independently downwind. Thus, while it would be good to use a whole new field equipment infrastructure to collect this new data, there are several advantages in fitting it into the current field site structure. The first of these is that the basic structure is already in place to collect this data. Secondly any new data and information can be: 1) easy incorporated with the existing data, 2) used to reanalyse the preexisting data and 3) used to gather additional information about the relative performance of each type of sampler.

A possible experimental scenario for collecting this data is shown in Figure 11.1. In this scenario both types of samplers used in the present study (wind vane and semi-isokinetic) are used to collected dust concentration data. In Figure 11.1, two experimental Sites (A and B) have been established, in areas which have similar surface conditions. At both sites a 2m (wind vane samplers) and 10m (semi-isokinetic samplers) tower are erected. Thus, providing two independent measures of dust concentration at each site. In addition Site B, would ideally be directly downwind of Site A. Information would also be collected about the surface conditions between Site A and B. The information obtained at Site A would be initially used to seed the DSism model. Theoretically, DSism could then be used to predict the vertical dust concentration profile at Site B.

A problem with this approach is that it is not possible to accurately estimate the relative strength of the dust sources between Site A and B from observed surface conditions alone. To ensure that correct estimates of the strength of these sources is used in DSism, further information is required. Assuming that the relative efficiency of the two samplers is the same at Site B as Site

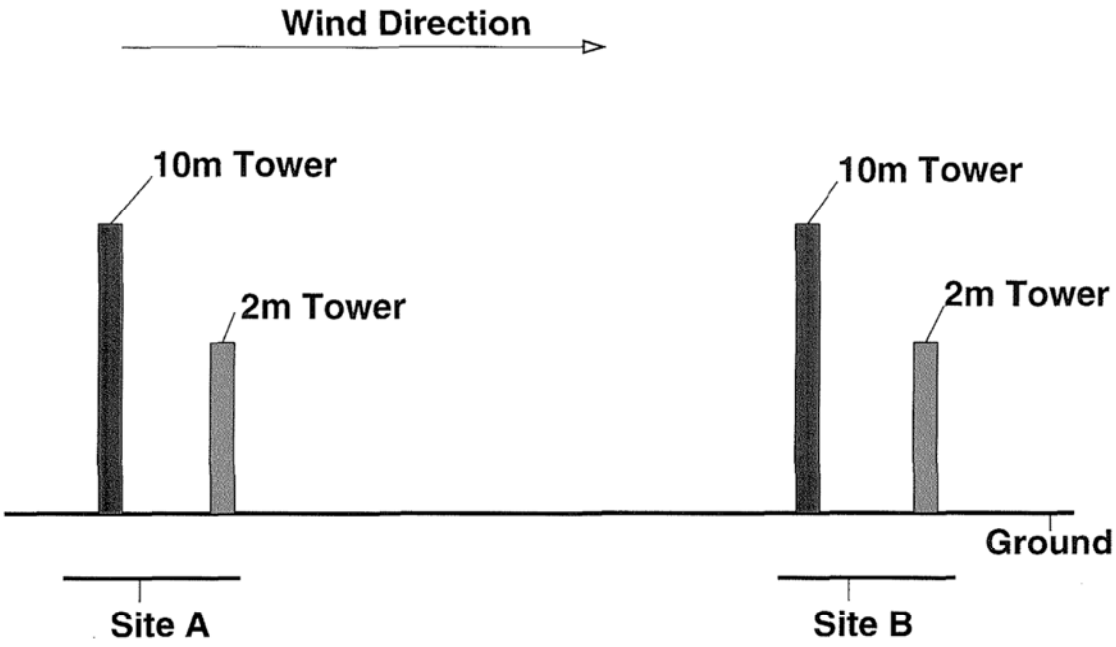

Figure 11.1: A possible scenario to test the predictive ability of DSism.

A, then it is possible to use the 2m wind vane sampler value at Site B and relative efficiency at Site A, to obtain a point on the vertical dust concentration. This point and the observed surface conditions between Site A and B, can be used to adjust the emission rates of the upwind dust sources. This process ensures that the dust source areas between Sites A and B are accurately simulated in DSism. Using all this information and assuming that atmospheric conditions are uniform within the study site, DSism can then be used to produce a predicted vertical dust concentration profile at Site B. This predicted profile can then be compared to the independently observed 10m vertical dust concentration at Site B. If DSism accurately reproduces the vertical dust concentration profile at Site B under these conditions, the predictive capacity of the model would have been demonstrated. By making such comparisons for a number of events and understanding the differences, it should be possible to gain a substantial new insight into the spatial and temporal aspects of wind erosion in rangeland environments.

11.2.2 Improving erodibility estimates used in DSism

A limitation of the Diamantina National Park data set used in the present study is that detailed experimental data on emission rates from different source areas were not readily available. Thus, in this thesis the Land Erodibility Index (LEI) developed by McTainsh et al. (1998) has been used to provided an initial estimate of the erodibility differences between the various land types (see Chapter 5 for details). Sensitivity testing was then used to determine spatial variability within a given land type, since the LEI as defined by McTainsh et al. (1998) could not be readily applied within land types. If however, better estimates of the erodibility of areas within land types could be obtained (i.e., the resolution of the LEI increased), then DSism's reliance on sensitivity testing could be significantly reduced. A recent study by Chappell et al. (2003) may provide a means by which the resolution of the LEI can be increased. In this study, also based at the Diamantina National Park, Chappell et al. (2003) use a geostatistical approach and a weighted average of wind vane sampler data within a given land type to calculate wind erodibility maps of the land type. These erodibility maps could be used to seed the spatial component of DSism, thereby increasing the spatial accuracy of the simulation. Further, by comparing the predicted dust concentration values using this coupled approach against those observed at several locations in the field, a much greater understanding of wind erosion processes within rangeland environments should be achievable. In addition the successful combination of these two approaches would make the resulting model an extremely useful predictive and analytical tool.

11.2.3 Crosswind improvements to DSism

The simulation results presented in Chapter 5, suggest that it is possible to have a substantial change in dust concentration at the edge of various crosswind sources. Other results presented in Chapter 8 indicated the presence of a dust source that was not located directly upwind of Site A. The existence of

this dust source provided a feasible explanation for second dust source area predicted by DSism analysis. These results, suggest that while, as shown in this thesis, the vertical dust concentration contains significant information about the upwind distribution of dust sources and the strength of these sources, it does not provide much information about the crosswind distribution of these sources. Clearly, more experimental and modelling work needs to be done, before it is possible to fully appreciate the importance of crosswind dust source variability.

DSism in its present form is clearly capable of simulating such spatial changes in erodibility and dust emissions. However, at present the Diamantina National Park data does not provide much information about crosswind variability in dust concentration. Therefore, the first priority in improving our understanding of crosswind processes has to be gathering more detailed crosswind information. Figure 11.2 shows a possible experimental scenario for collecting the extra experimental data. In this experiment, several 10m towers would be erected crosswind. (Note: while it is ideal to have three towers, the experiment could be set up in such a way that two or three towers could be used.) In particular if 2m towers are also setup at each site, the same experimental setup could be used to collect data either downwind for the experiment outlined in Section 11.2.1 or the crosswind experiment detailed here, depending on wind direction. These, 10m towers give crosswind dust concentration profiles at a variety of heights. Performing a similar analysis on the these crosswind dust profile to that undertaken in this thesis, should provide new insights into crosswind wind erosion processes within rangeland environments.

There are two advantages in using the experimental structure, shown in Figure 11.2. Firstly, the extra data can be easily integrated into the existing Diamantina National Park data set. That is the existing data can be reanalysed using the information gained from this new data. Secondly, using 10m towers in the crosswind array, means that it would be possible to have detailed 10m vertical dust concentration profiles at each tower within the array. Such data

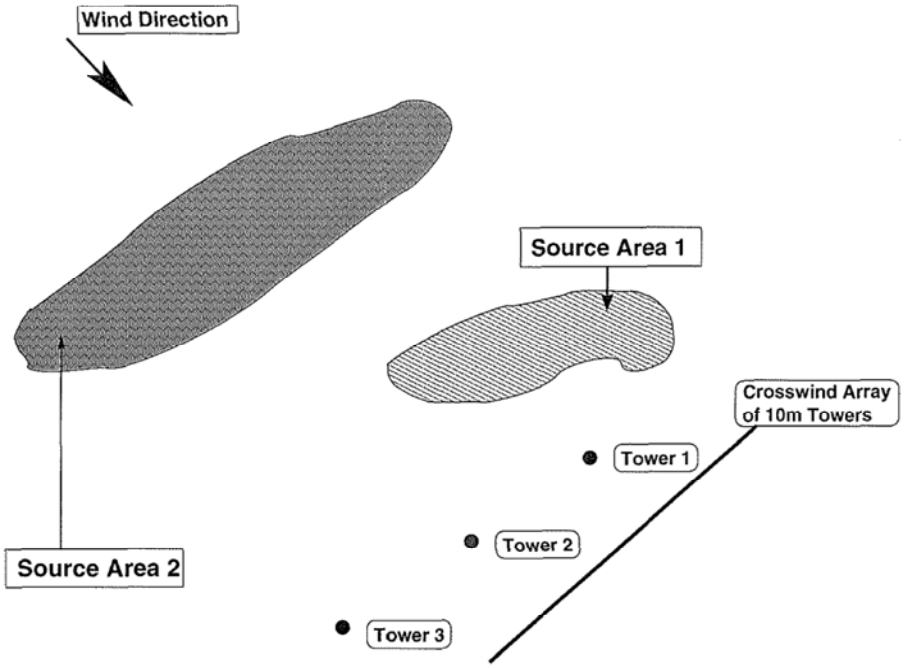

Figure 11.2: A possible scenario to collected further crosswind data on which to extend DSism.

would give a unique picture of the distribution of dust within rangeland environments during dust events and would be invaluable in understanding the spatial variability in dust concentration within such environments. If such detailed crosswind and vertical data is than coupled to a simulation model, such as the one presented in this thesis, it should be possible to gather new information about the wind erosion processes in rangeland environments.

11.2.4 Long term research goal

The work described so far has concentrated on the local scale and is achievable in the short term. A longer term research project could focus on how the spatial/temporal and process effects observed in this research, propagate through the various scales. Understanding this scaling problem is important as wind erosion is a scalable process, in that the same basic processes operate at all scales. Thus, it should be possible to scale DSism up from the claypan to, for example, the whole of Australia. The advantage of doing this is that for dust storms like the one that occurred in **Kazakhstan** on the 9th April,

2003 (Fig. 11.3), it would be possible to isolate how local spatial and temporal changes influence the structure of the dust plume at the regional and continental scale. In terms of Australia, this would also mean that it would be possible to understand, for example the impact that the Channel Country (and rangelands in general) have on urban pollution levels.

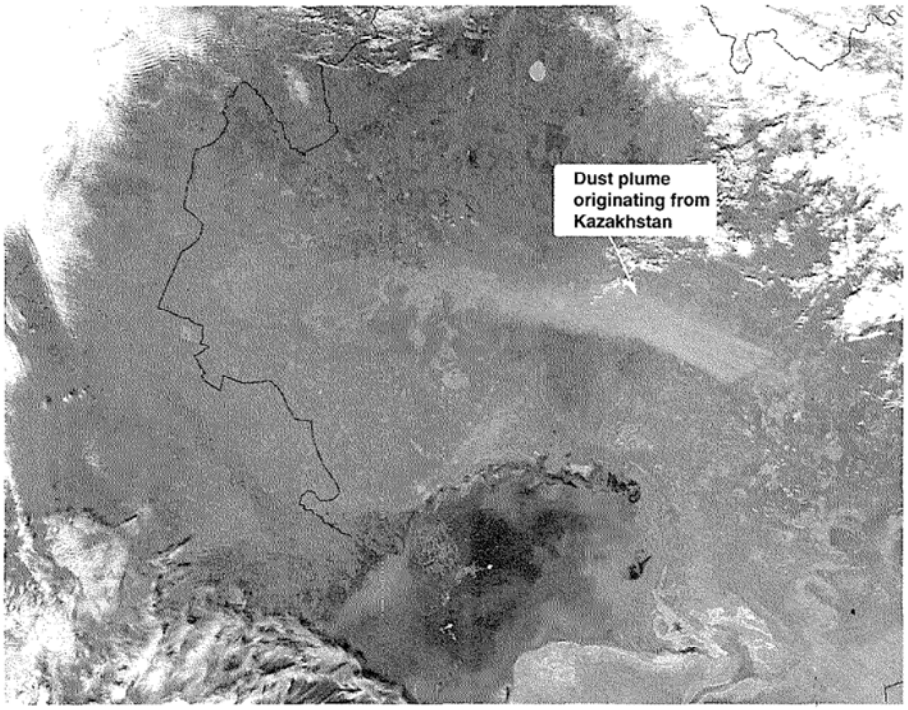

Figure 11.3: A satellite image of a dust plume blowing over the arid plains of **Kazakhstan**, on 9th April, 2003. Source: NASA (2003).

To achieve this, DSism needs to be modified to overcome the 20km modelling constraint imposed by the Gaussian assumption. There are several means of overcoming this limitation currently mentioned in the literature. The most promising approach at this stage is to use the DSism simulation results to seed a dispersion/transportation model, in a similar fashion to that used by Ilyushin and Kurbatskii (1996) to model atmospheric dispersion of contaminants. In this approach, a Gaussian air pollution model is coupled to a long range transportation model. If this is similarly applied to DSism, then it would be possible to produce a nested simulation model of the wind erosion events at a wide variety of scales.

References

Anderson, R. and P. Haff (1988). *Simulation of aeolian saltation.* Science, 241, pp. 820–823.

Argabright, M. (1991). *Evolution in use and development of the wind erosion equation.* Journal of Soil and Water Conservation, 46(2), pp. 104–105.

Armburst, D., W. Chepil, and F. Siddoway (1964). *Effects of ridges on erosion by wind.* Soil Science Society of America Proceedings, 28, pp. 557–560.

Bagnold, R. (1941). *The physics of blown sand and desert dunes.* Methuen London.

Baines, P. (1995). *Topographical effects in stratified flows.* Cambridge University Press.

Baines, P. and K. Hoinka (1985). *Stratified flow over two-dimesional topography in fluid of infinite depth: A laboratory study.* Journal of Atmospheric Sciences, 42(15), pp. 1614–1630.

Bondy, E., L. Lyles, and W. Hayes (1980). *Computing soil erosion by periods using wind-energy distributions.* Journal of Soil and Water Conservation, 35(4), pp. 173–176.

Briggs, L. and J. France (1982). *Mapping soil erosion by wind for regional environmental management.* Journal of Environmental Management, 15, pp. 158–168.

Brookshaw, L. (2001). Personal communication.

Burgess, R., G. McTainsh, and J. Pitblado (1989). *An index of wind erosion in Australia.* Australian Geographical Studies, 27(1), pp. 98–110.

Butler, H., W. Hogarth, and G. McTainsh (1996). *A source based model for describing dust concentrations during wind erosion events: An initial study.* Environmental Software, 11(1-3), pp. 45–52.

Butler, H., W. Hogarth, and G. McTainsh (2001). *Effects of spatial variations in source areas upon dust concentration profiles during three wind erosion events in Australia.* Earth, Surface Processes and Landforms, 26, pp. 1039–1048.

Butler, H., W. Hogarth, and G. McTainsh (2003). *"Kinks" in the dust concentration profile are they a natural part of the wind erosion process.* Submitted to JGR.

Carter, R. (1976). *Formation, maintenance and geomorpholical significance of an aeolian shell pavement.* Journal of Sedimentary Petrology, 46, pp. 418–429.

Chappell, A., G. McTainsh, J. Leys, and C. Strong (2003). *Using geostatistics to elucidate temporal change in the spatial variation of aeolian sediment transport.* Earth Surface Processes and Landforms, 28, pp. 567–585.

Chepil, W. (1945). *Dynamics of wind erosion, I: Nature of movement of soil by wind.* Soil Science, 60, pp. 305–320.

Chepil, W., F. Siddoway, and D. Armburst (1963). *Climatic index of wind erosion.* Proceedings, Soil Science Society of America, 27, pp. 449–452.

Chepil, W. and N. Woodruff (1957). *Sedimentary characterisitics of dust storms, II: Visibility and dust concentrations.* American Journal of Science, 255, pp. 104–114.

Chepil, W. and N. Woodruff (1963). *The physics of wind erosion and its control.* Advances in Agronomy, 15, pp. 211–302.

Cole, G., L. Lyles, and L. Hagen (1983). *A simulation model of daily wind erosion soil loss.* Transactions of the ASAE, 26(6), pp. 1758–1765.

Comis, D. and M. Gerrietts (1994). *Stemming wind erosion.* Agricultural Research, 42, pp. 8–15.

Cooke, R., A. Warren, and A. Goudie (1993). *Desert geomorphology.* UCL Press.

Dyke, M. V. (1982). *An album of fluid motion.* The Parabolic Press.

Eltayeb, I. and M. Hassan (2000). *Diffusion of dust particles from a point source above ground level and a line source at ground level.* Geophsyical Journal International, 142, pp. 426–438.

Findlater, P., D. Carter, and W. Scott (1990). *A model to predict the effects of prostate ground cover on wind erosion.* Australian Journal of Soil Research, 28, pp. 609–622.

Frank, A. and G. Kocurek (1994). *Effect of atmospheric conditions on wind profile and aeolian sand transport with an example from white sands national monument.* Earth Surface Processes and Landforms, 19, pp. 735–745.

Fryrear, D. (1986). *A field dust sampler.* Journal of Soil and Water Conservation, 41, pp. 533–552.

Fryrear, D. and A. Saleh (1993). *Field wind erosion:vertical distribution.* Soil Science, 155(4), pp. 294–300.

Gillette, D. (1977). *Fine particle emissions due to wind erosion.* Transactions of the ASAE, 20(5), pp. 890–897.

Gillette, D. (1979). *Saharan dust*, chap. Environmental Factors Effecting Wind Erosion. John Wiley, pp. 71–91.

Gillette, D. (1988). *Threshold friction velocities for dust production for agricultural soils.* Journal of Geophysical Research, pp. 12445–12462.

Gillette, D. (**1999**). *Aeolian environments, sediments and landforms*, chap. Physics of Aeolian Movement Emphasising Changing of the Aerodynamic Roughness Height by Saltating Grains (the Owen Effect). John Wiley and Sons Ltd, pp. 129–142.

Gillette, D., J. Adams, L. Endo, and D. Smith (**1980**). *Threshold velocities for input of soil particles into the air by desert soils*. Journal of Geophysical Research, 85, pp. 5621–5630.

Gillette, D., J. Adams, D. Muhs, and R. Kihl (**1982**). *Threshold friction velocities and rupture moduli for crusted desert soils for the input of soil particles into the air*. Journal of Geophysical Research, 87, pp. 9003–9015.

Gillette, D. and R. Passi (**1988**). *Modeling dust emissions caused by wind erosion*. Journal of Geophysical Research, 93(d11), pp. 14233–14242.

Goossens, D. (**2000**). *Dry aeolian dust accumulation in rocky deserts: A medium-term field experiment based on short term wind tunnel simulations*. Earth Surface Processes and Landforms, 25, pp. 41–57.

Goossens, D. and Z. Offer (**2000**). *Wind tunnel and field calibration of six aeolian dust samplers*. Atmospheric Environment, 34, pp. 1043–1057.

Greeley, R. and J. Iverson (**1985**). *Wind as a geological process on Earth, Mars, Venus and Titan*. Cambridge University Press.

Hagen, L. (**1991**). *A wind erosion prediction system to meet users needs*. Journal of Soil and Water Conservation, 46(2), pp. 106–111.

Hanna, S., G. Briggs, and R. Hosker (**1982**). *Handbook on atmospheric diffusion*. Technical Information Center US Department of Energy.

Hardisty, J. and R. Whitehouse (**1988**). *Evidence for a new sand transport process from experiments on Saharan dunes*. Nature, 332, pp. 532–534.

Hawthorne, S., D. Miller, P. Louie, R. Butler, and G. Mayer (**1996**). *Vapor-phase and particule associated pesticides and PCB concentrations in*

eastern North Dakota air samples. Journal of Environmental Quality, 25, pp. 594–600.

Horikawa, K. and H. Shen (1960). *Sand movement by wind action (on the characteristics of sand traps)*. Tech. Rep. Technical Memoir 119, US Army Corps of Engineers.

Ilyushin, B. B. and A. F. Kurbatskii (1996). *Modeling of contaminant dispersion in the atmospheric boundary layer*. Izvestiya, Atmospheric and Oceanic Physics, 32(3), pp. 283–297.

Iversen, J., W. Wang, K. Rasmussen, H. Mikkelsen, and R. Leach (1991). *Roughness element effect on local and universal saltation transport*. Acta Mechanica, suppl 2, pp. 65–75.

Knight, A., G. McTainsh, and R. Simpson (1995). *Sediment loads in an Australian dust storm: Implications for present and past dust processes*. Catena, 24, pp. 195–213.

Lancaster, N. and A. Baas (1998). *Influence of vegetation cover on sand transport by wind: Field studies at Owens Lake, California*. Earth Surface Process and Landforms, 23, pp. 69–82.

Lancaster, N., R. Greeley, and K. Rasmussen (1991). *Interaction between unvegetated desert surfaces and the atmospheric boundary layer: A preliminary assessment*. Acta Mechanica, suppl 2, pp. 89–102.

Leys, J. (1991a). *The threshold friction velocities and soil flux rates of selected soils in SW NSW*. Acta Mechanica, suppl 2, pp. 103–112.

Leys, J. (1991b). *Towards a better model of the effect of prostate vegetation cover on wind erosion*. Vegetatio, 91, pp. 49–58.

Leys, J. (1998). *Wind erosion process and sediments*. Ph.D. thesis, Griffith Univeristy.

Leys, J. (2001). Personal communication.

Leys, J., P. Butler, and C. McDonough (1993). *Wind erosion research at Borrika in the S.A Murray Mallee.* Tech. rep., CALM NSW.

Leys, J. and G. McTainsh (1996). *Sediment fluxes and particle grain-size charcteristics of wind-eroded sediment in southeastern Australia.* Earth Surface Processes and Landforms, 21, pp. 661–671.

Logie, M. (1981). *Wind tunnel experiments on sand dunes.* Earth Surface Processes, 6, pp. 365–374.

Love, B. (2001). *Changes in wind erosion rates in space and time in the Channel Country of western Queensland.* Griffith University Special Topic Project.

Lu, H. and Y. Shao (1999). *A new model for dust emission by saltation bombardment.* Journal of Geophysical Research, 104(D14), pp. 16827–16841.

Lu, H. and Y. Shao (2001). *Toward quantitative prediction of dust storms: An integrated wind erosion modelling system and its application,* Environmental Modelling and Software, 16, pp. 233–249.

Lyles, L. (1977). *Wind erosion: Processes and effects on soil productivity.* Transaction of the ASAE, 20, pp. 880–884.

Marshall, J. (1970). *Assessing the protective role of shrub-dominated rangeland vegetation against soil erosion by wind.* In *Proceedings of the XI International Grasslands Congress.* University of Queensland Press.

Marshall, J. (1972). *Principles of soil erosion and its prevention,* chap. The use of Tress and Shrubs in the Dry Country of Australia. Department of National Development–Forestry and Timber Bureau, AGPS, Canberra.

Marticorena, B. and G. Bergametti (1995). *Modelling the atmospeheric dust cycle: 1. design of a soil-derived dust scheme.* Journal of Geophyical Research, 100, pp. 16415–16430.

Marticorena, B., G. Bergametti, B. Aumont, Y. Callot, C. N'Doume, and M. Legrand (**1997**). *Modelling the atmospeheric dust cycle: 2. simulation of Saharan dust sources*. Journal of Geophyical Research, 102, pp. 4387–4404.

McEwan, I. (**1993**). *Bagnold's kink: A physical feature of the wind velocity profile modified by blown sand?* Earth Surface Process and Landforms, 18, pp. 18145–18156.

McEwan, I., B. Willetts, and M. Rice (**1992**). *The grain/bed collisions in sand transport by wind*. Sedimentology, 39, pp. 971–981.

McTainsh, G. (**1989**). *Quaternary aeolian dust processes and sediments in the Australian region*. Quatenary Science Reviews, 8, pp. 235–253.

McTainsh, G. (**1998**). Personal communication.

McTainsh, G. (**2002**). Personal communication.

McTainsh, G. and W. Boughton (**1993**). *Land degradation processes in Australia*. Longman Cheshire, Melbourne.

McTainsh, G. and J. Leys (**1993**). *Land degradation processes in Australia*, chap. Soil Erosion by Wind. Longman Cheshire, Melbourne, 1st edn., pp. 188–233.

McTainsh, G., J. Leys, and W. Nickling (**1999**). *Wind erodibility of arid lands in the Channel Country of western Queensland, Australia*. Zeitschrift für Geomorphologie, 116, pp. 113–130.

McTainsh, G., J. Leys, W. Nickling, and A. Lynch (**1996**). *Sediment loads, source areas and soil loss rates during a large dust storm in the Queensland Channel Country, Lake Eyre Basin.* Australian Rangelands Conference, Port Pirie, South Australia.

McTainsh, G., A. Lynch, and R. Burgess (**1990**). *Wind erosion in eastern Australia*. Australian Journal of Soil Research, 28, pp. 323–339.

McTainsh, G., A. Lynch, and R. Hales (1997). *Particle-size analysis of soils, dusts and other very small samples using a Coulter Mutlisizer.* Earth Surface Processes and Landforms, 22, pp. 1207–1216.

McTainsh, G., A. Lynch, and E. Tews (1998). *Climatic controls upon dust storm occurrence in eastern Australia.* Journal of the Arid Environments, 39, pp. 457–466.

Nanson, G., R. Young, and D. Price (1988). *Fluvial Geomorphology of Australia*, chap. Stratigraphy, sedimentology and late Quaternary chronology of the Channel Country of western Queensland. Academic Press, pp. 151–175.

NASA (2003). web page. NASA natural hazards web site. URL `http://naturalhazards.nasa.gov/shownh.php3?img_id=10161`

Nickling, W. (1978). *Eolian sediment transport during dust storms: Slims River Valley, Yukon Territory.* Canadian Journal of Earth Sciences, 15, pp. 1069–1084.

Nickling, W. (1988). *The initation of particle movement by wind.* Sedimentology, 35, pp. 499–511.

Nickling, W. and J. Gillies (1993). *Dust emission and transport in Mali, West Africa.* Sedimentology, 40, pp. 859–868.

Nickling, W., G. McTainsh, and J. Leys (1999). *Dust emissions from the Channel Country of western Queensland, Australia.* Zeitschrift für Geomorphologie, 116, pp. 1–17.

Offer, Z. and D. Goossens (2001). *Ten years of aeolian dust dynamics in a desert region (Negev desert, Israel): Analysis of airbourne dust concentration, dust accumulation and the high-magnitude dust events.* Journal of Arid Environments, 47, pp. 211–249.

Owen, P. (1964). *Saltation of uniform grains in air.* Journal of Fluid Mechanics, 20(2), pp. 225–242.

Phillips, N. (1957). *A coorindate system having some special advantages for numerical forecasting.* Journal of Meteorology, 14, pp. 184–185.

Pye, K. (1987). *Aeolian dust and dust deposits.* Academic Press.

Raupach, M. (1992). *Drag and drag partitioning on rough surfaces.* Boundary Layer Meteorology, 60, pp. 375–395.

Raupach, M. (1993). *Dry deposition of gases and particles to vegetation.* Clean Air, 27, pp. 200–203.

Raupach, M., D. Gillette, and J. Leys (1993). *The effect of roughness elements on wind erosion thresholds.* Journal of Geophsical Research, 98, pp. 3023–3029.

Raupach, M. and J. Leys (1992). *Wind tunnel studies of soil erodibility on western nsw.* In *Proceedings of the 5th Australian Soil Conservation Conference*, vol. 3.

Raupach, M. and J. Leys (1999). *The efficacy of vegetation in limiting spray drift and dust movement.* Tech. Rep. 47/99, CSIRO Divison of Land and Water, Canberra.

Raupach, M., G. McTainsh, and J. Leys (1994). *Estimates of dust mass in recent major Australian dust storms.* Australian Journal of Soil and Water Conservation, 7(3), pp. 20–24.

Shao, Y. (2000). *Physics and modelling of wind erosion.* Kluwer Academic Publishers.

Shao, Y. and L. Leslie (1997). *Wind erosion prediction over the Australian continent.* Journal of Geophysical Research, 102, pp. 30091–30105.

Shao, Y. and H. Lu (2000). *A simple expression for wind erosion threshold veolcity.* Journal of Geophysical Research, 105(D17), pp. 22437–22443.

Shao, Y., G. McTainsh, J. Leys, and M. Raupach (1993a). *Efficiences of sediment samplers for wind erosion.* Australian Journal of Soil Research, 31, pp. 519–532.

Shao, Y., M. Raupach, and P. Findlater (**1993**b). *The effect of saltation bombardment on the entrainment of dust by wind.* Journal of Geophysical Research, 98, pp. 12719–12726.

Shao, Y., M. Raupach, and J. Leys (**1996**). *A model for predicting aeolian sand drift and dust entrainment on scales from paddock to region.* Australian Journal of Soil Research, 34, pp. 309–342.

Sherman, D. (**1990**). *Evaluation of aeolian sand transport equations using intertidal-zone measurements, Sauton Sands, England-discussion.* Sedimentology, 37, pp. 385–389.

Sterk, G. and P. Raats (**1996**). *Comparison of models describing the vertical distribution of wind eroded sediments.* Soil Science Society of America Journal, 60, pp. 1414–1419.

Strong, C. (**2001**). Personal communication.

Sutton, O. (**1953**). *Micrometeorology.* McGraw-Hill.

Tegen, I. and I. Fung (**1994**). *Modeling the mineral dust in the atmosphere: Sources, transport and optical thickness.* Journal of Geophysical Research, 99, pp. 22897–22914.

Tegen, I. and I. Fung (**1995**). *Contribution to the atmsopheric mineral aerosol load from land surface modifications.* Journal of Geophysical Research, 100, pp. 18707–18726.

Thornthwaite, C. (**1931**). *The climates of North America according to a new classification.* Geographical Review, 21, pp. 633–655.

Tsoar, H. and K. Pye (**1987**). *Dust transport and the question of desert loess formation.* Sedimentology, 34, pp. 139–153.

Vories, E. D. and D. W. Fryrear (**1991**). *Vertical distribution of wind eroded soil over a smooth, bare field.* Transactions of the ASAE, 34(4), pp. 1763–1768.

Walmsley, J., J. Salmon, and P. Taylor (**1982**). *On the application of a model of boundary-layer flow over low hills to real terrain*. Boundary Layer Meteorology, 23, pp. 17–46.

Wasson, R. and P. Nanninga (**1986**). *Estimating wind transport of sand on vegetated surfaces*. Earth Surface Process and Landforms, 11, pp. 505–514.

Willetts, B. (**1983**). *Transportation by wind of granular materials of different grain shapes and densities*. Sedimentology, 30, pp. 669–680.

Willetts, B. and M. Rice (**1983**). *Practical representation of characteristic grain shape in sands: A comparison of methods*. Sedimentology, 30, pp. 557–565.

William, P. and M. Young (**1999**). *Costing dust: How much does wind erosion cost the people of South Australia*. final report, Policy and economic research unit, CSIRO Land and Water.

Wilson, P., R. Purdie, and C. Ahern (**1990**). *Western arid region land use study: Part 6*. Technical Bulletin 28, Divison of Land Utilisation, Queensland Department of Primary Industries. 234 pp.

Wind Erosion Research Unit (**2002**). web page. WERU web site. URL `http://www.weru.ksu.edu/weps.html`

Winges, K. (**1992**). *User's Guide for the Futive Dust Model (FDM) (revised): Volume I: User's Instructions*. US Environmental Protection Agency.

Woodruff, N. and F. Siddoway (**1965**). *A wind erosion equation*. Soil Science Society Proceedings, 29(5), pp. 602–608.

Yaalon, D. and E. Ganor (**1966**). *The climatic factor of wind erodibility and dust blowing in Israel*. Israel Journal of Earth Science, 15, pp. 27–32.

Yoshida, A. (**1991**). *Two-dimensional numerical simulation of thermal structure of urban polluted atmosphere (effects of aerosol characteristics)*. Atmospheric Environment, 25B(1), pp. 17–23.

Zannetti, P. (**1990**). *Air Pollution Modelling: Theories, Computational Methods and Available Software*. Van Nostrand Reinhold.